SURTSEY RESEARCH

14

SURTSEYJARFÉLAGIÐ

The Surtsey Research Society • Reykjavík

SURTSEY RESEARCH

Volume 14

THE SURTSEY RESEARCH SOCIETY

REYKJAVÍK, 2020

SURTSEYJARFÉLAGIÐ – The Surtsey Research Society
P.O.Box 352, 121 Reykjavík, Iceland
Website: www.surtsey.is

Surtsey Research is a continuation of Surtsey Research Progress Report I-X

Editors:
Bjarni D. Sigurdsson, ecosystem ecology (email: bjarni@lbhi.is)
Agricultural University of Iceland Hvanneyri, Borgarnes.

Borgthór Magnússon, terrestrial biology (email: borgthor@ni.is)
Icelandic Institute of Natural History P.O. Box 5320, Reykjavík, Iceland

Ingvar Atli Sigurðsson, geology and geophysics (email: ingvar.a.sigurdsson@ni.is)
Icelandic Institute of Natural History P.O. Box 5320, Reykjavík, Iceland

Kristján Jónasson, geology and geophysics (email: kristjan@ni.is)
Icelandic Institute of Natural History P.O. Box 5320, Reykjavík, Iceland

Karl Gunnarsson, marine biology (email: karl@hafro.is)
Marine Research Institute Skúlagata 4, Reykjavík, Iceland

Cover page: Drilling in Surtsey in 2017. The large photo was taken during the coring of the last of the three holes drilled. This hole had a 35° angle from vertical towards west. It retrieved a core through the island and the conduit that the eruption excavated into the pre-eruption seafloor. Inset left: The DOSECC drill rig. Inset right: The core from the bottom of the angled hole (about 290 m vertical depth below the surface), in the hands of the DOSECC drill crew (from left to right): Steve Cole, Justin Blouin, Anthony Vecchiarelli, Beau Marshall and Matthew Lyon.
Photos: Magnús Tumi Guðmundsson, August 29-September 4, 2017.

ISSN 1608-0998
https://doi.org/10.33112/surtsey.14

Contents

Introduction

The Surtsey Research Society aims to protect and raise the interest on scientific work related to the Surtsey island. The island has been a pristine natural laboratory for more than 55 year, where scientists have followed the island’s geological, geographical, biological and ecological evolution.

The island has been protected since its birth, which is unique for volcanic islands worldwide. In the documentation from the UNESCO World Heritage Centre it is stated that “Surtsey was born as a new volcanic island in 1963-67 and since that time has played a major role in studies of succession and colonisation. It has been the site of one of the few long-term studies worldwide on primary succession, providing a unique scientific record of the process of colonisation of land by plants and marine organisms.” It is as well stated that Surtsey will continue to provide invaluable data on biological colonisation long into the future. Every year a group of scientists fulfills this objective.

To pursue its main goal, the Surtsey Research Society now publishes the 14th volume of *Surtsey Research*. The first volume of the series was published already in 1965 and contained papers on oceanography, geology, geochemistry, geophysics and biology. Now, 55 years later there is more scientific interest than ever in this unique island. The present volume contains 11 papers that address different topics within meteorology, geology, biology and human geography.

On the cover page there is a picture taken during the SUSTAIN drilling operation on Surtsey in August 2017. The study focuses on the geology of the island, the birth and evolution by integrating volcanology, geophysics, geochemistry, mand microbiology. The SUSTAIN project extracted two vertical cores with the length of 344 m and one core from an inclined drill hole 354 m long. There was an earlier drilling on Surtsey done in 1979, so a comparison of the two cores was feasible. The study was to see how the details of the internal structure and thermal history has evolved, petrographic insight into time-lapsed alteration. Three papers in the current issue are from this research initiative.

Such a drilling operation is quite a venture, but every effort was made to preserve the sensitive surface and subsurface environments of the island during the drilling operation from end of July to beginning of September. At the termination of the drilling activities the restoration of the island environment was approved as correctly implemented by the Environmental Agency of Iceland. The Surtsey Research Society is pleased that the operation was successful and it acknowledges that the new boreholes offer unique future opportunities for continued monitoring of both geological and biological sub-surface processes.

Geology, biology and related sciences have been the most prominent research topics published in Surtsey Research from the beginning. However, in this volume a new chapter is being opened in the island’s research history, as it contains one study within the topic of human geography. It was done on the researchers themselves and the place names they have created on the island during its 57 years of existence.

Finally, I would like to thank the editorial committee: Bjarni D. Sigurðsson, Borþór Magnússon, Ingvar Atli Sigurðsson, Karl Gunnarsson and Kristján Jónasson for their editorial work, as well as Þórunn Edda Bjarnadóttir, for the layout. Also, I want to thank the 29 authors for submitting their papers for publication in *Surtsey Research*, but the continued interest and dedication of all those scientists is the main reason for continued existence of the Surtsey Research Society

Hallgrímur Jónasson,
Chairman Surtsey Research Society

METEOROLOGY

The climate of Surtsey

GUÐRÚN NÍNA PETERSEN AND TRAUSTI JÓNSSON

Icelandic Meteorological Office, Bústaðavegi 9, 108 Reykjavík, Iceland (gnp@vedur.is)

ABSTRACT

The first meteorological measurement in Surtsey were conducted before the eruption ended in 1967 and since 2009 there have been continous automatic measurements on the island. Here we give the first comprehensive analysis of the climate of Surtsey, based on these observations, and compare it to the climate at the two other stations in the Vestmannaeyjar archipelago, Vestmannaeyjabær and Stórhöfði. Surtsey experiences a relatively mild but windy climate, with monthly mean temperature above freezing during all calendar months and wind speed exceeding 20 m/s on average 30 days a year. Precipitation measurements are challenging but show, as expected, the summer months to be the driest and October to be both on average the wettest month but also the most variable month. The measurements show the climate of Surtsey to be similar to the climate of the other two stations in the archipelago with the largest difference in wind speed, where Vestamannaeyjabær is sheltered while at Stórhöfði strong winds are enhanced by the orography.

INTRODUCTION

Surtsey is the southernmost island of the Vestamannaeyjar archipelago as well as the southernmost point of Iceland, approximately 32 km from the southern coast. It is the second largest island of the archipelago. It rose from the sea floor during an eruption that lasted four years, 1963-1967, and at the end of the eruption the island covered an area of 2.65 km^2. However, due to erosion the island has undergone changes and e.g. in 2004 it had an area of 1.41 km^2 and a maximum elevation of 155 m a.s.l. (Baldursson & Ingadóttir (eds), 2007). The island was in 1965 declared a nature reserve owing to the scientific value of the new island (Surtseyjarfélagið, 2007) and in 2008 it was inscribed to the World Heritage List of UNESCO due to it being a pristine natural laboratory (UNESCO, 2008). Already in April-September 1967 the first routine meteorological measurements were conducted on the island (Sigtryggsson, 1968), with the eruption ongoing until 5 June. Observations were again obtained during April-September 1968, but during both years the measurements had several interruptions and could not be used to obtain direct information on the climate of Surtsey. However, by using the data in comparison to weather observations from Stórhöfði, at the south end of the largest of the Vestamannaeyjar islands Heimaey, Sigtryggsson (1968, 1970) could give an overview of the weather conditions during these two period, suggesting that the general climate is similar in both places and the main differences in temperature is due to differences in height above sea level. Automatic measurements over a two-month period in 1996 also strongly indicated the similarity between the weather conditions at the two stations (Baldursson & Ingadóttir (eds), 2007).

Since May 2009 there have been continuous automatic weather measurements in Surtsey. Here we analyse 10 years of data from Surtsey and compare to data from the other automatic stations in Vestmannaeyjar, namely Stórhöfði and Vestmannaeyjabær. Both stations have been operating automatically for over 15 years. In addition, Stórhöfði has a long record of manned observations extending back to 1921 but they were discontinued in 2014. Earlier observations in Vestmannaeyjar extend as far back as 1869. Although the stations are both on Heimaey and the distance between them, as the crow flies, is only 4.1 km there is a difference in climate, especially wind climate. Stórhöfði is known for high wind speed, due to the station being located at the top of the southernmost tip of Heimaey, at 118 m a.s.l. On the other hand, the station Vestmannaeyjabær is located within the town on the island, at 40 m a.s.l. and approximately at the centre of the island, sheltered by low mountains, vegetation and the town itself from the maritime winds. This results in a more pleasant wind climate than at Stórhöfði.

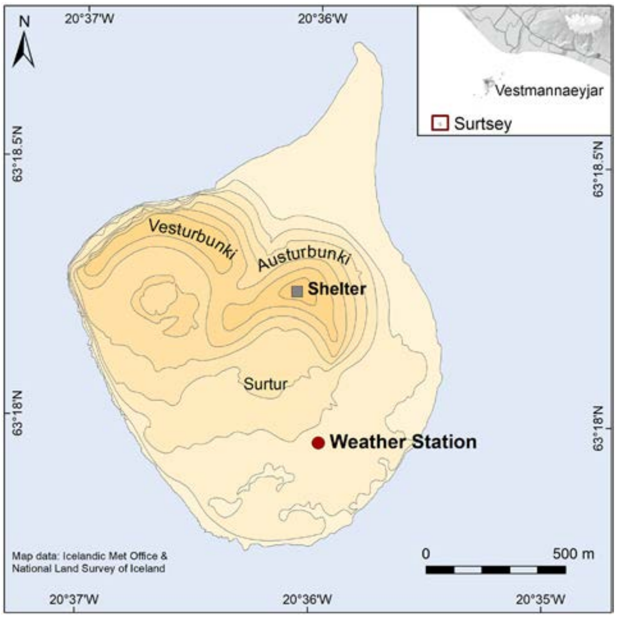

Figure 1. Map of Surtsey showing the location of the current weather station. Some earlier observations were conducted close to the shelter at the top of Austurbunki. The elevation is shown with contours, interval 20 m. Inset map shows location of Surtsey in relation to the Vestmannaeyjar archipelago as well as the southern coast of Iceland.

MATERIAL AND METHODS

The automatic weather station in Surtsey, Station No. 6012, is located on the south side of the island at 36 m a.s.l., see Fig. 1. A previous station was located at the top of the island on Austurbunki, at 154 m a.s.l., in the vicinity of a shelter, see Fig. 1 and Table 1. Some of the earlier measurements were conducted there. See Table 1 for further information on previous and current weather stations in Surtsey.

The station measures all the basic meteorological parameters, i.e. air pressure, temperature, humidity, precipitation, wind speed and wind direction. In addition, solar radiation is measured as well as soil temperature. The measurements are recorded every 10 minutes. Since 13 September 2018 the station is also equipped with a web camera, looking towards the mainland, and photos are saved hourly during daylight hours. Fig. 2 shows a photo of the station and Table 2 contains more detailed information on the equipment at the station. The station is visited every summer for regular maintenance. Sometimes it has been possible to add a visit in the case of instrumental failure but often maintenance has had to wait until the next summer visit. As a part of the regular maintenance of the station the temperature and humidity sensor has been replaced five times and the anemometer eight times. The solar radiation measurements are not analysed here as an analysis of all solar radiation measurements in Iceland and a comparison to sunshine hours and cloud cover measurements is yet to be conducted, prior to looking at measurements from an isolated automatic station. The soil temperature measurements are done in two locations, one with limited vegetation and another where vegetation covers the ground. They are done at two depths, 5 cm and 15 cm. The measurements

Table 1. Information on operational meteorological measurements in Surtsey as well as at the two other automatic stations in Vestmannaeyjar used in the study. The station number, where known, is shown in parenthesis.

	Period	Location	Height a.s.l.	Comments
Surtsey	April—Sept 1967	A few locations	_	Several interruptions
	April—Sept 1968	A few location	_	Several interruptions
Surtsey (814)	1969—1972	63.3N 20.6W	40 m	
Surtsey (6011)	Sept—Nov 1996	63.3N 20.6W	154 m	On Austurbunki
Surtsey (6012)	2009—	63.2993N 20.59947W	36 m	
Vestmannaeyjabær (6015)	2002—	63.43587N 20.27578W	40 m	
Stórhöfði (6017)	2004—	63.39957N 20.28825W	118 m	

Figure 2. The automatic station in Surtsey (No. 6012) with Austurbunki in the background. Some previous measurements were conducted close to the shelter seen at the top of the fell. Photo: Vilhjálmur S. Þorvaldsson, 17 July 2014.

are done in cooperation with the Surtsey Research Society. No attempts is made here to analyse these measurements. For information on the soil temperature measurements in Iceland see Petersen & Berber (2018).

The stations in Stórhöfði (Station No. 6017) and Vestmannaeyjabær (Station No. 6015) measure the basic meteorological parameters. However, the automatic precipitation measurements in Stórhöfði have been unreliable and are thus not included here.

For this analysis, 10 year of data from Surtsey, Stórhöfði and Vestmannaeyjabær were obtained from the database of the Icelandic Meteorological Office (IMO), for the period 01.06.2009—31.05.2019. For most calculations daily values are used but for diurnal variation and frequency roses hourly data is used.

Table 2. The instrumentation of the automatic station in Surtsey.

Parameter	Height	Instrument
Wind speed & direction	10 m a.g.l.	Young wind monitor
Temperature & Humidity	2 m a.g.l.	Rotronic temperature & humidity probe
Air pressure	37.5 m a.s.l.	Vaisala Barometric pressure transmitter
Precipitation	1.5 m a.g.l.	Lambrecht heated tipping bucket
Solar radiation	5 m a.g.l.	Type unknown
Cloud conditions, visibility & surface conditions	3 m a.g.l.	Web camera
Soil temperature	5 and 15 cm depth in an vegetated and a sparsely vegetated area.	Type unknown

RESULTS AND DISCUSSION

Annual variations

Surtsey has a maritime climate, e.g. the annual temperature variation in Surtsey is dampened by the sea that cools the climate during summer and warms it during winter. Fig. 3, top panel, shows the annual variation of temperature as a boxplot. The graph is based on monthly values and 50% of the values for each calendar month are inside the box (25-75% quantiles). The horizontal line inside each box is the median value, the whiskers (vertical lines) show outliers not further away from the box than 150% of its height. If there are outliers further away, they are depicted as points. The blue line represents monthly mean values. The figure shows a clear annual variability. December is the coldest month of the year with mean temperature of 3.2°C and August the warmest with 11.3°C, resulting in an annual amplitude of 8.1°C.

The monthly mean and median temperature in July and August are quite similar but there is more variability in July and outliers extend further away from the box. The same is true for January to March where the largest variation in temperature is seen in February. The temperature increases from spring into summer (April-July) with no overlapping of the boxes and decreases similarly from late summer to winter (August-December). In Iceland in general, July is the warmest month of the year and January the coldest, i.e. about a month after the sun is at its highest/lowest point in the sky (Einarsson, 1976). However, by the coast and on islands where the winds blow from the ocean the lag is often larger resulting in August being as warm or even warmer than July – as is true for Surtsey. Notice that this lag is not present during winter. In fact, December is in general colder than January. The reason for this is that during this century January-March have warmed more than other months of the year, in comparison to longer time periods, and December the least. This can be seen clearly in

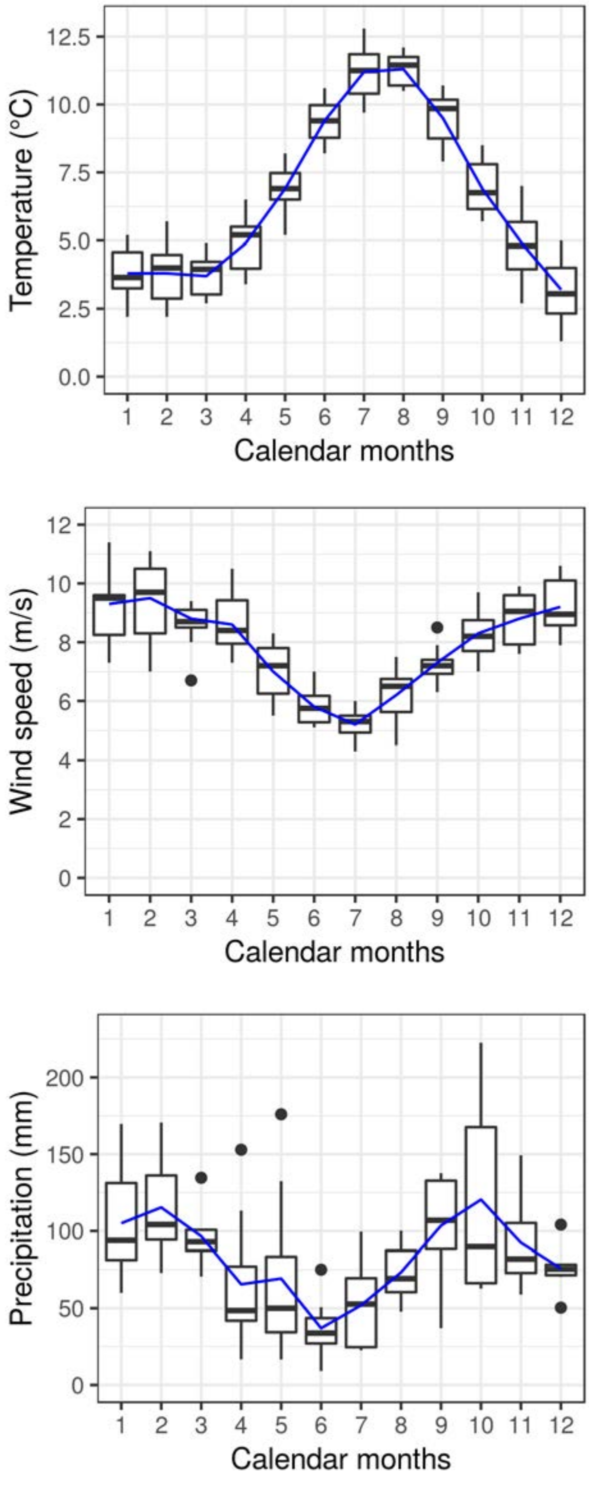

Figure 3. Annual variations of temperature (°C, top), wind speed (m/s, centre) and precipitation (mm, bottom) in Surtsey 2009-2019. The boxes contain 50% of the data (25-75% quantiles). The horizontal line is the median value and the whiskers show outliers within 150% of the height og the box. Outliers outside of that limit are shown with points. The blue line shows the monthly mean values.

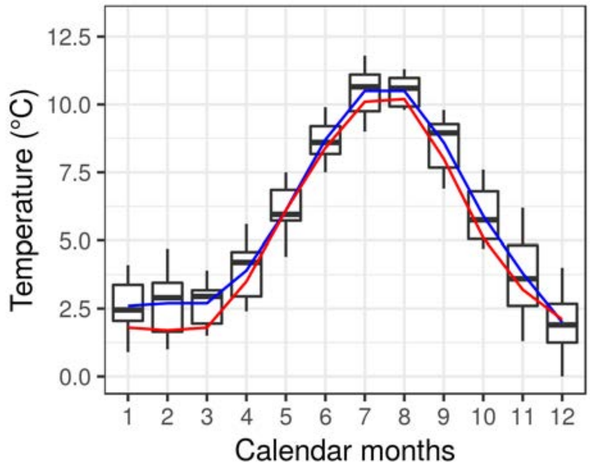

Figure 4. Annual temperature variations (°C) in Stórhöfði 2009-2019. The boxes contain 50% of the data (25-75% quantiles). The horizontal line is the median value and the whiskers show outliers within 150% of the height og the box. Outliers outside of that limit would be shown with points. The blue line shows the monthly mean values. The red line shows the monthly mean values for the 30-year period 1981-2010.

Fig. 4 that shows the annual temperature variations in Stórhöfði, for the applied period 2009-2019, with the monthly mean temperature for the 30-year period 1981-2010 inset. Similar results are found for other coastal stations e.g. Reykjavík (not shown).

The annual wind speed variations are shown in the centre panel of Fig. 3. The highest monthly mean wind speed is found in February, but also the most variable monthly values, emphasising how variable the weather can be in this month. In general, wind speed variations are large in most months with least variations in March, June, July and September. As expected, the lowest monthly mean wind speed is in July.

The wind roses in Fig. 5 show the frequency of wind directions and wind speed for the whole period as well as for the summer months (June-August). Although Surtsey is about 32 km from the southern coast of mainland Iceland it is clear that the mainland has a large impact on the wind directions in Surtsey. On an annual basis the most frequent wind directions are easterly (east-northeasterly to east-southeasterly) as well as north-northeasterly. Westerly winds are common, along the coast of Iceland, but northerly and southerly less common. Most windstorms, where wind speed exceeds 20 m/s, are easterlies. Low pressure systems approaching Iceland from the south frequently result in strong southeasterly and easterly winds in this region. The glacier mountains

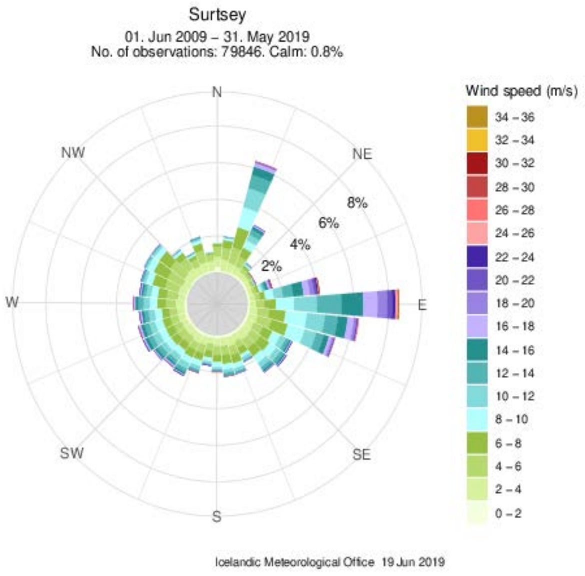

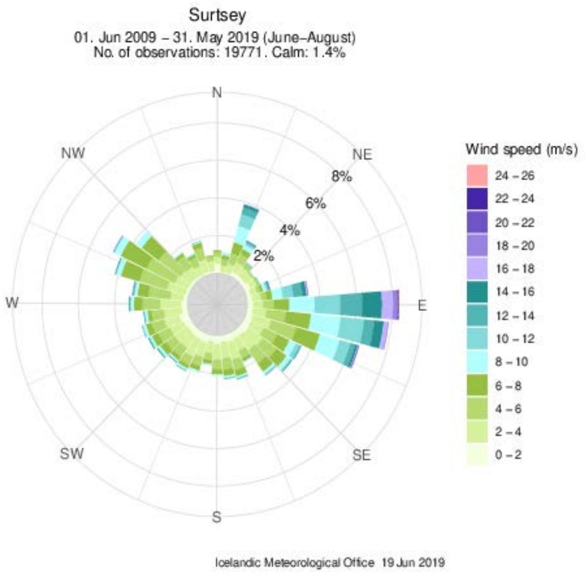

Figure 5. Wind roses showing the frequency of wind direction during (top) the whole year and (bottom) during June-August. The wind blows towards the centre of the wind rose. The colour show the wind speed. Hourly data from the time period 2009-2019.

at the southern tip of Iceland, Mýrdalsjökull and Eyjafjallajökull, can enhance these winds by forcing the air to flow on their south side and consequently increasing the easterly wind component. In addition, winds blow rarely from the northeast in Surtsey due to the same orographic features. The wind rose for the summer months shows a similar pattern but with increased west-northwesterly winds and decreased frequency of easterly winds as well as north-northeasterly winds. However, the strongest winds are still easterly.

The annual precipitation is shown in the bottom panel of Fig. 3. It is worth bearing in mind that precipitation measurements are challenging in Iceland. Firstly, there is an increasing undercatch of precipitation with increased wind speed. Pollock *et al.* (2018) estimate that at an exposed upland site the underestimation can be more than 23% on average. Secondly, solid precipitation is more difficult to catch than liquid precipitation due to the distortion of snowflake trajectories by the airflow around the gauges (e.g. Rasmussen *et al.*, 2012). Heated rain gauges, such as the one in Surtsey, melt snow so that the amount catched can be measured although the precipitation intensity is in these cases not reliable. Given that Iceland is a windy country in general undercatch of precipitation is expected at most locations. However, as Surtsey is the southern point of Iceland, in maritime location and the station at low elevation winters are in general mild and solid precipitation can be expected to be much less common than liquid precipitation. Here, no attempt is made to correct for undercatch. In general the driest month of the year is June and the wettest months September and October as well as January and February during the winter. The largest variability is in October and least in December, although that may be due to undercatch of solid precipitation.

Diurnal variations

Due to limited solar radiation there is little diurnal variation of temperature during winter. Indeed, during December the mean temperature of each hour of the day is in the range 3.1-3.3°C. Also, the highest temperature can be at any time of the day as heat is transported into the region by synoptic systems pushing warm air masses northward. The lowest temperatures occur in calm conditions during winter darkness when long wave radiation results in heat loss from the surface and the surface then subsequently cools the adjacent air. The diurnal temperature variations in July in Surtsey and Vestmannaeyjabær are shown in Fig. 6. While the mean and median values are similar, the number of outliers differs greatly. The mean diurnal amplitude is 1.7°C and 2.3°C in Surtsey and Vestmannaeyjabær, respectively, with both lower minimum and higher maximum value at Vestmannaeyjabær. At both stations the lowest temperature is measured in early morning, at 4-5 UTC, and the highest temperature in the afternoon, at 15-16 UTC. However, while in Surtsey most outliers

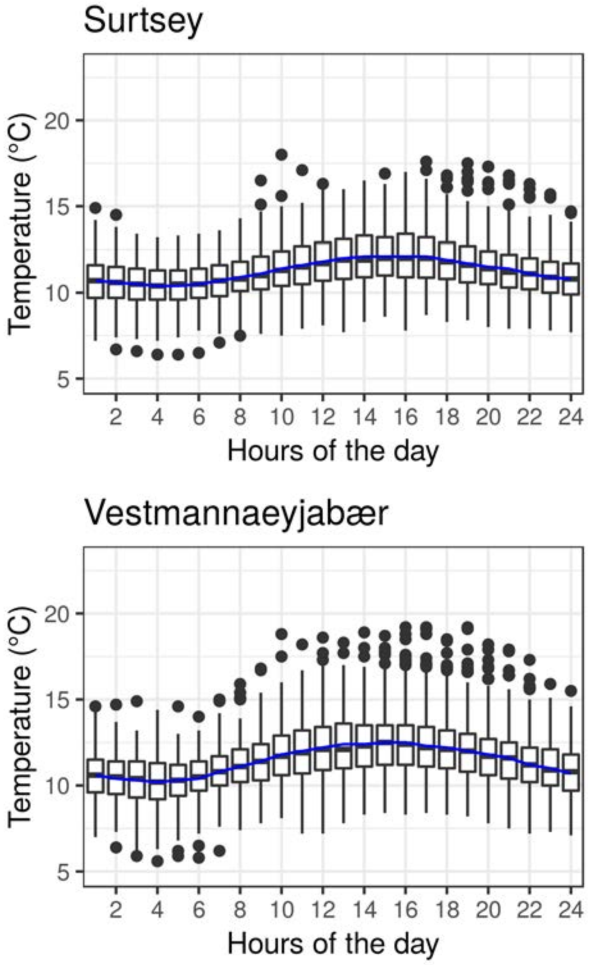

Figure 6. Diurnal variation of temperature (°C) in Surtsey (top) and Vestmannaeyjabær (bottom) in July during the period 2009-2019.

lie within the maximum whiskers length (150% of the height of the box), in Vestmannaeyjabær there is a considerable number of outliers that exceed these limits, especially with higher values during the day and evening. This suggests that the station Vestmannaeyjabær is less affected by the sea than the station in Surtsey, with the former located close to the centre of Heimaey and sheltered from the sea. For example, the highest hourly temperature measured in Surtsey is 18.0°C at 10 UTC on 29 July 2018 when Vestmannaeyjabær measured 18.8°C.

Comparison of mean values and outliers

The annual mean values for Surtsey, Vestmannaeyjabær and Stórhöfði are shown in Table 3 and maxima and minima in Table 4. Note that at Stórhöfði no data is retrieved from the manned station, only the automatic. Of these three stations Surtsey has the highest mean temperature, the fewest days where temperature falls below freezing level and fewest freezing days, i.e. where the temperature never exceeds freezing level. In addition, the station has on average the longest period of non-freezing temperatures, 199 days (approximately 6 months annually). The difference in elevation of Surtsey and Stórhöfði explains most

Table 3. Mean values during the period 2009—2019 at Surtsey, Vestmannaeyjabær and Stórhöfði.

	Surtsey	**Vestmanna-eyjabær**	**Stórhöfði**
Temperature	6.6°C	6.3°C	5.7°C
Days with minimum temperature below 0°C	45 days	66 days	67 days
Days with maximum temperature below 0°C	2 days	5 days	7 days
Length of frost-free period	199 days	175 days	184 days
Annual precipitation	1009.3 mm	1327.9 mm	_
Days with precipitation	229 days	239 days	_
Wind speed	7.8 m/s	5.0 m/s	10.7 m/s
Days with wind speed exceeding 20 m/s	30 days	5 days	120 days

Table 4. Maxima and minima during the period 2009—2019 at Surtsey, Vestmannaeyjabær and Stórhöfði. If higher records exist at Vestmannaeyjabær and Stórhöfði outside of this period they are shown in parenthesis. Note that pressure measurements in Stórhöfði ended 9 June 2015 while the lowest pressure at the other stations is measured at the end of that year.

	Surtsey	**Vestmanna-eyjabær**	**Stórhöfði**
Maximum temperature	18.3°C	19.8°C (23.6°C)	18.4°C (21.6°C)
Minimum temperature	-9.7°C	-10.6°C	-11.3°C
Maximum wind speed	35.2 m/s	28.0 m/s	46.7 m/s
Maximum wind gust	47.8 m/s	45.8 m/s	56.6 m/s
Maximum annual precipitation	1071.8 mm	1485.4 mm	_
Maximum daily precipitation	67.5 mm	85.6 mm	_
Maximum hourly precipitation	13.8 mm	16.8 mm	_
Maximum sea level pressure	1041.6	1040.9 hPa (1044.8 hPa)	1038.4 hPa (1044.4 hPa)
Minimum sea level pressure	936.7	934.5 hPa	949.1 hPa
Minimum relative humidity	41%	32%	38%

of the difference in mean temperature between the stations, given the dry adiabatic lapse rate of 9.8°C/km. However, it is also clear that the sheltering of Vestmannaeyjabær decreases slightly the impact of the sea on air temperature. This results in the period of non-freezing temperatures being on average 24 days shorter than in Surtsey and the days of freezing on average five but only two in Surtsey. The sheltering of Vestmannaeyjar is also clearly detected in the mean wind speed which is by far the lowest of the three stations and rarely exceeds 20 m/s. In comparison, at Stórhöfði the same limit is reached on average 120 days a year, or about one third of the year. On average it rains about 300 mm more in Vestmannaeyjabær than Surtsey as well as more frequently.

The maximum temperature measured during the period was 19.8°C in Vestmannaeyjabær and 18.3°C and 18.4°C in Surtsey and Stórhöfði, respectively. The lowest temperature measured at Surtsey was higher than at the two other station, or -9.7°C compared to -10.6°C at Vestamannaeyjabær and -11.3°C at Stórhöfði. Again, this illustrates the impact of the sea as well as the low elevation in decreasing temperature variations. The maximum wind speed and wind gust where both measured at the windy Stórhöfði with considerably lower values at the other two stations. In particular, the maximum wind speed at Vestmannaeyjabær is low in comparison, only 28.0 m/s while the values are 35.2 m/s in Surtsey and 46.7 m/s in Stórhöfði. For wind gust the highest measurement in Stórhöfði is 56.6 m/s while at the other stations the maxima are 45.8 m/s and 47.8 m/s, with the higher value at Surtsey.

Fig. 7 shows the monthly values of a few parameters for all stations. The variations in time are similar at all stations, as expected due to their proximity to each other. In general, the winter temperature is milder in Surtsey than at the other two stations, but summer temperature similar to the one in Vestmannaeyjabær. The wind speed lies within the values for the other

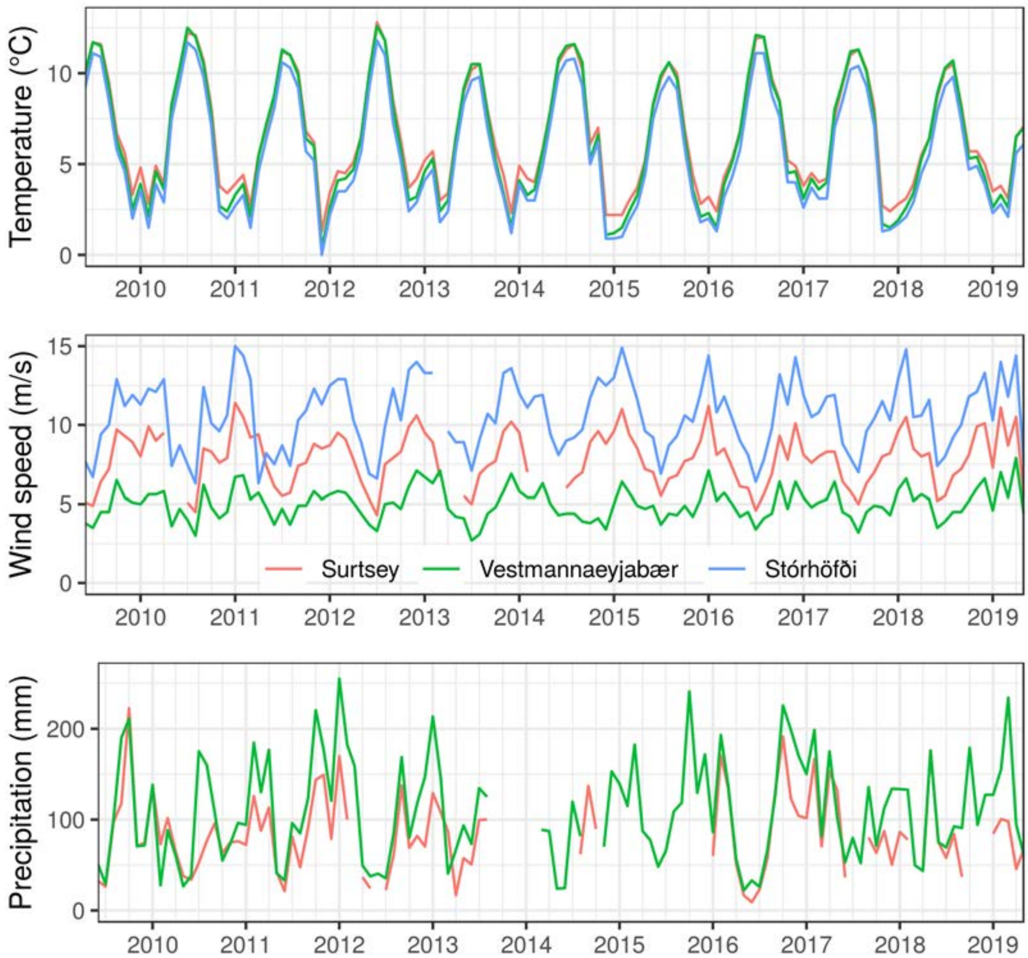

Figure 7. Monthly values of temperature (°C, top), wind speed (m/s, centre) and precipitation (mm, bottom) at Surtsey, Vestmannaeyjabær and Stórhöfði, 2009-2019.

stations; the sheltering of Vestmannaeyjabær is seen clearly as well as the wind enhancement at Stórhöfði. Precipitation is only measured at Surtsey and in Vestmannaeyjabær. Both time series have periods of missing data but there are indications that in general it rains more in Vestmannaeyjabær than in Surtsey and with higher intensity.

CONCLUSION

Surtsey is the southernmost part of Iceland. A weather station is on the island, located at 36 m a.s.l. and open to the sea. Measurements have been conducted continuously on the island since 2009 but the first routine measurments were conducted already in 1967. Here we inspect the time series June 2009-May 2019.

Given the southerly location, the closeness to the sea and low elevation the station experiences a relatively mild but windy climate.

The monthly mean temperature is above freezing during all calendar months, December is the coldest month and August the warmest. A comparison with a 30 year time series, 1981-2010 at Stórhöfði, on Heimaey, shows that the last decade has seen warmer January-March months than earlier when these months were the coldest of the year.

The wind speed is rather high as the winds blow in from the sea and there is little surface friction to decrease the wind speed. The wind speed is in general between the one measured at Stórhöfði and Vestmannaeyjabær, with both stations located in Heimaey, the largest island of the archipelago. At Stórhöfði the wind speed is considerably higher mainly due to the fact that the station is at the top of a hill that enhances the wind speed. On the other hand Vestmannaeyjabær is sheltered from the sea by the orography and the town itself. The wind directions in Surtsey are highly impacted by the mainland which can be seen clearly by the frequency of easterly winds as well as lack of northeasterly winds.

Precipitation measurements are in general challenging. A considerable undercatch can be expected in Surtsey, mainly because of the windy conditions. However, the pattern of summer months being the driest and winter months the wettest is consistent with expectations. The same is true for October being in general the wettest but also the most variable month, related to the prevalence of cyclones in the region.

The measurements show that the climate of Surtsey is similar to the climate at the other two stations in the Vestmannaeyjar archipelago with the largest difference being in wind speed.

This is the first time a comprehensive analysis of the climate in Surtsey has been done. It is the hope that this summary will be useful for anyone conducting research in Surtsey where weather plays a part as well as informative for those that have a general interest in Surtsey and its evolution.

ACKNOWLEDGEMENT

The authors would like to thank Ragnar Heiðar Þrastarson for producing the map of Surtsey and Vilhjálmur Smári Þorvaldsson for the photo of the weather station. Thanks also to the weather measurement team at the Icelandic Meteorological Office for their contribution.

REFERENCES

Baldursson, S. & Á. Ingadóttir (eds.) 2006. Nomination of Surtsey for the UNESCO World Heritage List. Icelandic Institute of Natural History, Reykjavík, 120 p.

Einarsson, M. Á. 1976. Veðurfar á Íslandi. Reykjavík: Iðunn.

Petersen, G. N. & D. Berber 2018. Jarðvegsmælingar á Íslandi. Staða núverandi kerfis og framtíðarsýn. Icelandic Meteorological Office, VÍ 2018-009.

Pollock, M. D., G. O'Donnell, P. Quinn, M. Dutton, A. Black, M. E. Wilkinson, M. Colli, M. Stagnaro, L.G. Lanza, E. Lewis, C. G. Kilsby, & P. E. O'Connell, 2018. Quantifying and mitigating wind-induced undercatch in rainfall measurements. WaterResources Research, 54 3863–3875. https://doi.org/10.1029/2017WR022421

Rasmussen, R., B. Baker, J. Kochendorfer, T. Meyers, S. Landolt, A. P. Fischer, J. Black, J. M. Thériault, P. Kucera, D. Gochis, C. Smith, R. Nitu, M. Hall, K. Ikeda & E. Gutmann, 2012: How Well Are We Measuring Snow: The NOAA/FAA/NCAR Winter Precipitation Test Bed. Bull. Amer. Meteor. Soc., 93, 811–829, https://doi.org/10.1175/BAMS-D-11-00052.1

Sigtryggsson, H. 1968. Preliminary report on meteorological observations in Surtsey 1967. Surtsey Research Progress Report IV, 167-170.

Sigtryggsson, H. 1969. Preliminary report on the results of meteorological observations on Surtsey 1968. Surtsey Research Progress Report V, 119-120.

Surtseyjarfélagið 2007. Visited 30 July 2019 at surtsey.is.

UNESCO 2008. Visited 30 July 2019 at unesco.org.

GEOLOGY

Lithofacies from the 1963-1967 Surtsey eruption in SUSTAIN drill cores SE-2a, SE-2b and SE-03

JOCELYN McPHIE[1], JAMES D.L. WHITE[2], CAROLYN GORNY[3], MARIE D. JACKSON[4], MAGNÚS TUMI GUDMUNDSSON[3] AND SAMANTHA COUPER[4]

[1]School of Natural Sciences, University of Tasmania, Hobart, Tasmania 7000, Australia j.mcphie@utas.edu.au. (Corresponding author). [2]Geology Department, University of Otago, Dunedin 9016, New Zealand. [3]Nordvulk, Institute of Earth Sciences, University of Iceland, Sturlugata 7, 101 Reykjavik, Iceland. [4]Department of Geology and Geophysics, University of Utah, Salt Lake City, Utah, USA

ABSTRACT

Surtsey was drilled in 2017 in the context of the Surtsey Underwater volcanic System for Thermophiles, Alteration processes and INnovative Concretes (SUSTAIN) project. Vertical drill holes, SE-02a and SE-02b (drilled to 191.64 m), and angled drill SE-03 (drilled to 354.05 m), intersected armoured lapilli tuff and lapilli tuff generated mainly by explosive eruptions at Surtur from November 1963 to January 1964. The top ~20 m of lapilli tuff was erupted from Surtungur. Intervals of coherent basalt in SE-02b (15.7 to 17 m and <15 cm at the end) and in SE-03 (<1 m at ~60 m and ~238 m, and 10 m near the base) are probably intrusions that may have fed the small lavas erupted at Surtur ~2.5 years later. Although collared only a few m from the 1979 drill hole, neither SE-02a nor SE-02b intersected the 13-m-thick interval of basalt found in the 1979 drill hole. The 2017 drill cores are entirely lithified and variably altered, reflecting the effects of hydrothermal alteration and cement deposition on the originally fresh, unconsolidated ash and lapilli. Drill hole SE-03 was drilled on an azimuth of 264° and at 55° from horizontal, obliquely crossing the crater- and conduit-fill of Surtur. Although the exact trajectory of SE-03 is unknown (the drill hole was not surveyed), the drill hole ended at a vertical depth of ~100 m below the pre-eruption sea floor, however, sedimentary facies known to underlie the sea floor nearby were not intersected. Surtur eruptions therefore excavated the pre-eruption sea floor to a depth of several tens of m.

INTRODUCTION

Surtsey was created by submarine and then subaerial basaltic eruptions from 1963 to 1967 (Thórarinsson *et al.* 1964; Jakobsson & Moore 1982; Jakobsson *et al.* 2009). The eruptions began in sea water ~130 m deep, eventually building an island that grew to a height of 150 m above sea level. Two vents were active on Surtsey during the main subaerial activity. Explosive eruptions began at Surtur and lasted for about 2.5 months (visible from 14 November 1963 to 31 January 1964). Explosive eruptions then began at a second vent, Surtungur, ~500 m to the northwest of Surtur. Explosions at Surtungur stopped on 4 April 1964, when fountains and effusion of lavas began. After a hiatus of over two months during May to July 1964, lava eruption continued at Surtungur until 17 May 1965. No further eruptions occurred at Surtungur. However, effusive activity resumed at Surtur in August 1966, and continued until the end of the eruption in 5 June 1967. During this period (12 December 1966 to 8 January 1967), four very small lavas, some associated with tiny spatter ramparts, were erupted from four separate vents within and on the upper outer flanks of Surtur.

In 1979, a vertical hole 181 m deep was drilled through the rim of Surtur (SE-01; Jakobsson & Moore 1982, 1986), providing information on the lithofacies, structure, alteration and temperature. In 2017, the Surtsey Underwater volcanic System for Thermophiles, Alteration processes and INnovative Concretes (SUSTAIN) project, sponsored partly by the International Continental Scientific Drilling Program (ICDP), drilled three cored holes on Surtsey (Jackson *et al.* 2019; Weisenberger *et al.* 2019). Here we review the characteristics of the lithofacies in the three SUSTAIN drill holes and compare our data with those on the 1979 drill core (Jakobsson & Moore 1982, 1986).

The four drill hole collars, SE-01 (1979) and SE-02a, SE-02b, and SE-3 (2017), lie within a 10-m-wide area on the southeastern rim of Surtur (Fig. 1). The drill holes intersected eruptive products from November 1963 to April 1964 and slightly younger intrusions, probably emplaced 1966-1967 (Jakobsson & Moore 1986). SE-02a is a vertical cored drill hole that was abandoned at depth 151.57 m following collapse. A second vertical hole, SE-02b, was then drilled adjacent to SE-02a to a depth of 191.64 m (recovered drill core extends to 185.85 m). SE-03 is inclined, plunging 55° to the west (264°) across the vent of Surtur, and extends downhole to 354.05 m (recovered drill core extends to 353.7 m). None of the drill cores were oriented. No borehole orientation surveys were conducted on SE-03 during or after drilling so the vertical thickness intersected is not exactly known but it is expected to be close to 290 m.

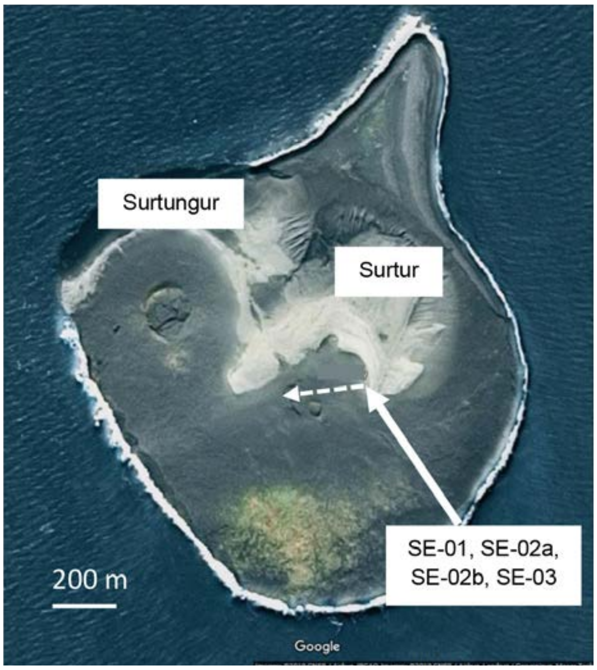

Figure 1. Map of Surtsey showing Surtungur, Surtur and the location of the drill hole collars for SE-01 (drilled in 1979) and SE-02a, SE-02b and SE-03 (drilled in 2017). The white dashed line is the approximate planned trace of angled drill hole SE-03 (plunge 55°, azimuth 264°). Base from Google Maps.

METHODS

We logged the drill core from the base upward, in stratigraphic order, concentrating on textures, components, grain size and layers (Figs 2, 3). The drill core was wet when logged and the surface was intermittently moistened with sprays of fresh seawater. Most observations were made using a hand lens and, in some cases, using a binocular microscope. Data were entered into the ICDP Digital Information System (http://surtsey.icdp-online.org) and compiled as summary graphic logs, similar to those in Figures 2 and 3.

PRINCIPAL LITHOFACIES

Three main lithofacies have been defined: lapilli tuff (lithified), coherent basalt, and volcanic sandstone.

Lapilli tuff

At least 95% of the drill core consists of lapilli tuff (Fig. 4a). Weakly altered lapilli tuff is black or yellowish brown whereas more altered lapilli tuff is green, dark green or greenish black, depending on the intensity and type of alteration. In SE-02b, weakly lithified grayish black lapilli tuff (Fig. 4b, c) occupies a <2-m-thick section at 146 m depth and a 3-m-thick section close to the base (Fig. 2). These intervals are more friable and less altered than the rest. The lapilli tuff is poorly sorted, everywhere comprising components from ash (<2 mm) to medium lapilli (typically 8 to 10 mm). Coarse lapilli (typically 4 to 6 cm) are commonly present. Coarser fragments (7 to 30 cm) are minor.

Lapilli tuff composed of armoured lapilli (Fig. 4d) is the dominant facies in SE-02a at four levels (~9 to 20 m, ~24 to 26 m, ~38 to 40 m and ~55 to 66

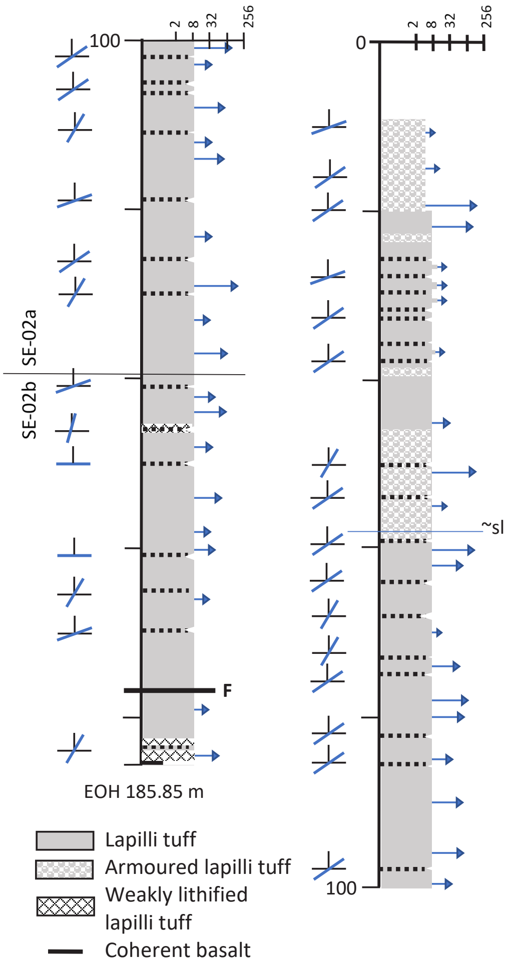

Figure 2. Simplified graphic log of the lithofacies in vertical drill holes SE-02a and SE-02b. The boundary between SE-02a (above) and SE-02b (below) occurs at 139.29 m. The grain size scale across the top is in mm and depths are in m; blue arrows give the size of the maximum clast. Beds defined by grain size differences are shown by dashed lines. Approximate orientations of beds (LHS) are given by the blue lines with respect to the drill core axis (vertical). The bold black line and "F" indicate the position of a fault in the section marked by slickensides. The fine blue line is approximate sea level (~sl; ~58 m depth in the drill core). EOH, end of recovered drill core (185.85 m).

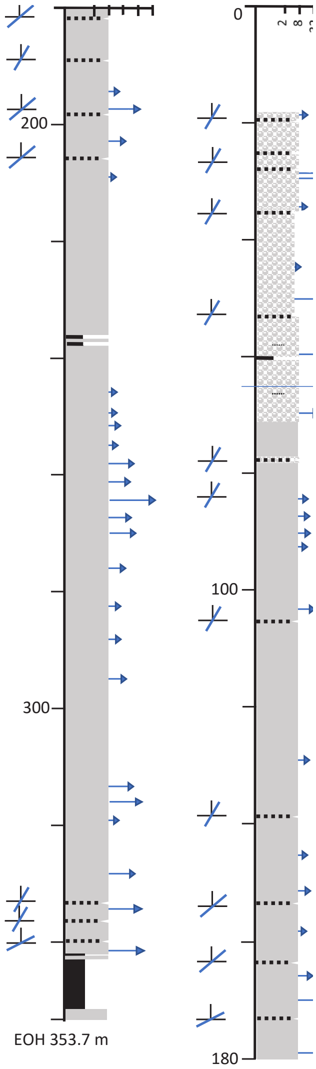

Figure 3. Simplified graphic log of the lithofacies in angled drill hole SE-03. This drill hole plunges 55° toward 264° but was not surveyed so the exact trajectory is not known. The legend for the patterns is given on Figure 2. The grain size scale across the top is in mm and depths are in m; blue arrows give the size of the maximum clast. Beds defined by grain size differences are shown by dashed lines. Approximate orientations of beds (LHS) are given by the blue lines with respect to the drill core axis (vertical). The fine blue line is approximate sea level (~sl; ~65 m down-hole depth in the drill core). EOH, end of recovered drill core (353.7 m).

m; Fig. 2) and in SE-03, at various levels above 70 m (Fig. 3). Armoured lapilli may be present in the deeper, altered parts of the drill cores but could not be confirmed using a hand lens.

Coherent basalt

Coherent basalt is a minor facies (<4% of the stratigraphic section), occurring in SE-02b from 15.7 to 17 m and in the lowest 15 cm, and in SE-03 from 60.2 to 61.0 m, between 236.3 and 238.7 m and from 342.4 to 352.0 m. The basalt is dark gray, vesicular, aphanitic, almost aphyric and magnetic; coarse tabular translucent feldspar crystals (3-4 mm) are present and subtle changes in vesicle abundance define subparallel mm-thick bands (Fig. 5a). In SE-03, a second, weakly vesicular, feldspar-phyric basalt type is present (~347.87 m; Fig. 5b). The contacts of the basalt intervals are sharp and planar, and in some cases, clearly intrusive (e.g. Fig. 5b).

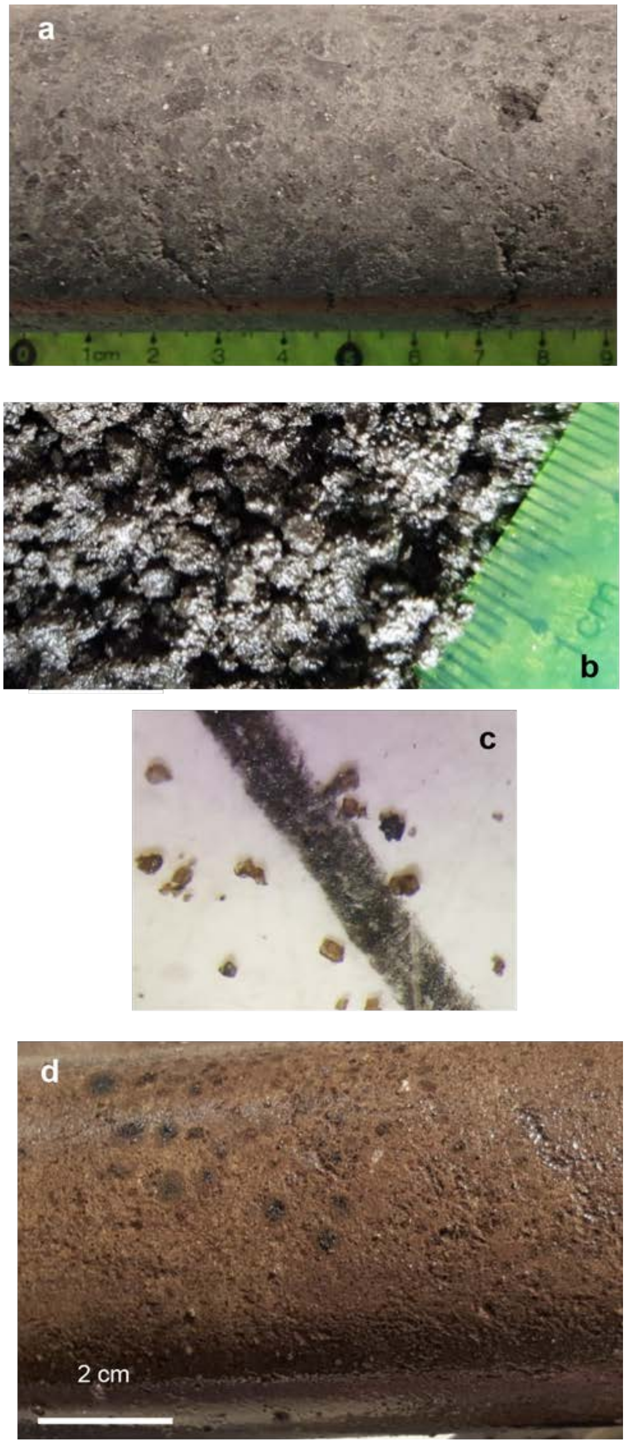

Figure 4. (a) Greenish black lapilli tuff, SE-03, 334.9 m. Scale in cm. (b) Weakly lithified lapilli tuff, SE-02b, 185.2 m. (c) Magnified view of ash particles disaggregated from weakly lithified lapilli tuff (pencil line is 0.5 mm wide), SE-02b, 185.2 m. (d) Armoured lapilli tuff, SE-02a, 9.74 m. Drill core top to the left in (a) and (d).

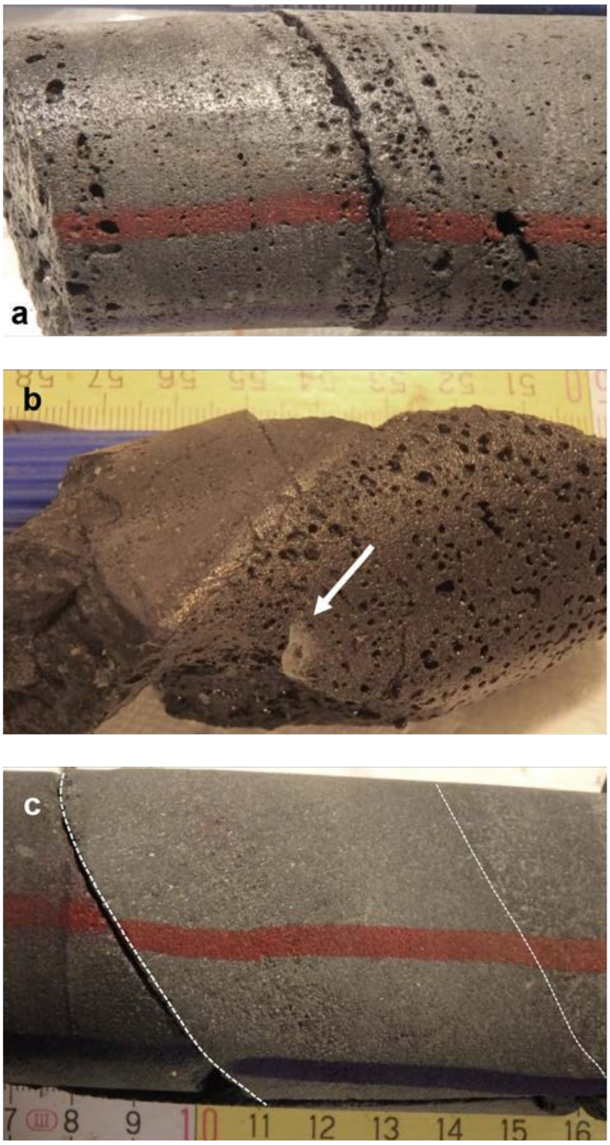

Figure 5. (a) Coherent basalt with bands of vesicles, SE-03, 350.5 m. Drill core diameter is 6 cm. (b) Feldspar-phyric basalt dyke (LHS) intruding aphyric vesicular basalt (RHS), SE-03, 347.87 m. Note the coarse feldspar crystal (arrow) in the aphyric vesicular basalt. Scale in cm. (c) Pale gray volcanic sandstone, SE-03, 349.60 to 349.65 m. White dotted lines delineate the top and base of the sandstone; the top contact at 349.60 m is a fracture. Scale in cm. Drill core top is to the left in (a), (b) and (c).

Volcanic sandstone

Volcanic sandstone is the least abundant facies (<0.1% of the section), found only in SE-03 near the base. Two layers are present (one at 339.86 m, 1 cm thick, and the other at 349.60, ~5 cm thick; Fig. 5c). Both consist of sub-mm relatively well sorted grains presumed to be volcanic. The upper layer (339.86 m) is interbedded with greenish black lapilli tuff. The lower layer (349.6 m) separates two intervals of coherent basalt.

CLAST TYPES IN LAPILLI TUFF

The lapilli tuff consists of ash (<2 mm) and several different types of coarser clasts. The ash, vesicular lapilli, armoured lapilli and composite clasts are considered to be juvenile whereas other clast types are non-juvenile and/or have more complex origins.

Ash (matrix)

In the lapilli tuff, ash is present in varying proportions and altered to different degrees. In the weakly lithified lapilli tuff in SE-02b, the ash grains are predominantly (75-90%) sideromelane (basaltic glass) fragments, based on their translucence and shiny appearance (Fig. 4c). Small (<0.1 mm) vesicles are present in coarse to very coarse ash grains (0.5-2 mm). Very fine to medium ash grains (0.063-0.5 mm) are inferred to vary in vesicularity, based on observations of the 1979 core samples. The finest components of the lapilli tuff could not be resolved with a hand lens and probably include mineral cements, especially in the more strongly altered lapilli tuff.

Vesicular lapilli

Black or dark gray, vesicular basaltic lapilli make up the main volume of the drill core (Fig. 6a). Hand lens and binocular examination of fresh vesicular lapilli indicate they are sideromelane, consistent with observations of vesicular lapilli in the 1979 drill core (Jakobsson & Moore 1986). Vesicles are typically round and small (<0.5 mm), and most obvious where partly filled by white mineral cement (Fig. 6b). Within single lapilli, there are different patterns of vesicularity: (1) homogeneous, composed of a single dominant vesicle size (~0.1 mm), with or without an additional population of smaller barely visible vesicles; and (2) banded or zoned, in which vesicles are arranged according to vesicle size, shape and abundance (Fig. 6b).

Armoured lapilli

Armoured lapilli are common in the upper one third of the drill cores. The armoured lapilli consist of a fragment of basaltic glass, commonly finely vesicular, surrounded by a rim of fine ash (Figs 4d, 6c). The ash rims are typically very thin, ~1-2 mm, though rare examples are up to ~4 mm. The visual effect of the ash rims is to prominently outline the interior clast, particularly if the central clast has vesicles filled with white mineral cements. We could not confidently identify armoured lapilli using a hand lens in the lower two-thirds of the drill cores; this part of the section is, overall, the most altered (Jackson, 2020).

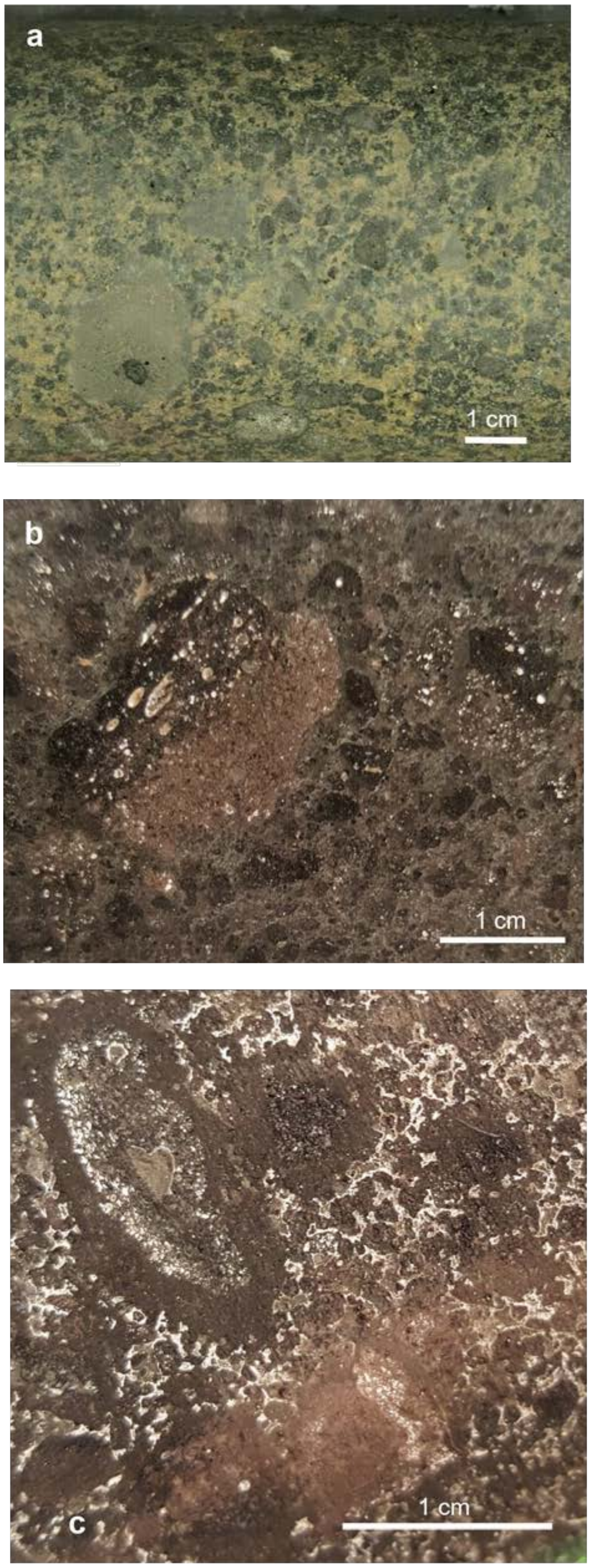

Figure 6. (a) Black, finely vesicular lapilli in weakly altered lapilli tuff, SE-03, 61.05 m. The vesicles are round, open and <0.5 mm across. (b) Vesicular lapillus in which vesicle sizes and shapes are zoned, defining bands, SE-02a, 131.5 m. (c) Armoured lapilli, SE-02a, 61.55 m. Lapilli cores consist of brown, very finely vesicular basalt and rims are dark gray ash.

Composite clasts (lapilli and rare bombs)

Lapilli and bombs that have a composite structure occur at all levels in the section but amount to only ~10 modal%. "Composite" means that the clast contains, or consists of, multiple smaller clasts (Fig. 7; Schipper & White 2016). Composite clasts typically have highly irregular shapes and consist of vesicular tachylitic (microlite-rich, basaltic) lapilli (0.5-2.5 mm) loosely held within a larger, less vesicular fragment. Vesicle sizes (0.1 mm to cms) and abundance (<10 to ~60 modal%) within composite clasts vary widely. Fluidal layers defined by variations in vesicularity are present inside the clasts and separate different clusters of internal grains. It is notable that in altered parts of the drill cores, the composite clasts appear to be less altered and typically retain original porosity; vesicles remain open and have less secondary mineral surface coatings than adjacent altered lapilli.

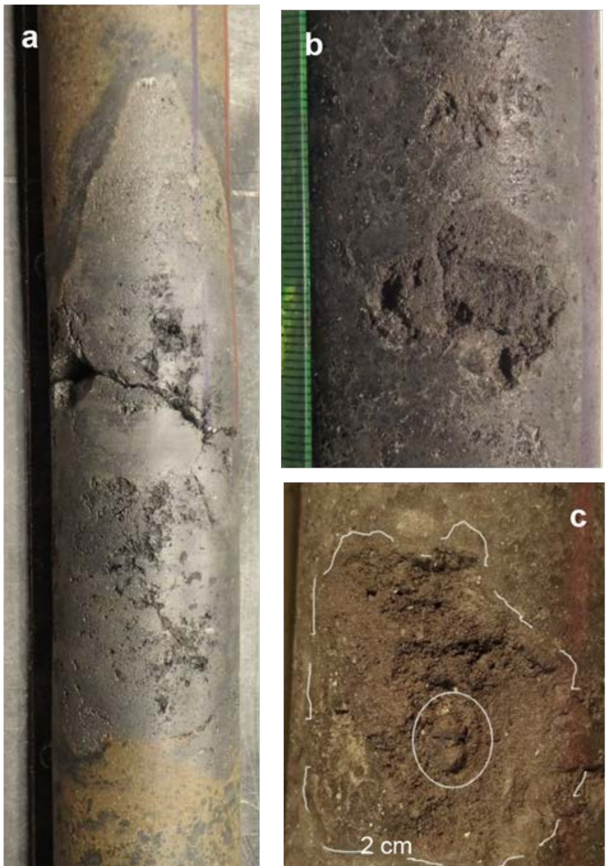

Figure 7. Composite lapilli. (a) Large composite clast (22 cm in maximum length), SE-03, 59.5 m. Drill core diameter is 6 cm. (b) Composite lapillus in greenish black lapilli tuff, SE-03, 336.42 m. Scale in mm. (c) Composite lapillus, SE-02b, 158.95 m. Dashed outline shows the margin of the lapillus; circle encloses two distinct internal lapilli contained within the larger lapillus. Drill core top is at the top of each photo.

Feldspar crystals (Labradorite)

Translucent or white, coarse (0.5-2 cm) feldspar crystals (Fig. 8a) are present in low abundance (~1 modal%) throughout the lapilli tuff. The feldspar crystals have been identified as labradorite and their crystal structure has been defined (Steinthorsson 1965; Wenk 1985). Many crystals are broken and comprise independent grains within the lapilli tuff, but some have narrow vesicular basalt selvages.

Lapilli tuff clasts

There are rare (<0.5 modal%) lapilli tuff fragments (Fig. 8b) in the lapilli tuff above a depth of about 60 m. The particles within these clasts appear to

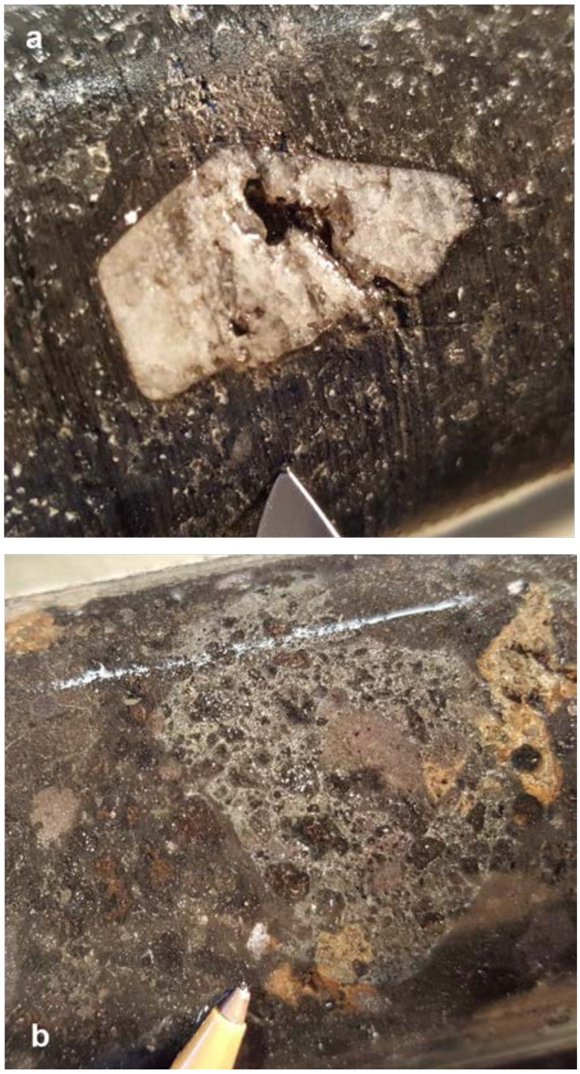

Figure 8. (a) Coarse feldspar (labradorite) crystal fragment in lapilli tuff, SE-02b, 102.84 m. Scale is the tip of a pocket-knife blade (~3 mm visible). (b) Clast of lapilli tuff, interpreted on the basis of the gray color and texture, to be intraformational, SE-02a, 43.43 m. The host rock is lapilli tuff. Scale is the tip of a ballpoint pen. Drill core top is to the left in (a) and (b).

be vesicular basalt, and hence are inferred to have been erupted and deposited during an earlier stage of the Surtur eruption. In one case (Fig. 8b), a white mineral cement is distinctly more abundant in the intraformational clast than in the host lapilli tuff, implying that some mineral cements were precipitated in the deeper parts of the succession before Surtur's explosive activity had ended.

Dense basalt clasts

Dark gray, aphanitic or fine-grained, non-vesicular or weakly vesicular, strongly magnetic basalt clasts (Fig. 9) are scattered through the lapilli tuff. Both rounded and angular shapes occur, and some examples contain abundant polymictic inclusions (Fig. 9b, c).

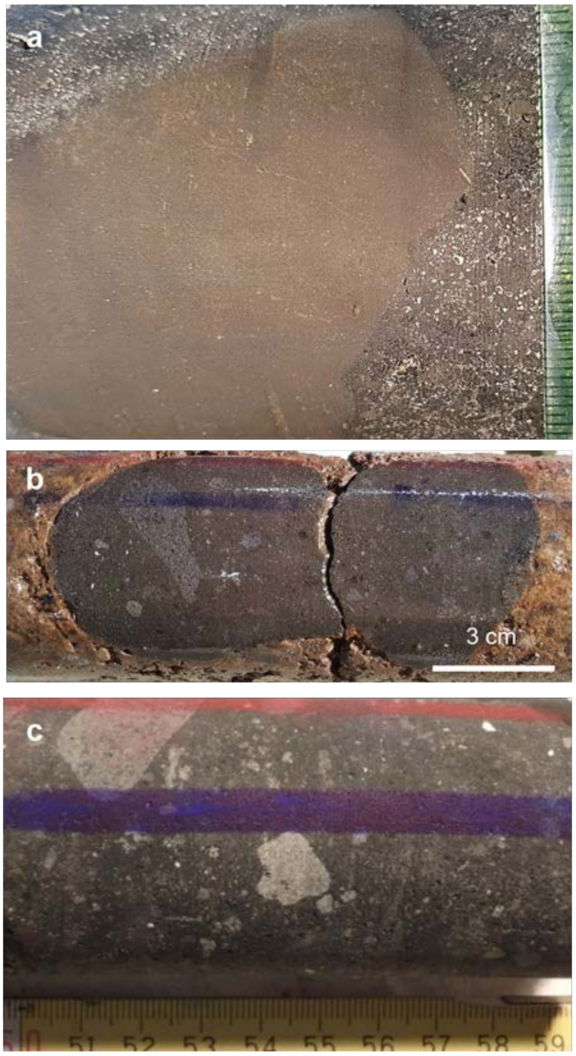

Figure 9. Dense basalt clasts in the lapilli tuff. (a) Uniformly fine-grained basalt clast, SE-02a, 80.52 m. Scale in mm. (b) Round basalt clast(s?) that contains abundant inclusions, SE-02a, 21.1 m. (c) Basalt clast (maximum dimension 11 cm) that contains abundant inclusions, SE-03, 342.35 m. Scale in cm. Drill core top is to the left in (a), (b) and (c).

Wispy fluidal clasts

Dark gray, wispy fluidal clasts occur in the lapilli tuff in SE-03 below ~250 m (down-hole depth). One of the best examples (Fig. 10a) has an amoeboid shape from which elongate narrow wisps only 1-3 mm wide extend several cm. Although it is clear that these clasts were soft when deformed into their present shapes, their nature and origin have not been resolved.

Crystalline clasts

There are rare, rounded, holocrystalline igneous clasts in the lapilli tuff (Fig. 10b).

Sedimentary clasts

Pale gray clasts of fine-grained sandstone (Fig. 10c) are present but are very rare (<0.5 modal%) in the drill cores.

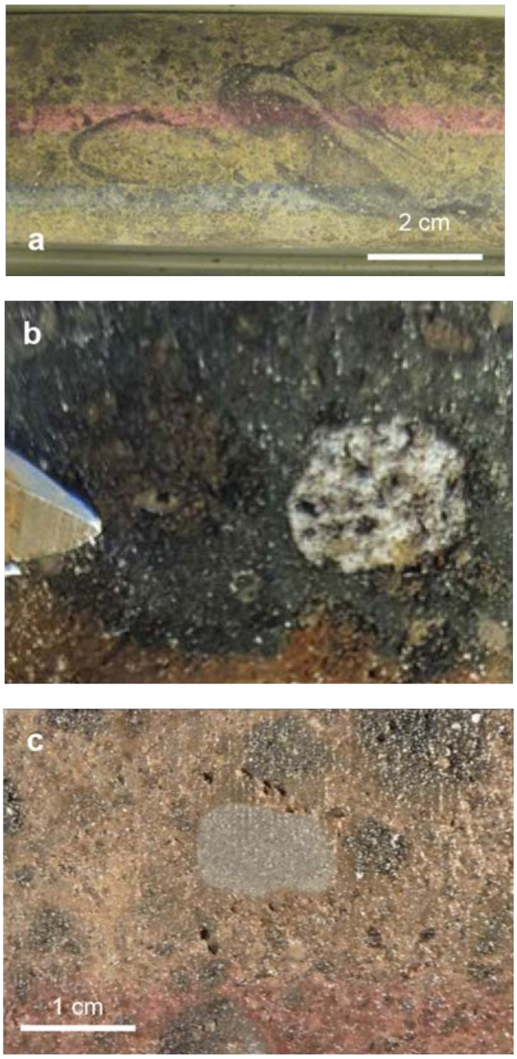

Figure 10. (a) Wispy fluidal clast in lapilli tuff, SE-03, 266.26 m. (b) Equigranular crystalline igneous clast in lapilli tuff, SE-02a, 41.4 m. Scale is the tip of pocket-knife blade (~2 mm visible). (c) Gray fine sandstone clast in lapilli tuff, SE-02a, 14.6 m. Drill core top is to the left in (a), (b) and (c).

BEDS AND OTHER LAYERS

Beds defined by grain size and color differences occur throughout the drill cores but are more distinct in the less altered upper part above ~70 m, vertical depth. They are hard to discern below ~150 m, vertical depth. Bed thickness ranges from ~1 cm to tens of cm. A small proportion (10%) of the beds are slightly better sorted, comprising framework-supported lapilli and minor ash; one example of a very thin, laminated ash bed was noted in SE-03 (334.3 m down hole).

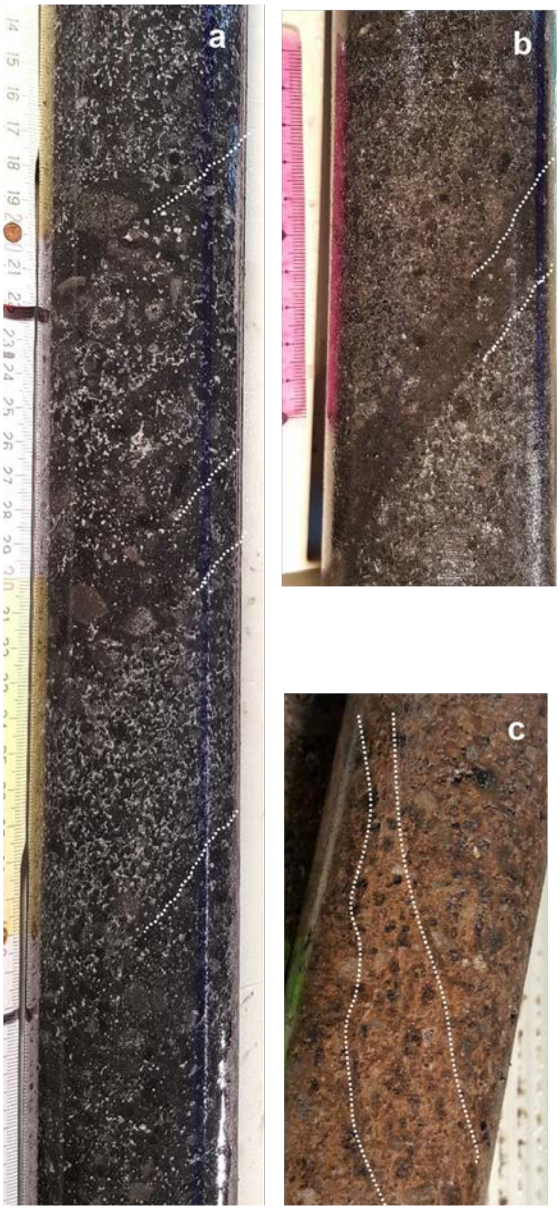

Figure 11. (a) Coarser versus finer beds in lapilli tuff, SE-02a, 82 m. Scale in cm. (b) Very thin, ash-rich bed in lapilli tuff, SE-02a, 111.7 m. Scale in cm. (c) Network of anastomosing, narrow cracks in lapilli tuff, SE-02a, 26.65 m. Drill core diameter is 6 cm. Dotted white lines in (a) and (b) highlight the beds. Dotted white lines in (c) mark the boundaries of the fracture network. Drill core top is at the top in (a), (b) and (c).

In the vertical drill holes (SE-02a, SE-02b), almost all the beds dip between ~20^o and 60^o (Fig. 11a); we noted one example of almost vertical beds (~146 m, SE-02b) and one example of horizontal beds (~148 m, SE-02b). At the scale of logging used, no clear pattern in bed dip was recognised vertically through the section. Moore & Jackson (2020) present data on bed orientations determined from unrolled digital core scans from the ICDP Digital Information System.

Very thin layers apparently defined by more abundant ash (Fig. 11b) are also present but may not be genuine beds; they may instead be either alteration artefacts or structural artefacts, such as the layers identified in Jakobsson & Moore (1982) and Moore (1985) as shear planes. A subvertical structure ~5 cm wide in SE-02a (from 20 to 30 m and at 36 m) comprises an anastomosing network of very narrow cracks (Fig. 11c).

DISCUSSION

Vertical variations in lithofacies

The main variations in grain size and components in vertical drill holes SE-02a and SE-02b (Fig. 2) are as follows:

(a) Maximum clast size (commonly >4 cm, some clasts 7 to 15 cm) is largest between ~160 m and ~50 m; above and below, the maximum clast size is <4 cm;

(b) Most vesicular basaltic lapilli from the base to ~20 m depth are 8 to 10 mm, coinciding with but overlapping the interval of the coarsest maximum clast sizes; in the shallowest ~20 m, most vesicular basaltic lapilli are <7 mm (typically 5 mm);

(c) Composite clasts appear to be more abundant in the interval that contains the coarsest maximum clast sizes, between ~160 m and ~50 m; they are also conspicuous at ~18 to 24 m;

(d) Armoured lapilli appear to be common above ~70 m and are either not present, not common or not preserved below that depth.

Both Jakobsson & Moore (1982) and Moore (1985) noted that at the 1979 drill hole site, there is a 10- to 20-m-thick section of tephra that was erupted from Surtungur (western vent) overlying the products of Surtur (eastern vent). Moore (1985, p. 657) stated that this unconformity had not been identified in the 1979 drill core. Our log of SE-02a (Fig. 2) shows that the average grain size of the vesicular basaltic lapilli in the top ~20 m is finer than in the rest of the section. The grain size change most likely corresponds to the unconformity between Surtur products below and Surtungur products above. Surtungur deposits are farther from their source vent and hence, overall finer grained than Surtur deposits.

Effects of alteration in 2017 drill cores

By alteration, we mean processes that result in changes in texture, composition, mineralogy and physical properties (density, porosity, permeability, competency). When first deposited, the subaerial tephra on Surtsey was unconsolidated, unaltered and yellowish brown or gray (e.g. Thorarinsson 1966, Figs. 18, 28 and 31). The color of the 2017 drill core varies among black, dark gray, dark greenish gray, brown, yellowish brown and pinkish brown, and all of it is altered and lithified to some extent.

In the vertical drill holes (SE-02a, SE-02b; Fig. 12), a weakly altered interval extends from the top to ~54 m depth. This interval is lithified and mostly brown or yellowish brown (Fig. 13a) although gray patches, bands and domains are locally conspicuous (Fig. 13b, c). The black vesicular basaltic lapilli appear glassy and vesicles are only partly filled; minor white mineral cement is present. There are many examples of armoured lapilli (Fig. 4d); the textural preservation is moderate to good.

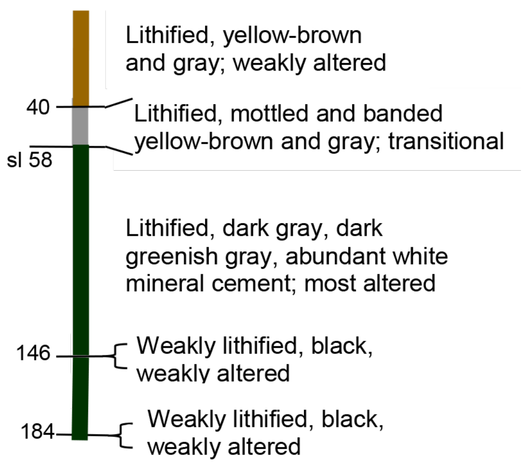

Figure 12. Schematic section showing the macroscopic vertical variations in alteration intensity in the SE-02a – SE-02b drill core. Note that the most altered lapilli tuff (~58 m to ~182 m) includes a weakly altered, weakly lithified interval (~146-148 m) and overlies weakly altered, weakly lithified lapilli tuff (~182-185 m). sl, sea level.

There is a gradation into progressively more-altered lapilli tuff with depth. From ~54 m to ~70 m, the vesicular basaltic lapilli are dull grayish black; a white mineral cement infills or lines intraparticle pores (Fig. 13d). Overall, the textural preservation is moderate and the alteration intensity is lower than in the underlying interval. From ~70 to ~182 m, the duller grayish black colour of the basaltic lapilli suggests the glass has been altered; white mineral cement is abundant and pores have been at least partially infilled (Fig. 13e). Textural preservation is moderate to poor and beds are difficult to discern. This interval is the most altered interval.

In the lowermost core retrieved from near the bottom of SE-02b (~182 to 185 m), there is an abrupt change to weakly altered, weakly lithified lapilli tuff (Fig. 4c) that consists of glassy black vesicular basaltic fragments and lacks abundant mineral cement. A similarly narrow, weakly altered, weakly lithified interval occurs at 146 to 148 m (SE-02b; Fig. 13f).

The entire section of lapilli tuff and armoured lapilli tuff in angled drill hole SE-03 (Fig. 3) is lithified and altered. Shallower than ~40 m (down-hole depth), the lapilli tuff is tan-brown or black and weakly altered; armoured lapilli are abundant and easy to identify. From ~40-65 m, weakly altered brown-black lapilli tuff and more altered dark gray lapilli tuff are both present. Below ~65 m (roughly equivalent to sea level), the lapilli tuff is dull and dark gray or dark greenish gray. Below ~100 m (equivalent to ~80 m below the surface), white mineral cement is conspicuous and armoured lapilli are either not present, not common or not preserved.

The contrast between the fresh, unconsolidated Surtsey tephra and the rock in the 2017 drill cores reflects the effects of alteration during the ~50 years since deposition. Jakobsson & Moore (1982, 1986) attributed the alteration to a hydrothermal system generated by heat from basaltic dykes emplaced mainly in December 1966. Jakobsson & Moore (1986) also concluded that there were no significant differences in the hydrothermal assemblages in the 1979 drill core above and below sea level but that the relative abundances of the minerals in the assemblages varied. Our qualitative review of the 2017 drill cores suggests that the intensity of alteration increases with depth below sea level, with the exception of the narrow weakly altered intervals in SE-02b at about 146 m and at the base. Fluid temperature also

Figure 13. (a) Weakly altered armoured lapilli tuff, SE-02a, 17.4 m. (b) Weakly altered lapilli tuff composed of irregular yellowish brown versus dark gray domains, SE-02a, 41.7 m. (c) Weakly altered lapilli tuff composed of yellowish brown versus dark gray bands, SE-02a, 36 m. (d) Mottled dark versus pale gray, altered lapilli tuff, SE-02a, 68.4 m. White mineral cement occurs in pores. Scale is the tip of a ballpoint pen. (e) Dark gray, altered lapilli tuff with abundant white mineral cement in pores, SE-02b, 129.8 m. (f) Black, weakly altered, weakly lithified lapilli tuff, SE-02b, 146.2 m. Note the well-defined boundary between coarser (above) and finer (below) beds. In all cases, drill core diameter is 6 cm and drill core top is to the left.

increases with depth below sea level to a maximum at 40-60 m below sea level and declines at deeper levels (Jakobsson *et al.* 2000; Jackson *et al.* 2019). It is likely that being saturated with warm sea water has promoted alteration of the sub-sea-floor section.

Comparison of the 2017 and 1979 vertical drill cores

There are macroscopic similarities and differences between the geology of the 2017 vertical drill cores (SE-02a, SE-02b) and the geology of the 1979 drill core as recorded by Jakobsson & Moore (1982). The three drill holes were collared at ~58 m above sea level; SE-02a and SE-02b collars are about 2 m apart and ~8 m from the 1979 drill hole collar.

The main similarities are:

(a) The range of dips of beds logged in the 2017 drill core is similar to that recorded by Jakobsson & Moore (1982).

(b) In both the 1979 and 2017 drill core, the lapilli tuff is more altered below sea level (~58 m depth) than above sea level.

(c) Neither the 1979 nor the 2017 vertical drill holes intersected the pre-eruption sea floor. Jakobsson & Moore (1982) estimated the pre-1963 sea floor to be ~130 m below sea level. The 1979 drill hole reached 180.1 m depth, ~8 m above the inferred pre-1963 sea floor. The deepest drill core recovered from SE-02b at 185.85 m was as little as ~2 m above the inferred pre-1963 sea floor position.

The main differences are:

(a) Coherent basalt is restricted to two thin intervals in SE-02b (15.7 to 17 m and the lowermost 15 cm). In contrast, it is the dominant lithology from 71.9 to 84.8 m in the 1979 drill core. Jakobsson & Moore (1982) interpreted these intervals of basalt to be dykes.

(b) In the 1979 drill core, unaltered unlithified tephra occupies more than 80% (~35 of 42 m) of the section below ~138 m to the bottom of the drill hole at ~181 m (unaltered and unlithified from 138.1 m to 143.8 m, 148.5 m to 149.7 m, 157.4 m to 168.6 m, 170.5 m to 180.6 m) (Fig. 14). The entire section of lapilli tuff in the 2017 drill core (SE-02b) is lithified and variably altered. Weakly altered, weakly lithified lapilli tuff is restricted to the lowest few metres (below ~182 m) and ~146 m to 148 m (~10% of the section from 138 m to the end of the drill core). The weakly altered, weakly lithified lapilli tuff at ~146 m in SE-02b was unaltered and unlithified in 1979. The reduction in the amount of unlithified tephra from 1979 to 2017 presumably reflects ongoing lithification through alteration of glass and crystallization of zeolite and Al-tobermorite mineral cements.

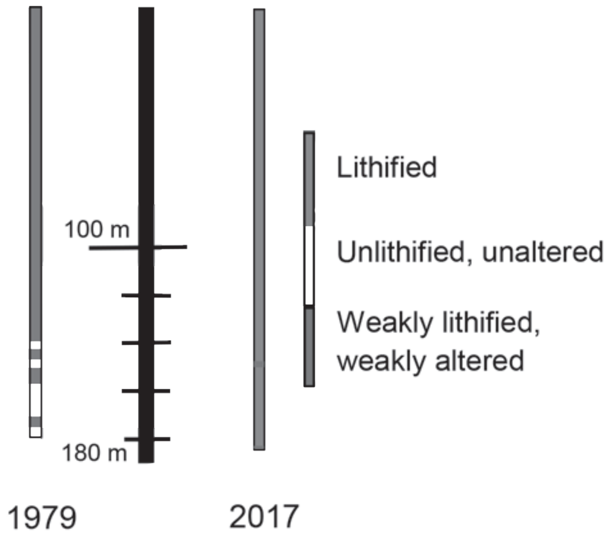

Figure 14. Simplified vertical distribution of lithified versus unlithified, unaltered facies in the 1979 drill core (LHS) compared with the 2017 drill core (RHS, SE-02a, SE-02b). About 20% of the 1979 drill core is unlithified and unaltered (all below ~138 m; Jakobsson & Moore 1982). All of the 2017 drill core is lithified and altered to some extent; <3% is weakly lithified and weakly altered.

(c) Jakobsson & Moore (1982) recorded about 50 "pre-solidification slump planes commonly associated with reworked sedimentary layers" in the section from ~45 m to ~165 m in the 1979 drill core. In the 2017 drill cores, layers defined by grain size changes are interpreted to be beds. A few instances of steep and/or apparently discordant beds were noted, and some of these beds might be equivalent to what were described in the 1979 core as reworked sedimentary layers associated with slumps. Other layers of uncertain origin are also present in the 2017 drill cores. Jakobsson & Moore (1982) recorded post-solidification shear planes (13 examples from 88 m to 157 m). Only two examples of structures interpreted to be shear-related were noted in the 2017 vertical drill core SE-2a, extending from 20 to 30 m and at 36 m (Fig. 11c), at a much shallower depth than those identified by Jakobsson & Moore (1982). Also, these two occurrences may be connected, representing a single subvertical anastomosing structure.

(d) We recognise composite clasts, at low abundances, throughout the cores. Composite clasts were not previously identified in published core descriptions but have been characterized from surface deposits (Schipper & White 2016).

The depth range of the armoured lapilli is contentious. Armoured lapilli (called "accretionary lapilli" by Jakobsson & Moore, 1982) are discernible above ~70 m and conspicuous above ~50 m in SE-02a. This distribution closely matches the depth range reported by Jakobsson & Moore (1982). However, according to Moore (1985, his Figure 6), armoured lapilli occur the full length of the 1979 drill core. Using a hand lens, we have noted possible armoured lapilli in SE-02a (119.7 m) and SE-02b (146.5 m, 155.8 m) but alteration has also produced "haloes" around lapilli, so confirmation that armoured lapilli are present requires examination of these samples in thin section.

The depth range of vesicular tuff is similarly contentious. Many examples of vesicular tuff (called "vesiculated tuff" by Jakobsson & Moore, 1982) were observed in the 1979 drill core above 34.2 m, and they have been recorded in the subaerial tephra on Surtsey (Lorenz 1974). However, Moore (1985, his Figure 6) indicated that vesicular tuff occurs the full length of the 1979 drill core. Interstitial void space is common in the lapilli tuff and armoured lapilli tuff in the 2017 vertical drill cores (e.g., Figs 6c, 13e). The most obvious examples are partly lined by white mineral cement. In some cases, the voids appear to be spaces between armoured lapilli. However, much of the section that includes well-preserved armoured lapilli lacks voids or else the voids are not obviously confined to spaces between armoured lapilli. Voids are also present in more strongly altered drill core in which armoured lapilli cannot be identified in hand sample with confidence.

Moore (1985) interpreted the depth distribution of the armoured lapilli and vesicular tuff to mean that the section below sea level was in fact originally emplaced subaerially and was later moved to below-sea-level positions by inward slumping of the crater walls. Indeed, Moore (1985, his Figure 9) considered the entire section of lapilli tuff in the 1979 drill hole to consist of down-dropped beds that were originally deposited subaerially.

SE-03 and Surtur crater- and conduit-fill

SE-03 was drilled to explore the crater- and conduit-fill of Surtur and perhaps help constrain the depth excavated into the pre-Surtsey sea floor by the 1963 to 1964 explosions. Because no borehole survey was conducted, the amount of deviation from the plan and the exact trajectory of SE-03 are not known. The section in SE-03 comprises texturally uniform, variably altered, lithified lapilli tuff for some 342 m of the total drilled length of ~354 m (97%). This continuous section of lithified lapilli tuff presumably originated as unconsolidated pyroclastic deposits that formed Surtur crater walls and that filled the crater and conduit. In such a proximal setting, it is likely that the section almost entirely comprises facies resedimented from unstable depositional sites and/or recycled through the vent perhaps multiple times. SE-03 appears to include much thicker massive intervals compared with SE-02a and SE-02b (Figs 2, 3), possibly because the complex intra-crater depositional processes favoured preservation of thick massive beds, and/or because more intense alteration in this more proximal setting has obliterated layers, and/or because the inclined drill hole obliquely crossed dipping beds at a low angle. Although not shown on the logs, the composite clasts in SE-03 appear to be smaller and less abundant than in SE-02a and SE-02b. These relatively fragile clasts would have been easily destroyed by re-cycling through the vent and repeated intra-crater slumping events.

The most significant lithofacies change in SE-03 is the appearance of thick coherent basalt just above the end of the drill hole (~342 to 352 m) and much thinner intervals at two shallower levels (~60 m and ~238 m; Fig. 3). At least two feeder dykes are evident in the thick coherent basalt interval. These dykes intruded the deepest part of the lapilli tuff section, consistent with the expectation that the end of this drill hole crossed Surtur's conduit.

The pre-Surtsey sea floor was ~130 m below sea level (Jakobsson & Moore 1982) and underlain by volcanogenic sedimentary rocks (Alexandersson 1970). Although the exact vertical depth of the end of SE-03 is not known, the planned depth of the end was ~100 m below the pre-eruption sea floor. However, no in situ sedimentary rocks were intersected in SE-03. There are three possible explanations: (1) the pre-Surtsey sea floor was locally deeper than 130 m below sea level; (2) the drill hole deviated to the extent that it ended in Surtur products above the former sea floor; or (3) Surtur's explosions deeply excavated the pre-Surtsey sea floor at the vent. Options (1) and (2) cannot be confirmed or eliminated but are both considered highly unlikely. The sea floor surrounding Surtsey is presently ~110 to 130 m deep over a radial distance of 2-3 km from the island coast, except for a narrow zone to the southeast where the sea floor reaches 139 m (Jakobsson *et al.* 2009). Regionally to the west, north and east of Surtsey, the sea floor is shallower than 130 m and it deepens only to ~150 m about 10 km to the south (Jackson *et al.* 2019). Some deviation of the SE-O3 drill hole is to be expected but the deviation would have to be extreme for option (2) to be correct. If option (3) is correct, then the Surtur crater was excavated ~100 m below the paleo-sea floor, as shown in the reconstruction in Jackson *et al.* (2019). It remains a puzzle that non-juvenile clasts in general, and clasts of sedimentary rock in particular, apparently amount to such a low percentage (<5 modal%) of the lapilli tuff in SE-03.

CONCLUSIONS

The SUSTAIN project drilled three holes into the products of Surtsey's 1963 to1967 eruptions. Variably altered lapilli tuff composed of vesicular basaltic lapilli and ash is the most abundant lithofacies in the 2017 drill holes. Armoured lapilli are common in the sections above ~ 70 m depth. All of the lapilli tuff except the top ~20 m was erupted from Surtur during its 1963 to 1964 activity; the top ~20 m was erupted from Surtungur in 1964. Coherent basalt occurs in two narrow intervals in SE-02b, and in two narrow (<1.5 m) and one thick (~10 m) intervals in the angled drill hole, SE-03. The angled drill hole also includes very minor volcanic sandstone.

The originally unconsolidated pyroclastic deposits produced by Surtur and Surtungur were entirely lithified and variably altered when drilled in 2017. In comparison, when drilled in 1979 (Jakobsson & Moore, 1982), ~20% of the section was unlithified and unaltered. The difference reflects ongoing lithification in response to alteration of glassy components and crystallisation of mineral cements.

Although the exact depth of the end of the angled drill hole, SE-03, is not known, this drill hole ended in altered lapilli tuff intruded by basalt dykes probably several tens of m below the pre-eruption sea floor. None of the sedimentary rocks expected to underlie the sea floor, nor modern sediment, were intersected. Eruptive activity at Surtur must therefore have excavated to a depth of several tens of m below the pre-eruption sea floor.

ACKNOWLEDGMENTS

Funding for this project was provided by the International Continental Scientific Drilling Program (ICDP) through a grant to the SUSTAIN project; a grant of excellence from the Icelandic Research Fund, ICF-RANNÍS; the Bergen Research Foundation and K.G. Jebsen Centre for Deep Sea Research at the University of Bergen, Norway; the German Research Foundation (DFG); and DiSTAR, Federico II, University of Naples, Federico II, Italy. The University of Utah, USA, the University of Tasmania, Australia, and Icelandic power companies, Reykjavík Energy and Landsvirkjun, contributed additional funds. The logistical support provided by the Icelandic Coast Guard was instrumental in carrying out the drilling operation. We gratefully acknowledge the DOSECC drilling team led by Beau Marshall with drillers Steve Cole, Justin Blouin, A. J. Vecchiarelli, Matthew Lyon, and Michael Vinson, and all members of the science and technical teams of the SUSTAIN project.

REFERENCES

Alexandersson, T., 1970. The sedimentary xenoliths from Surtsey: Marine sediments lithified on the sea-floor. A Preliminary Report. Surtsey Research Progress Report V, 83-89.

Jackson, M.D., M.T. Gudmundsson, T.B. Weisenberger, J.M. Rhodes, A. Stefánsson, B. I. Kleine, P. C. Lippert, J. M. Marquardt, H. I. Reynolds, J. Kück, V. Th. Marteinsson, P. Vannier, W. Bach, A. Barich, P. Bergsten, J. G. Bryce, P. Cappelletti, S. Couper, M. F. Fahnestock, C. F. Gorny, C. Grimaldi, M. Groh, Á. Gudmundsson, Á. Th. Gunnlaugsson, C. Hamlin, Th. Högnadóttir, K. Jónasson, S. S. Jónsson, S. L. Jørgensen, A. M. Klonowski, B. Marshall, E. Massey, J. McPhie, J. G. Moore, E. S. Ólafsson, S. L. Onstad, V. Perez, S. Prause, S. P. Snorrason, A. Türke, J. D. L. White & B. Zimanowski, 2019. SUSTAIN drilling at Surtsey volcano, Iceland, tracks hydrothermal and microbiological interactions in basalt 50 years after eruption. Scientific Drilling, 25, 35-46.

Jakobsson, S.P. & J.G. Moore, 1982. The Surtsey research drilling project of 1979. Surtsey Research Progress Report IX, 76-93.

Jakobsson, S. P. & J.G. Moore, 1986. Hydrothermal minerals and alteration rates at Surtsey volcano, Iceland. Geol. Soc. Am. Bull. 97, 648–659.

Jakobsson, S.P., G. Guðmundsson & J.G. Moore, 2000. Geological monitoring of Surtsey, Iceland, 1967-1998. Surtsey Research XI, 99-108.

Jakobsson, S. P., K. Thors, Á.T. Vésteinsson, & L. Ásbjörnsdóttir, 2009. Some aspects of the seafloor morphology at Surtsey volcano: The new multibeam bathymetric survey of 2007. Surtsey Research XII, 9–20.

Lorenz, V., 1974. Vesiculated tuffs and associated features. Sedimentology 21, 273-291.

Moore, J. G., 1985. Structure and eruptive mechanisms at Surtsey Volcano, Iceland, Geol. Magazine 122, 649–661.

Schipper, C.I. & J.D.L. White, 2016. Magma-slurry interaction in Surtseyan eruptions. Geology 44, 195-198.

Steinþórsson, S., 1965. Surtsey: Petrology and chemistry. Surtsey Research Progress Report I, 41-49.

Thorarinsson, S., 1966. Surtsey. The new island in the Atlantic. Almenna Bókafélagið, Reykjavík. 47 pp, 53 photos.

Thórarinsson, S., Th. Einarsson, G. Sigvaldason & G. Elísson, 1964. The submarine eruption off the Vestmann Islands 1963–64. Bull.Volcanol. 29, 435–455.

Weisenberger, T. B., M.T. Gudmundsson, M.D. Jackson, C. Gorny, A. Türke, B. I. Kleine, B. Marshall, S. L. Jørgensen, V. Th. Marteinsson, A. Stefánsson, J. D. L. White, A. Barich, P. Bergsten, J. G. Bryce, S. Couper, M. F. Fahnestock, H. Franzson, C. Grimaldi, M. Groh, Á. Gudmundsson, Á. Th. Gunnlaugsson, C. Hamelin, Th. Högnadóttir, K. Jónasson, S. S. Jónsson, A. Klonowski, J. Kück, R. L. Magnússon, E. Massey, J. McPhie, E. S. Ólafsson, S. L. Onstad, S. Prause, V. Perez, Velveth, J. M. Rhodes, S. P. Snorrason, 2019. Operational Report for the 2017 Surtsey Underwater volcanic System for Thermophiles, Alteration processes and INnovative Concretes (SUSTAIN) drilling project at Surtsey Volcano, Iceland. GeoForschungs Zentrum (GFZ) German Research Centre for Geosciences, 98pp.

Wenk, H.-R., W. Joswig, T. Tagai, M. Korekawa & B.K. Smith, 1980. The average structure of An 62-66 labradorite. American Mineralogist, 65, 81–95.

Observations on the structure of Surtsey

JAMES G. MOORE[1] AND MARIE D. JACKSON[2]

[1] U.S. Geological Survey, Menlo Park, California, U.S.A.
[2] Department of Geology and Geophysics, University of Utah, Salt Lake City, Utah, U.S.A.

ABSTRACT
Comparison of investigations of the 1979 and 2017 cored boreholes coupled with continued observations of the dynamic surface of Surtsey has modified our concepts of the subsurface structure of the volcano. A geometrical analysis of the 2017 vertical and inclined cores indicates that near-surface layering dips westerly, indicating that the boreholes are located inside the Surtur crater. In subaerial deposits, as well as in deep deposits below sea level and below the pre-Surtsey seafloor, there are zones of porous tuff that contain abundant pyroclasts with narrow rims of fine ash. These features, typical of near-surface deposits, could have been carried down the vent by downslumping during fluctuating explosive activity. They support the hypothesis that a broad diatreme underlies the Surtur vent. No major intrusions were encountered in the 2017 drilling except for coherent basalt in deep sub-seafloor deposits below the center of Surtur crater. The 2017 borehole temperature measurements indicate that the peak temperature in the vertical boreholes was 124 °C at 105 meters below the surface (m.b.s.) and that in the inclined hole it was 127 °C at 115 m.b.s. immediately after drilling. These peak temperatures are 72 meters apart horizontally yet closely resemble each other in shape and magnitude, suggesting a broad heat source. In addition, measurements in the inclined hole from 200 to 290 m.b.s. indicate a temperature of 60±2 °C. This is apparently residual heat from the volcanic action that created the diatreme. These facts cast doubt on the previous concept that the heat anomaly in the 1979 borehole was due to a nearby intrusion. Instead they suggest that heat would have been conducted down from the 85-meter-thick hot lava shield within the Surtur crater into a warm diatreme substrate containing original volcanic heat. As the conducted heat moved down into the water-saturated substrate it would have elevated the temperature above the boiling point curve, baked out water, and created a vapor-dominated system below sea level. Eventually loss of heat by boiling and rise of steam caused the vapor-dominated system to retreat upward. The resulting steam rose and warmed the tephra adjacent to the lava shields where it produced broad areas of palagonitized tuff.

INTRODUCTION
A new era in Surtsey investigations began in 1979 when a 181 m deep borehole was drilled on the eastern flank of the Surtur vent (Fig. 1). The cored borehole was a cooperative venture between the Icelandic Natural History Museum, the Surtsey Research Society, and the Geothermal Program of the U.S. Geological Survey (Jakobsson & Moore 1982a). The Icelandic National Energy Authority conducted the drilling. This work led to a better understanding of the sub-surface structure and

This study is dedicated to Sveinn Jakobsson, the man who with his spirit and his boots has taken the pulse of Surtsey for five decades.

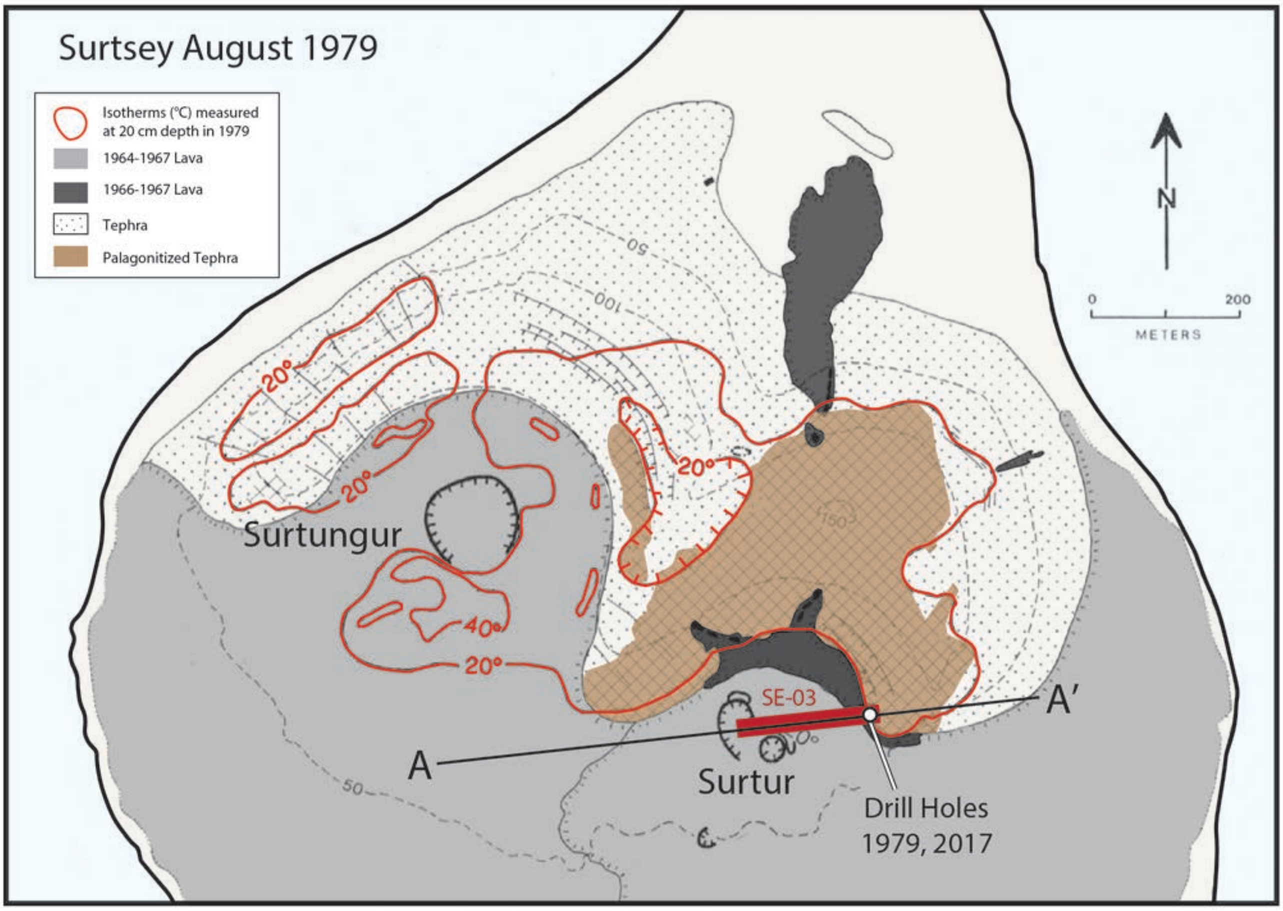

Figure1. Map of central Surtsey in 1979 showing lava of 1964–1967, in shades of gray. Tephra is dotted and the extent of palagonitized tephra in 1979 is shown in brown. Temperature of the 1979 hydrothermal area measured at depths of 20 cm is shown by red isotherms. Profile of Figure 10 is shown by the black line, with the red segment depicting the surface projection of the 2017 inclined borehole SE-03. Vertical boreholes SE-01, SE-02A and SE-02B occur at the east end of the red segment. After Jakobsson & Moore (1982b) and Jackson *et al.* (2019a).

thermal history of the volcano and characterized the time-dependent growth of secondary hydrothermal minerals (Jakobsson & Moore 1986). One result was the proposition that the Surtur and adjacent Surtungur vents are each underlain by a funnel-shaped diatreme (Moore 1985).

In 2017, 38 years after the completion of this first borehole (SE-01), three new cored boreholes were drilled (SE-02A, SE-02B, and SE-03) by the Surtsey Underwater volcanic System for Thermophiles, Alteration processes and INnovative Concretes (SUSTAIN) drilling project, sponsored by the International Continental Scientific Drilling Program (Jackson *et al.* 2019a, Weisenberger *et al.* 2019). Two new vertical boreholes (SE-02A, SE-02B) were placed within seven meters of the 1979 SE-01 borehole and a third new borehole (SE-03) was drilled such that it plunged 55° W toward the Surtur crater and through the tuff deposits at the center of the postulated Surtur diatreme (Fig. 1). The holes were spudded in 170 meters east of the Surtur crater at an elevation of 58 meters. This work outlines some of the findings obtained from a comparative study of the two drilling projects.

Sequence of events at the Surtur vent

First observations of the Surtur vent occurred when explosions emerged above the sea surface and rapidly began building a tuff cone on November 14, 1963 (Thórarinsson 1965, 1967). The explosive activity continued until January 31, 1964, during which time continuous uprush explosions alternated with sea wave erosion of the crater rim allowing water to have access to the vent. A hypothesized diatreme is believed to have fed this 78-day explosive phase in late 1963 and early 1964 (Moore 1985). The eruption began when rising magma approached the ocean floor and heated interstitial water. When the boiling point was attained the generation of steam produced explosions that cleared the vent of rubble, tephra and water and built the edifice toward the sea surface. When the vent was open to the atmosphere continuous uprush explosions carried tephra to great heights and then deposited it within and around the crater. As the rim surrounding the vent was eroded by the sea, water poured down into the open vent, and landslides followed, cooling and quenching the explosions. This explosive cycle was repeated when debris in the diatreme was heated by new magma rising from below. The oscillation of material that was ejected from the vent and then returned to it by downfall, slumping, and landsliding can account for the deep occurrence of the vesicles in tuff deposits and lapilli with ash coatings observed in the 1979 core (Moore 1985). A variety of fine ash coatings on glass fragments occurs in submarine and sub-seafloor tuff deposits in the 2017 drill cores; these likely record diverse depositional processes (Jackson 2020).

Explosions ceased at Surtur on January 31, 1964 and then began at the new Surtungur vent 450 meters west-northwest (Fig. 1). These explosions occurred for 64 days covering the island and vicinity with air fall tephra. Eventually Surtungur grew well above the sea and sea incursion was suspended. Explosions ceased and effusive activity began April 4, 1964. Lava flows poured from Surtungur for more than two years. The flows built a lava shield, enlarged the island to the south and flowed east around the south side of Surtur until May 17, 1966. During this Surtungur effusive phase, the crater of Surtur remained largely empty. The crater of the Surtur vent is depicted on a map made from aerial photographs taken October 23, 1964 (Iceland Survey Department 1965) six months after the Surtungur lava flows had begun. It shows lava banked up against the south side of the Surtur crater with the crater floor now less than 20 m above sea level.

Effusive activity began at Surtur on August 19, 1966 and was active for nine months. A lava lake grew in the crater and lava fountains fed overflowing lava flows that built a lava shield above the original crater to 80 meters above sea level (Norrman 1970, Moore 1982). These flows overflowed to the south and east covering almost half of the area covered by the Surtungur lava flows and further enlarging the island. The eruption stopped on June 5, 1967.

In April 1968 elevated temperatures were first noticed in areas north of the Surtur lava shield that had been cool in July 1967 (Jakobsson 1978). By 1979 the surface temperature measurements of tephra at 20 cm depths exceeded 20 °C in sizable areas north of both lava shields (Fig. 1) (Jakobsson & Moore 1982b). Areas within these warm zones became lithified as the glassy tephra underwent palagonitization to form resistant tuff (Fig. 1).

Sizes of volcanic clasts

Surtsey tephra is poorly sorted with the largest clasts up to about one meter in size and the smallest comprising fine ash. The overall average grain size is about 0.5 mm with 60–70 % in the coarse ash (0.06–2 mm) fraction, and less than 0.5 % in the block and bomb (>64 mm) fraction (Sheridan 1972, Jakobsson *et al.* 2000).

Much of the tephra is made up of angular to sub-rounded lapilli of vesicular basalt, which is commonly grayish orange (10YR 7/4 Munsell color) sideromelane, and less abundant, dark gray opaque tachylite (N3) in hand sample. Olivine and plagioclase phenocrysts occur throughout. Glass lapilli commonly have rims of accretionary ash in the subaerial tuff cone and the borders of the fragments are variously altered and palagonitized (Lorenz 1974, Moore 1985). Narrow rims of fine ash also occur on altered glass pyroclasts in the submarine and sub-seafloor tuff deposits (Jackson 2020). Fragments of bombs are present as rounded or ribbon-like lava masses (McPhie *et al.* 2020). Xenocrysts of pre-Surtsey volcanic rock, sediment, and ice-rafted exotic rocks are present in the subaerial tephra and in the drill cores.

The 2017 drill core was photographed around its circumference in unrolled digital scans. The maximum size of clasts displayed in these scans was measured in each segment in the core trays, a sample size about one-meter long (Fig. 2). Clast sizes less than one centimeter were not recorded. This maximum clast size, as recorded in the core scans, is only one gauge of clast size because the HQ (6.35 cm diameter) and NQ (4.3 cm diameter) cores cannot encompass clasts of greater dimension. However, the measurements are useful for comparative purposes. Only a few unrolled digital scans were created for the 75–200 m.b.s. interval of the inclined SE-03 core.

In the SE-02A, SE-02B, and SE-03 cores most of the largest clasts fall in the range of 1–4 cm with perhaps 10 % being larger (Fig. 2). Interestingly, this size range remains quite constant down to the bottom

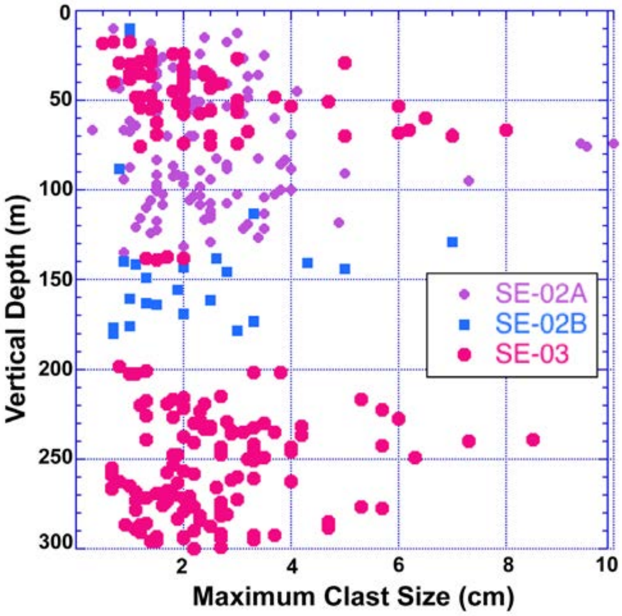

Figure 2. Maximum size of clasts in each approximately one-meter-long section of the three 2017 drill cores as measured in unrolled digital scans.

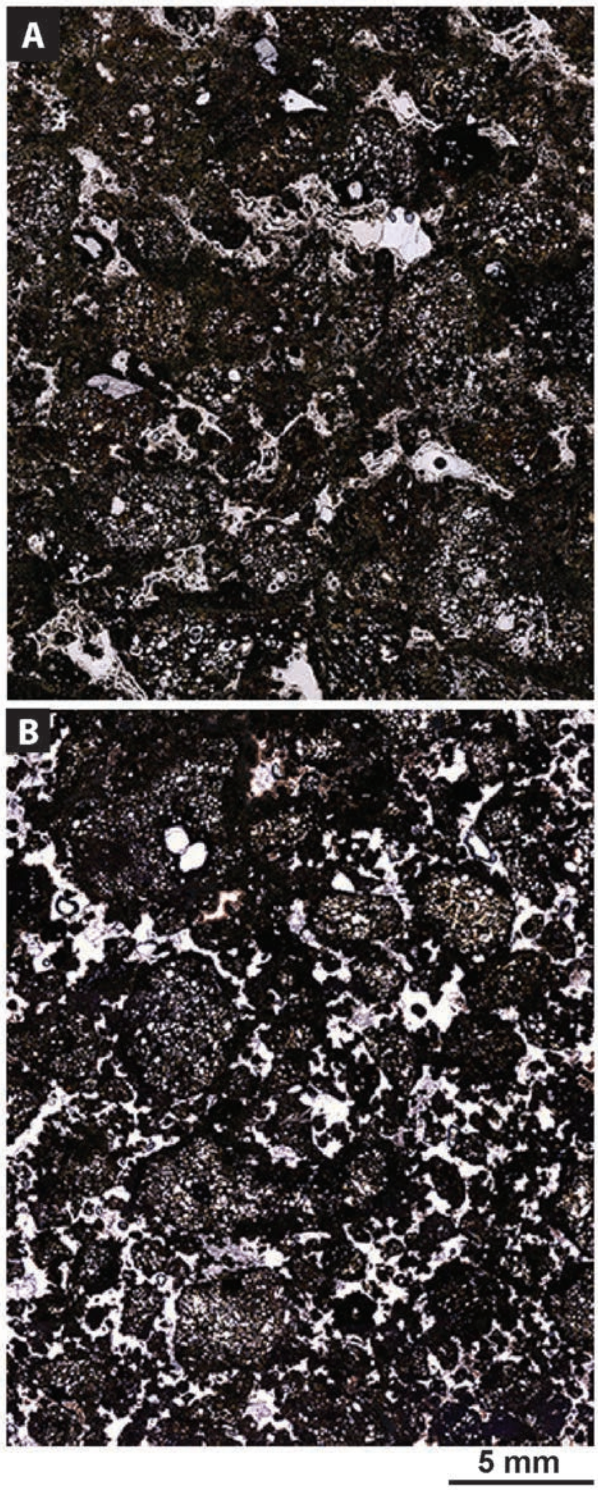

Figure 3. Scans of thin sections showing vesicles (white) in porous submarine and sub-seafloor basaltic lapilli tuff, plane polarized light. A) Borehole SE-02B, 77.9 m.b.s., Reference Sample 6; 12 volume % vesicles. B) Borehole SE-03, 259 m measured depth, Reference Sample 24; 12 volume % vesicles.

of the inclined borehole, SE-03, at a depth of 290 m.b.s. and horizontally 205 m west of the vertical holes. Such uniformity in the clast size distribution could imply extensive mixing from crater edge to center as might occur during the repetitive explosions in a diatreme.

Vesicles in the tuff

Vesicles that occur as open spaces in the ash matrix of the lapilli tuff are widespread in the Surtsey deposits. They are commonly 0.3–0.6 mm in diameter when spherical but exceed one cm when irregular in shape (Moore 1985). These vesicles are distinct from the much smaller vesicles (< 0.1 mm), which are contained within glassy lapilli. The vesicles in tuff often show an amoeboid shape with small lobate peripheral protrusions that penetrate between lapilli. They may surround glass fragments with narrow rims of fine-ash (Jackson 2020). At deeper levels the vesicles are generally less abundant and take on a more jagged outline (Fig. 3).

The vesicles are well shown as open spaces in thin sections (Fig. 3) but cannot be readily identified in photographs and scans of the cores. Those measured through point counts of thin sections from the 1979 SE-01 core (see Moore, 1985, *his* figures 6 B, C, and D) commonly attain 25 volume % of the lapilli tuff near the surface but are less abundant in the deeper samples (Fig. 4). A similar pattern of decreasing vesicular space with depth occurs in the 2017 SE-02B core. Here, point counts of 32 reference sample thin

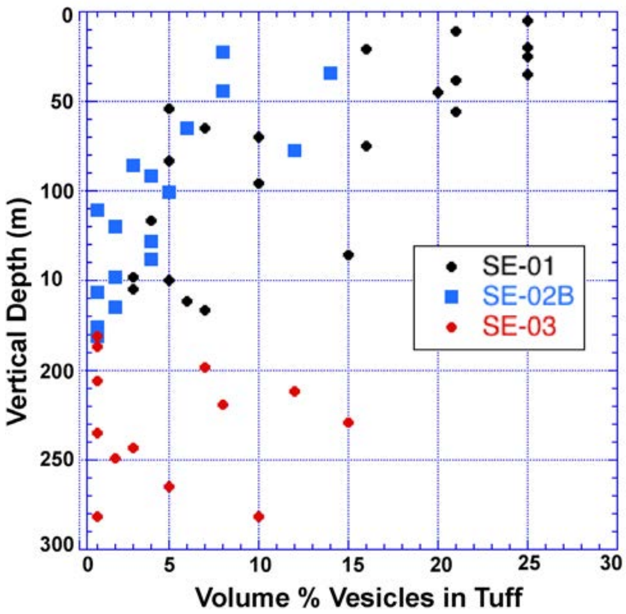

Figure 4. Volume % vesicles in lapilli tuff as measured in thin sections of samples from boreholes SE-01, SE-02B, and SE-03.

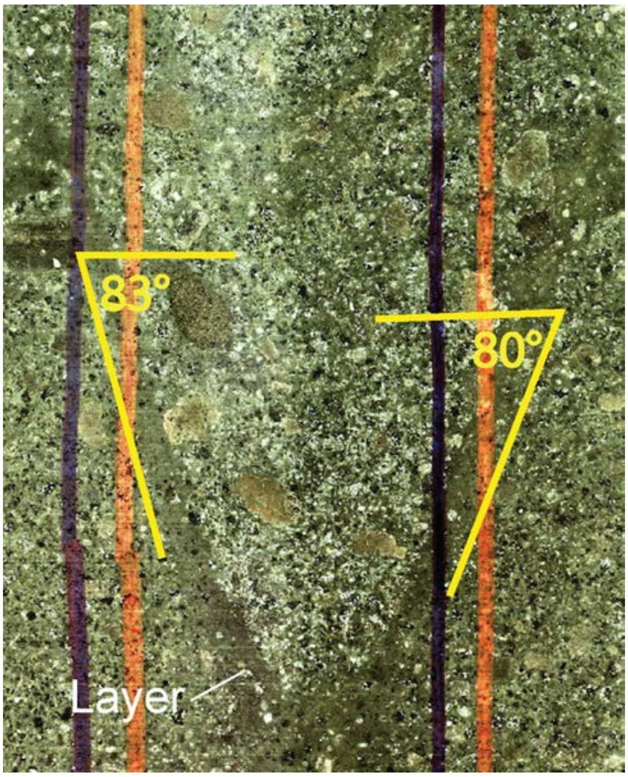

Figure 5. Unrolled digital scan (20 cm across) of the 2017 borehole SE-2A core at 38.3 m.b.s. A planar dipping dark ash layer is expressed as a sine curve. The dip is the angle between each of the steep parts of the curve and a plane normal to the core axis. The average dip is 71°.

sections were achieved through placing a transparent grid of 100 points on an enlarged high-resolution scan of the thin section. However, in the lower part of the SE-03 inclined core below 200 m, 13 samples of lapilli tuff show a somewhat higher average volume of vesicles. Seven samples contain 3 or fewer volume percent vesicles and the remaining 6 contain 5–15 volume % vesicles (Fig. 4). The more porous deposits have lower bulk density and higher water absorption than more compact deposits (Jackson 2020).

Tuff vesicles described at phreatomagmatic centers (Lorenz 1974a, 1974b) commonly form near the surface where air is trapped in water-saturated fine ash, or mud. It is unlikely that the vesicles could persist in lapilli or ash that has fallen on the sea surface and then descended to the sea floor. Hence the presence of the vesicles down to the lower sections of the cored boreholes could suggest that tephra which entrapped air or other gases near the surface was carried down by slumping and landslides into the sub-seafloor deposits (Moore 1985).

Dip of layering

Measurement of the dip of layering on the digital scans of the 2017 cores utilizes the expression of each planar layer boundary as a sine curve on the unrolled image (Fig. 5). As the bed dip steepens the amplitude of the sine curve increases. The dip is defined as the angle between the normal to the axis of the core and the steepest part of the curve (Fig. 5). The dip is measured on both sides of the sine curve crest, and the average is recorded.

In the SE-01 core the dip of planar surfaces, as bedding, slump and shear planes, in the upper 50 m of the borehole is generally 10°–45°, averaging 30° (Moore, 1985). From 50–100 m.b.s. the dip increases generally to 40°–60° and below this the dips broaden in value generally from 15°–80°. The dip of layering in the upper part of borehole SE-2A shallower than 100 m.b.s. is generally 20°–50°, averaging 30°. Below this depth the dip broadens, generally between 10° and 70° (Fig. 6).

The apparent dip of planar surfaces in inclined borehole SE-03 is largely measurable only above 75 m.b.s. and from 230–290 m.b.s. Only a few digital unrolled scans of the core were made at intermediary depths, for example, at about 140 m. Above 50 m.b.s., the apparent dips are rather tightly clustered between 60°–80°, averaging 70° (Fig. 6). In the lower interval the apparent dips are largely between 40°–80°.

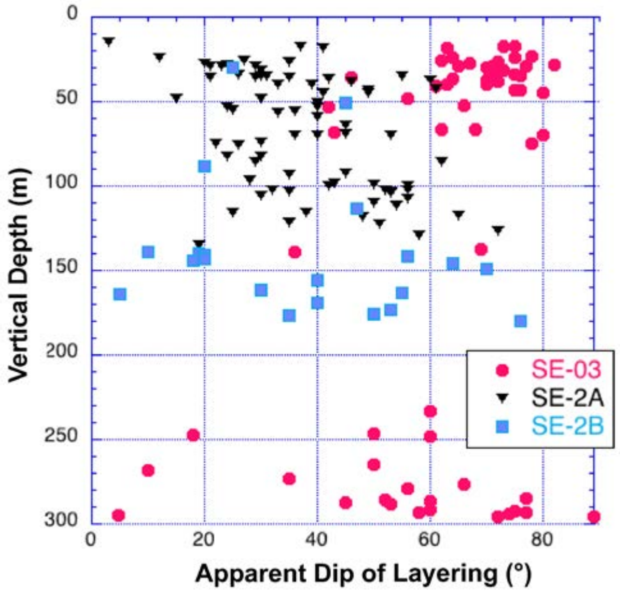

Figure 6. Dip of layering in boreholes SE-02A, SE-02B, and SE-03 as measured from unrolled digital scans.

Since the azimuth of the core was not fixed during drilling, the direction of the dip of planar surfaces is not defined in any of the 1979 or 2017 cores. However, there is a relation of the measured apparent dip in the inclined SE-03 core with the equivalent true dip if it is assumed that the layering dips either west or east, along the azimuth of the inclined borehole (azimuth 264°, plunge 55° W) (Fig. 7). This assumption is reasonable because the axis of the borehole is radial to the volcanic vent (Fig. 1) and it is considered likely that the layering will be dipping toward the vent (inner crater wall) or away from the vent (outer crater slope).

The relation of the apparent dip to the true dip relative to the horizontal in the inclined SE-03 core is such that steep apparent dips are more common in westerly true dips, and gentle apparent dips are more common in easterly true dips (Fig. 7). If the layering is at right angles to the inclined core (that is, 0° apparent dip) then the true dip will be 35° E. If the layering has an apparent dip of 10° then the true dip may dip either 25° E or 45° E relative to the horizontal. If the layering has an apparent dip of 90° (that is, parallel to the axis of the inclined core) then the true dip is 55° W. Hence, true dip can be assessed by comparison of measurements of apparent dip in the inclined SE-03 core and true dip in the vertical cores provided the boreholes are close together.

The dip of layering in the upper part of vertical borehole SE-02A above 50 m.b.s. is generally 20°–50°, averaging 35° (Fig. 6). In contrast, the apparent dip in the upper part of inclined borehole SE-03 is 60°–80°, averaging 70° (Fig. 6). The 70° apparent dip is equivalent to a true dip of either 35° W or 85° W relative to the horizontal (Fig. 7). The correspondence of the 35° W true dips in the SE-03 core with the 35° dips in the three vertical holes establishes that the layering above 50 m.b.s. in the cores dips west at an inclination averaging about 35°. Therefore, the boreholes are all located in the inner wall of the Surtur crater and not on the outer volcano slope. The dip of layers deeper in the boreholes cannot be quantified because the horizontal distance between vertical boreholes and the inclined borehole increases to about 200 m. It is evident, however, that the dispersion of dips increases with depth. The structures deeper in the subsurface apparently become more complex.

On the western side of Surtsey the sea has eroded several hundred meters into the Surtungur vent complex (Fig. 8). This has produced a cliff 140 m high that exposes a rhythmically-bedded section of tuff that dips east (Jakobsson *et al.* 2013). The dip of layering becomes steeper downward attaining approximately 45° near the bottom of the cliff at sea level. It therefore resembles the inner-dipping, downward-

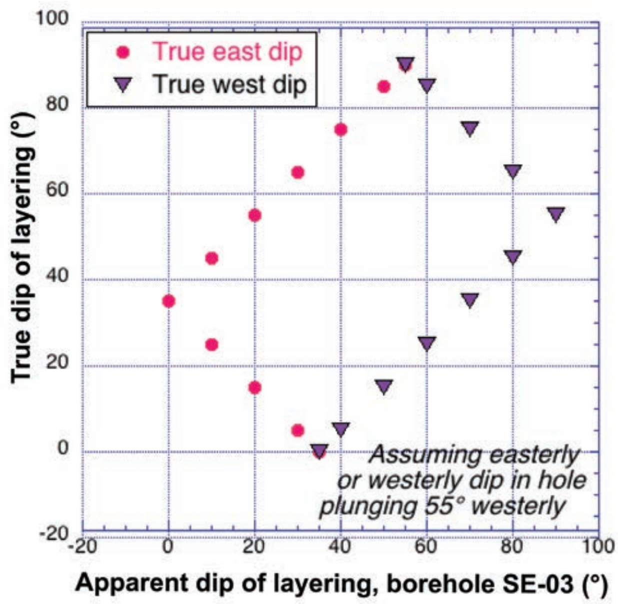

Figure 7. Relation between the apparent dip of bedding in the inclined borehole SE-03 that plunges 55° westerly and the true dip, assuming that the dip is either easterly or westerly. Note that gentle apparent dips in the drill core generally indicate true easterly dips and steep apparent dips generally indicate true westerly dips.

Figure 8. Looking east to the 140 m-high seacliff on the west side of Surtsey. The east-dipping tuff layers apparently belong to the west side of the postulated diatreme beneath the Surtungur vent complex. Note that the dip of layering becomes steeper downward. After Jakobsson *et al.* (2013).

steepening layers that are a hallmark of diatremes (Lorenz 1986, *his* fig. 1). This cliff exposure of the postulated Surtungur diatreme (Moore 1985) is 400 m from the center of the vent suggesting that the radius of the Surtungur structure is at least that dimension at sea level. In comparison the radius of the postulated Surtur diatreme is approximately 250 m at sea level.

The Surtungur tuff sequence as exposed in the cliff consists of alternating light and dark beds with each couplet averaging about 1.5 m thick. The beds were perhaps alternately deposited during (1) a vent-clearing process when water, rubble, and tephra was expelled from the vent by steam explosions (light layer), and (2) a continuous-uprush magmatic explosion process when incandescent tephra was erupted to a great height and fell back into the crater (dark layer).

Lava shields

During the nine and a half months of the Surtur effusive eruption beginning August 19, 1966 a lava shield was built within the Surtur tephra crater. A similar, though somewhat larger, shield grew earlier in the Surtungur crater for 19 months from April 4, 1964 to October 17, 1965. These lava shields consist of a central cone surrounded at a distance of 350–450 m by a lower gradient lava apron. The Surtur cone is 85 m above sea level and the Surtungur cone, 110 m above sea level. Slopes of the Surtur cone average 6°–7° and its outer lava slopes average 2°–5° (Thórdarson 2000).

Leveling surveys showed that the center of the island subsided as much as 30 cm relative to the east and west sides from 1967 to 1968 in the year after the eruption stopped (Tryggvason 1972). Subsidence continued at a reduced rate through 1970 and beyond (Moore 1982). Hence, the lava shields were actively subsiding at the end of volcanic activity, perhaps because the weight and heat of the newly grown shields compressed the loose tephra on which they rest. Subsidence was possibly more rapid earlier when the lava shields were actively growing. The amount of thickening of the lava shields and lowering of their bases below sea level is unknown but is possibly several meters or more.

The initially hot lava shields may be important heat sources for the early hydrothermal system of the volcano. During the months of their eruption, an active lava lake occurred within the craters, lava fountains played, and lava overflowed the crater rims (Thórarinsson 1965). The flows stacked one upon another with little time to cool between overflows. Some flows were fed through tubes from the central lake to the shield flanks. The measured temperature of molten lava during the Surtungur effusive phase was 1138–1182 °C (Sigurgeirsson 1965), and magmatic temperatures at the Surtur shield were similar. The 80-m-thick lava shield should take decades to cool. Moreover, the substrate beneath the Surtur shield retained a part of its original volcanic heat. The lower 90 meters of the SE-03 inclined borehole was a uniform 60 °C in 2017 immediately after drilling (Fig. 9) about one-half the peak temperature at about 115 m.b.s.

The cooling of ponded Hawaiian basalts has been studied by drilling programs that are useful in assessing the cooling of the Surtsey lava shields. Recent Hawaiian lava lakes overlay non-saturated

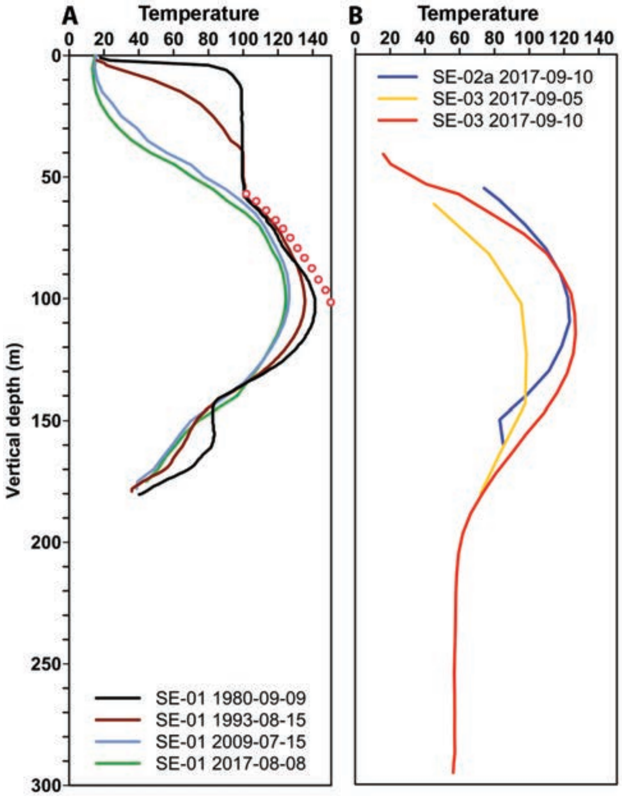

Figure 9. Temperatures measured in the Surtsey boreholes relative to vertical depth. A) 1979 SE-01 borehole temperatures measured in 1980, 1993, 2009, and 2017; red dotted line is boiling point curve. B) Borehole temperatures, SE-02a and SE-03 measured in 2017. After Jackson *et al*. (2019a).

substrates whereas the Surtsey lava shields overlay water saturated substrates. However, precipitation is three times greater in Hawaii and perched water tables are common.

The 1963 Alai lava lake (15-m-thick and 300 m in diameter) became solid about one year after eruption. Two years after the eruption the temperature in the substrate 8 m beneath the lava lake was estimated to be 250 °C (Peck *et al.* 1977). The 1959 Kilauea Iki lava lake (130 m thick and 750 m by 1350 m in areal extent) became solid about 20 years after eruption. Magnetic measurements indicate that it will cool below the Curie Point (540 °C) in 2037 (Gailler & Kauahikaua 2017).

Magnetic measurements on the southern margin of the Surtungur lava shield showed a marked increase in magnetization between 1969 and 1970. This increase indicates that large amounts of the basalt shield cooled below the Curie Point (500–580 °C) and became magnetized (Sigurgeirsson 1974). Hence, 4 to 5 years after eruption the temperatures in the lava comprising the Surtungur lava shield had decreased to below 580 °C .

In 1987, temperature measurements in fissures on the top of the Surtungur lava shield yielded values up to 300 °C (Jakobsson & Moore 2000, *their* fig. 4). This near-surface high temperature (22 years after the end of lava effusion) implies that the core of the shield was at a still higher temperature,

Borehole temperature measurements

In 1980, the temperature profile in the 1979 SE-01 borehole showed a positive bulge, or anomaly, at 105 m.b.s. peaking at 141 °C. Traced upward from the top of this bulge the temperature profile is slightly below and nearly parallel to the boiling point curve (Fig. 9). At the crest of the bulge the temperature is about 10 °C below the curve. Near sea level (58 m.b.s.) the profile joined the boiling point curve (Jakobsson & Moore 1982b) (Fig. 9). In 1979 measurements of the depth of the water level in the borehole were difficult to establish because the water surface was boiling (Moore 1982). In 1993 (26 years after the eruption ceased) the temperature at sea level was still at the boiling point curve (Fig. 9). Measurements after 1993 show that the borehole temperature was cooler than the boiling point curve.

Since 1979 the maximum temperature in the bulge has decreased. It was 135 °C in 1993, 126 °C in 2009, and 124 °C in 2017 (Jackson *et al.* 2019a). Even in 2017 the upper limb of the temperature profile mimicked the boiling point curve but was 20 – 30 °C cooler (Fig. 9). On September 10, 2017, 24 days after drilling ceased on August 17, the shape of the temperature profile in the SE-02A borehole was very similar to that measured August 8, 2017 in the 1979 SE-01 borehole located 7 m to the east (Fig. 9).

The drilling of the inclined SE-03 borehole was completed September 4, 2017. The temperature measured the next day already showed the temperature bulge despite the cooling induced by drilling fluids. Five days later on September 10, the temperature anomaly in borehole SE-03 had increased to a peak of 127 °C at 115 m.b.s., slightly deeper and hotter than that in the SE-02A borehole (Fig. 9). The temperature presumably continued to rise slightly as the borehole attained equilibrium. It is clear, however, that the general shape and depth of the temperature anomaly in the inclined borehole is remarkably similar to that of the vertical boreholes even though the site of the temperature bulge is 72 m to the west. This suggests that the heat source, or sources, are laterally large. The slightly higher temperature of the anomaly crest in the inclined hole suggests that the heat source(s) may be more pronounced toward the west.

The temperature measured in 1980 at the bottom of the SE-01 borehole at 180 m.b.s. was 40 °C (Jakobsson & Moore 1982, *their* figure 5). By 2017 it was only a few degrees cooler (Fig. 9). In contrast, the 2017 temperature in the inclined SE-03 borehole at 180 m vertical depth was 75 °C. At this level 125 m to the west, the interior deposits were 35 °C warmer than the exterior deposits.

Proceeding downward in the SE-03 inclined borehole, the temperature decreases to 60±2 °C and remains constant from 200 m.b.s. to 290 m.b.s., near the center of the vent (Fig. 9). This suggests that the sub-seafloor lapilli tuff has retained residual heat from the series of phreatomagmatic explosions that created the deposits. Previously, this lower zone could have been hotter but in the 52 years since it was deposited in the earliest Surtsey activity it has probably cooled. This residual heat may have played a role in enhancing the temperature of the peak anomalies above. Future monitoring of temperature in the lower part of borehole SE-03 could determine the rate of cooling of this sector of the Surtur diatreme. Back plotting of this rate may help in an estimate of the initial temperatures.

The subaerial tephra deposits north of the Surtur vent began warming in April,1968. In September 1969, temperatures of 48–84 °C were measured at approximate depths of 5 cm in the hottest areas where steam escaped to the surface (Jakobsson 1972). In August 1979, many measurements of ground temperature were made with probes placed at a uniform depth of 20 cm in the tephra deposits. These show zones hotter than 20 °C spanning broad areas adjacent to the Surtur and Surtungur vents (Fig. 1). Areas of palagonitized tuff generally occur within the 20 °C isotherms (Jakobsson & Moore 1982b). In subsequent years these palagonitized areas grew larger. However, much of this expansion was due to wind erosion of unpalagonitized tephra from atop palagonitized tuff (Jakobsson *et al.*, 2000). In 2002–2008 a hot spring appeared on the northwestern shore north of the Surtungur vent. The maximum water temperature measured was 82 °C (Ólafsson & Jakobsson 2009, *their* figs. 1 and 5).

Surtur hydrothermal system

Previously the measured heat anomaly within the 1979 SE-01 borehole was believed to have been caused by the intrusion of nearby feeder dikes (Jakobsson & Moore 1986). This concept is now considered unlikely since the small dike cluster encountered in the SE-01 borehole (Jakobsson & Moore 1982) is too small to produce the elevated temperatures (Axelsson *et al.*, 1982) and also because no major intrusions were encountered in the 2017 drilling except near the bottom of the inclined SE-03 borehole.

The revised interpretation considered here points to both the residual heat within the diatreme (Fig. 9) and the overlying hot Surtur lava shield as possible heat sources (Fig. 10). These could account for the similarity in shape and magnitude of the 2017 high temperature anomalies in both the vertical and inclined boreholes even though they are 72 m apart horizontally (Figs. 9, 10). As the lava shield cools heat is conducted from its upper zones to the atmosphere, enhanced by wind and precipitation. The heat in its lower zones could be conducted downward where it would be dissipated in three ways: (1) by conduction of heat into the previously heated water-saturated tephra and tuff below sea level, (2) by the phase change that occurs when interstitial water boils in the substrate, and (3) by upward convection of rising steam.

After the growth of each lava shield heating of the substrate could have occurred by conduction of heat downward from the hot lava. This could have rapidly heated the warm substrate above the boiling point and created a vapor-dominated system that grew downward as it heated. The greatest depth that it attained would have been at the depth of the maximum heat anomalies (at about 105 m.b.s. in the vertical boreholes and 115 m.b.s. in the inclined borehole).

Eventually, as interstitial water boiled the downward conducted heat was offset by the loss of the heat of vaporization of the interstitial water and by the convection of steam upward. The vapor-dominated system then began to shrink upward as the temperature fell below the boiling point curve at depth. At the time of the 1979 drilling (13 years after eruptions terminated) the system had shrunk back to a thin zone below sea level where water was still actively boiling in the borehole and the steam was able to heat the borehole to 100 °C up to 50 meters above sea level (Jakobsson & Moore 1982, Fig. 9).

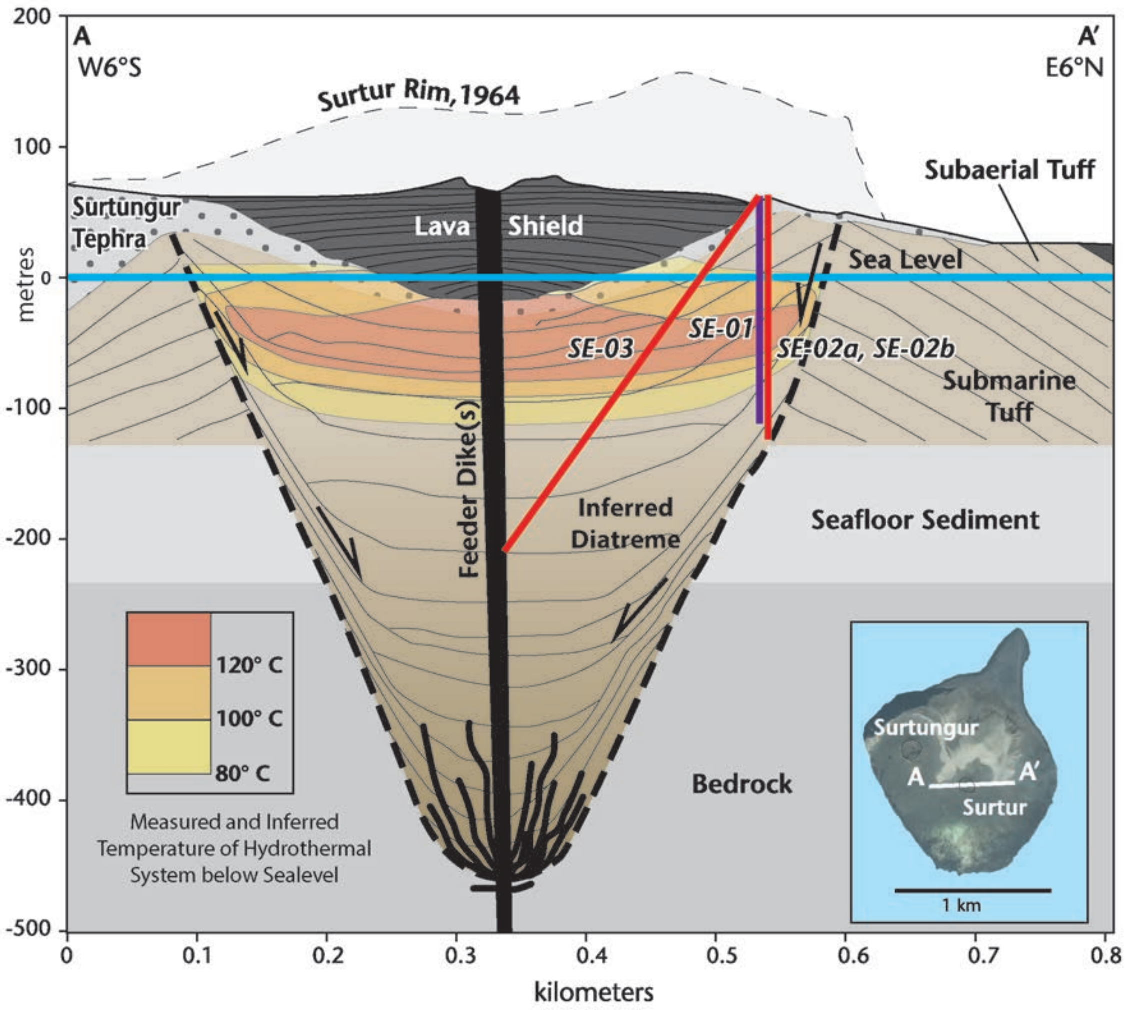

Figure 10. Structure of the Surtur vent and hypothesized diatreme as deduced from eruptive history and cored boreholes (red). Tephra from Surtungur (dotted pattern) and from Surtur (undotted), and the lava shield (dark gray). Conjectural temperatures in the 2017 hydrothermal system beyond those measured in boreholes are shown only below sea level.

By 1993 (26 years after eruptions terminated) the peak of the temperature profile had cooled slightly but the profile still joined the boiling point curve near sea level, indicating the vapor-dominated system still existed at this site. At this time rising steam was able to heat the borehole to 100 °C up to 20 m above sea level (Fig. 9). The vapor-dominated system was possibly hotter and deeper to the west.

Somewhat after 1993, the vapor-dominated systems disappeared in the 1979 SE-01 borehole and the copious steam that was previously detected at the surface abated. Later temperature measurements in 2009 and 2017 were below the boiling point curve (Fig. 9). Cooling was retarded because the formation of steam and the movement of steam ceased. However, even in 2017 the close parallelism of the upper limb of the temperature profiles with the boiling point curve immediately after drilling points to previously hotter profiles constrained by the curve.

The hydrothermal zone under the Surtur lava shield and beneath sea level may be symmetrical as depicted in Figure 10. However, the zone may be deeper toward the vent where there is a thicker pile of lava flows. The western part of the hydrothermal zone may also be enhanced by heat from the neighboring Surtungur lava shield contributing to the overall heating of the substrate. The temperature of the Surtungur hydrothermal system is possibly higher than that of the Surtur system because the lava shield is thicker and because the hypothesized diatreme grew upward through the edge of the warm Surtur submarine tephra deposits rather than entirely through seawater as was the case with Surtur. The hot spring on the northwest coast of Surtsey apparently taps hot water from the Surtungur hydrothermal system.

During the life of the vapor-dominated system steam moved upward to the subaerial deposits on the volcano where it was diverted around the hot lava shield and heated the tephra to the north of the Surtur shield thereby producing palagonitized tuff (Fig. 1). The area of palagonitization first noticed in 1969 (Jakobsson 1972) grew until it encompassed much of the tephra deposits of Surtur and Surtungur by 2006 (Ólafsson & Jakobsson 2009, *their* fig. 1).

CONCLUSIONS

The 2017 SUSTAIN drilling project provides new constraints on the structure of Surtsey volcano and supports the hypothesis that both the Surtur and Surtungur vents are underlain by broad diatremes. Fragment size and sorting in samples from the inclined SE-03 borehole that reaches the approximate center of the Surtur vent are similar to those in the vertical boreholes near the east edge of the Surtur crater. Zones of porous tuff with vesicular fabrics and narrow rims of fine ash on glassy pyroclasts occur in lapilli tuff deposits deep below water level in the vertical boreholes and below the pre-eruption sea floor in the inclined borehole (Fig. 3). These features could have formed in near-surface deposits produced by explosive eruptions. That they occur at depth supports the notion of diatreme growth by deep explosions that repeatedly cleared the vent and then were followed by down-slumping that partly filled the vent with re-mobilized surficial tephra. Likewise, the similarity in clast size in the cores traversing the Surtur deposits horizontally and vertically could indicate mixing induced by a diatreme explosion process (Fig. 4).

Analysis of the orientation of layering in the vertical and inclined Surtur cores indicates that the layering dips systematically west in the lapilli tuff deposits above 50 m.b.s. The westward dip of the layering supports the concept of a wide diatreme with a rim east of the vertical boreholes (Fig. 10). Deeper submarine and sub-seafloor tuff deposits show more complex orientations of layering, perhaps related to structures produced by explosions and subsidence. A 140-meter-high sea cliff on the west side of Surtsey exposes a thick sequence of east-dipping tuff layers that increase in dip downward. They apparently belong to the west side of the crater that merges downward into the postulated diatreme underlying the Surtungur lava shield.

The general absence of basaltic intrusions in the 2017 boreholes except in the lowest part of the inclined SE-03 borehole near the central axis of the Surtur vent casts doubt on the supposition that the heat anomaly measured in the 1979 SE-01 borehole results from nearby intrusions (Jakobsson & Moore 1986). Borehole measurements in 2017 revealed a maximum temperature anomaly in the vertical borehole SE-01 of 124 °C at 105 m.b.s. This anomaly closely duplicates the maximum temperature anomaly in the inclined borehole SE-03, which is 127 °C at 115 m.b.s. The similarity of these anomalies that are 72 meters apart horizontally suggests that their temperature source(s) were laterally broad.

The temperature measured in 2017 in the lower part of the inclined borehole SE-03 at 200–290 m.b.s. was remarkably uniform at 60±2°. This warm temperature is believed to reflect residual heat from the hydromagmatic explosive eruption that created the postulated diatreme that led to the birth of Surtsey island. Such heat, no doubt, has contributed to the elevated temperatures in the hydrothermal system.

Another source of heat in the hydrothermal system may be the 85-meter-thick lava shield that grew in the Surtur crater in 1966–1967. Downward conduction of heat from the lava could have heated the water-saturated substrate above the boiling point creating a downward migrating vapor-dominated system. The greatest depth that it attained is recorded by the sites of the maximum heat anomalies (at about 105 m.b.s. in the vertical boreholes and 115 m.b.s. in the inclined borehole). As downward conducted heat waned the generation of steam eventually began to cool the system at depth by removing the heat of vaporization of the interstitial water and by convection of steam upward. As the temperature fell below the boiling point curve, the vapor dominated systems shrank. In 1979 the system was limited to a narrow zone somewhat below sea level where water was actively boiling in the SE-01 borehole. After 1993 the substrate steadily cooled; temperatures fell below the boiling point curve (Fig. 9) and the vapor-dominated zone disappeared. When the vapor-dominated system was most active steam from boiling interstitial water rose above sea level, heated the surrounding glassy tephra, and increased the rates of palagonitization of the lapilli tuff.

ACKNOWLEDGEMENTS

Funding for 2017 drilling was provided by the International Continental Scientific Drilling Program (ICDP) through a grant to the SUSTAIN project; a grant of excellence from the Icelandic Research Fund, ICF-RANNÍS; the Bergen Research Foundation and K.G. Jebsen Centre for Deep Sea Research at the University of Bergen, Norway; the German Research Foundation (DFG), and DiSTAR, Federico II, University of Naples, Federico II, Italy. The University of Utah, USA, and the two Icelandic power companies Reykjavík Energy and Landsvirkjun contributed additional funds. The logistical support organized by Magnús T. Gudmundsson and provided by the Icelandic Coast Guard was instrumental in carrying out the drilling operation. The DOSECC drilling team was led by Beau Marshall with drillers Steve Cole, Justin Blouin, A. J. Vecchiarelli, Matthew Lyon, and Michael Vinson. The 1979 drilling team was led by Sigidur Sveinsson with drillers Jon Stefansson, Helgi Arsaelsson, Eirikur Stigsson, and Gudmundur Sigurdsson. Kristján Jónasson maintains the Surtsey drill core archive at the Iceland Institute of Natural History. Bronze Black drafted figures 1 and 10. We thank Michael Clynne, Kristján Jónasson, and J. Michael Rhodes for reviews which have substantially improved the manuscript.

REFERENCES

Axelsson, G., V. Stefánsson, G. Gudmundsson & B. Steingrímsson, 1982. Thermal condition of Surtsey. Surtsey Research Progress Report 9, 102–110.

Gailler, L. & J. Kauahikaua, 2017, Monitoring the cooling of the 1959 Kilauea Iki lava lake using surface magnetic measurements. Bulletin of Volcanology 79. DOI 10.1007/s00445-017-1119-7

Iceland Survey Department, 1965, Map of Surtsey volcano, October 23, 1964. Surtsey Research Progress Report 1, 4.

Jackson, M. D., 2020. Petrographic and material observations of basaltic lapilli tuff, 1979 and 2017 Surtsey drill cores, Iceland. Surtsey Research, Surtsey Research 14, 47-62.

Jackson, M. D., M. T. Gudmundsson, T. B. Weisenberger, J. M. Rhodes, A, Stefánsson, B. I. Kleine, P. C. Lippert, J. M. Marquardt, H. I. Reynolds, J. Kück, V. Th. Marteinsson, P. Vannier, W. Bach, A. Barich, P. Bergsten, J. G. Bryce, P. Cappelletti, S. Couper, M. F. Fahnestock, C. F. Gorny, C. Grimaldi, M. Groh, Á. Gudmundsson, Á. Th. Gunnlaugsson, C. Hamlin, Th. Högnadóttir, K. Jónasson, S. S. Jónsson, S. L. Jørgensen, A. M. Klonowski, B. Marshall, E. Massey, J. McPhie, J. G. Moore, E. S. Ólafsson, S. L. Onstad, V. Perez, S. Prause, S. P. Snorrason, A. Türke, J. D. L. White & B. Zimanowski, 2019a, SUSTAIN drilling at Surtsey volcano, Iceland, tracks hydrothermal and microbiological interactions in basalt 50 years after eruption, Scientific Drilling, 25, 35-46, DOI: https://doi.org/10.5194/sd-25-35-2019.

Jackson, M. D., S. Couper, C. V. Stan, M. Ivarsson, M. Czabaj, N. Tamura, D. Parkinson, L. M. Miyagi & J. G. Moore, 2019b. Authigenic mineral texture in submarine 1979 basalt drill core, Surtsey volcano, Iceland. Geochemistry, Geophysics, Geosystems 20 (7).
DOI: https://doi.org/10.1029/2019GC008304.

Jakobsson, S. P., 1972. On the consolidation and palagonitization of the tephra of the Surtsey volcanic Island, Iceland: Surtsey Research Progress Report 6, 121–128.

Jakobsson, S.P., 1978. Environmental factors controlling the palagonitization of the Surtsey tephra, Iceland. Geological Society of Denmark Bulletin 27, Special Issue, 91–105.

Jakobsson, S. P. & J. G. Moore, 1982a. Introduction to the Surtsey Research Drilling Project of 1979. Special Issue of Surtsey Research Progress Report 9, I-II.

Jakobsson, S. P. & J. G. Moore, 1982b. The Surtsey Research Drilling Project of 1979. Surtsey Research Progress Report 9, 76–93.

Jakobsson, S. P. & J. G. Moore, 1986. Hydrothermal minerals and alteration rates of Surtsey volcano, Iceland. Geological Society of America Bulletin 97[5], 648–659.

Jakobsson, S. P. & J. G. Moore, 2000. Geological monitoring of Surtsey, Iceland, 1967-1997. Surtsey Research 11, 99–108.

Jakobsson, S. P., J. G. Moore & I. H. Thorseth, 2013. Palagonitization and lithification of the Surtsey tephra, Iceland. Proceedings of the Surtsey 50th Anniversary Conference, 12–15 August 2013, Reykjavík, Iceland.

Lorenz. V., 1974a. Vesiculated tuffs and associated features. Sedimentology 21, 273–291.

Lorenz, V., 1974b. Study of the Surtsey tephra deposits. Surtsey Research Progress Report 7, 72–79.

Lorenz, V., 1986. On the growth of maars and diatremes and its relevance to the formation of tuff rings. Bulletin of Volcanology 48, 265–274.

McPhie, J., J. D. L. White, C. Gorny, M. D. Jackson, M. T. Gudmundsson & S. Couper, 2020. Lithofacies from the 1963-1967 Surtsey eruption in SUSTAIN drill cores SE-2a, SE-2b and SE-03. Surtsey Research 14, 19-32.

Moore, J. G., 1982. Tidal and leveling measurements on Surtsey, July-August, 1979. Surtsey Research Progress Report 9, 98–101.

Moore, J. G., 1985. Structure and eruptive mechanism at Surtsey Volcano, Iceland. Geological Magazine 122, 649–661.

Norrman, J. O., 1970. Trends of post volcanic development of Surtsey Island. Progress on geomorphological activities in 1968. Surtsey Research Progress Report 5, 95–112.

Ólafsson, M. & S. P. Jakobsson, 2009. Chemical composition of hydrothermal water and water-rock interactions on Surtsey volcanic island, a preliminary report. Surtsey Research 12, 29–38.

Peck, D.L., M.S. Hamilton & H.R. Shaw, 1977. Numerical analysis of lava lake cooling, Part II, application in Alai Lava Lake, Hawaii: American Journal of Science, 277, 415-437.

Sheridan, F. F., 1972. Textural analysis of Surtsey tephra, a preliminary report. Surtsey Research Progress Report, 6, 150–151.

Sigurgeirsson, T., 1965. Some geophysical studies in Surtsey in 1964. Surtsey Research Progress Report 1, 61–57.

Sigurgeirsson, T., 1974. Final report on geomagnetic measurements on Surtsey. Surtsey Research Progress Report VII, 91–84.

Thórarinsson, S., 1965. The Surtsey eruption, course of events and the development of the new island. Surtsey Research Progress Report 1, 52–59.

Thórarinsson, S., 1967. Surtsey, The New Island in the North Atlantic. The Viking Press, New York, 54 p.

Thórdarson, Th., 2000. Physical volcanology of lava flows on Surtsey, Iceland: a preliminary report. Surtsey Research 11, 109–126.

Tryggvason, E., 1972, Precision levelling in Surtsey: Surtsey Research Progress Report VI, 158–162.

Weisenberger, T. B., M. T. Gudmundsson, M. D. Jackson, C. F. Gorny, A. Türke, B. I. Kleine, B. Marshall, S. L. Jørgensen, V. Th. Marteinsson, A. Stefánsson, J. D. L. White, A. Barich, P. Bergsten, J. G. Bryce, S. Couper, M. F. Fahnestock, H. Franzson, C. Grimaldi, M. Groh, Á. Gudmundsson, Á. Th. Gunnlaugsson, C. Hamelin, Th. Högnadóttir, K. Jónasson, S. S. Jónsson, A. Klonowski, J. Kück, R. L. Magnússon, E. Massey, J. McPhie, E. S. Ólafsson, S. L. Onstad, S. Prause, V. Perez, Velveth, J. M. Rhodes, S. P. Snorrason, 2019.Operational Report for the 2017 Surtsey Underwater volcanic System for Thermophiles, Alteration processes and INnovative concretes (SUSTAIN) drilling project at Surtsey Volcano, Iceland: GFZ German Research Centre for Geosciences.
DOI: http://doi.org/10.2312/ICDP.5059.001

Petrograpic and material observations of basaltic lapilli tuff, 1979 and 2017 Surtsey drill cores, Iceland

MARIE D. JACKSON[1]

[1]Department of Geology and Geophysics, University of Utah, Salt Lake City, Utah, U.S.A., m.d.jackson@utah.edu

ABSTRACT

Petrographic studies of thin sections from the 1979 and 2017 Surtsey drill cores provide new insights into microstructural features in basaltic lapilli tuff sampled from the principal structural and hydrothermal zones of the volcano. These describe narrow rims of fine ash on altered glass pyroclasts in thin sections of the 2017 cores, characteristics of granular and microtubular structures in the original thin sections of the 1979 core, and glass alteration in diverse environments. The narrow ash rims follow the outlines of glass pyroclasts in the subaerial tuff cone and in submarine and sub-seafloor deposits; they suggest complex eruptive and depositional processes. The tubular microstructures resemble endolithic microborings in older oceanic basalt; they suggest possible microbial activity. Tubule lengths indicate rapid growth rates, up to 30 µm in ~15 years. Comparisons of glass alteration in thin sections prepared immediately after drilling in 1979 and 2017 indicate differential time-lapse alteration processes in the structural and hydrothermal zones of the volcano. In contrast, thin sections of the 1979 core prepared after 38 years in the repository reveal labile glass alteration during archival storage. The oven-dry density of the sub-seafloor lapilli tuff decreases in 2017 samples with high porosity and water absorption and increases in 2017 samples with a compact ash matrix and lower water absorption. The petrographic descriptions and material measurements provide a foundational reference for further investigations of explosive eruption and deposition of basaltic tephra at Surtsey and the subsequent alteration of these deposits in the volcanic environment and, potentially, the curatorial environment.

INTRODUCTION

Explosive and effusive eruptions of basalt created the very young island of Surtsey from 1963 – 1967 in the southernmost offshore extension of Iceland's southeastern volcanic zone (Thórarinsson *et al.* 1964, Thórarinsson 1965, 1967) (Fig. 1). Cored boreholes through the still hot volcano in 1979 and 2017 provide a precise time-lapse record of hydrothermal rock-water interactions and chemical, mineralogical, and physical change in the 50-year-old basaltic tephra and tuff. The 1979 drilling project at Surtsey produced a 181 m vertical core (SE-01) through Surtur, the eastern vent and tuff cone (Jakobsson & Moore 1982, 1986). The 2017 Surtsey Underwater volcanic System for Thermophiles, Alteration processes and INnovative Concretes (SUSTAIN) drilling project, sponsored by the International Continental Scientific Drilling Program, produced the adjacent vertical SE-02A and SE-02B cores and the inclined SE-03 core that probes the deeper structure of the volcano, as well as a subsurface observatory in the SE-02B borehole (Jackson *et al.* 2019a, Türke *et al.* 2019, Weisenberger *et al.* 2019). Studies of drill core samples and borehole fluids have provided new insights into the processes of explosive Surtseyan

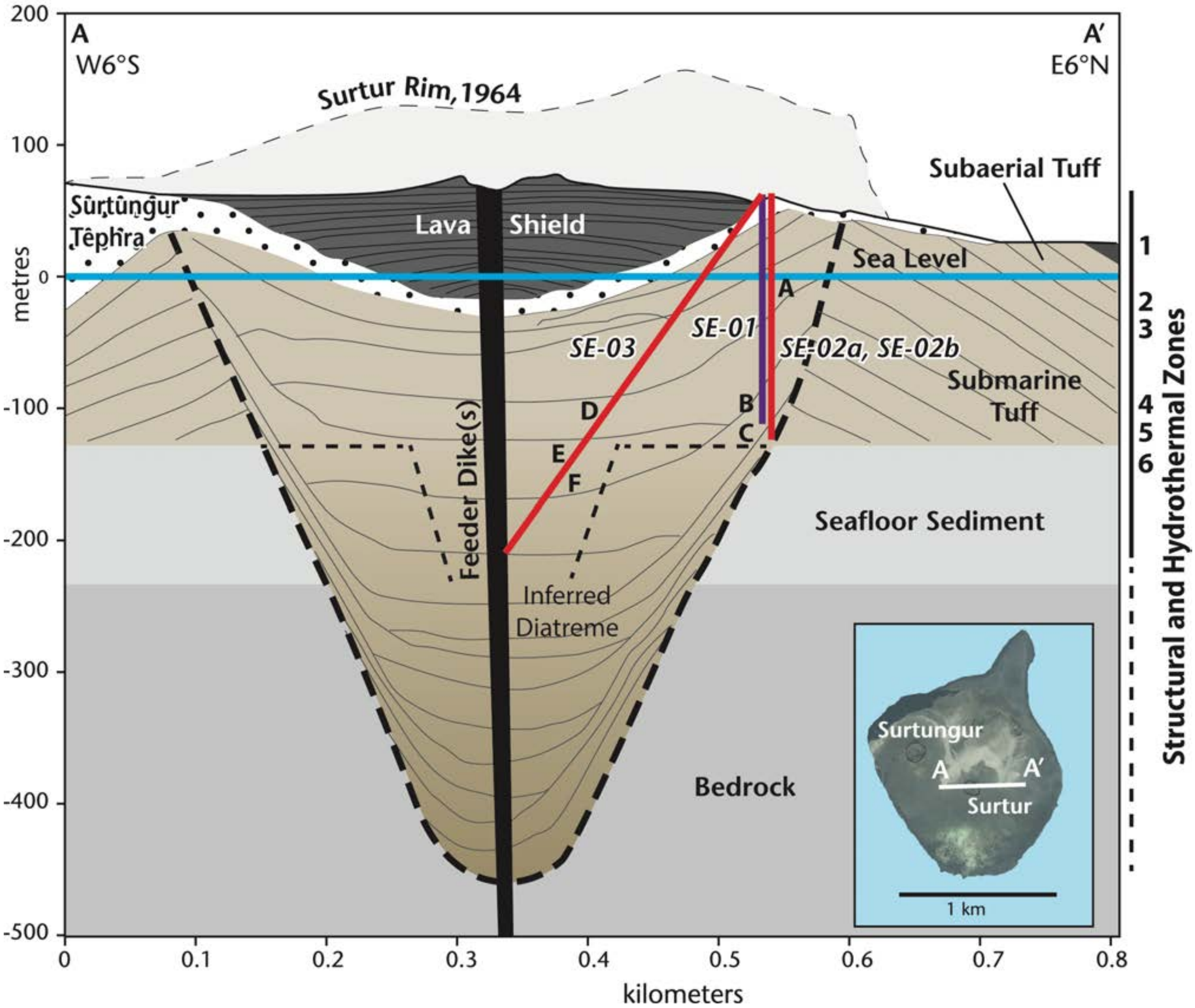

Figure 1. Interpretative, diagrammatic cross-section of Surtur, the eastern crater of Surtsey, showing eruptive deposits, seafloor sediments and sedimentary rocks, and a lava shield in the central crater (modified from Moore 1985, Jakobsson *et al.* 2009, Jackson *et al.* 2019a, Moore & Jackson 2020). The heavy dashed line shows the sub-seafloor diatreme inferred by Moore (1985). The lighter dashed line shows the minimum subsurface vent and conduit deposits that will fit the 2017 drilling results (Jackson *et al.* 2019a). Layering orientations follow the geometrical analysis in Moore & Jackson (2020). Petrographic studies (Figs. 2, 4, 6) describe features in 1979 and 2017 basaltic lapilli tuff drill core samples from (1) the subaerial tuff cone (0 – 58 m.b.s.), (2) the upper submarine tuff (58 – 85 m.b.s.), (3) the maximal temperature zone (85 – 115 m.b.s.), (4) the submarine inflow zone (140 – 155 m.b.s.), (5) the lowermost borehole deposits above the pre-eruption seafloor (155 – 180 m.b.s.), and (6) the sub-seafloor tuff deposits (below 185 m.b.s.). A – F indicate examples of glass pyroclasts with ash rims in the submarine and sub-seafloor tuff (Fig. 2).

submarine and emergent volcanism, the palagonitic alteration of basaltic glass (sideromelane) in diverse fluid and temperature environments and associated changes in rock material characteristics, and the potential for rapid initiation of microbial activity in freshly erupted tephra (Jakobsson & Moore 1982, 1986, Moore 1985, Marteinsson *et al.* 2015, Schipper *et al.* 2015, Jackson *et al.* 2019a, 2019b, Prause *et al.* 2020, McPhie *et al.* 2020, Moore & Jackson 2020). Many aspects of these processes are currently under investigation. This article describes fine-scale features in thin sections of basaltic lapilli tuff from the 1979 and 2017 drill cores with petrographic microscopy. Changes in the density and water absorption characteristics of drill core samples are also recorded. The principal objective is to provide a reference for further investigations of the basaltic tephra at Surtsey and the subsequent alteration of these deposits under diverse environmental conditions.

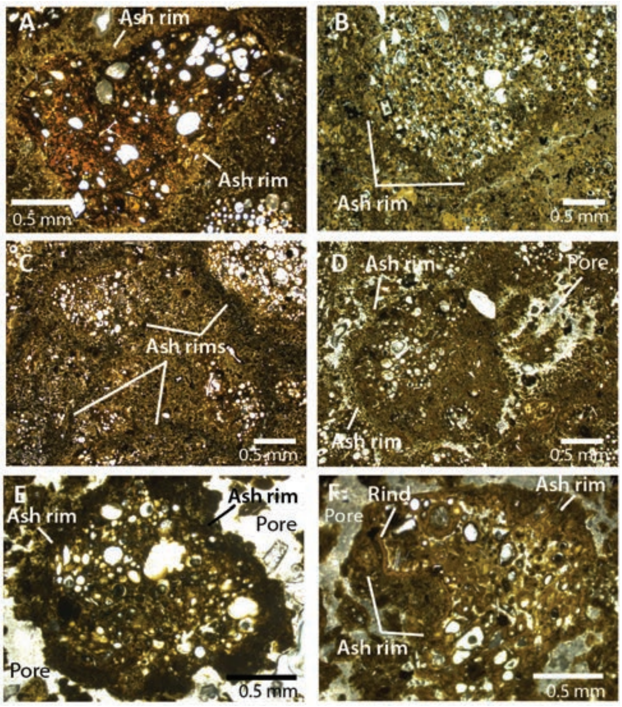

Figure 2. Petrographic images of coarse ash- and lapilli-sized particles with rims of fine ash in submarine and sub-seafloor lapilli tuff in 2017 Surtsey drill cores, plane polarized light (ppl) except (A). A) Near water level, 65.8 m.b.s., 110.3 °C in 1980, 102.8 °C in 2017; highly altered glass particle with a rim of birefringent fine ash, SE-02B core, cross polarized light (xpl). B) Near the submarine inflow zone, 154.1 m.b.s., 83°C in 1980, 82 °C in 2017, SE-02B core; weakly altered glass lapillus with an opaque, non-birefringent, altered fine ash rim. C) Lowermost submarine zone, 170 m.b.s., 68.6 °C in 1980, 62.1 °C in 2017, SE-02B core; clot of weakly consolidated tephra agglomerations surrounded by fine, dark gray ash rims. D) Sub-seafloor lapilli tuff, 220.4 m measured depth, 58 °C post-drilling in 2017, SE-03 core (sample RS19); altered glass particle with a rim of angular fine ash, surrounded by narrow cavities partially filled with mineral cements. E) Sub-seafloor lapilli tuff, 258.9 m measured depth, 57 °C post-drilling in 2017, SE-03 core (sample RS24); altered glass particle with a dense rim of fine ash, surrounded by large, open cavities. F) Sub-seafloor lapilli tuff, 267.2 m measured depth, 57 °C post-drilling in 2017, SE-03 core (sample RS25); altered glass particle with a thick rim of sub-angular coarse and fine ash, surrounded by large cavities filled with mineral cements. Temperature measurements from Jakobsson & Moore (1982), Jackson *et al.* (2019a).

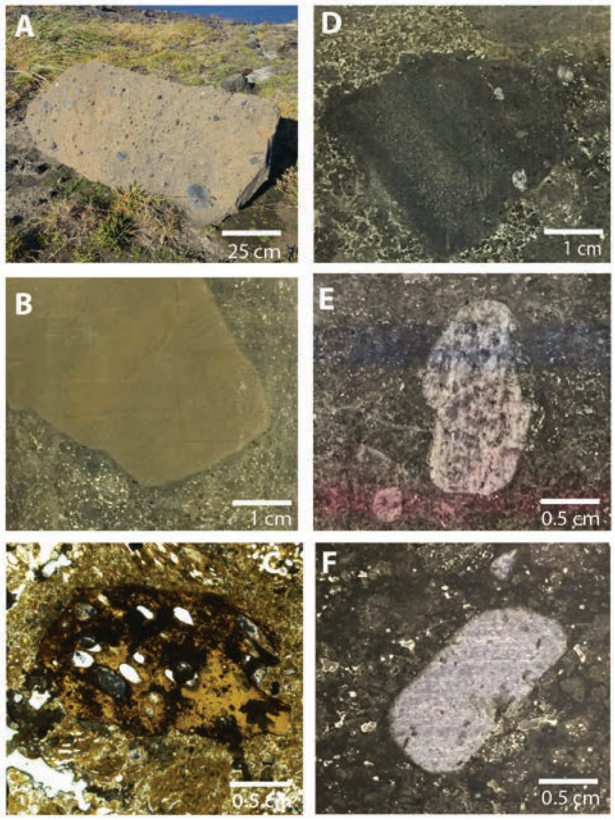

Figure 3. Examples of xenolithic fragments in 2017 Surtsey drill cores. A) Block of seafloor sedimentary rock, Surtur subaerial tuff cone. B) Subangular clast of basaltic glass , 80.5 m.b.s., SE-02A core. C) Photomicrograph of a subangular basaltic clast similar to (B) but strongly altered, 120.0 m.b.s., SE-03. D) Subangular basaltic clast with layering and plagioclase phenocrysts, 83.1 m.b.s., SE-02A. E) Two subrounded gneissic rock fragments, 125.1 m.b.s., SE-02A. F. Subrounded granitic rock fragment, 99.6 m.b.s., SE-02A. (A) Field photo, (B, D, E, F) Core photos, (C) Petrographic microscope image, ppl.

The petrographic studies first describe narrow rims of fine ash approximately 15 – 800 µm in thickness that follow the outlines of vesicular, glassy coarse ash and lapilli in thin sections from the 2017 drill cores (Fig. 2). Subaerially-deposited tephra of the Surtur and Surtungur tuff cones contains abundant armoured lapilli (Lorenz, 1974b, Jakobsson & Moore 1982, Jackson *et al.* 2019a, McPhie *et al.* 2020). These are commonly associated with large vesicles in the tuff that record entrapment or entrainment of steam (or liquid water) (Lorenz 1974a, Lorenz 1986). In deeper lapilli tuff of the 1979 SE-01 Surtsey drill core, observations of narrow ash rims on lapilli and large irregularly-shaped pores (> 1 mm) have been interpreted as indicators of landslides and slumps that re-mobilized freshly erupted subaerial tephra, along with steam or atmospheric gases (Moore 1985). Lithic fragments of seafloor rocks and exotic clasts (Alexandersson 1970, 1972, Baldursson & Ingadóttir 2007, Reynisson & Jakobsson 2009) (Fig. 3) in the lapilli tuff originated from the wall rock around the vent and conduit. They have been

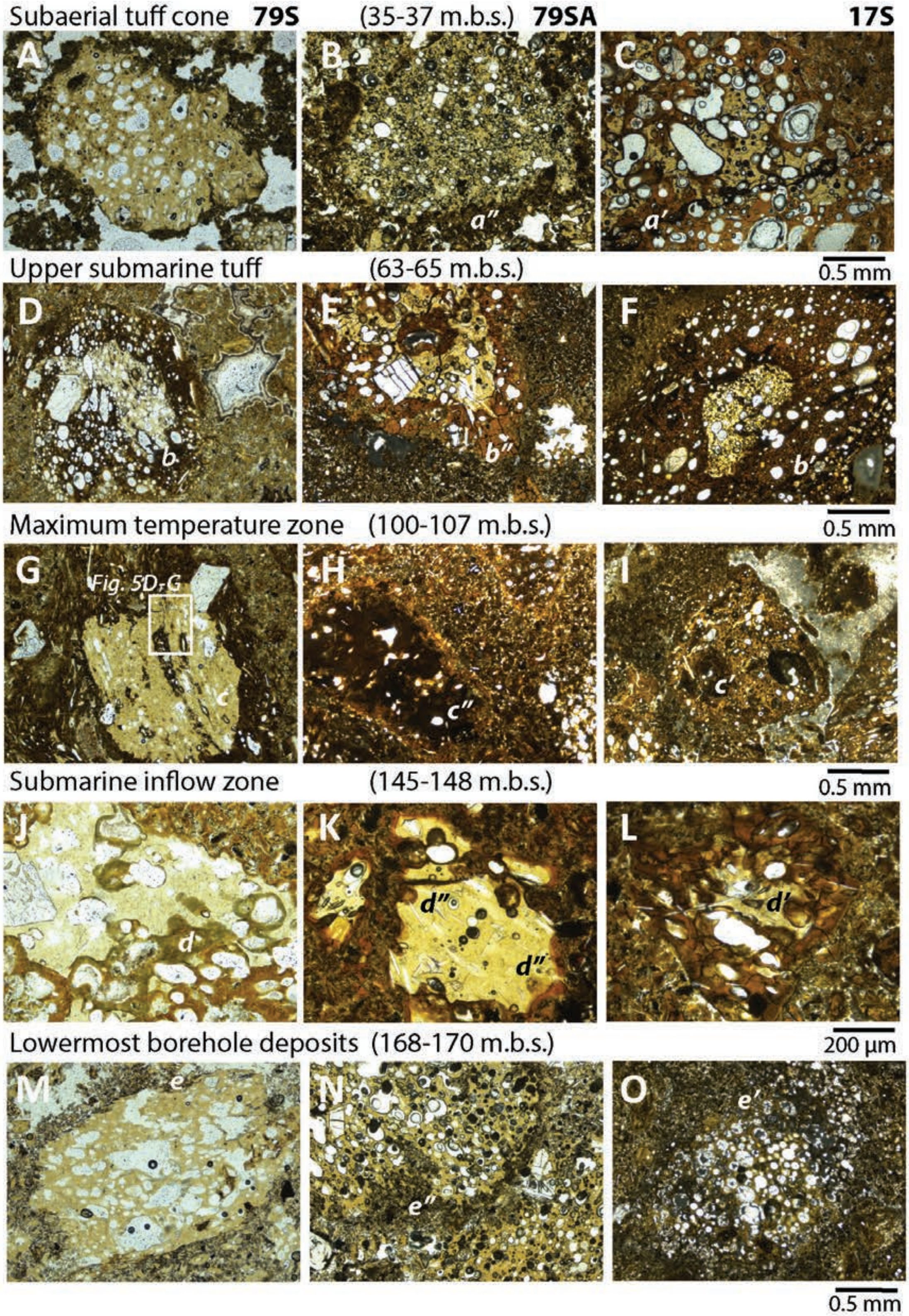

Figure 4. Petrographic images of glassy Surtsey pyroclasts in thin sections from samples of the 1979 drill core prepared in 1979 immediately after drilling (*79S*), the archived 1979 drill core prepared in 2016 – 2018 (*79SA*), and the 2017 drill cores prepared in 2017 – 2019 (*17S*), ppl except (H). See Table 1 for Munsell Colours. Labels *a*, *a'*, *a"*, etc. refer to sites in the *79S*, *79SA* and *17S* thin sections described in the text. A) *79S*, 37.0 m.b.s., 70.8 °C in 1980, B) *79SA*, 37.3 m.b.s., C) *17S*, 34.5 m.b.s., 36 °C in 2017, D) *79S*, 63.1 m.b.s., 107.8 °C in 1980, E) *79SA*, 65.5 m.b.s., F) *17S*, 65.8 m.b.s., 101 °C in 2017, G) *79S*, 107.5 m.b.s., 140.8 °C in 1980, H) *79SA*, 102.6 m.b.s. (xpl) I) *17S*, 100.0 m.b.s., 125 °C in 2017, J) *79S*,147.7 m.b.s., 82.5°C in 1980, K) *79SA*, 145.0 m.b.s., L) *17S*, 145.6 m.b.s., 85°C in 2017, M) *79S*, 168.9 m.b.s., 70.6 °C in 1980, N) *79SA*, 170.1 m.b.s., O) *17S*, 170.6 m.b.s., 51 °C in 2017. Temperature measurements from Jakobsson & Moore (1982), Jackson *et al.* (2019a).

inferred to derive from explosive excavation of the seafloor by continuous uprush eruptions underlying the Surtur and Surtlungur craters (Moore 1985). The altered glass pyroclasts with narrow ash rims (Fig. 2) do not precisely resemble typical armoured lapilli, which have a round outer margin and fine ash coating that is millimeters in thickness (McPhie *et al.* 2020, *their* figs. 4d, 6b).

The petrographic studies then describe characteristics of altered glass in the original thin sections of the 1979 SE-01 drill core prepared in 1979 (*79S*) and thin sections from the 2017 SE-02A, SE-02B and SE-03 drill cores prepared in 2017 – 2019 (*17S*) (Fig. 4). These samples record changes in glass alteration that occurred over 38 years within the principal hydrothermal and structural zones of the volcano: (1) the subaerial tuff cone above water level at approximately 0 – 58 m below surface (m.b.s.), (2) the upper submarine tuff, (3) the higher temperature hydrothermal zone, (4) the submarine inflow zone of weakly-lithified tephra where cooler water of higher salinity enters the borehole (Jackson *et al.* 2019a), (5) the lowermost tephra and tuff above the pre-eruption seafloor at approximately 168 – 181 m.b.s., and (6) the sub-seafloor tuff at approximately 185 – 290 m.b.s. (Fig. 1, zones 1 – 6). The depths do not necessarily indicate where the tephra was first deposited or where the characteristics of the sample first formed.

Associated changes in the oven dry density and water absorption characteristics of drill core samples from these deposits are briefly described (Fig. 5). The labile nature of Surtsey basaltic glass and a possible propensity to undergo change in the repository environment is then explored with descriptions of altered glass in thin sections prepared from the 1979 drill core archive (*79SA*) in 2016 – 2018 from the same alteration zones. These samples experienced about 12 years in the volcanic environment and about 38 years in the repository environment, while stored in wooden core boxes under room temperature conditions. The comparison of petrographic features of glass alteration in the 1979 and 2017 volcanic environments (*79S* and *17S*) with the 1979 mixed volcanic and archival environments (*17SA*) provide reference guidelines for assessing the instability of the glass phase under the evolving conditions of the volcanic environment as well as the curatorial conditions of the repository environment.

The petrographic studies also explore the presence of microtubular structures that resemble endolithic microborings in the original thin sections of the 1979 drill core (Fig. 6). The term, endolith, defines an organism that penetrates actively into the interior of rocks forming tunnels or microborings (Fisk *et al.* 2003, Staudigel *et al.* 2008, Walton 2008, Fisk & McLoughlin 2013). The main threat to the survival of organisms in basalt seems to result from increases in temperature. Hyperthermophile organisms, commonly in domain Archaea, can thrive in extremely hot environments, 80 °C, and some bacteria are able to tolerate temperatures of 100 °C. However, the inferred temperature maximum for functional microbial life is thought to be 120 °C (Ivarsson *et al.* 2015, Kashefi & Lovley 2003, Prieur & Marteinsson 1998). This implies that submarine deposits at Surtsey from 80 – 130 m.b.s. that reached 120 – 141 °C borehole temperatures in 1980 (Jakobsson & Moore 1982) (Fig. 1) could be

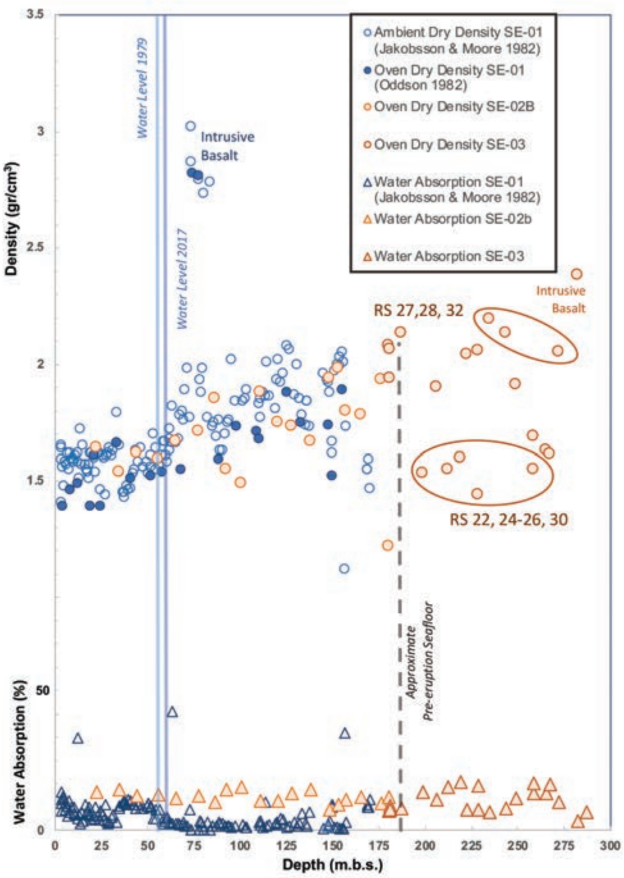

Figure 5. Water absorption and rock density of Surtsey lapilli tuff and basaltic intrusions, based on measurements by Jakobsson & Moore (1982), Oddson (1982), and Jackson *et al.* (2019a).

inhospitable environments for functional microbial activity. By contrast, the possible preservation of traces of endolithic microbial activity in residual fresh glass of the highly altered tuff would suggest that the initial temperatures of the freshly erupted tephra deposits were less than about 80 – 100 °C, as hypothesized by Jakobsson & Moore (1982).

MATERIAL AND METHODS

Petrographic studies of thin sections used an Olympus BX53M microscope in the Department of Geology and Geophysics, University of Utah, to compare features in thin sections of Surtsey basaltic tuff samples from the 1979 SE-01 core prepared immediately after drilling in 1979 (the *79S* sections), the 1979 SE-01 core prepared in 2016 – 2018 after archival storage for 38 years in wooden core boxes (the *79SA* sections), and the 2017 SE-02A, SE-02B and SE-03 cores, prepared in 2017 – 2019 (the *17S* sections). The 2017 samples are wrapped tightly in plastic and stored under refrigeration at 2 °C. All sections were prepared at standard 0.3 mm thickness. The *79S* thin sections were first described by Jakobsson & Moore (1982, 1986); they have glass cover slips. The *79SA* and *17S* thin sections were polished and prepared with superglue and no heat treatment in the laboratory of Burnham Petrographics, L.L.C. to facilitate detachment of the rock slice for fine-scale diffraction and spectroscopic investigations (e.g. Jackson *et al.* 2019b). A suite of 32 reference samples (RS) from the 2017 cores was distributed to the SUSTAIN science team to facilitate collaborative research; these are designated by an RS sample name. All colours are described with Munsell Colour notation, as distinguished by the

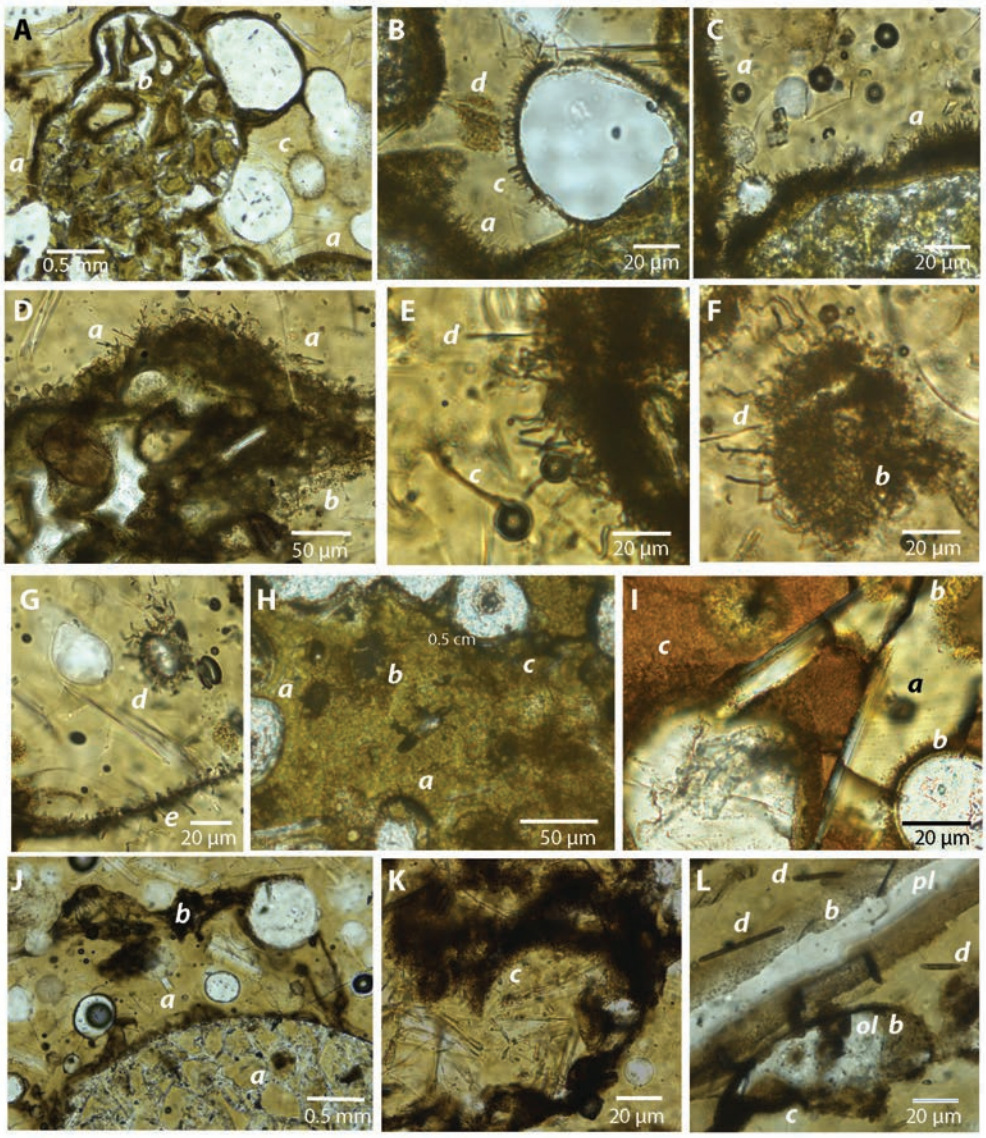

Figure 6. Petrographic images of microtubule and granular microstructures, interfacial zones with narrow protrusions, and possible endolithic microborings in glass lapilli in the original 1979 Surtsey thin sections (*79S*), ppl. Labels *a*, *b*, *c*, *d* refer to sites described in the text; ol, olivine, pl, plagioclase. A, B, C) *79S*, 36.4 m.b.s., 70.8 °C in 1980. D, E, F, G) *79S*, 107.5 m.b.s., 140.8 °C in 1980 (see Fig. 4G). H) *17S*, 100.1 m.b.s., 141.3 °C in 1980, 126 °C in 2017. I) *17S*, 145 m.b.s., 82.5 °C in 1980, 100.2 °C in 2017. J, K, L, M) *79S*, 168.9 m.b.s., 70.6 °C in 1980. Temperature measurements from Jakobsson & Moore (1982), Jackson *et al.* (2019a).

Table 1. Munsell colours of altered glass in the plane polarized light of petrographic microscopy. Surtsey drill cores SE-01 and SE-02A, SE-02B.

Sample Name	Translucent "Glass" Pyroclast Interior	Altered Glass Palagonitized Rind Pyroclast Margin	Altered Glass Fine Ash
Subaerial Tuff Cone 35 – 37 m.b.s.			
79S-37.0m	Yellowish gray 5Y 7/2	Moderate yellow brown 5Y 4/4 to Olive gray 5Y 3/2 (rare)	Dark greenish yellow 10Y6/6 to Moderate greenish yellow 10Y6/4
79SA-37.3m	Yellowish gray 5Y 7/2	Dusky olive brown 5Y 3/4 (rare)	Light olive brown 5Y 4/4 to Olive gray 5Y 3/2
17S-34.5m	Yellowish gray 5Y 7/2 (rare)	Moderate yellowish orange 10YR 7/6 to Light brown 5YR 5/6 (common) (birefringent)	Yellowish orange 10YR 7/6 to Dark yellowish orange 10 YR 5/6 (very weakly birefringent)
Upper Submarine Zone 63 – 65 m.b.s.			
79S-63.1m	Yellowish gray 5Y 7/2	Moderate yellow 5Y 6/6 to Moderate olive brown 5Y 4/4 (birefringent)	Moderate yellow 5Y 7/6 to Dusky yellow 5Y 6/4 (very weakly birefringent)
79SA-65.6m	Yellowish gray 5Y 7/2	Pale yellowish orange 10YR 8/6 to Light brown 5YR 5/6 (birefringent)	Pale yellowish orange 10YR 8/6 to Moderate olive brown 5Y 4/4 (weakly birefringent)
17S-65.8m	Not present	Dark yellowish orange 10YR 6/6 to Light brown 5YR 6/6 (rare) (birefringent) Moderate brown 5YR 3/4 (common) (not birefringent)	Dark yellowish orange 10YR 5/6 to Dark yellowish brown 10YR 3/2 (very weakly birefringent)
Maximal Temperature Zone 100 – 107 m.b.s.			
79S-107.5m	Yellowish gray 5Y 7/2 (rare)	Light olive 10Y 5/4 to Grayish olive 10Y 4/2 to Olive gray 5Y 4/2 (rare) (weakly birefringent)	Pale olive 10Y 6/2 to Light olive brown 5Y 5/6 (very weakly birefringent)
79SA-102.6m	Not present	Moderate yellowish brown 10YR 6/4 to Moderate yellow orange 10YR 7/6 (rare) (birefringent)	Light brown 5YR 4/6 to Grayish brown 5YR 3/2 (very weakly birefringent)
17S-100.1m	Not present	Moderate yellow brown 5Y 6/6 to Moderate olive brown 5Y 4/4 to Olive gray 5Y 3/2 (rare) (birefringent)	Moderate olive brown 5Y 4/4 to Olive gray 5Y 3/2 (weakly birefringent) (also lapilli interiors)
Submarine Inflow Zone 145 – 148 m.b.s.			
79S-147.7m	Yellowish gray 5Y 7/2	Light olive 10Y 5/4 (vesicle rims, not birefringent) Moderate greenish yellow 10YR 6/4 to Light olive brown 5Y 5/6 (weakly birefringent)	Moderate greenish yellow 5Y 6/6 to Moderate yellow 5Y 6/6 (very weakly birefringent)
79SA-145.0m	Grayish yellow 5Y 8/4	Moderate yellow 5Y 7/6 (not birefringent) Moderate yellow orange 10YR 7/6 to Light brown 5YR 5/6 (weakly birefringent)	Moderate yellow 5Y 7/6 (not birefringent) Moderate yellow orange 10YR 7/6 (weakly birefringent)
17S-148.4m	Yellowish gray 5Y 7/2 (rare)	Dark yellowish orange 10YR 6/6 to Light brown 5YR 5/6 (weakly birefringent)	Moderate yellow 5Y 6/6 to Dark yellowish orange 10YR 6/6 to Light brown 5YR 5/6 (very weakly birefringent)
Lowermost borehole deposits 168 – 170 m.b.s.			
79S-168.9m	Yellowish gray 5Y 7/2	Moderate yellow brown 5Y 4/4 (opaque borders and zones)	Yellowish gray 5Y 7/2 Dark gray N2 (fine dark gray ash)
79SA-170.1m	Dusky yellow 5Y 6/4	Grayish brown 5YR 3/2 (opaque borders and zones)	Dusky yellow 5Y 6/4 Dark gray N2 (fine dark gray ash)
17S-170.6m	Not present	Moderate yellow 5Y 6/6 to Light yellow brown 5Y 5/6 Moderate olive brown 5Y 4/4 (weakly birefringent)	Light olive brown 5Y 5/6 to Moderate olive brown 5Y 4/4 to Olive gray 5Y 3/2 (weakly birefringent)

Geological Society Rock Colour chart (Table 1). Colours were noted in plane polarized light (ppl) at 10X magnification and matched with the color chart in the light of a sunlit window. Note that the colours shown by the micrographs (Figs. 2, 4, 5) do not always represent the true colours in ppl (Table 1). Rock density measurements by Oddson (1982) and this study and measurements of water absorption, [(weight in air$_{\text{water saturated}}$ – weight in air$_{\text{oven dry}}$)/ weight in air$_{\text{oven dry}}$], follow the guidelines of the American Standards of Testing Materials (ASTM C97/C97M-18). Measurements recorded by Jakobsson & Moore (1982) did not oven dry specimens before water saturation and so give lower water absorption values (Fig. 5). Temperatures refer to measurements in borehole SE-01 in September 1980 and August 2017 and in borehole SE-03 ten days post-drilling in September 2017 (Jakobsson & Moore 1982, Jackson *et al.* 2019a).

RESULTS

Narrow ash rims on glass pyroclasts

Armoured lapilli tuff is the dominant facies in 2017 borehole SE-02A above water level and in 2017 borehole SE-03, at various levels above 70 m measured depth (McPhie *et al.* 2020). Some glassy coarse ash and lapilli in thin sections from the subaerial tuff cone deposits are outlined by a narrow rim of fine ash (Fig. 4A). The fine ash rims differ in particle shape, size, packing, porosity and/or colour from the surrounding altered vitric ash matrix. The narrow rims do not precisely resemble the typical rounded form and thicker rims of very fine accretionary ash on armoured lapilli (Lorenz 1974a). Lapilli and coarse ash in certain submarine (Fig. 2A–C) and sub-seafloor (Fig. 2D–F) tuff deposits from the 2017 SE-02B and SE-03 drill cores also have these unusual, narrow rims of fine ash. For example, in submarine tuff at 65.8 m.b.s., just below the zone of tidal flux (Fig. 1), a vesicular, highly altered glass fragment has a 200 – 400 µm border composed of fine ash and opaque, sub-angular, coarser ash that is more birefringent than the fine ash of the altered vitric matrix (Fig. 2A). In less altered tuff at 154.1 m.b.s., a weakly altered, vesicular glass fragment has an intermittent, 200 – 300 µm thick rim composed of dark gray (N2) fine ash and sparse moderate yellow (5Y 6/6) coarser ash (Fig. 2B); the fine ash is darker and more opaque than that of the altered vitric matrix. In the lowermost SE-02B core at 170.6 m.b.s., clots of ash 0.5 – 1.5 cm in diameter have 100 – 300 µm rims of moderate olive brown (5Y 4/4) subangular fine ash (Fig. 2C). At 220.3 – 220.7 m measured depth (180.5 m.b.s.) in the SE-03 core, a highly altered, vesicular glass fragment has a porous 50 – 100 µm rim of angular, light to moderate olive brown (5Y 5/6 – 5Y 4/4) fine ash; the rim is separated from the ash matrix by pores 1 – 2 mm in length, now partially filled with mineral cements (Fig. 2D, sample RS19). Tuff samples from porous zones at 258.9 – 259.3 m measured depth (212.0 m.b.s.) and 267.2 – 267.6 m measured depth (218.9 m.b.s.), about 25 – 35 m below the pre-eruptive seafloor (Fig. 1), contain abundant altered glass fragments outlined with narrow rims of ash (Fig. 2E-F, samples RS24, RS25). For example, the vesicular glass fragment at 212 m.b.s. is isolated from the altered vitric matrix by nearly contiguous pores 0.25 – 2 mm in length and width. It has a 300 – 500 µm rim of very fine, compact, olive gray (5Y 3/2) ash (Fig. 2E). The vesicular glass pyroclast at 219 m.b.s. has an intermittent rind of altered glass, about 15 µm in thickness (Fig. 2F). It is also isolated from the vitric matrix by large, irregularly-shaped pores, but these are filled with mineral cements. The rim, 15 – 800 µm in thickness, is composed of sub-angular, olive gray (5Y 3/2) fine ash and light brown (5YR 4/6) coarser ash. The vesicular pyroclast has an intermittent rind of altered glass, about 15 µm in thickness.

Examples of lithic fragments

The tuff deposits on the surface of Surtsey contain two principal groups of xenoliths: pre-eruption seafloor sedimentary rock deposited on the insular terrace underlying the volcano during and following glacial periods, and ice-rafted debris carried in from afar before the growth of the volcano (Alexandersson 1970, 1972, Baldursson & Ingadóttir 2007, Reynisson & Jakobsson 2009). The marine sedimentary rock of volcanic origin was lithified before Surtsey erupted. The largest rock fragments exposed on the subaerial tuff cone are about one meter in diameter (Fig. 3A). These commonly have a compact matrix of sub-rounded glass particles and abundant sub-angular, sand- to coarse gravel-sized clasts of coherent basalt The fragments in the drill cores range from relatively unaltered (Fig. 3B) to highly altered with authigenic mineral cements (Fig. 3C), principally zeolites and Al-tobermorite growing in relict pores. Angular fragments of coherent basalt (Fig. 3D) are common. Exotic crystalline rocks, gneissic and granitic pebbles most likely derived from Greenland (Fig. 3E, F), were transported by icebergs into the region and deposited with the sediments underlying the volcano (Reynisson & Jakobsson 2009). The volume of sedimentary rock that underlay the volcano and was carried to the surface is difficult to estimate, since only the largest xenoliths are clearly recognizable.

Petrographic comparisons of glass alteration

Rates of glass alteration in the SE-01 drill core were quantified immediately after drilling in 1979 through measurements of the thicknesses of palagonitized rinds on coarse ash- and lapilli-sized glass fragments and alteration rims on olivine crystal fragments (Jakobsson & Moore 1986). The growth rates ranged from about 1 µm/year at 60 °C to 5 – 10 µm/year at 100 °C. Examples of those alteration features are shown in the first panel of Figure 4 (*79S*) and described with Munsell Colours in Table 1. At 37.0 m.b.s. in the subaerial tuff cone a translucent, yellowish gray (5Y 7/2) glass fragment with a narrow irregular rim of fine ash shows little palagonitic alteration (Fig. 4A). By contrast, the glass fragment at 63.1 m.b.s. in the upper submarine zone has a thick rind (up to 500 µm) of moderate yellow (5Y 6/6) to moderate olive brown (5Y 4/4) palagonitized glass (Fig. 4D, site *b*). At 107.5 m.b.s. in the higher temperature hydrothermal zone, most lapilli are pervasively altered. However, one pyroclast preserves translucent, yellowish gray (5Y 7/2), apparently fresh glass that contains granular and tubular microstructures (Figs. 4G, site *c*, 6D-G). In the submarine inflow zone at 147.7 m.b.s., a lapillus also preserves apparently fresh, yellowish gray (5Y 7/2) glass. The internal vesicles have 20 – 30 µm light olive (10Y 5/4) alteration rinds; broad zones of unusual moderate greenish yellow (10YR 7/6) to light olive brown (5Y 6/6) altered glass occur around the perimeter (Fig. 4J, site *d*). In the lowermost core at 168 m.b.s., apparently fresh, yellowish gray (5Y 7/2) glass is preserved, but opaque, isotropic, moderate yellow brown (5Y 4/4) zones of altered fine ash are common in the matrix surrounding larger clasts (Fig. 4M, site *e*).

Vesicular, glassy coarse ash and lapilli in *17S* thin sections show a pronounced progression of palagonitic alteration relative to that recorded in the *79S* thin sections. In the subaerial tuff cone at 34.5 m.b.s. and in the uppermost submarine zone at 65.8 m.b.s., the yellowish gray (5Y 7/2) clast interiors do not have the clear and translucent aspect of apparently fresh *79S* glass (Fig. 4A, C). The altered rinds range from yellowish orange (10YR 7/6) to dark yellowish orange (10YR 5/6) and dark yellowish brown (10YR 3/2) (Fig. 4C, F, site *a'*, Table 1); smaller glass particles are more pervasively altered. In the higher temperature hydrothermal zone at 100.1 m.b.s., the palagonitized rinds have become birefringent (Fig. 4I). Areas occupied by apparently fresh, yellowish gray (5Y 7/2) glass in the *79S* thin sections (Fig. 4G, site *c*) are opaque and isotropic in the *17S* thin sections (Fig. 4I, site *c'*). The *17S* palagonitized glass rinds retain the same olive brown (5Y 4/4) and olive gray (5Y 3/2) hues as the *79S* rinds, but have developed weak birefringence (Table 1). In the submarine inflow zone at 148.4 m.b.s. only sparse glass particles retain yellowish gray (5Y 7/2) interiors; thick rinds (up to 450 µm) of weakly birefringent, dark yellowish orange (10YR 6/6) and light brown (5YR 5/6) palagonitized glass occur at clast perimeters (Fig. 4L, site *d'*). In the lowermost SE-02B core at 170.6 m.b.s., the altered glass of clast interiors is opaque and non-birefringent (Fig. 4O); palagonitized glass rinds, however, preserve the same moderate yellow (5Y 6/6) and light yellow brown (5Y 5/6) colours of *79S* rinds at the same depth (Fig. 4M, site *e*, Fig. 4O, site *e'*, Table 1).

The submarine 1979 core was dusky green to grayish olive green (5G 3/2 to 5GY 3/2) when drilled and first placed in core boxes (Jakobsson & Moore 1982), but after years of storage the green colour has vanished and the surface colour of the *79SA* core is now dark to moderate yellowish brown (10YR 4/2 to 10YR 5/4). Petrographic features of altered glass in the *79SA* thin sections differ from those of the *79S* thin sections — and also from the *17S* thin sections. In the subaerial tuff cone at 37.3 m.b.s., internal zones retain a yellowish gray (5Y 7/2) colour (Fig. 4B) but lack the clear, translucent aspect of the apparently fresh glass of the *79S* thin section at 37.0 m.b.s. (Fig. 4A). Rare palagonitized rinds resemble those of the *17S* thin section at 34.5 m.b.s. (Fig. 4C, site *a'*), but are dusky olive brown (5Y 3/4) and more opaque (Fig. 4B, site *a''*, Table 1). In the upper submarine zone at 65.6 m.b.s., the thicknesses of palagonitized rinds on glassy particles (Fig. 4E, site *b''*) are similar to those of the *79S* thin section (Fig. 4D, site *b*) but the colours more closely resemble the pale yellowish orange (10YR 7/6) of *17S* rinds (Figs. 4F, site *b'*).

In the high temperature hydrothermal zone at 102.6 m.b.s., the internal zones of some *79SA* glass fragments are altered to an opaque, isotropic mass (Fig. 4H, site *c''*). X-ray microdiffraction analyses demonstrate that this is mainly nano-crystalline nontronite (Jackson *et al.* 2019b, *their* fig. 4) and record the progressive organization of the incipient clay mineral structure. Altered glass rinds are weakly birefringent. None of the apparently fresh, yellowish gray (5YR 7/2) glass of the *79S* thin section at 107.5 m.b.s. (Fig. 4G, site *c*) is present. The greater opacity of the ash matrix in the submarine *79SA* thin sections (Fig. 4E, H) may result from crystallization of analcime. By contrast in the submarine inflow zone at 145.0 m.b.s., a *79SA* glass fragment has a weakly altered, grayish yellow (5Y 8/4) interior (Fig. 4K). The altered glass rinds around internal vesicles are moderate yellow (5Y 7/6) (Fig. 4K, site d'') and preserve none of the light olive (10Y 5/4) hue of the internal rinds in the *79S* thin section at this depth (Fig. 4J, site *d*); instead, they more closely resemble the moderate yellow (5Y 6/6) of *17S* rinds (Fig. 4L, site *d'*, Table 1). In the lower core at 170.1 m.b.s., internal zones of *79SA* lapilli remain yellowish gray (5YR 7/2) (Fig. 4N); at 157.1 m.b.s., X-ray microdiffraction investigations of a similar *79SA* yellowish gray (5YR 7/2) internal zone indicates that fresh unaltered glass does indeed persist (Jackson *et al.* 2019b, *their* fig. 2). The opaque borders and irregular alteration zones are grayish brown (5YR 3/2) (Fig. 4N, site *e''*), however, rather than the moderate yellow brown (5Y 4/4) of *79S* lapilli (Fig. 4M, site *e*).

Rock density and water absorption

The oven-dry density of 2017 SE-02B drill core samples shows a wide range of scatter in the approximately 180 m thick sequence of lapilli tuff also sampled by the 1979 SE-01 drill core (Fig. 5). Measurements of the SE-02B samples were made in 2017 immediately after drilling. They yield an average oven-dry density, 1.70 g/cm^3, which is slightly higher than the average of the oven-dry SE-01 measurements made in 1980, 1.60 g/cm^3 (Oddson 1982, Jackson *et al.* 2019a). The SE-01 core samples measured by Jakobsson & Moore (1982) were not oven-dried and so yielded higher values.

Measurements of water absorption in the SE-01 core samples show a pronounced increase at 35 – 55 m.b.s. (Jakobsson & Moore 1982). This increase may reflect higher porosity near the zone of tidal flux in samples that were not oven-dried (J. G. Moore, personal communication, 2019). By contrast, water absorption measurements of the oven-dried SE-02B core samples at these depths show little or no change. There, oven-dried densities range from 1.62 – 1.71 g/cm^3 compared with 1.51 – 1.55 g/cm^3 for the oven-dried SE-01 core samples (Oddson 1982, Jackson *et al.* 2019a). The development of mineral cements that now fill much of the original porosity seems to have slightly increased the density of the lapilli tuff.

The oven-dried density of the lapilli tuff in the lower sections of the 2017 SE-03 drill core also shows a great deal of variation. Lapilli tuff samples at 198.7, 212.0, 218.9, 228.6 and 258.5 m.b.s. (242.6, 258.9, 267.3, 279.1 and 315.6 m measured depth) give low oven-dried density, 1.40 – 1.70 g/cm^3 (Jackson *et al.* 2019a, samples RS 22, 24, 25, 26, 30). Thin sections of these samples show abundant mm-scale pores in the ash matrix (e.g. Fig. 2E, F) (Moore & Jackson 2020, *their* fig. 3). Water absorption is high, 16 – 19%; the water-saturated density, 1.80 – 2.02 g/cm^3, may approximate the *in situ* density of the porous sub-seafloor deposits. By contrast, tuff samples at 235.1, 243.4, 271.9 m.b.s. (287.1, 297.2 and 303.8 m measured depth) have higher oven-dried density, 2.05 – 2.19 g/cm^3 (Jackson *et al.* 2019a, samples RS27, 28, 32). Thin sections of these samples show a compact ash matrix and a general absence of mm-scale pores. Water absorption is lower, 8 – 12% and the water-saturated density, 2.21 – 2.38 g/cm^3, may approximate the *in situ* density of the more compact sub-seafloor deposits. The coherent basalt at 282.1 m.b.s. (344.7 m measured depth) has 2.38 g/cm^3 oven-dry density, 0.04% water absorption, and 2.48 g/cm^3 water-saturated density.

Granular and tubular microstructures

Fine-scale (5 – 30 µm) linear features are preserved in translucent, yellowish-gray zones (5YR 7/2) within the glassy ash and lapilli of many *79S* thin sections (Fig. 6). These linear features resemble microtubules thought to record endolithic microborings produced by microbial dissolution and alteration of glass (Fisk *et al.* 2003, Thorseth *et al.* 1991, 2001, Walton 2008, Fisk & McLoughlin 2013). The tubular features are much finer than the thickness of the thin section (Fig. 6E, F). Tiny "hair-like", overlapping protrusions are arranged roughly perpendicular to contacts between fresh and altered glass (Fig. 6A-C); these protrusions are similar to tubules described by Fliegel *et al.* (2012, *their* fig. 4) in ancient basaltic pillow lavas from DSDP Hole 418A. There are abundant granular features, as well (Thorseth *et al.* 1991, Furnes *et al.* 2001, Staudigel *et al.* 2008) (Fig. 6B, D, L).

In the *79S* 36.4 m.b.s. sample from the subaerial tuff cone, 70.8 °C in 1980 (Jakobsson & Moore 1982), protrusions < 1 µm in width and up to 25 µm in length emerge from the contact between translucent, yellowish-gray (5Y 7/2) glass and opaque, altered glass selvages (Figs. 6A, B, C). They occur on the surfaces of alteration rinds along the perimeter of the lapillus (Figs. 6A, B, C, *a*), on accretionary ash particles (Fig. 6A, site *b*) and along internal vesicles (Figs. 6A, B, site *c*). There are also opaque, olive gray (5Y 3/2) granular features (Fig. 6B, site *d*).

In the submarine *79S* 107.5 m.b.s. sample, 140.8 °C in 1980 (Jakobsson & Moore 1982), coarse ash- to lapilli-sized particles locally preserve translucent, yellowish-gray (5Y 7/2), apparently fresh glass (Fig. 4G). In one example, irregular linear features < 1 µm in width and up to 30 µm in length protrude from the altered selvage of an internal vesicle into the yellowish-gray glass (Fig. 6D, site *a*). They radiate from the alteration rinds along other internal vesicles (Figs. 6E, F, site *d*; 6G, site *d*), as well. The linear features also form in the glass (Fig. 6E, *c*), along micro-fractures (Fig. 6G, *e*) and within granular features (Fig. 6D, F, site *b*). No vestiges of translucent fresh glass remain in the correlative 100.1 m.b.s., SE-02A *17S* thin section, 141.3 °C in 1980 and 126 °C in 2017 (Jakobsson & Moore 1982, Jackson *et al.* 2019a). Here, dark olive gray (5Y 3/2) opaque zones obscure radially-oriented protrusions up to 20 µm in length (Fig. 6H, site *a*), granular features (Fig. 6H, site *b*), and a possible microcrack (Fig. 6H, site *c*). The progressive development of weakly birefringent, nano-crystalline clay mineral in the altered glass conceals the fine-scale features. By contrast, in the 145 m.b.s., SE-02A *17S* thin section, 82.5 °C in 1980 and 100.2 °C in 2017 (Jakobsson & Moore 1982, Jackson *et al.* 2019a), translucent, yellowish-gray, apparently fresh glass persists (Fig. 6I, site *a*). Here, the contact of fresh glass with opaque altered glass around internal vesicles is occupied by granular features (Fig. 6I, site *b*). Nearby, a shadowy tangle of linear features up to 30 µm in length (Fig. 6I, site *c*) occurs in the very weakly birefringent, light brown (5YR 5/6) altered glass rind of a vesicle filled with zeolite. These may represent microtubules produced in fresh glass before progressive alteration to authigenic minerals.

In the submarine *79S* sample at 168.9 m.b.s., 70.6 °C in 1980 (Jakobsson & Moore 1982), translucent, yellowish-gray, apparently fresh glass is preserved in coarse ash and lapilli (Fig. 6J, site *a*). However, opaque, moderate yellow brown (5Y 4/4) selvages and zones make diffuse, irregular boundaries with the fresh glass (Fig. 6J, site *b*). Discrete protrusions are not detected at the petrographic scale (Figs. 6K, site *c*; 6L, site *c*), but these do occur in glass lapilli and along micro-fractures at 157.1 m.b.s. (Jackson *et al.* 2019b). The dissolved perimeters of olivine and plagioclase crystals (Fig. 6L, site *b*) also contain traces of granular features. In addition, chambered, opaque rods 1– 2 µm in width and up to 50 µm in length occur in the translucent glass (Fig. 6L, site *d*).

DISCUSSION

Narrow ash rims

At least two processes are known to produce ash rims on glass pyroclasts. Accretionary ash coatings on lapilli commonly form in an eruption column or cloud when ash attaches to a larger particle and then further ash accretes before falling from the cloud onto Earth's surface (Lorenz 1974a, Gilbert & Lane 1994, Schumacher & Schmincke 1995, Mueller *et al*. 2016). These armoured lapilli may be deposited into water; some survive (and some are destroyed). Furthermore, accretionary lapilli that have been deposited on land may be re-deposited into water. Alternatively, enveloping fine ash particles may be produced through *in situ* granulation of the surfaces of hot juvenile lapilli, caused by thermal stress as the hot pyroclasts briefly travel through water and are quenched during Surtseyan eruptions (Colombier *et al.* 2019). In addition, it has been hypothesized that landslides and slumps of freshly erupted subaerial deposits during explosive eruptions (Moore 1985, Lorenz *et al*. 2017) may carry subaerial lapilli with accretionary ash coatings into submarine and sub-seafloor environments; these eruptive and depositional processes remain poorly understood.

Armoured lapilli that formed in an ash-charged atmosphere are common in the Surtur sub-aerial tuff cone deposits (Fig. 4A, B). They have been described and mapped by Lorenz (1974b) and are recorded in the SE-01 (Jakobsson & Moore 1982, *their* fig.

8) and the SE-02B drill cores (McPhie *et al.* 2020, *their* figs. 4d, 6c). By contrast, the narrow ash rims that outline the outer surfaces of glass particles in some submarine (Figs. 2A-C) and sub-seafloor tuff deposits (Figs. D-H) show variations in thickness, composition, particle sizes and shapes that differ from the altered vitric ash matrix. These features appear to record diverse depositional processes. For example, in lapilli tuff at 170.6 m.b.s. dark gray (N2) ash rims cover sub-rounded clots of altered vitric ash (Fig. 2C); the clast composed of the agglomerated clots is also rimmed with dark gray ash. The origins of these rims remain unknown. By contrast, at the approximate depth of the pre-eruptive seafloor, 180.5 m.b.s., a narrow rim of angular olive brown (5Y 5/6 – 5Y 4/4) fragments resembles the enveloping ash that may be produced by *in situ* granulation as a hot juvenile pyroclast travels though water and is quenched (Fig. 2D) (Colombier *et al.* 2019). Similar fractured lapilli with jigsaw cracks in submarine *79SA* samples have been described by Jackson *et al.* (2019b). At 212.03 and 218.86 m.b.s., ash rims adhere to the surfaces of altered vesicular glass fragments; the rims are composed of dense, homogeneous fine ash (Fig. 2E) and poorly sorted, sub-angular ash (Fig. 2F). Large, nearly contiguous pores 1 – 3 mm in length, now partially filled with mineral cements, surround these features and follow the intergranular outlines of the narrow ash rims. It has been suggested that these clasts and vesicles could represent freshly erupted tephra from subaerial deposits that were remobilized by submarine landslides and slumps, which incorporated steam and atmospheric gases (Lorenz 1974a, 1986, Moore 1985). However, the forms of the ash rims differ from the thicker, rounded surface coatings of typical armoured lapilli. The origins of these complex features thus remain unclear.

Glass alteration

The original thin sections from the 1979 drill core (*79S*) preserve translucent, yellowish-gray (5Y 7/2) glass in all hydrothermal and structural zones traversed by the SE-01 borehole (Figs. 1, 4, Table 1), although this glass is very rare in the high temperature hydrothermal zone at 85 – 115 m.b.s. By contrast, the thin sections from the 2917 drill cores (*17S*) preserve little yellowish-gray (5Y 7/2) glass and palagonitized glass rinds are thicker and more birefringent that those of the *79S* thin sections at parallel depths. This difference indicates that substantial alteration occurred during the intervening 38 years of hydrothermal alteration at diverse temperatures and fluid compositions in the volcano. The average density of the oven-dried lapilli tuff increased slightly from 1979 to 2017 (Fig. 5) probably through the growth of mineral cements in the vesicles of glass fragments and the ash matrix of the tuff (Fig. 4).

The moderate yellow (5Y 6/6) and olive brown (5Y 5/6 – 5Y 4/4) colours of palagonitized glass rinds in the *79S* thin sections (Fig. 4A, G, M, Table 1) are preserved in some *17S* thin sections, especially in samples from the submarine lapilli tuff (Fig. 4I, O, Table 1). In *79S* thin sections from the subaerial tuff cone and the submarine inflow zone, however, some palagonitized glass rinds have an unusual moderate to dark greenish yellow (10Y 6/6 – 10Y 6/4) colour (Fig. 4A, J, Table 1). This colour has been transformed to dark yellowish orange (10YR 6/6) and light brown (5YR 5/6) in the *17S* thin sections. The associated differences in authigenic mineral assemblages are not yet known.

Marked differences also exist in altered glass of the *79S* and *79SA* thin sections. Altered glass rinds in the *79SA* thin sections are more orange (Fig. 4E), more brown (Fig. 4K, N), and more birefringent (Fig. 4H) than those of the original *79S* thin sections at similar depths (Table 1). The unusual moderate to dark greenish yellow of altered glass in the *79S* thin sections from the subaerial tuff cone (sample *79S*-37.0 m) and submarine inflow zone (sample *79S*-147.7 m) (Fig. 4A, J) is dull olive brown (5Y 4/4) and olive gray (5Y 3/2) in the *79SA* thin sections (Fig. 4B, K, Table 1). The moderate greenish yellow (5Y 6/6) and olive brown (5Y 4/4) of altered glass rinds in *79S* thin sections from the upper submarine lapilli tuff (Fig. 4E) are pale yellowish orange (10YR 8/6) and light brown (5YR 5/6) in the equivalent *79SA* thin section (Fig. 4D). The rare yellowish-gray glass of lapilli in the *79S* thin section from the high temperature hydrothermal zone appears as dense, opaque nano-crystalline clay mineral in the equivalent *79SA* thin section (Fig. 4G, H); no translucent glass persists. The opaque moderate yellow brown (5Y 4/4) of altered fine ash in the *79S* thin section at 168.9 m.b.s. is grayish brown (5YR 3/2) in the *79SA* thin section at 170.1 m.b.s. (Fig. 4M, N). Overall, the internal zones of *79SA* glass fragments appear less translucent and tend to grayish yellow (5Y 8/4) or dusky yellow (5Y 6/4), as compared with the apparently fresh glass of *79S* thin sections (Fig. 4B, E, K, N, Table 1).

Storage conditions evidently had a pronounced influence on the surface colour of the submarine SE-01drill core, transforming it from grayish-green to yellowish brown over time in the repository environment. The thin section investigations (Figs. 4, 6) indicate that alteration under ambient conditions also influenced the petrographic characteristics of the lapilli tuff. The petrographic studies suggest the oxidation of iron in altered glass rinds (Fig. 4D, E, sites *a*, *a"*, Fig. 4J, K, sites *c, c"*), the transformation of fresh glass to nano-crystalline clay mineral (Fig. 4G, H, sites *b*, *b"*) and the possible crystallization of fine-grained, isotropic analcime that lends opacity to the *79SA* ash matrix (Fig. 4E, H).

A recent article describes the differences in the petrographic characteristics of the archived 1979 SE-01 drill core (*79SA*) and the 2017 SE-02B drill core (*17S*) as a means to estimate time-lapse alteration in the volcano from 1979 to 2017 (Prause *et al.* 2020). The study provides an important empirical record of alteration processes. The present investigations indicate, however, that the *79SA* samples do not provide a clear reference framework for alteration progress uniquely in the volcanic environment because they have undergone considerable change during the 38 years they resided in the core boxes. It also indicates that further sealing of the 2017 cores from atmospheric contamination in order to preserve their true alteration fabrics should be considered.

Possible endolithic microborings

Fine-scale microtubules similar to those inferred to be endolithic microborings indicative of microbial activity (Fisk *et al.* 2003, Staudigel *et al.* 2008, Walton 2008) occur in the apparently fresh glass of *79S* thin sections from the subaerial tuff cone, the *79S* and *17S* thin sections from the higher temperature hydrothermal zone, and the *17S* thin sections from the submarine inflow zone and the deeper submarine deposits (Fig. 6). Traces of microtubular structures along the surfaces of glass vesicles and microcracks also occur in a *79SA* thin section at 157.1 m.b.s. (Jackson *et al.* 2019b). The overall diameter of the tubules is remarkably constant, < 1 micron, whereas lengths show considerable variation. Generally, the tubules are straight or gently curved and they are usually of a constant length at a given site, 10 µm in some locations and 20 µm in others. The tubules mainly have a constant diameter, do not pinch and swell, and are not sharp at the tip but, instead, maintain diameter out to a blunt end. They protrude into apparently fresh glass and are packed together side-by-side where they emerge on the contact of fresh glass with the altered glass rind of a glass particle or the inner wall of a vesicle or a microcrack surface.

Microbiological analyses of fluids extracted from the SE-01 borehole in 2009 indicate traces of potentially indigenous thermophilic bacteria and archaea at 145 m.b.s. and 174 m.b.s. (Marteinsson *et al.* 2015). These studies suggest the possibility that some alteration could have occurred through biotic activity deep in the submarine lapilli tuff deposits of Surtsey. The tubular features suggestive of possible endolithic microborings are especially well-developed in a lapillus with apparently fresh glass in a *79S* thin section at 107.5 m.b.s. (Figs. 4G, 6D-G). There, the growth rate of microtubule lengths is about 2 µm/yr (30 µm since 1964). This rate is far more rapid than rates predicted by Staudigel *et al.* (2008) for tubular bioalteration in soils, which requires >1000 years to initiate. The borehole temperature measured at 107.5 m.b.s. in 1980, 140.8 °C (Jakobsson & Moore 1982), exceeded an inferred limit for functional microbial life, 120 °C (Ivarsson *et al.* 2015, Kashefi & Lovley 2003, Prieur & Marteinsson 1998). It is possible that an early low-temperature episode of functional microbial activity could have persisted for a few years before progressive heating produced the 141 °C temperature maximum measured in 1980 (Jakobsson & Moore 1982), which had decreased to 126 °C in 2017 (Jackson *et al.* 2019a).

CONCLUSIONS

Petrographic studies of thin sections from the 1979 and 2017 Surtsey drill cores describe narrow ash rims on coarse ash- to lapilli-sized basaltic glass pyroclasts in subaerial, submarine, and sub-seafloor lapilli tuff (Fig. 2), the progression of glass alteration in diverse environments from 1979 to 2017 (Fig. 4), and the characteristics of tubular microstructures in apparently fresh glass (Fig. 6). The origins of the narrow ash rims that outline altered glass pyroclasts in submarine and sub-seafloor deposits remain unclear. Some rims may record *in situ* granulation by thermal stress during submarine eruption. Other rims record alteration and/or depositional processes in the submarine and sub-seafloor environments that are poorly understood. In porous lapilli tuff 70 – 80 m below the pre-eruption seafloor, altered glass fragments with narrow rims of fine ash are surrounded by large, irregularly-shaped cavities that may be filled with mineral cements (Fig. 2E-F). These samples have low oven-dry density, 1.4 – 1.6 gr/cm^3 and high water absorption, 19 – 21 wt % (Fig. 5) (Jackson *et al*. 2019a, *their* table S1). Nearby samples, however, have a compact ash matrix with few vesicular cavities; they have higher dry density, 2.13 – 2.19 gr/cm^3 and low water absorption, 8 – 9 wt %. These differences produce a heterogeneous fabric in the submarine and sub-seafloor deposits.

Comparisons of the petrographic characteristics of glass fragments in the original thin sections of the 1979 drill core (*79S*) and the thin sections of the 2017 drill cores (*17S*) at corresponding depths indicate that alteration has progressed rapidly in all structural and hydrothermal environments over the past 38 years (Fig. 4, Table 1). Microtubules and narrow protrusions along contacts between fresh and altered glass are common in the apparently fresh glass of *79S* thin sections (Fig. 6). These features resemble endolithic microborings but further analyses are needed to determine possible traces of microbial activity. The microtubules have become obscured by progressive glass alteration in the *17S* thin sections (Fig. 6H, I).

The marked differences in the petrographic characteristics of the altered glass in the *79S* thin sections and the *79SA* thin sections, prepared after 38 years of archival storage (Fig. 4, Table 1), are verified through precise correlations with Munsell colours in plane polarized light and isotropic and birefringent characteristics (Table 1). The present investigations indicate that Surtsey glass remains labile at ambient temperatures and atmospheric conditions. This reactive propensity suggests that the 2017 cores may also evolve in the repository environment. The colours and fabrics of fresh and altered glass preserved in the original thin sections of the 1979 drill core (*79S*) therefore provide a critical reference for establishing past and future rates of alteration in the volcano (Figs. 4, 6). Measurements of rock material characteristics were made immediately post-drilling in 1979 and 2017 (Fig. 5) and so provide an accurate reference for changes in physical properties produced uniquely in the volcanic environment. Although many 2017 core sections are stored in nitrogen gas or under refrigeration, additional conservation efforts should be put into place and a reference suite of glass-covered thin sections prepared for the future core archive.

ACKNOWLEDGEMENTS

Funding for the SUSTAIN project was provided by the International Continental Scientific Drilling Program (ICDP); a grant of excellence from the Icelandic Research Fund, ICF-RANNÍS; the Bergen Research Foundation and K.G. Jebsen Centre for Deep Sea Research at the University of Bergen, Norway; the German Research Foundation (DFG); and DiSTAR, Federico II, University of Naples, Federico II, Italy. The University of Utah, USA, and the Icelandic power companies, Reykjavík Energy and Landsvirkjun, contributed additional funds. The logistical support organized by M. T. Gudmundsson and provided by the Icelandic Coast Guard was instrumental in carrying out the drilling operation. I gratefully acknowledge S. P. Jakobsson and J. G. Moore for their contributions to drilling on Surtsey, and the 2017 DOSECC drilling team led by B. Marshall with drillers S. Cole, J. Blouin, A. J. Vecchiarelli, M. Lyon, and M. Vinson along with all members of the science and technical teams for their contributions to the SUSTAIN project. K. Jónasson maintains the Surtsey drill core archive at the Iceland Institute of Natural History. Figure 1 was drafted by B. Black. J. Fisher contributed to measurements of material properties and high resolution scans of reference sample thin sections. The article has benefitted from reviews by J. McPhie, J. G. Moore, K. Jónasson and M. Ivarsson.

REFERENCES

Alexandersson, T., 1970. The sedimentary xenoliths from Surtsey: marine sediments lithified on the sea floor. Surtsey Research Progress Report 6, 101–116.

Alexandersson, T., 1972. The sedimentary xenoliths from Surtsey: turbidites indicating shelf growth. Surtsey Research Bulletin 5, 83–89.

ASTM C97/C97M-18, 2018. Standard Test Methods for Absorption and Bulk Specific Gravity of Dimension Stone, ASTM International, West Conshohocken, PA. DOI: https://doi.org/10.1520/C0097_C0097M-18.

Baldursson, S. & Á. Ingadóttir, 2007. Nomination of Surtsey for the UNESCO World Heritage List, Icelandic Institute of Natural History, Reykjavik.

Colombier, M., B. Scheu, U. Kueppers, S. J. Cronin, S. B. Mueller, F. B. Wadsworth, M. Tost, K. J. Dobson, B. Ruthensteiner & D. B. Dingwell, 2019. In situ granulation by thermal stress during subaqueous volcanic eruptions. Geology 47, 1–4.

Fisk, M. R. & N. McLoughlin, 2013. Atlas of alteration textures in volcanic glass from the ocean basins. Geosphere 39 (2), 317–341.

Fisk, M. R., M. C. Storrie-Lombardi, S. Douglas, R. Popa & C. Di Meo-Savoie, 2003. Evidence of biological activity in Hawaiian sub-surface basalts. Geochemistry Geophysics Geosystems 4 (12).
DOI: https://doi.org/10.1029/2002GC000387.

Fliegel, D., E. Knowles, R. Wirth, A. Templeton, H. Staudigel, K. Muehlenbachs & H. Furnes, 2012. Characterization of alteration textures in Cretaceous oceanic crust (pillow lava) from the N-Atlantic (DSDP Hole 418A) by spatially-resolved spectroscopy. Geochimica and Cosmochimica Acta 96, 80–93.

Furnes, H., H. Staudigel, I. H. Thorseth, T. Torsvik, K. Muehlenbachs & O. Tumyr, 2001. Bioalteration of basaltic glass in the oceanic crust. Geochemistry Geophysics Geosystems, 2 (8).
DOI: https://doi.org/10.1029/2000GC000150.

Gilbert, J. S. & S. J. Lane, 1994. The origin of accretionary lapilli. Bulletin of Volcanology 56, 398–411.

Ivarsson, M., S. Bengtson, H. Skogby, P. Lazor, C. Broman, V. Belivanova & F. Marone, 2015. A fungal-prokaryotic consortium at the basalt-zeolite interface in subseafloor. PLoS ONE 10 (10), e0140106.
DOI: https://doi.org/10.1371/journal.pone.0140106

Jackson, M. D., M. T. Gudmundsson, T. B. Weisenberger, J. M. Rhodes, A, Stefánsson, B. I. Kleine, P. C. Lippert, J. M. Marquardt, H. I. Reynolds, J. Kück, V. Th. Marteinsson, P. Vannier, W. Bach, A. Barich, P. Bergsten, J. G. Bryce, P. Cappelletti, S. Couper, M. F. Fahnestock, C. F. Gorny, C. Grimaldi, M. Groh, Á. Gudmundsson, Á. Th. Gunnlaugsson, C. Hamlin, Th. Högnadóttir, K. Jónasson, S. S. Jónsson, S. L. Jørgensen, A. M. Klonowski, B. Marshall, E. Massey, J. McPhie, J. G. Moore, E. S. Ólafsson, S. L. Onstad, V. Perez, S. Prause, S. P. Snorrason, A. Türke, J. D. L. White & B. Zimanowski, 2019. SUSTAIN drilling at Surtsey volcano, Iceland, tracks hydrothermal and microbiological interactions in basalt 50 years after eruption, Scientific Drilling, 25, 35–46.
DOI: https://doi.org/10.5194/sd-25-35-2019.

Jackson, M. D., S. Couper, C. V. Stan, M. Ivarsson, M. Czabaj, N. Tamura, D. Parkinson, L. M. Miyagi & J. G. Moore, 2019b. Authigenic mineral textures in submarine 1979 basalt drill core, Surtsey volcano, Iceland. Geochemistry, Geophysics, Geosystems 20 (7).
DOI: https://doi.org/10.1029/2019GC008304.

Jakobsson, S. P. & J. G. Moore, 1982. The Surtsey Research Drilling Project of 1979. Surtsey Research Progress Report 9, 76–93.

Jakobsson, S. P. & J. G. Moore, 1986. Hydrothermal minerals and alteration rates of Surtsey volcano, Iceland. Geological Society of America Bulletin 97 (5), 648–659.

Jakobsson, S. P., K. Thors, Á. T. Vésteinsson & L. Ásbjörnsdóttir, 2009. Some aspects of the seafloor morphology at Surtsey Volcano: the new multibeam bathymetric survey of 2007. Surtsey Research 12, 9–38.

Kashefi, K. & D. R. Lovley, 2003. Extending the upper temperature limit for life. Science 301, 934.

Lorenz, V., 1974a. Vesiculated tuffs and associated features. Sedimentology 21, 273–291.

Lorenz, V., 1974b. Study of the Surtsey tephra deposits. Surtsey Research Progress Report 7, 72–79.

Lorenz, V., 1986. On the growth of maars and diatremes and its relevance to the formation of tuff rings. Bulletin of Volcanology 48, 265–274.

Lorenz, V., S. Suhr & P. Suhr, 2017. Phreatomagmatic maar-diatreme volcanoes and their incremental growth: A model. In Németh, K., G. Carrasco-Nuñez, J. J. Aranda-Gómez & , I. E. M. Smith (eds), Monogenetic Volcanism. Geological Society, London, Special Publications, 446.
DOI: http://doi.org/10.1144/SP446.4

Marteinsson, V., A. Klonowski, E. Reynisson, P. Vannier, B. D. Sigurdsson & M. Ólafsson, 2015. Microbial colonization in diverse surface soil types in Surtsey and diversity analysis of its subsurface microbiota. Biogeosciences 12, 1191–1203.

Moore, J. G., 1985. Structure and eruptive mechanism at Surtsey Volcano, Iceland. Geological Magazine 122, 649–661.

McPhie, J., J. D. L. White, C. Gorny, M. D. Jackson, M. T. Gudmundsson & S. Couper, 2020. Lithofacies from the 1963-1967 Surtsey eruption in SUSTAIN drill cores SE-2a, SE-2b and SE-03. Surtsey Research 14, 19-32.

Moore, J. G. & M. D. Jackson, 2020. Observations on the structure of Surtsey. Surtsey Research 14, 33-45.

Mueller, S. B., U. Kueppers, P. M. Ayris, M. Jacob & D. B. Dingwell, 2016. Experimental volcanic ash aggregation: Internal structuring of accretionary lapilli and the role of liquid bonding. Earth and Planetary Science Letters 433, 232–240.

Oddson, B., 1982. Rock quality designation and drilling rate correlated with lithology and degree of alteration in volcanic rocks from the Surtsey 1979 drill hole. Surtsey Research Progress Reports 9, 94–97.

Prause, S., T. B. Weisenberger, P. Cappelletti, C. Grimaldi, C. Rispoli, K. Jónasson, M. D. Jackson & M. T. Gudmundsson, 2020. Alteration progress within the Surtsey hydrothermal system, SW Iceland – a time-lapse alteration study of cores drilled in 1979 and 2017. Journal of Volcanology and Geothermal Research 392, 106754.

Prieur, D. & V. Th. Marteinsson, 1998. Prokaryotes living under elevated hydrostatic pressure. Advances in Biochemical Engineering / Biotechnology 61, 23–35.

Reynisson, R. F. & Jakobsson, S. P., 2009. Xenoliths of exotic origin at Surtsey volcano, Iceland. Surtsey Research Bulletin 12, 21–27.

Schipper, C. I., S. P. Jakobsson, J. D. L. White, J. M. Palin & T. Bush-Marcinowski, 2015. The Surtsey magma series. Scientific Reports 5, 11498.
DOI: 10.1038/srep11498.

Schumacher, R. & H.-U. Schmincke, 1995. Models for the origin of accretionary lapilli. Bulletin of Volcanology 56 (8), 626–639.

Staudigel, H., H. Furnes, N. McLoughlin, N. R. Banerjee, L. B. Connell & A. Templeton, 2008. 3.5 billion years of glass bioalteration: Volcanic rocks as a basis for microbial life? Earth Sciences Reviews 89, 156–176.

Thorseth, I. H., H. Furnes & O. Tumyr, 1991. A textural and chemical study of Icelandic palagonite of varied composition and its bearing on the mechanism of the glass-palagonite transformation, Geochimica and Cosmochimica Acta 55, 731–749.

Thorseth, I. H., T. Torsvik, V. Torsvik, F. L. Daae & R. B. Pedersen, 2001. Diversity of life in ocean floor basalt. Earth and Planetary Science Letters 194 (1-2), 31–37.
DOI: https://doi.org/10.1016/S0012-821X (01)00537-4

Thórarinsson, S., 1965. The Surtsey eruption, course of events and the development of the new island. Surtsey Research Progress Report 1, 52–59.

Thórarinsson, S., 1967. Surtsey, The New Island in the North Atlantic. The Viking Press, New York.

Thórarinsson, S., Th. Einarsson, G. Sigvaldason & G. Elísson, 1964. The submarine eruption off the Vestmann Islands 1963–64. Bulletin of Volcanology 29, 435–455.

Türke, A., M. D. Jackson, W. Bach, W.-A. Kahl, B. Grzybowski, B. Marshall, M. T. Gudmundsson & S. L. Jørgensen, 2019. Design of the subsurface observatory at Surtsey Volcano, Iceland. Scientific Drilling 25, 57–62.
DOI: https://doi.org/10.5194/sd-25-57-2019

Walton, A. W., 2008. Microtubules in basalt glass from Hawaii Scientific Drilling Project #2 phase 1 core and Hilina slope, Hawaii: evidence of the occurrence and behavior of endolithic microorganisms. Geobiology 6, 351–364.

Weisenberger, T. B., M. T. Gudmundsson, M. D. Jackson, C. F. Gorny, A. Türke, B. I. Kleine, B. Marshall, S. L. Jørgensen, V. Th. Marteinsson, A. Stefánsson, J. D. L. White, A. Barich, P. Bergsten, J. G. Bryce, S. Couper, M. F. Fahnestock, H. Franzson, C. Grimaldi, M. Groh, Á. Gudmundsson, Á. Th. Gunnlaugsson, C. Hamelin, Th. Högnadóttir, K. Jónasson, S. S. Jónsson, A. Klonowski, J. Kück, R. L. Magnússon, E. Massey, J. McPhie, E. S. Ólafsson, S. L. Onstad, S. Prause, V. Perez, Velveth, J. M. Rhodes & S. P. Snorrason, 2019. Operational Report for the 2017 Surtsey Underwater volcanic System for Thermophiles, Alteration processes and INnovative concretes (SUSTAIN) drilling project at Surtsey Volcano, Iceland: GFZ German Research Centre for Geosciences.
DOI: http://doi.org/10.2312/ICDP.5059.001

Erosion and sedimentation in Surtsey island quantified from new DEMs

BIRGIR VILHELM ÓSKARSSON [1], KRISTJÁN JÓNASSON [1], GUÐMUNDUR VALSSON [2] AND JOAQUÍN M. C. BELART [2,3]

[1]Icelandic Institute of Natural History, Urriðaholtsstræti 6–8, 210 Garðabær, birgir@ni.is (corresponding author).

[2]National Land Survey of Iceland, Stillholt 16–18, 300 Akranes.

[3]Institute of Earth Sciences, University of Iceland, Sturlugata 7 - Askja, 101 Reykjavík.

ABSTRACT

We present data from a photogrammetric study on Surtsey island that generated three new DEMs and orthoimages, two from scanned aerial images from 1967 and 1974 and one from high-resolution close-range images from a survey in 2019. DEM differencing allowed for quantification of the erosion and the sedimentation in the island since 1967. Of the subaerial volcanics, about 45% of the lava fields have eroded away but only about 16% of the tuff cones. The prevailing SW coastal wave erosion is evident from the erosive pattern in Surtsey, and the cumulative loss of the coastal margins amounts to $28\pm0.9\text{x}10^6$ m^3 since 1967, with the current average erosion rate of $0.4\pm0.02\text{x}10^6$ m^3/yr. Wind deflation and runoff erode the tuff cones and the sediments at the flanks of the cones, with the total volume loss amounting to $1.6\pm0.2\text{x}10^6$ m^3 and the current erosion rate of $0.03\pm0.004\text{x}10^6$ m^3/yr. A rapid decline in erosion rates characterized the first years post-eruption, and the coastal erosion rate during the winter of 1967–68 was about 5–6 times higher than the current erosion rate due to the thinner and less cohesive nature of the lava apron at the edge of the shelf. The cones eroded at a rate about 2–3 times higher during the first years due to the uncompacted and unconsolidated nature of the cones at that time. The 2019 area of 1.2 km^2 and an extrapolation of the current erosion rate fits well with the projected erosion curve of Jakobsson et al. (2000) with the island becoming a tuff crag after approximately 100 years.

INTRODUCTION

Since the emergence of Surtsey island from the sea on November 14th 1963, researchers have monitored the island from air, sea and land; systematically documenting its growth during the eruption and its rapid post-eruption erosion (e.g. Einarsson 1965, Thorarinsson 1964, 1966, 1968, Norrman 1970, 1978, 1985, Jakobsson & Gudmundsson 2003, Jakobsson et al. 2009, Romagnoli & Jakobsson 2015). During the early stages of Surtsey, the active involvement of seawater with the erupting basalts in the relatively shallow subaqueous environment (130 m depth), generated high energy phreatomagmatic eruptions, the eruption becoming a "type" in the international classification scheme for explosive eruptions known as "Surtseyjan eruption" (Walker 1973). The eruption formed two crescent shaped tephra cones and the primary constituents were intercalated layers of fine and coarse-grained tephra, lithics, accretionary lapilli and fusiform bombs (e.g. Lorenz 1974, Norrman 1974). The non-cohesive tephra, saturated with water, was easily eroded by the waves and washed away with the swash. Two adjacent syn-eruptions, Syrtlingur and Jólnir, formed ephemeral islands that eroded completely within months and a third eruption, Surtla, only formed a seamount (e.g. Thorarinsson 1964, 1966, 1968). With the isolation of the vent area in Surtsey from the sea around April 1964, and the transition to effusive volcanism, two half lava shields formed, one in the Surtungur cone from April 1964 to May 1965 and the other in the Surtur cone from August 1966 to June 1967. Lava entering the sea built a delta of foreset breccia and quenched vitric fragments (Thorarinsson 1968, Kjartansson 1966). Subaerial lava flows that were emplaced on top of the delta extended the coastline to the south and eventually protected the cones from the strong coastal erosion and allowed the tephra to palagonitize and consolidate into tuff. The process of palagonitization turned out to be surprisingly fast and in 10 years about 64% of the total tephra had already palagonitized, significantly increasing the resistance of the cones to erosion (Jakobsson 1972, 1978).

Despite the lava fields to the south shielding the cones, erosion progresses at a remarkably high rate and in 2019 the maximum coastal retreat reached 720 m and the total area lost because of erosion since 1965 accumulated to 1.8 km^2 (e.g. Norrman 1970, 1978, 1985, Jakobsson et al. 2009). The steep submarine slope of Surtsey volcano and its location at the outer margin of the Iceland shelf create conditions for high energy waves to converge and break full-force on the island (Norrman 1970, 1978). Moreover, strong submarine currents circle the island and wave erosion extends down to depths of >50 m as seen in the eroded mounds of Jólnir, Syrtlingur and Surtla (Normann 1970, Jakobsson et al. 2009). Extreme erosion was observed in the first years, notably during the winter of 1967–1968, when the southeastern lava apron retreated by up to 140 m (Norrman 1970). Before that year or since 1965, the lava field of Surtungur had already retreated by about 150 m (Thorarinsson 1968). The structure of the lava flows, with close-spaced (cm to 1–2 m) vertical and subvertical polygonal joints, makes them susceptible to brittle fracturing and failure under stress. The eroded lava cliffs collapse in large blocks, the talus is grinded by the swash and the boulders are heavily polished and rounded in a matter of days (Thorarinsson 1966). Boulders, gravel and sand are then transported and graded along the shores to a spit north of the island (Thorarinsson 1966, Norrman 1970, Calles et al. 1982), the supply decreasing in recent years leading to a recession of the spit. Erosion of the west coast has led to a steepening of the western side of the tuff cone, the cliff developing a notch with overhanging scarps. Moreover, wind erosion is intense and storms with hurricane force are frequent (Petersen & Jónsson 2020). With compaction, alteration and subsequent palagonitization of the cones, the erosion rate has decreased, but by 1980 the cones had in localized areas lowered by 1.5–2 m (Ingólfsson 1982) and by up to 4 m in 2004 (Baldursson & Ingadóttir 2007). Wind-blown tephra accumulates in natural traps within the lava fields and around the cones, parts of this tephra originating from the eruptions of Jólnir and Syrtlingur (Thorarinsson 1968). Runoff from seasonal rain erodes rills and gullies in the unconsolidated tephra and sediments. Slumps, mudflows and solifluction mobilize the tephra on the slopes of the cones that accumulate in taluses (Norrman 1970, Calles et al. 1982, Ingólfsson 1982).

Despite the numerous studies documenting the geomorphic change in Surtsey, only minor reference is to the volumetric quantification (e.g. for coastal erosion in Norrman 1970). The total volumetric change was estimated from topographic maps and scanning airborne laser altimetry showing a volumetric decrease of about 25% from 1968 to 1998 (Garvin et al. 2000). Nevertheless, quantification of the total material loss by erosion and the sediments deposited or redeposited on the island is lacking.

Photogrammetry techniques allow for the generation of high-quality digital elevation models (DEMs) from overlapping nadir and oblique photographs, including from scanned aerial images (e.g. Pedersen et al. 2018, Belart et al. 2019), and nowadays image acquisition with unmanned aerial vehicles (UAVs) is a rapid and cost-effective way to monitor natural environments. Geodetic techniques allow measurements with centimeter precision and geolocation of points in the images yield precise 3D models.

This article presents data processed with digital photogrammetric techniques generating a high-resolution DEM for 2019 in addition to two DEMs, one for 1967, the year the eruption ceased, and one for 1974, when the tephra cones had become largely palagonitized and denudation rate had declined significantly. Available is a rich archive of quality photosets with good overlap that can be used to generate DEMs for past years (Landmælingar Íslands 2020, Loftmyndir ehf 2020). Differencing these models yields an overall quantification of the elevation and volume changes since 1967. In addition, we present field observations from a survey in 2019 that aid in the interpretation of the photogrammetric data. Although the comparison in this study is limited to three DEMs, we will here describe the methods and set the stage for future studies quantifying in higher temporal resolution the geomorphic changes in Surtsey.

The Surtsey volcano

Surtsey is a volcanic island located about 30 km from the south coast of Iceland and a part of the Vestmannaeyjar archipelago. The eruption of Surtsey began in 1963 and was active intermittently for a period of 3.5 years, terminating in mid-1967 (Einarsson 1965, Thorarinsson 1964, 1966, 1968). The eruption formed a submarine ridge, about 5.8 km long trending SW–NE, that fed four long-lived eruptions, three of which formed islands and one a seamount. Only Surtsey remains as an island. The Surtsey volcano, with two vents, formed two tephra cones in phreatomagmatic eruptions and two half lava shields in effusive eruptions, with a total area of 2.7 km^2. The total volume of Surtsey volcano was estimated to be about 1.1–1.2 km^3 of which 70% was tephra and 30% lava (Thorarinsson 1968). The subaerial volume of the island at the end of the eruption in 1967 was estimated to be about 0.1 km^3 and the highest point of the island 173 m a.s.l. (Thorarinsson 1968, Jakobsson et al. 2000). In total, lava comprised about 0.3–0.4 km^3 of the total erupted volume, including the submarine foreset breccia but of this volume, only about 0.07 km^3 was estimated to be subaerial (Thordarson 2000). The tephra comprised about 0.7–0.8 km^3 of which only 0.04–0.05 km^3 was subaerial.

METHODS

Surtsey was visited in July 18–22, 2019 in the yearly monitoring expedition led by the Icelandic Institute of Natural History. A geodetic survey measured ten ground control points (GCPs) marked with targets (Fig. 1A, label Flagg) along with ten other nearby natural points (Flagg_ex, Nat1), an old benchmark (626, Fig. 1B) and the center of the helipad (THP_C_f). The location of the GCPs are shown in Fig. 2B and the coordinates and labels given in Table 1. The benchmark SURS (Fig. 2B, Sturkell et al. 2009) was occupied with a Trimble NetR5

Table 1. GPS coordinates of ground control points, and their numbers, labels and reference stations. The height h and H are in meters, h is in an ellipsoidal geodetic reference system and H in a vertical reference system.

Nr.	GCP'S	Lat	Lon	h (GRS80)	H (ISH2004)
1	626	63°18'00.69806"	-20°36'38.08563"	118,67	53,89
2	Flagg1	63°18'07.60633"	-20°36'48.81971"	142,94	78,17
3	Flagg1_ex	63°18'07.37060"	-20°36'48.98645"	141,76	76,98
4	Flagg2	63°18'14.19832"	-20°36'55.43431"	159,24	94,46
5	Flagg2_ex	63°18'13.92611"	-20°36'55.48831"	159,99	95,20
6	Flagg3	63°18'14.67978"	-20°36'23.70404"	175,48	110,70
7	Flagg3_ex	63°18'14.55741"	-20°36'23.33110"	175,26	110,49
8	Flagg4	63°17'51.17985"	-20°35'54.95749"	89,10	24,33
9	Flagg4_ex	63°17'50.82319"	-20°35'53.84254"	90,49	25,73
10	Flagg5	63°17'48.80348"	-20°36'18.18708"	87,44	22,68
11	Flagg5_ex	63°17'48.39999"	-20°36'17.21318"	87,20	22,43
12	Flagg6	63°18'12.82605"	-20°35'35.81968"	78,00	13,23
13	Flagg6_ex	63°18'12.81001"	-20°35'35.05744"	79,84	15,07
14	Flagg7	63°18'22.59821"	-20°35'48.54144"	71,21	6,43
15	Flagg7_ex	63°18'22.12830"	-20°35'47.89453"	71,78	7,00
16	Flagg8	63°18'32.00115"	-20°35'55.75310"	70,28	5,50
17	Flagg8_ex	63°18'32.03681"	-20°35'55.79452"	70,30	5,51
18	Flagg9	63°18'25.15451"	-20°36'11.09302"	77,33	12,55
19	Flagg9_ex	63°18'25.19063"	-20°36'11.08543"	77,19	12,40
20	Nat1	63°18'11.59753"	-20°36'51.60637"	156,14	91,36
21	THP_C_f	63°18'01.04796"	-20°35'50.81561"	98,84	34,07
	Reference	**Lat**	**Lon**	**h (GRS80)**	**H (ISH2004)**
22	SURS	63°18'00.79004"	-20°36'20.00381"	115,10	50,33
23	VMEY	63°25 37.16530"	-20°17'36.81215"	135,28	70,31
24	SELF	63°55 44.33199"	-21°01'56.00393"	79,97	13,94

Figure 1. Images from the field work in July 2019. A) Targets used for marking ground control points. B) Surveyor measuring an old benchmark on a lava flow. C) Photographing from the Coast Guard helicopter. Courtesy Barbara Klein. D) The Phantom 4 Pro UAV used in the mapping.

receiver and an NAX3G+C antenna from July 19–22. This benchmark served as a base for the GCP campaign. After choosing suitable locations for the GCP signals and the natural ex-center points a Fast-Static survey was carried out with a Trimble R10 Global Navigation Satellite System (GNSS) receiver. The occupation time was about 8–12 minutes at each point. Additionally, a Network Real-Time Kinematic (RTK) measurements using the National Land Survey of Iceland´s (NLSI's) IceCORS Network were performed at the same GCPs where there was mobile connection. In total 21 points were measured with Fast-Static and 15 points with Network RTK. The GNSS data was processed with a GrafNet GNSS post-processing software. The first step was to compute an accurate position for SURS. The coordinates were computed using the permanent station VMEY in Heimaey and SELF in Selfoss as reference stations. Then the GCP coordinates were computed using SURS and VMEY as reference stations. A network adjustment was performed, giving 1.2 cm rms (root mean square) in plane and 1.5 cm rms in height. Comparison with the Network RTK measurements showed good agreement where the biggest difference was 1.4 cm in plane and 2.7 cm in height. Finally, ISH2004 heights were computed using NLSI's geoid model in the Cocodati transformation application.

Geotagged nadir and oblique photographs were taken from a helicopter with a Nikon D850 45 MP with a 35 mm Zeiss Distagon lens with a B+W 72 mm MRC Nano XS-pro filter (Fig. 1C). Photographing was also done from a DJI Phantom 4 Pro drone mounted with a FC6310 20 MP camera and an 8.8 mm lens (Fig. 1D). About 1500 nadir and oblique photographs were taken at altitudes of 80–340 m. The average ground sampling distance of the images (GSD) was 5.49 cm/pixel.

The field and analytical workflow is described in (Sørensen & Dueholm 2018) and the data processed in Pix4Dmapper (Pix4Dmapper 2019), a commercial digital photogrammetric software. The resulting products were a DEM, an orthoimage, a point cloud and a mesh model (Fig. 2A–B and 4A–D).

The Pix4Dmapper reported optimum results for all processing steps of the 2019 model. Georeferencing was achieved with 18 GCPs with an error less than

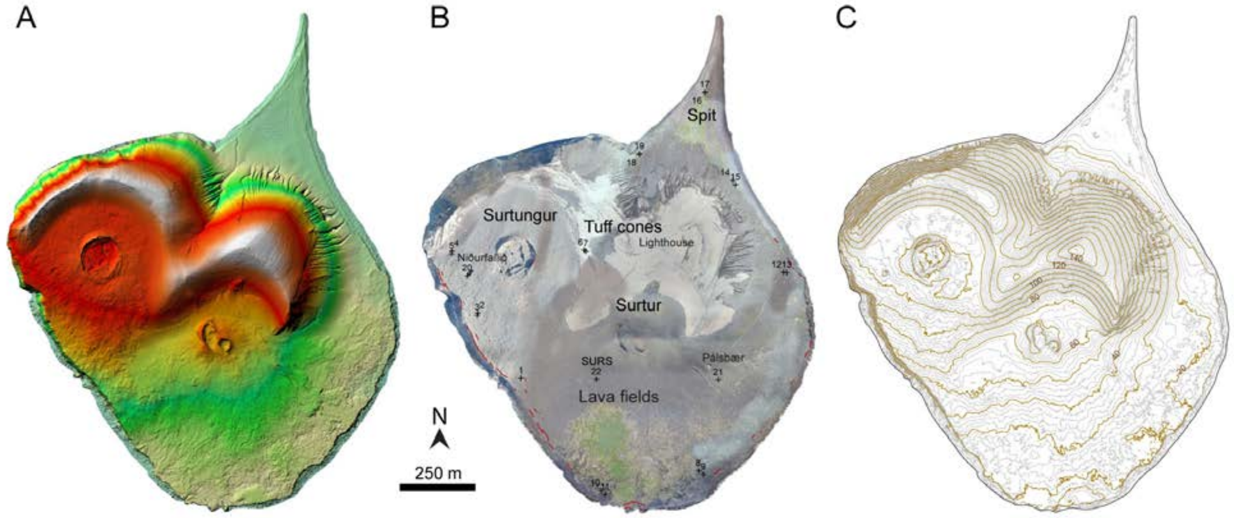

Figure 2. The products of the 2019 photogrammetry project. A) A DEM of Surtsey in 10x10 cm, visualized as a color-coded shaded relief. B) An orthophoto of Surtsey showing the main geologic formations on the island, the location of reference points as the hut Pálsbær, the lighthouse and the "Niðurfallið" (Icelandic for "drain pipe", a pit crater above a lava tube), the locations of the GCPs (crosses, see locations of numbers in Table 1) and the crack systems from wave loading at the margins of the lava fields (red lines). C) Contour lines generated from the DEM with line interval of 2 m (gray) and 10 m (yellow).

two times the average GSD (rms of 0.061 m). The number of 3D points had an average density of 29 pts m^{-3}. The point cloud was linearly interpolated into a 10x10 cm DEM, and an orthoimage was created in 5x5 cm. Both DEM and orthoimage were projected in the ISN2016 reference system. The DEM displayed minor artefacts, only small holes from shadows in the south cliff region and on the west slope of Surtungur tuff cone. The resulting DEM was compared to the GPS points surveyed, yielding a median elevation difference of 0.01 m and a Normalized Mean Absolute Deviation (NMAD, Höhle & Höhle, 2009) of 0.11 m.

The aerial photographs of 1967 and 1974 were processed following the method described in Belart et al. (2019). This consists of a semi-automatic workflow where the photogrammetric software MicMac (Pierrot Deseilligny & Clery 2011; Rupnik et al. 2017) is used, and the only input required is the digitization of GCPs. The GCPs were extracted from the 2019 DEM and orthoimage, and additional GCPs were included at different locations along the coast of the 1967 and 1974 datasets, assumed to have zero elevation. As a result, DEMs in 2x2 m and orthoimages in 50x50 cm were created from the 1967 and 1974 datasets. Gaps and outliers in the resulting DEMs and orthoimages were due to bad matching because of shadows or surfaces such as homogeneous tephra. These areas were manually masked out for visualization (Fig. 3), and for volume calculation they were linearly interpolated using a Delaunay triangulation.

The volume of the different lithologies on the island in 2019, that include the lava fields, the tuff cones, the cone sediments (sediments on the flanks of the tuff cones comprised of aeolian sand, talus and debris fans) and the spit sediments, were calculated in Pix4Dmapper using a reference base-plane of zero m elevation while the base of the cone sediment was triangulated. The areal distribution of each lithology was based on field reconnaissance, nadir images and the geological maps of Sveinn Jakobsson (Náttúrufræðistofnun Íslands, Reykjavík, unpublished maps of Surtsey in 1:5,000: 1967, 1977, 2016). The erosion and sedimentation volumes were calculated from the DEM differences (dDEMs) of 1967–1974 and 1974–2019 (Fig. 3). To quantify the processes, i.e. coastal erosion, wind and runoff erosion as well as sedimentation, we specified areas based on the results of the dDEMs and the different lithologies on the geological maps (Fig. 3 and Table 2). The pixels of the analyzed area were summed up and multiplied by the pixel area (e.g. McNaab et al. 2019). Uncertainties in elevation of the DEMs of 1967 and 1974 and the volume calculations were estimated assuming an uncertainty of 1 m for the marginal areas (areas 1, 2 and 5 in Fig. 3) and

Table 2. Areas and volumes of Surtsey island from the 1967, 1974 and 2019 DEMs , and of the main lithologies measured from the 2019 DEM and point cloud. Below are the volume changes from the 1967–1974 and 1974–2019 dDEMs. The area for each location numbered 1–7 is shown in Figure 3.

DEM	**Month**	**Area m^2**	**Volume (x 10^6 m^3)**	**Vol% of 1967**
2019	19–21 July	1251310	70.69±0.12	71,0
1974	16 July	2117962	90.71±2.12	91,1
1967	18 July	2659034	99.63± 2.66	100,0
2019 DEM and point cloud		**Area m^2**	**Volume (x 10^6 m^3)**	**Vol% of 2019**
Lava fields	July	660976	31.8±0.06	44,8
Tuff cones	July	443220*	38.6±0.04	54,4
Spit sediment	July	122542	0.3±0.005	0,4
Sediment	July	153930	0.3±0.008	0,4
Volume change 1967–1974				
	Area m^2	**Volume (x 10^6 m^3)**		**Avg./yr (x 10^6 m^3) loss**
		Positive	Negative	
1-Cliff lava	491435	0.026±0.036	-6.999±0.553	-0.999±0.079
2-Cliff tephra/tuff	121284	0.011±0.009	-2.658±0.113	-0.380±0.016
3-Tephra/tuff cones	408544	0.336±0.117	-0.248±0.088	-0.035±0.013
4-Lava fields	1122572	0.430±0.280	-0.417±0.281	-0.060±0.04
5-Spit sediment	—	0.181±0.048	-0.507±0.244	-0.072±0.035
6-Sediment	216916	0.447±0.091	-0.091±0.018	-0.013±0.003
7-Scoria cones	32928	0.033±0.014	-0.011±0.002	-0.0016±0.0003
Total		1.464±0.595		
Total			-10.931±1.299	-1.562±0.186
Net loss			-9.467±1.894	-1.352±0.271
Volume change 1974–2019				
1-Cliff lava	615928	0.031±0.035	-15.484±0.693	-0.344±0.015
2-Cliff tuff	112809	0.003±0.001	-2.931±0.113	-0.065±0.003
3-Tuff cones	287104	0.011±0.005	-0.922±0.276	-0.020±0.004
4-Lava fields	535010	0.055±0.078	-0.199±0.188	-0.004±0.004
5-Spit sediment	—	0.051±0.027	-0.735±0.214	-0.016±0.005
6-Sediment	191071	0.257±0.046	-0.384±0.063	-0.009±0.001
7-Scoria cones	31953	0.003±0.003	-0.034±0.014	-0.0008±0.0003
Total		0.409±0.193		
Total			-20.689±1.422	-0.459±0.032
Net loss			-20.280±1.615	-0.451±0.036

* Sediments around the tuff cones included in area.

0.5 m for central areas (areas 3, 4, 6 and 7). This uncertainty is estimated based on similar datasets processed in Iceland between 1960s and 1970s, which have uncertainties ranging from 0.3 m to 0.8 m (Magnússon et al. 2016, Belart et al. 2019), since no unchanged terrain can be used in Surtsey as a proxy for uncertainties. The lower uncertainty of 0.5 m is assumed based on the difference of elevation observed in areas with little changes (Fig. 3). The uncertainty of the DEM of 2019 was estimated as 0.2 m, based on the difference between the DEM and the GPS measurements. For simplicity, the uncertainty neglects errors due to subsidence post-eruption and errors in the definition of the "zero" elevation at the sea level, which do not consider effects of tides or changing waves during the acquisition of photographs. The subsidence post-eruption in Surtsey is attributed to a compaction of the volcanic material and the underlying sediments and a down sagging of the volcano, totaling 1.1 m in 1991 (greatest in the Surtur vent area), followed by a continuous subsidence rate of approximately 1 cm/yr until 2000 (Moore et al. 1992, Sturkell et al. 2009). For the purpose of this study, this subsidence, that could amount to 1–2% of the original volume, was not included in the interpolation in order not to skew the quantification of the erosive and sedimentary products.

RESULTS

Area and volume calculations from the DEMs

The total area and volume calculations of the DEMs are given in Table 2. In addition, we include the calculated area and volume from the 2019 DEM

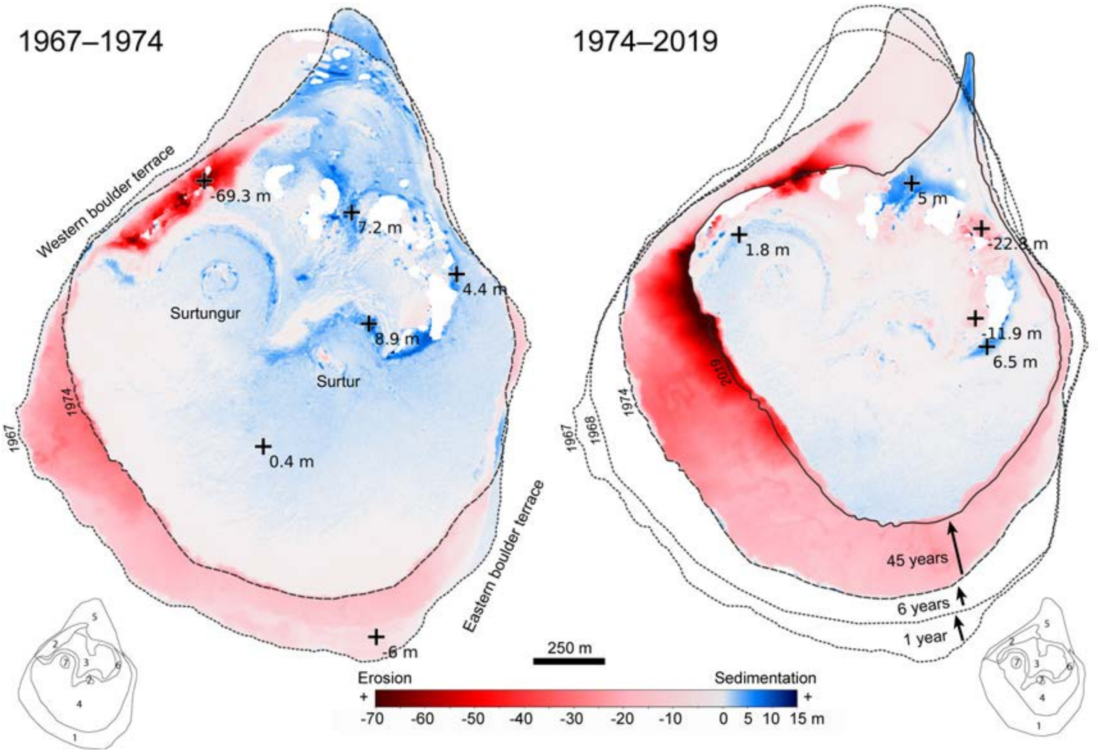

Figure 3. Elevation differences from the 1967–1974 and 1974–2019 dDEMs showing the main geomorphic changes in Surtsey since the end of the eruption. The colors give the values in meters of material eroded (red) or deposited (blue). The thickness in meters for selected locations (crosses) is shown for reference. Stippled lines show the areal change since 1967 and arrows the respective years between them. The numbers in the overview maps on the sides show the areas used in the calculations in Table 2.

and point cloud for the lava fields, the tuff cones, the sediments around the cones and the spit.

Difference in elevation

The positive and the negative volume change for the dDEMs of the 1967–1974 models and the 1974– 2019 models is shown in Figure 3. The values reflect the volume lost by erosion or gained with sedimentation and are in good agreement with documented field observations. The 1967–1974 dDEM shows the extensive erosion of the southern lava fields (totaling about 0.49 km^2) and the erosion of the northwestern part of the tephra/tuff cones (the cones were undergoing palagonitization during this period and changing from tephra to cemented tuff and are thus referred to here as tephra/tuff cones). It shows the sedimentation and the erosion of the southeastern boulder terrace that eroded away in 1968 (Norrman 1970) as well as the shrinking and migration to the east of the spit. It also shows marked erosion of the inner flanks of the tephra/tuff craters and the early sediment accumulation at the base of the cones (4–9 m). Evidence of sedimentation and possibly mass wasting is seen in the positive areas of the upper rims and northern flanks of the tephra/ tuff cones. A negative area inside the scoria cone of Surtur was verified on the aerial photographs to be the collapse of a small intra-crater scoria cone, the remains of which can still be found inside the larger Surtur scoria cone.

The 1974–2019 dDEM shows extensive erosion of the southern lava fields (totaling about 0.61 km^2) and the west side of Surtungur (Fig. 3). Negative areas of the tuff cones show pronounced erosion, especially on the eastern side where the gullies are found. Continuous accumulation of sediments is seen on the northern and eastern flanks of the tuff cones and within the craters. The spit continues to undergo recession and eastward migration. The crest of the scoria cones has undergone minor degradation.

It is worth presenting a few additional observations from the field survey in 2019. From oblique images and the mesh model we observe and measure a notch 2–4 m deep and 14–90 m high in the western tuff cone (Fig. 4A). Also seen are cave formations 10–30 m deep and 10–20 m high in the

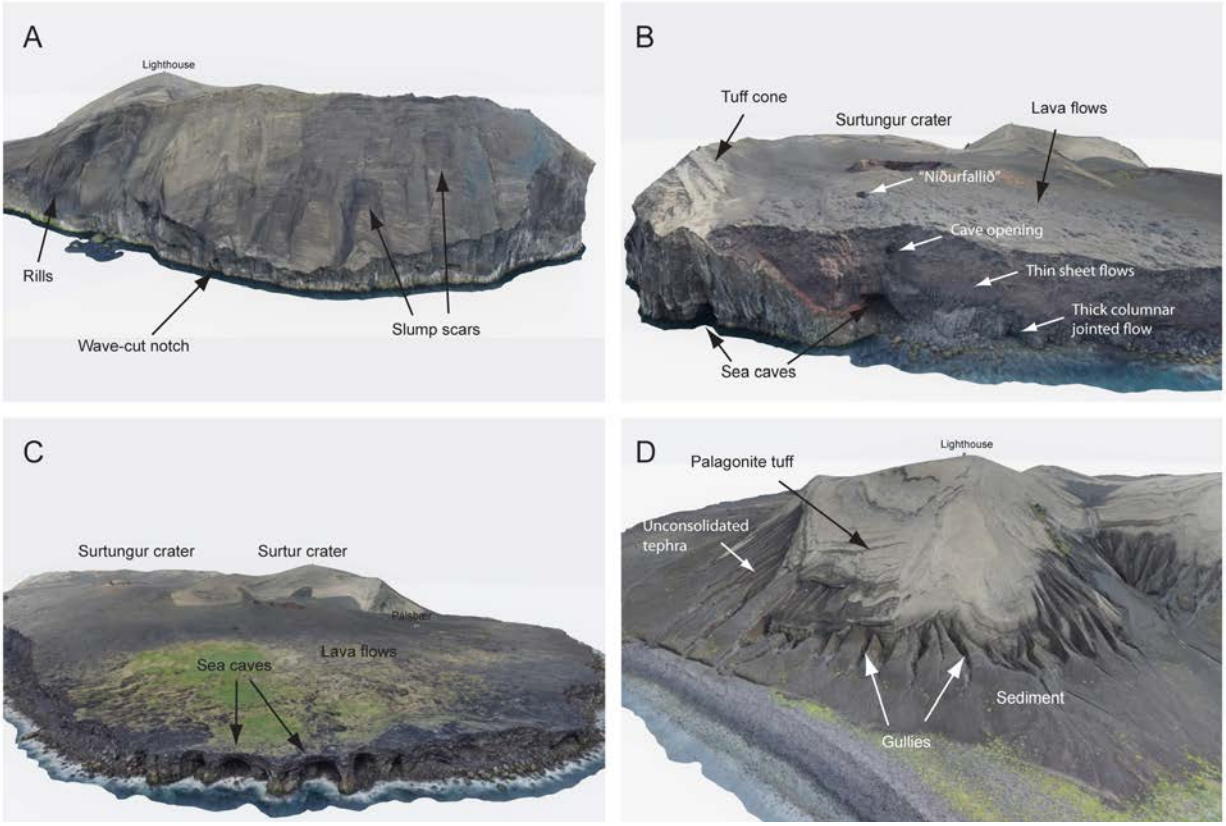

Figure 4. Images of the mesh model showing erosion features in Surtsey (the mesh model can be viewed at www.ni.is/surtsey-i-thriv-idd). A) The NW side of Surtsey showing the notch and slump scars in the Surtungur tuff cone. Field of view is about 800 m. B) The SW side of Surtsey showing the sea caves forming in the tuff cone and at the contact between the tuff cone and the lava flows. Field of view is about 600 m. C) The SE side of Surtsey showing the sea caves in the apron of the Surtur lava field. Field of view is about 1.2 km. D) The NE side of Surtur tuff cone showing the gullies forming at the boundary between the unconsolidated sediments (dark brown) and the palagonitized tuff (light brown). Field of view is about 700 m.

tuff and the lava flows (Fig. 4B–C). A conspicuous system of cracks was mapped parallel to the cliffs along the entire southern coast, most 1–5 m into the lava fields, up to 170 m long, and a less conspicuous system of cracks can be found 25–47 m further into the fields in the western area (Fig. 2B and 5A). The cracks in the southern coastal areas above the caves in Figure 4C, are inflation clefts that formed during the emplacement of the lava flows and are not fractures from wave loading (Fig. 5B). The inner south flank of Surtur tuff crater, which is now mostly palagonitized, has developed a large 30 m wide and 1–2 m deep wind-eroded pothole (Fig. 5C). The unconsolidated tephra and sediment on the eastern and northeastern flanks of Surtur is cut by numerous (>50) 3–30 m wide, 2–14 m deep and 20 to over 300 m long gullies. At one location rills merge to form a prominent 10–20 m deep gully at the boundary between the palagonitized part of the cone and the sediment (Fig. 4D). A standing 4–5 m feeder dyke on the eastern slopes of Surtur shows the extent of the erosion into the palagonitized Surtur tuff cone (Fig. 5D), and consolidated material around hydrothermal fissures standing 0.5–1 m above their surroundings on top of Surtungur cone show the minimum extent of the erosion since the formation of the fissures at those locations. Driftwood accumulates mostly on the western boulder shore on the spit, 20–55 m inland and at 4 m a.s.l. A few pieces of driftwood are found 100 m away from the shore on a small sand and gravel patch where plants thrive.

Output and input quantified

Quantification of the erosion and sedimentation from the dDEMs is given in Table 2 for the specified areas shown in Figure 3. Noteworthy is the high erosion for the first 7 years from 1967–1974 totaling 10.9±1.3x10^6 m^3, of which 9.7±0.7x10^6 m^3 is from coastal wave erosion of areas 1 and 2. Total sedimentation or resedimentation is also high or

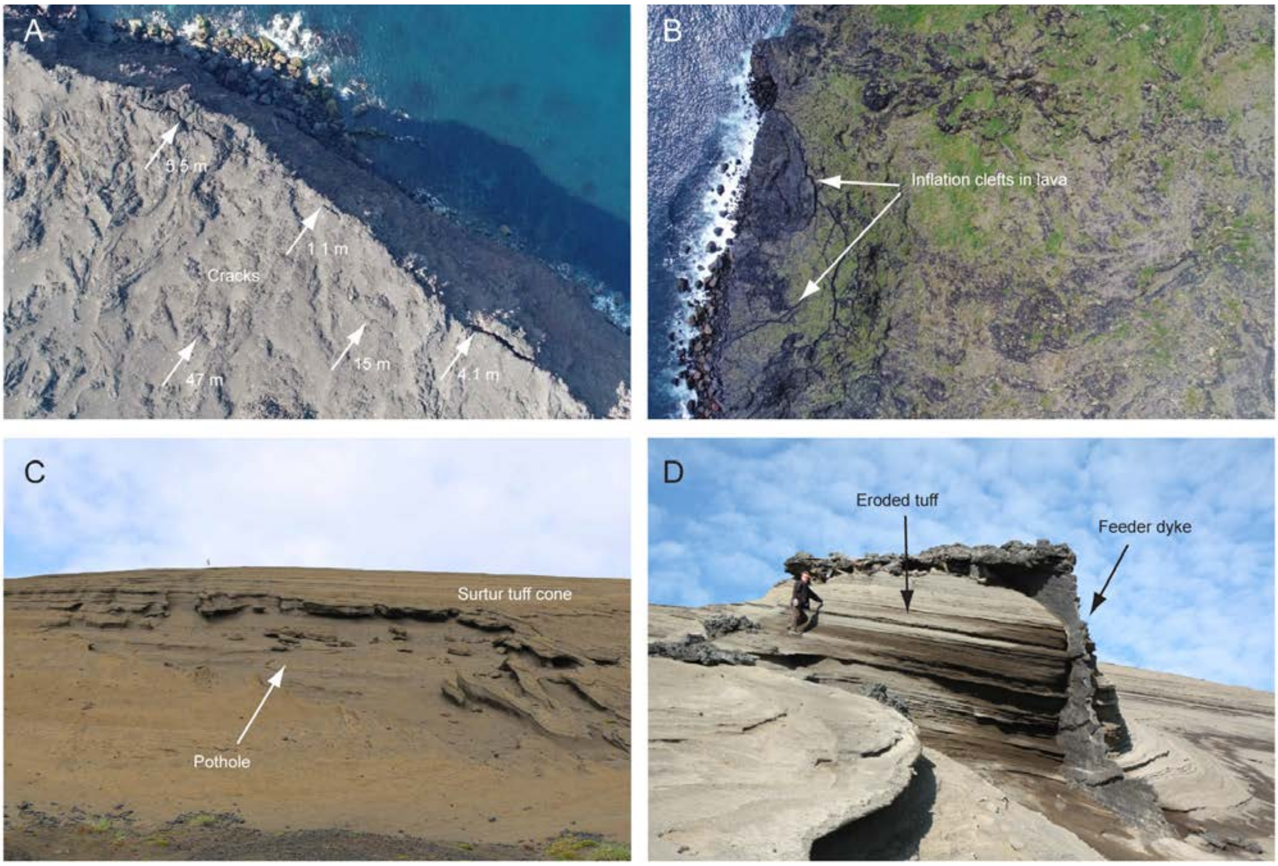

Figure 5. Close-up images of erosion features. A) Cracks along the coastal lava edges. The arrows show the location of the cracks and their respective distances from the margins. B) Inflation clefts in the lava apron. C) Wind-eroded pothole in the inner slopes of Surtur tuff crater. D) Erosion of the Surtur palagonite tuff exposing a feeder dyke. Person for scale.

about 1.5±0.6x10^{6} m^{3}. Wind and runoff erosion of the tephra/tuff cones and the sediments in areas 3 and 6 amounts to 0.3±0.1x10^{6} m^{3} while sedimentation amounts to 0.8±0.2x10^{6} m^{3}. The spit (area 5) lost 0.5±0.2x10^{6} m^{3} and about 0.2±0.05x10^{6} m^{3} was redeposited. Only average erosion rates are given and they do not reflect the rapid decline in erosion during the first year's post-eruption.

Erosion rate decreases significantly from 1974–2019 with a total loss of 20.7±1.4x10^{6} m^{3}, of which 18.4±0.8x10^{6} m^{3} was by coastal wave erosion of the cliffs in areas 1 and 2 at rates of 0.4±0.02 m^{3}/yr, 1.3±0.3x10^{6} m^{3} by wind and runoff erosion of the partly palagonitized tuff cone and the sediments in areas 3 and 6 at rates of 0.03±0.005 m^{3}/yr. The spit lost 0.74±0.2x10^{6} m^{3}, eroding at a rate of 0.016±0.005 m^{3}/yr. Total sedimentation was about 0.41±0.2x10^{6} m^{3}, mostly tephra accumulating around the tuff cones in area 6. The cumulative loss since 1967 is 28±1.5x10^{6} m^{3} for the coastal areas (areas 1 and 2), 1.6±0.4x10^{6} m^{3} for the tuff cones and sediments (areas 3 and 6) and 1.2±0.5x10^{6} m^{3} for the spit (area 5).

A few areas were sampled for assessing the denudation rate. An area of 20,970 m^{2} within area 2 of the 1967–1974 dDEM, yielded a negative volume of -0.883±0.021x10^{6} m^{3} and calculated denudation rate of 600±14 cm/yr. The value agrees well with measured coastal retreat rates for the NW tephra/tuff cone from maps from this period. An area of 13,734 m^{2} within area 2 of the 1974–2019 dDEM yielded a negative value of -0.674±0.014x10^{6} m^{3} and calculated denudation rate of 100±2 cm/yr. The volume is also in good agreement with the calculated coastal retreat for the NW tuff cone for this period. The total denudation rate of the tephra/tuff cones during the first years from 1967–1974 given the sum of the average erosion rates for areas 3 and 6 and total area of 515,286 m^{2} yield a denudation rate of 9±3 cm/yr. For the same areas from 1974–2019 and a total area of 478,175 m^{2} we derive a denudation rate of 6±1 cm/yr. An area of 19,595 m^{2} sampled within the consolidated palagonite tuff of Surtur in area 3 in the 1974–2019 dDEM yielded a negative volume of -0.018±0.009x10^{6} m^{3} and calculated denudation rate of 2±1 cm/yr.

Statistical uncertainty is high for a few areas, making their interpretation more difficult. However, the estimated values when compared with independent measurements, show in general good agreement. For example, the 2019 volume of the sediments on the margins of the tuff cones of 0.3±0.01x10^6 m^3 agrees well with the sum of the net volumes from the dDEMs of area 6 (total=0.23±0.2x10^6 m^3). The 1967–1974 positive volume of 0.430±0.28x10^6 m^3 of the aeolian sediments on the lava fields of area 4 within an area of 1,122,572 m^2 yield average sediment thickness of 38±24 cm. The 1974–2019 positive volume of 0.055±0.08x10^6 m^3 of area 4 divided by an area of 535,010 m^2 gives an average sediment thickness of 10±14 cm. The sum is thus 48±38 cm average sediment thickness for area 4 while the measured average thickness is of 49±7 cm (Ilieva-Makulec et al. 2015, densely vegetated area excluded).

Volumes of subaerial lithologies revised

Our results allow for a revision of the estimated total volumes for the main lithologies on Surtsey. The lava fields have a cumulative loss of 22.5x10^6 m^3 and the current volume of uneroded lava is 31.8x10^6 m^3 which gives a total volume in 1967 of about 54x10^6 m^3. Together with subsidence and the volume of the lava eroded since 1965 a total initial volume for the subaerial lava flows is likely in the range of 58x10^6 m^3, lower than the initial estimate of 70x10^6 m^3. The tuff cones have a cumulative loss of 6.7x10^6 m^3 and with a current volume of 38.6x10^6 m^3 we derive a total volume of about 45x10^6 m^3 in 1967. The initial volume of the tephra/tuff cones considering the volume loss since 1964 may be around 46x10^6 m^3 which is within the upper range of the initial estimate.

DISCUSSION

The dynamic geomorphic processes at work in Surtsey since the eruption ceased are vividly portrayed by the dDEM's (Fig. 3). These can be summarized into three processes: 1) The rapid incipient erosion. 2) The prevailing SW coastal wave erosion. 3) Intense wind and runoff erosion and a decrease in sediment availability.

The rapid incipient erosion

Our results show that rapid erosion characterized the first years of Surtsey, in accord with the field observations (Fig. 3 and Table 2). A better temporal control for the first year's post-eruption would allow for a more accurate assessment, but contemporaneous studies documented a rapid decline in erosion rate, the rate varying between lithologies and erosive processes. As mentioned above, especially noticeable was the decline in coastal wave erosion following the winter of 1967–1968 when up to 140 m of the southern side of the lava fields eroded away with an average retreat of 75 m and a total volume loss of 2x10^6 m^3 (Norrman 1970). This volume is twice as high as the average of 1967–1974 and renders an erosion rate 5–6 times the average rate of 0.3±0.02x10^6 from 1974–2019. Rapid coastal retreat is attributed primarily to the thinner (<14 m) and less cohesive nature of the distal margins of the lava apron. As noted by Norrman (1972a, 1972b), after passing these margins or terraces, and entering thicker and more cohesive pile of lava, the erosion rate of the lava fields decreased significantly, or to an average of 25–35 m and a maximum retreat of 40–50 m the following year. The rate of wave erosion is likely also influenced by the growth of the insular shelf (e.g. Ramalho et al. 2013). The thinner terraces were located near the break of the shelf along the steep submarine flanks of the Surtsey volcano, unprotected from high wave energy loading. According to the bathymetry map of Jakobsson et al. (2009) the width of the insular shelf of Surtsey had grown to about 900 m in the SW in 2007, extending to 1100 m when including the mound of Jólnir. The average slope is 1.7° from the coast to the break of the shelf of Jólnir at about 60 m depth. The erosion of the satellite mounds down to depths of 50 m suggests that wave energy is dissipated even to these depths. Therefore, the widening of the shallower shelf is expected to increase wave attenuation and protect the coastal margins.

Our results also show a rapid denudation rate for the tephra/tuff cones the first years. As shown above, we acquire average vertical denudation rate of 9±3 cm/yr for 1967–1974 while the rate decreased to 6±1 cm/yr in 1974–2019. Despite the higher statistical uncertainty for the first years, denudation rate about 2–3 times higher than the 1974–2019 average is realistic. Ingólfsson (1982) reported localized measurements on vertical stakes conducted by Sigurður Þórarinsson, that showed that the north side of the Surtungur tephra/tuff cone was lowered by up to 92 cm in the first three years from 1967–1970 and the top of the Surtur cone by 52 cm. Denudation rate decreased to 10 cm at Surtungur from 1970–1976

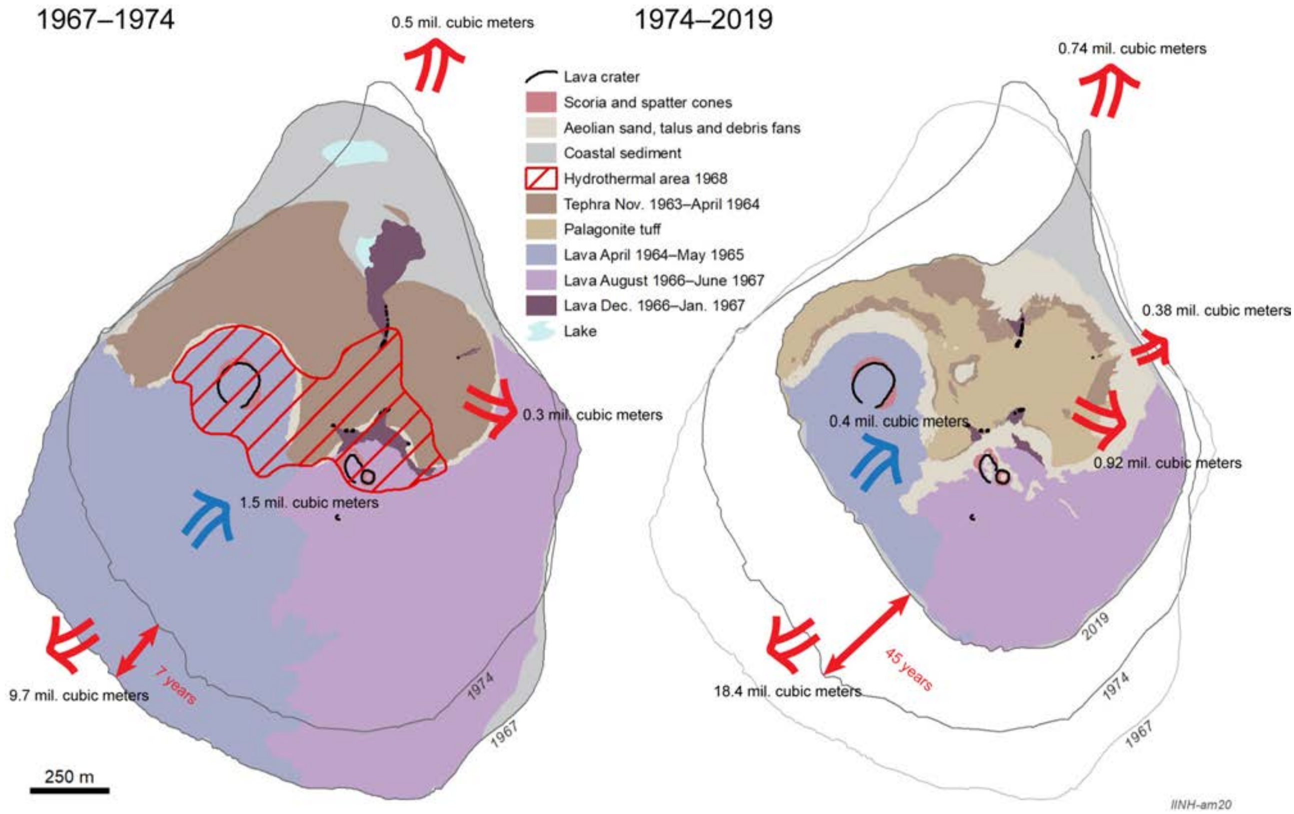

Figure 6. Simplified geological maps of Surtsey as in 1967 and 2019 summarizing the geomorphic and geological changes highlighted in this study. The values with arrows display the most significant volumetric estimates of erosion (red) or sedimentation (blue) from the 1967–1974 and 1974–2019 dDEMs, in million cubic meters (see Fig. 3 and Table 2). Processes in focus are coastal wave erosion (sum of areas 1 and 2), total sedimentation on land, erosion of the spit and wind and runoff erosion of the cones and the marginal sediment (sum of areas 3 and 6). In the figure to the right, the erosion values for the tuff cones and sediments are shown separately.

and to 40 cm at Surtur; and to 5 cm at Surtungur from 1976–1979. Rapid denudation rate of the tephra/tuff cones during these first years is explained by the uncompacted and unconsolidated (unaltered) nature of the cones at this time. The subsidence measured by Moore et al. (1992) was about 15–20 cm for the year 1967–1968 decreasing to 1–2 cm/yr to 1991 and compaction of the volcanic material was one of the factors. A hydrothermal anomaly was observed in 1968 in the unconsolidated tephra cones (Fig. 6, Jakobsson 1978), and palagonite tuff was discovered in 1969, meaning alteration was rapidly speeding up diagenesis (Jakobsson 1972), and rates of denudation of the cones declined after the cones became largely palagonitized.

The prevailing SW coastal wave erosion

Oceanographic studies have confirmed the prevailing SW direction of coastal waves (Romagnoli & Jakobsson 2015), evident in the prominent erosion of the SW side of the island and the E-NE migration of the spit. The retreat for the last 45 years has progressed at a relatively uniform pace into the lava pile and is about 8 m/yr with volume loss of $0.3 \pm 0.02 \times 10^6$ m^3/yr. Of the revised initial subaerial lava volume of 58×10^6 m^3, about 45% has eroded away. The dynamics of failure and retreat of the rocky coast in Surtsey is mainly controlled by the cyclical but persistent wave loading, intensified in heavy storms. The waves hammer the base of the lava cliffs causing flexural fatigue, the strain leading to the propagation of cracks preparing the cliffs for failure (Hapke et al. 2014). The hydraulic action of the waves increases air pressure in the cracks, inducing further propagation of the tip of the cracks (Hansom et al. 2008). A notch develops through abrasion which grows with time to extend an unsupported cantilevered mass (e.g. Sunamura 1992, Young & Ashford 2008). Failure and collapse of the fractured rocks and unsupported masses form taluses that are entrained as tools in the orbital and turbulent motion of the waves prompting further abrasion and speeding the growth of a new notch. Alongside these processes, other weathering mechanisms such as the role of expansion and contraction of cracks with freezing and thawing during winter months and possibly thermal expansion of salts during summer months, are also likely to play a role in the degradation of the lava margins and other parts of Surtsey (e.g. Hansom et al. 2014).

The SW wave current erodes a transect at right angle to the prevailing wave loading. The transect varies in thickness and morphology along the coast, the variation originating from the buildup of the lava shields. Thicker pile of flows builds the proximal areas of the vent (the cone of the shield), while the pile thins out towards distal areas that make the lava apron. Erosion of the SW coast has exposed the thicker lava sequence of Surtungur cone, and the lava morphology there is mostly a pile of thin (<2 m) surface (overbank) vesicle-poor sheet lobes of smooth or slabby pahoehoe and clinckery a'a types (Fig. 4B, Thordarson 2000). An exception is a >35 m thick columnar jointed flow at the base of the sequence (Fig. 4B). The apron is composed of mostly tube-fed hummocky pahoehoe (Thordarson 2000) that feature hollow cavities, caves, and inflation clefts (Fig. 4C and 5B). It is notable that coastal erosion rates seem indifferent to the various morphologies and thicknesses within the lava pile. Norrman (1970) mapped the cracks on the margins of the cliffs from wave loading up to 20 m into the lava apron in 1968. The cracks mapped in 2019 were found within similar range as in 1968 along the cone and apron. The most distant cracks up to 47 m are found in the thicker western cliff region (Fig. 2B and 5A) and can be explained as forming at a right angle to the SW current, and/or be the result of the stronger gravitational pull of the thicker cliff section at that location. However, the pace of fracturing of the lava cliffs by the wave action appears to be continuous independent of the thickness of the lava pile. In principle, the base of the lava cliffs is of similar properties and with abrasion and formation of a notch, failure and collapse of the unsupported cantilevered mass takes place independent of the thickness above.

On the other hand, the coastal erosion of the tuff cones, still largely protected by the lava fields, advances at slower rates and only 16% eroded away. The NW side of Surtungur cone was exposed to wave erosion shortly after formation and waves quickly penetrated the sides of the cone abrading parts of the unconsolidated tephra (Thorarinsson 1968, Norrman 1970, 1974). Steepening of the sides led to slumps and rapid lowering of the west crest of Surtungur, that was about 169 m a.s.l. in 1965 according to Thorarinsson (1966), to approximately 150 m a.s.l. in 1968 (Norrman 1970). After 1967 a boulder terrace formed, partly protecting the tephra wall but retreat by erosion was still high reaching 6 m/yr. With the removal of the boulder terrace sometime in the early 1980´s, wave abrasion has resulted in the formation of a notch and cave (Fig. 4A). With palagonitization, the tuff cones which now form a compact mass without jointing or cleavage (Jakobsson 1978), have become more resistant to erosion, and the current rates of retreat of the western palagonite cliff seems to be in the range of 1 m/yr.

The boulder coast that extends to the tip of the spit (Fig. 2) gives further evidence of the strength of the prevailing SW ocean currents, where large boulders, up to 2 m in diameter, have been transported from the southern parts of the island to the spit, a distance over a kilometer. Eyewitnesses reported the tip of the spit to flip from having a hook to the west to having a hook to the east during a day of heavy storm in 2017. Driftwood 100 m into the central parts of the spit testify to strong flooding events that can sweep material over the berms and far into the spit. Events of this scale can easily account for the disintegration of the spit, and with the retreat of the lava fields with erosion and decrease in sediment on the island, less sediment supplies the spit, which is eroding and shrinking. Since finer particles are more easily washed away with the swash or subject to deflation, the boulder concentration in the spit has increased with time (Norrman 1970, 1972a, Ingólfsson 1982).

Intense wind and runoff erosion and decrease in sediment availability

Meteorological data from Surtsey and Heimaey show that the prevailing wind direction is easterly and about 30 days per year on average have wind speed exceeding 20 m/s (Petersen and Jónsson 2020). The prevailing easterly direction is not obvious from the erosion pattern in Surtsey but could account for the more pronounced erosion of the northeast side of Surtur (Fig. 3 and 4D). Wind erosion intensified in storms causes differential erosion of the palagonitized tephra layers and marked erosion of the inner flanks of the craters, including the potholes in the Surtur tuff crater (Fig. 5C), may be the result of vortex shedding (e.g. Bauer et al. 2013) induced by wind-driven currents around the tuff cones.

Seasonal runoff, common during the rainy months of September and October deepens gullies and rills in the unconsolidated tephra and sediments opening new surfaces for erosion (Fig. 4D). Gullies deepen down to the boundary between the unconsolidated tephra and the palagonitized tuff and enlarge where water streams converge (Fig. 4D). Although the average denudation rate of the tuff cones and sediments by wind and runoff reaches 6 cm/yr, the current erosion of the consolidated palagonitized areas in the tuff cones is estimated at rates of about 2 cm/yr. In total the denudation by wind deflation and runoff from the tuff cones and sediments removes approximately $0.029\pm0.005\text{x}10^6$ m^3/yr of the unconsolidated tephra and sediments.

The lava fields are covered largely by a sediment cover about 50 cm thick and do not show much evidence of degradation, the only visible changes are on the fragile crust of the hollow shelly pahoehoe flows which at many locations are fragmented, partly by human activity. The scoria cones show only minor evidence of slumps on the crests of the cones but the cumulative material mobilization within both cones since 1967 could amount to $0.033\pm0.014\text{x}10^6$ m^3. A significant change was the collapse of the small cone within the scoria cone of Surtur sometime between 1967 and 1974.

The volume of material eroded by wind or surface waters available for sedimentation or resedimentation on the island is of about $0.03\pm0.01\text{x}10^6$ m^3/yr (predominantly material from areas 3, 4, 5 and 6). However, from the 1974–2019 total sediment average, only about $0.008\pm0.004\text{x}10^6$ m^3/yr remains on the island, meaning approximately $0.02\pm0.01\text{x}10^6$ m^3/yr of the eroded material is removed away. Overall, with the prevalence of erosive processes, less sediment is available for plant colonization while vegetation binds and protects parts of the sediment cover for longer periods.

The future of Surtsey

In terms of predictions for the future development of Surtsey, the 2019 area of 1.2 km^2 fits well in the area-based, least-square equation of Jakobsson et al. (2000), but the volume of 0.0707 km^3 is larger than predicted by the volume-based equation of Garvin et al. (2000). An erosion rate estimate from the 45-year average given in Table 2 allows for some additional quantification. The erosion rate of $0.02\pm0.005\text{x}10^6$ m^3/yr of the spit yield a 15–25 year life expectancy for the bulk of the spit. The lava fields with an erosion rate of $0.3\pm0.02\text{x}10^6$ m^3/yr have a life expectancy of about 100 years while the palagonitized tuff cones could survive for centuries eroding at a rate of $0.02\pm0.004\text{x}10^6$ m^3/yr, although wave erosion will speed up the erosion of the palagonitized tuff when the lava fields have eroded away. This is in line with Jakobsson et al. (2000) prediction that the island will likely reach the palagonite core in about 100 years, but the core itself, with an area of about 0.39 km^2, may survive for centuries as a palagonite tuff crag.

CONCLUSIONS

Differencing of high-resolution DEMs allows for quantitative analyses of the erosive and depositional processes that have been active in Surtsey since its emergence. Extreme rate of erosion and sedimentation characterized the first-years post-eruption with the rapid removal of the thin and less cohesive margins of the lava apron by wave erosion. Furthermore, there was rapid erosion of the uncompacted and unconsolidated tephra from the tephra cones by wind and runoff erosion and mass wasting. In the following years, the erosion rate decreased but prevailing SW coastal erosion, runoff and strong winds continue to erode the island, totaling today over 53% areal loss and 29% volume loss. The future development of Surtsey projecting current erosion rate predicts that the island will become a palagonite tuff crag in about 100 years.

ACKNOWLEDGEMENTS

The authors want to thank the rescue team in Vestmannaeyjar for ferrying the expedition over to Surtsey. We also thank the Icelandic Coast Guard for helicopter transport to Reykjavík and for flying around Surtsey for photography. Carsten Kristinsson is acknowledged for the scanning of the historical aerial photographs. We thank Bjarni Sigurðsson for editorial work and Ingvar Atli Sigurðsson for review.

REFERENCES

Baldursson, S. & Á. Ingadóttir (Eds.) 2007. Nomination of Surtsey for the UNESCO World Heritage List. Icelandic Institute of Natural History, Reykjavík, 123 p.

Belart, J.M.C., E. Magnússon, E. Berthier, F. Pálsson, G. Aðalgeirsdóttir, & T. Jóhannesson 2019. The geodetic mass balance of Eyjafjallajökull ice cap for 1945–2014: processing guidelines and relation to climate. Journal of Glaciology 65, 395–409.

Bauer, B., I. Walker, A. Baas, D. Jackson, C. McKenna Neuman, G. Wiggs & P. Hesp 2013. Critical Reflections on the Coherent Flow Structures Paradigm in Aeolian Geomorphology. Coherent Flow Structures at Earth's Surface, 111–134.

Calles, B., K. Lindé & O.J. Norrman 1982. The geomorphology of Surtsey island in 1980. Surtsey Research Progress Report IX, 117–132.

Einarsson, T. 1965. Gosið í Surtsey í máli og myndum. Heimskringla, Reykjavík, 53 pp.

Garvin, J.B., R.S. Williams, J.J. Frawley & W.B. Krabill 2000. Volumetric evolution of Surtsey, Iceland, from topographic maps and scanning airborne laser altimetry. Surtsey Research 11, 127–134.

Hansom, J.D., N.D.P. Barltrop & A.M. Hall 2008. Modelling the processes of cliff-top erosion and deposition under extreme storm waves. Marine Geology 253, 36–50.

Hansom, J. D., D. L. Forbes, & S. Etienne 2014. The rock coasts of polar and sub-polar regions. Geological Society, London, Memoirs 40, 263–281.

Hapke, C.J., P.N. Adams, J. Allan, A., Ashton, G.B. Griggs, M.A. Hampton, J. Kelly, & A.P. Young 2014. Chapter 9 The rock coast of the USA. Geological Society. London, Memoirs 40, 137.

Höhle, J. & M. Höhle 2009, Accuracy assessment of digital elevation models by means of robust statistical methods, ISPRS J. Photogramm. Remote Sens. 64, 398–406.

Ilieva-Makulec, K., B. Bjarnadottir & B. Sigurdsson 2015. Soil nematode communities on Surtsey, 50 years after the formation of the volcanic Island, Icelandic Agric. Sci. 28, 43-58.

Ingólfsson, Ó. 1982. Some observations on the sediments of Surtsey. Surtsey Research Progress Report IX,133–141.

Jakobsson, S.P. 1972. On the consolidation and palagonitization of the tephra of the Surtsey volcanic island, Iceland. Surtsey Research Progress Report VI, 121–129.

Jakobsson, S.P. 1978. Environmental factors controlling the palagonitization of the Surtsey tephra, Iceland. Bull. Geol. Soc. Denmark, Special Issue 27, 91–105.

Jakobsson, S.P., G. Gudmundsson & J.G. Moore 2000. Geological monitoring of Surtsey, Iceland. Surtsey Research 11, 99–108.

Jakobsson, S.P. K. Thors, Á.T. Vésteinsson & L. Ásbjörnsdóttir 2009. Some aspects of the seafloor morphology at Surtsey volcano: The new multibeam bathymetric survey of 2007. Surtsey Research 12, 9–20.

Jakobsson, S.P. & G. Gudmundsson 2003. Rof Surtseyjar: Mælingar 1967–2002 og framtíðarspá [The marine abrasion of Surtsey, Iceland: areal changes 1967–2002 and future development]. Náttúrufræðingurinn 71, 138–144 (in Icelandic with English summary).

Kjartansson, G., 1966. Stapakenningin og Surtsey [A comparison of table mountains in Iceland and the volcanic island of Surtsey off the south coast of Iceland]. Náttúrufræðingurinn 36, 1–34 (in Icelandic with English summary).

Landmælingar Íslands 2020. www lmi.is.

Loftmyndir ehf. 2020. www.loftmyndir.is.

Lorenz, V. 1974. Studies of the Surtsey tephra deposits. Surtsey Research Progress Report VII, 72–79.

Magnússon, E.; J. M.C. Belart, F. Pálsson, H. Ágústsson, & P. Crochet 2016. Geodetic mass balance record with rigorous uncertainty estimates deduced from aerial photographs and lidar data – Case study from Drangajökull ice cap, NW Iceland. The Cryosphere 10, 159–177.

McNabb, R., C. Nuth, A. Kääb, & L. Girod 2019. Sensitivity of geodetic glacier mass balance estimation to DEM void interpolation. The Cryosphere 13, 895–910.

Norrman, J.O. 1970. Trends in post-volcanic development of Surtsey island. Progress report on geomorphological activities in 1968. Surtsey Research Progress Report V, 95–112.

Norrman, J.O. 1972a. Coastal development of Surtsey Island, 1968–69. Surtsey Research Progress Report VI, 137–143.

Norrman, J.O. 1972b. Coastal development of Surtsey Island, 1969–70. Surtsey Research Progress Report VI, 145–149.

Norrman, J.O. 1974. The geomorphology of Surtsey Island in 1972. Surtsey Research Progress Report VII, 61–71.

Norrman, J.O. 1978. Coastal changes in Surtsey Island, 1972–75. Surtsey Research Progress Report VIII, 53–59.

Norrman, J.O. 1985. Stages of coastal development in Surtsey island, Iceland. *In* Sigbjarnarson, G. (ed.). Proceedings of the Iceland Coastal and River Symposium, pp. 33–40.

Moore, J.G., S.P. Jakobsson & J. Holmjarn 1992. Subsidence of Surtsey volcano, 1967–1991. Bulletin of Volcanology 55, 17–24.

Pedersen, G. B. M., J. M. C. Belart, E. Magnússon, O. K. Vilmundardóttir, F. Kizel, F. S. Sigurmundsson, G. Gísladóttir & J. A. Benediktsson 2020. Hekla Volcano, Iceland, in the 20th Century: Lava Volumes, Production Rates, and Effusion Rates. Geophys. Res. Lett. 45, 1805–1813.

Petersen, G.N. & T. Jónsson 2020. The climate of Surtsey. Surtsey Research 14, 9–16.

Pierrot Deseilligny, M. & I. Clery 2011. Apero, An Open Source Bundle Adjusment Software for Automatic Calibration and Orientation of Set of Images. ISPRS - International Archives of the Photogrammetry. Remote Sensing and Spatial Information Sciences 3816, 269–276.

Pix4Dmapper 2019. Pix4D SA. www.pix4d.com.

Ramalho, R. S., R. Quartau, A. S. Trenhaile, N. C. Mitchell, C. D. Woodroffe, & S. P. Ávila 2013. Coastal evolution on volcanic oceanic islands: A complex interplay between volcanism, erosion, sedimentation, sea-level change and biogenic production. Earth-Science Reviews 127, 140–170.

Romagnoli, C. & S. P. Jakobsson 2015. Post-eruptive morphological evolution of island volcanoes: Surtsey as a modern case study, Geomorphology 250, 384–396.

Rupnik, E., M. Daakir & M. Pierrot Deseilligny 2017. MicMac – a free, open-source solution for photogrammetry. Open Geospatial Data, Software and Standards, 2: 14.

Sturkell, E., P. Einarsson, H. Geirsson, E. Tryggvason, J.G. Moore & R. Ólafsdóttir 2009. Precision levelling and geodetic GPS observations performed on Surtsey between 1967 and 2002. Surtsey Research 12, 39–47.

Thorarinsson, S. 1964. Surtsey: The new island in the North Atlantic [Surtsey: Eyjan nýja í Atlantshafi]. Almenna Bókafélagið, Reykjavík, 108 p. (in Icelandic with English summary).

Thorarinsson, S. 1966. Some facts about the Surtsey eruption [Sitt af hverju um Surtseyjargosið]. Náttúrufræðingurinn 35, 153–181 (in Icelandic with English summary).

Thorarinsson, S. 1968. The last phases of the Surtsey Eruption [Síðustu þættir Eyjaelda]. Náttúrufræðingurinn 38, 113–135. (in Icelandic with English summary).

Thordarson, T. 2000. Physical volcanology of lava flows on Surtsey, Iceland: A preliminary report. Surtsey Research 11, 109–126.

Sørensen, E.V. & M. Dueholm 2018. Analytical procedures for 3D mapping at the Photogeological Laboratory of the Geological Survey of Denmark and Greenland. Geological Survey of Denmark and Greenland Bulletin 41, 99–104.

Sunamura, T. 1992. Geomorphology of Rocky Coasts. John Wiley & Sons., New York. 302 p.

Walker, G.P.L. 1973. Explosive volcanic eruptions a new classification scheme. Geol. Runds. 62, 431–446.

Young, A.P. & S.A. Ashford 2008. Instability investigations of cantilevered sea cliffs. Earth Surface Processes and Landforms 33, 1661-1677.

HISTORICAL GEOGRAPHY

A short note on place-names in Surtsey

BIRNA LÁRUSDÓTTIR

The Árni Magnússon Institute for Icelandic studies, Laugavegur 13, 101 Reykjavík, Iceland
(birna.larusdottir@arnastofnun.is / birnalar@gmail.com)

INTRODUCTION

In the summer of 2019 the author joined a field team of biologists on Surtsey with the aim of conducting a survey of place-names on the island. This was the first comprehensive survey of this kind on Surtsey.[1]

From the beginning, Surtsey has been the focus of nature-driven perspectives as a scientific oasis for geological, biological and ecological research, a place to study the formation of a new landmass, erosion and the colonization and progress of flora and fauna. One species has been more or less left out on purpose in this process, namely humans. The island nevertheless offers a rare opportunity to study interactions between man and nature and human aspects of colonization and place-making processes from the beginning of the island's existence. The act of naming can be seen as an important indicator of these processes.

Often the study of place-names involves interpreting old names which may have lost their original context, appearance or meaning. Surtsey offers the rare opportunity to investigate an assemblage of names from the beginning of its history: the processes by which names appeared as people set foot on the island and started to make the landscape familiar through using names can be identified, as well as the motivations behind them – and how and why some of them survive while others have already disappeared.

[1] This study is a part of an ongoing Phd-project carried out by the author at the University of Iceland, Faculty of Life- and Environmental Sciences.

HISTORY AND METHODS

In general, place-names are seen as an important part of a nation´s heritage and as vital sources about the past. They are often been referred to as such, for example by historians and archaeologists as they can contain information (although sometimes fragmented) about bygone landscapes, landuse patterns, settlement history and environmental change, to name a few examples.

Conventional place-name research has been criticized for relying excessively on „the collection and description of data (see e.g. Alderman 2008, 198), ignoring the social processes behind them“ and even for being one of the driest specialist branches of linguistics (Levinson 2008, 256). However, recent advances in the field, especially within cultural geography, have brought to light the more problematic and political sides of place-names and naming processes. Much of this new research has focused on how government elites have manipulated place-names to strengthen national identity – sometimes undermining indigenous histories. Scholars have started to view landscapes as "documents of power", rather than as mere reflections of culture (Alderman 2008, pp. 196-198). Thus space (seen as a socially produced phenomenon) is viewed as a *medium* rather than a *container* for action (Tilley 1998, p. 10). This relates directly to the act of naming, as „names act so as to transform the sheerly physical and geographical into something that is historically and socially experienced… . In a fundamental way names create landscapes.“ (Tilley 1998, 18-19)

The aim of this project is to investigate the dynamics of place-names and how people inscribe meaning, claim and connect to the landscape by naming and using names. Surtsey was seen as an ideal place to carry out this kind of research and a fascinating case study for many reasons, not least that the biographies of individual place-names would most likely be known due to the young age of the new land. Conducting a field survey was seen as fundamental to the project, which is inspired both by ethnological approaches and phenomenology. The plan was to analyse names through discussion and observing the daily routines of people familiar to the place, as well as to directly experience the landscape through fieldwalking in different circumstances to discover its many layers of meaning.

Figure 1. Þóra Pétursdóttir hiking up Austurbunki on her way to the lighthouse.

BACKGROUND

The name Surtsey

The naming of Surtsey itself was quite a famous process that was much debated in Iceland soon after the initial creation of the island in 1963. The debate has been interpreted as a manifestation of territorial disputes between locals of the Vestmannaeyjar Islands and academics in Reykjavík who represented the State (Lárusdóttir 2017). Much of the discourse took place in the media in the days and weeks following the start of the eruption. Several names for the new land were suggested by journalists, readers, local people in the Vestmannaeyjar Islands or by scientists. These names included *Nýey* (New Island), *Gosey* (Volcanic Island), *Ólafsey* (Ólaf´s Island) after the man who first spotted the eruption, and *Bjarnaey* (Bjarni´s Island) after the new Prime Minister of Iceland at the time, Bjarni Benediktsson. *Frakkey* (French Island) was also mentioned (most likely as a joke) after three French journalists from the newspaper *Le Paris Match* surreptitiously landed on the still erupting island before any locals had. This was not well received in the Vestmannaeyjar Islands.

On the 10th of December 1963 the Ministry of Education announced the official name of the island, *Surtsey*, after having consulted the Icelandic place-name committee (Örnefnanefnd) that was made up of prominent academics. The new name referred to the giant Surtur who was in charge of fire according to the famous medieval Icelandic poem *Völuspá*, which describes the creation (and the end) of the world. This decision about the new name caused an uproar in the Vestmannaeyjar Islands. It even led to a nearly fatal boat trip taken by some locals to the site of eruption a few days later with the aim of erecting a home-made sign with their preferred name, *Vesturey* (West Island), referring to its geographical location as a part of the bigger cluster of islands. Despite their efforts, the name Surtsey stuck. Knowledge of this highly political naming process was an important prelude to the forthcoming fieldtrip to Surtsey.

PREPARATION

Maps and written sources

In preparation, all known names were collected from some key sources. A total of around 40 names were collected before the journey. Some seemed well established and appeared repeatedly, i.e. the name of the crater *Surtur*; the two prominent hills around the craters, *Austur*- (Fig. 1) and *Vesturbunki*; and *Svartagil*, a gully leading up from the old Pálsbær location up between the craters. *Pálsbær*, the cabin built in the 1960s and named in honour of scientist Paul Bauer whose donation made the building possible, was also mentioned in many sources. Later, the hut was threatened by erosion, moved to a new location and named *Pálsbær II* (Fig. 2). More places were named after the legendary Paul, e.g. *Pálstindur*, the name of the highest peak of the island and *Bóndi* (farmer), an Icelandic translation of his last name Bauer. Neither name is in use today.

Figure 2. A view over Pálsbær. Paths appeared after a few days, marking the most commonly walked routes of visitors.

One of the newest maps of Surtsey and a key source shows a total of 21 names, including names in the northern part of the island of features which now have disappeared (Ólafsson & Ásbjörnsdóttir 2014, p. 13). What is unusual about this map is that the authors distinguish between established and unestablished names. This raises some questions about the basic nature of names. When does a reference to a place in fact become a place-name and what elements does it need to include in order for it to be accepted on a map? What was the difference between established names and the other references? Were the names perhaps seen as being on different levels in the place-naming process?

Figure 3. A human figure just visible in the fog north of the crater Surtungur.

Some features seemed to have more than one name, perhaps because different groups of people referred to them differently. New names seemed to have been added over time, perhaps by new scientists or because the island was evolving –whether due to erosion or the expanding vegetation. There were also examples of names which appeared early on but fell out of use. It should be noted that the maps and other sources cannot be seen as giving complete overviews of existing place-names at certain points in time but rather as indicators for them. It was hoped that the field trip would answer some questions and fill in some gaps.

Figure 4. Mávasteinn („Seagull Rock”) is visible from the cabin Pálsbær

THE SURVEY

The trip to Surtsey was a very meaningful experience and it provided invaluable insights into the naming process on Surtsey and beyond: what motivates and affects the giving of names, how names are used and how meaning is created in landscapes. Despite foggy—even mystical— conditions during the first two days (Figs. 1 and 3), the island slowly emerged and materialized through the visible features, histories and names of places. A total of around 80 names has now been collected. The data are still being processed and theorized and will have to await further discussion and analysis although a few notes are given below.

Even if Surtsey has never been permanently settled in the conventional sense, many names indicate a certain process of place-making which relates noticeably to perspectives from dwellings, routes between key areas, and permanent research plots defined by biologists to monitor the development of life. Examples include Svartagil, a gully between the two hills which was the main route between the old *Pálsbær* cabin and the craters; and *Rauðabrík*, an informal name for one of the smaller craters that derives from the red colour of one of the crater sides most visible from the area now referred to as *máfabyggðin* (the seagull colony), where scientists often conduct their research. Research plots are usually identified by numbers (10, 12) but there are some examples of those references behaving like names (e.g. *Tían*), and this shows an interesting combination of two different reference systems.

Figure 5. This cliff is often referred to as Sfinxinn („The Sphinx”) for obvious reasons although some other naming suggestions have been discussed.

Scales of names are very different: thus, there are names for very prominent landscape features that can be viewed from a long distance (Figs. 4 and 5). Other examples are e.g. *Austur*- and *Vesturbunki*, which interestingly seem to relate to similar crater-hills also called *bunkar* in other small islands near by); and there are also names for small patches which have originally been defined by a plant species (e.g. *Muruhóll* and *Hvanndalur*).

Some earlier names are not in use anymore (e.g. *Mávaból* and *Pálstindur*); some places were referred to as if they had names but my travel companions nevertheless did not perceive them as such (e.g. tanginn, ‚the spit‘-, and vitinn, ‚the lighthouse‘). There were also examples of names that had been contemplated and discussed at some point but dismissed for various reasons. Some names obviously had a humorous element, e.g. a new name relating to the very primitive toilet facilities under a cliff on the east coast of the island called *Gústavsberg*, which is a well known manufacturer of toilets and sinks. Furthermore, there were examples of landscape features which have now disappeared on account of the dramatic landscape change on the island – but somehow, these places live on through the names, e.g. *Fjallið eina* and *Bólfell*.

The complexity of the data underlines how names connect to the everchanging nature of the landscape and the angle of the viewer – and how place-names encapsulate the fascinating network of natural/human relations.

ACKNOWLEDGEMENTS

I sincerely thank the Surtsey society for permitting fieldwork undertaken on the island. I am also most grateful to the field team: Bjarni Diðrik Sigurðsson, Borgþór Magnússon, Erling Ólafsson, Matthías Alfreðsson and Pawel Wasowicz were all extremely friendly and generous in passing on their knowledge of place-names and the legacy of earlier scientists in Surtsey. I also want to express gratitude to my colleague Þóra Pétursdóttir at the University of Oslo and another Surtsey-enthusiast, for many inspiring conversations during our time in Surtsey. Emily Lethbridge read a draft of this short paper, detected some errors and gave some very useful comments.

This study is supported thanks to a research position linked to the name of Sigurður Nordal at the Árni Magnússon Institute for Icelandic studies, Reykjavík.

REFERENCES

Alderman, D. H., 2008. Place, Naming and the Interpretation of Cultural Landscapes. *In* Graham, B. and P. Howard (eds), The Ashgate Research Companion to Heritage and Identity, Farnham: Ashgate, pp. 195-213.

Lárusdóttir, B., 2017. Að nema land með nafni. Skírnir 191 (spring), 166-185.

Levinson, S. C., 2008. Landscape, seascape and the ontoology of places on Rossel Island, Papua New Guinea. Language Sciences 30, 256-290.

Ólafsson E. & L. Ásbjörnsdóttir, 2014. Surtsey í sjónmáli. Edda útgáfa.

Tilley, C., 1994. A Phenomenology of Landscape. Places, Paths and Monuments. Oxford: Berg.

BIOLOGY

Effects of sea birds and soil development on plant and soil nutritional parameters after 50 years of succession on Surtsey

RIEN AERTS[1], RICHARD S.P. VAN LOGTESTIJN[1], NIKI I.W. LEBLANS[2] AND BJARNI D. SIGURDSSON[3]

[1] Dept of Ecological Science, 1081HV Vrije Universiteit Amsterdam, The Netherlands (m.a.p.a.aerts@vu.nl)

[2] Climate Impact Research Centre, Umeå University, Sweden

[3] Agricultural University of Iceland, Hvanneyri 311 Borgarnes, Iceland

ABSTRACT

Surtsey, the island that rose from the sea in a submarine eruption during 1963 to 1967, has been the subject of many studies on primary succession. These studies have intensified after the establishment of a seagull colony on the island in 1986. This paper reports on the results of a short sampling expedition in 2013 that intended to characterize the interactive effects of the seagull colony and of soil development on soil nutritional characteristics in the tephra sands that cover the underlying lava, as well as in plants growing inside and outside the seagull colony. Feces and pellets of the gulls were extremely rich in both nitrogen (N) and phosphorus (P) and $\delta^{15}N$ analyses showed that N was transferred from pellets and feces to the tephra soils and subsequently taken up by the plants. The tephra soils not affected by the birds showed a high concentration of P compared to N. The concentration of both nutrients was much lower than in the soils of the bird colony. In general, variation in tephra soil depth had little effect on nutritional characteristics, except for the very low N concentration in deep soils. Thus, our results confirm the overriding effect of the seagull colony on Surtsey on nutritional characteristics of the developing soils and vegetation. Due to the very high P availability of the volcanic soils in combination with the high P input by the birds, vegetation productivity is N limited, despite the extremely high N input of 47 kg N ha^{-1} yr^{-1} that the birds add to the system. Our findings emphasize the extreme importance of bird colonies on the nutritional ecology of young, N-poor ecosystems.

INTRODUCTION

Since the submarine eruption that took place during 1963-1967 and its subsequent further development, Surtsey has been the subject of many studies on primary succession, soil development, vegetation development and ecosystem respiration (e.g. Sigurdsson & Magnusson 2010, Leblans *et al.* 2014, Magnusson *et al.* 2014). From these studies, it is clear that both the autonomous soil development and the establishment of a seabird colony has had a great impact on the aforementioned processes. In this context it is important to study plant and soil mineral nutrition as it is critical to our understanding of the functioning of Surtsey ecosystems. It feeds back on photosynthesis, primary production, herbivore forage quality, leaf litter and soil organic matter decomposition and, ultimately, plant-mediated nutrient and carbon cycling pathways and rates (Aerts *et al.* 2009). Apart from the standard nutritional analyses, the natural abundance of ^{13}C ($\delta^{13}C$) and especially of ^{15}N ($\delta^{15}N$) is a good proxy for tracing nutrient transfer in food webs (Bokhorst *et al.* 2019). In the present study the impact of the presence of a sea bird colony (both through feces and regurgitatad pellets) and of soil development on soil and leaf

https://doi.org/10.33112/surtsey.14.7

nutritional characteristics were studied by analysing soil- and leaf nutrients and isotopic composition. This was done in a expedition to the island in 2013, after 50 years of primary succession and after 26 years of seagull (*Larus* sp.) nesting in a confined area on the island. Sampling was performed both inside and outside the seabird colony on the southern part of Surtsey, on shallow soils formed on lava surfaces and on deeper soils formed in tephra (volcanic ash) deposited during the eruption.

MATERIAL AND METHODS

Study area

The study was conducted in a series of permanent plots that were already established between 1990 and 1995 (Fig. 1), both inside and outside the permanent breeding colony of seagulls (mainly *Larus fuscus* L.). In this area many other studies have already taken place (Magnusson *et al.* 2014). The seagull colony was originally established in 1986 on the south-western part of the island and by time it has grown in size as the number of birds has increased (Fig. 1). The study was conducted in plots with shallow soils (≤10 cm soil) formed by wind-borne tephra sands that had covered the basaltic lava surfaces and in deep soils (> 30 cm soil) in areas where the tephra sands had been deposited during the eruption (see Leblans *et al.* 2014 for further details). The vegetation on the sandy areas outside the colony was dominated by *Honckenya peploides* (L.) Ehrh. and *Leymus arenarius* (L.) Hochst. The dominant plant species inside the seagull colony were *Poa pratensis* L., *P. annua* L., *Festuca richardsonii* (Hook.) Hultén., with some *Leymus arenarius* and *Stellaria media* (L.) Vill. in the deeper soils (Table 1).

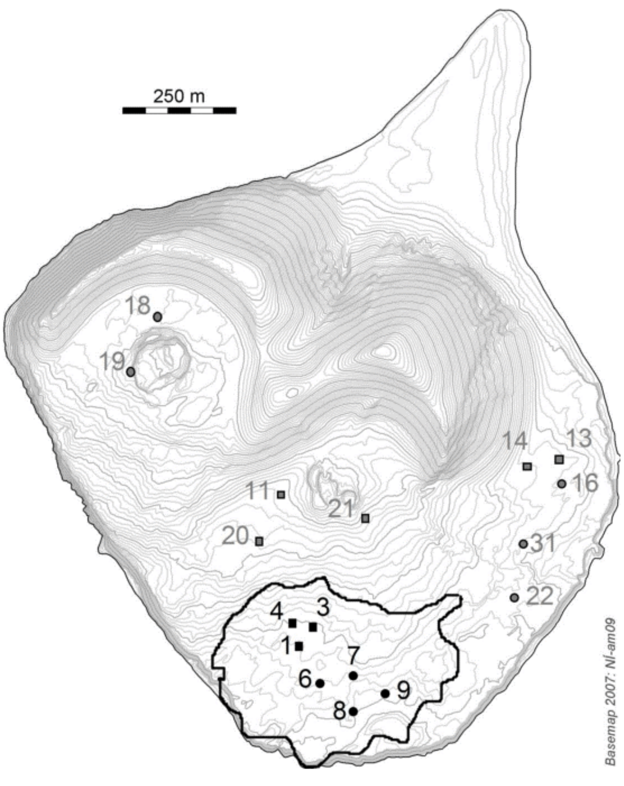

Figure. 1. Location of the permanent study plots on Surtsey that were sampled in the study, shown on a topographical map from 2007. Contour intervals are 2 m, the highest point of the island is 152 m a.s.l. The sea bird colony plots in the southern part are marked with the solid line and black plot numbers. Outside the colony the plots have grey plot numbers. Circles indicate plots with shallow soils (< 10 cm soil depth), squares indicate plots with deep soil (≥ 30 cm soil depth).

Table 1. Distribution of the treatments over the plots used in this study (see Fig. 1 for their locations). Shallow: up to 10 cm deep; Deep: at least 30 cm deep.

Treatment	Plotnumbers	Dominant plant species
Shallow, no birds	16, 18, 19, 22	*Leymus arenarius, Honckenya peploides*
Shallow, + birds	6, 7, 9, 23	*Festuca richardsonii, Poa* sp.*, Pucinellia capillaris*
Deep, no birds	11, 13, 14, 20, 21	*Leymus arenarius, Honckenya peploides*
Deep, + birds	1, 3, 4	*Leymus arenarius, Poa* sp.*, Stellaria media*

Sampling

In July 2013, when the biomass was at its maximum, the sampling was carried out according to the two-factorial design (soil depth and bird presence) as described above. To characterize the nutritional composition of the sea bird input to the ecosystem, we collected sea gull feces and pellets. Additionally, we took a sample of mature leaves from a representative species mix in each plot (see Table 1) and a soil sample down to a standard depth of 15 cm in each plot (deep soils) or to the depth that the underlying lava allowed (shallow soils). The samples were air-dried in Surtsey and after the expedition transported to Amsterdam, where they were dried at 70 ^{o}C for further analysis.

Chemical analyses

After drying, the samples were ground for chemical analyses. The C and N concentration and the δ^{13}C and $\delta^{15}N$ signature of each sample was quantified by dry combustion in an NC 2500 elemental analyzer (Carlo Erba, Rodana, Italy) coupled with a Delta^{plus} continuous-flow isotope ratio mass spectrometer (Thermo Finnigan, Bremen, Germany). The isotopic ratios were converted to delta units (δ) in parts per thousand, according to the formula:

$$\delta(‰) = (R_{sample}/R_{standard} - 1) * 1000$$

in which R is the molar ratio of heavy to light isotopes ($^{13}C/^{12}C$ or $^{15}N/^{14}N$). The $R_{standard}$ for C was VPDB and for N it was the ratio for atmospheric N_2 (air).

Leaf P and soil P concentrations were determined by digesting ground leaf material in 37% HCl : 65% HNO_3 (1:4, v/v). Phosphorus was measured colorimetrically at 880 nm after reaction with molybdenum blue.

RESULTS AND DISCUSSION

Both the gull feces and pellets had extremely high concentrations of N and, especially, of P. This resulted in very low C/N ratios and an extremely low N/P ratio (Table 1). There were no significant differences between feces and pellets for any of the nutritional parameters. The nutrient ratios observed are far below the lowest values reported for both living and dead leaves (Aerts & Chapin 2000), but are characteristic for bird excrements (Bokhorst *et al.* 2019). This implies that input of gull feces and pellets into soils results in a different ratio of N to P input compared to the input of leaf litter.

As is usually found for soils with low carbon content soil N and P concentrations were relatively low. However, higher soil N and P concentrations were found inside than outside the seagull colony (Tables 2 and 3). The N concentration of the shallow soil in the colony was higher than in the deeper soil, where it was extremely low. This is probably due to the fact that most of the N is concentrated in the top layer. Therefore the N is more “diluted” in a deeper soil. The dilution can even have been underestimated in the present study, as we did not sample the whole tephra soil profile in the deep soils. Stefansdottir *et al.* (2014) sampled tephra soil profiles down to 80 cm. They found that considerable amounts of accumulated SOC and N were found below 15 cm depth where the deep-rooted *Honckenya peploides and Leymus arenarius* were growing.

The C/N ratios in the soil were not affected by bird presence or soil depth. This was in contrast with the N/P ratios where bird presence led to higher ratios. Higher N/P ratios were also found in the shallow soils compared to the deep soils (Tables 2, 3). As clearly shown by the extremely low soil N/P ratios outside the bird colony, these young volcanic soils are very rich in P compared to N. This is a general characteristic of volcanic soils (Arnalds 2015).

In southern Iceland, Edlinger (2016) found that $\delta^{15}N$ values in bulk soil (0-10 cm) varied between 0.3 to 1.3 in developed, dryland volcanic (Brown Andosol) soil and in grasses the $\delta^{15}N$ value varied between 1.0 to 1.8 at the same site (unpublished). The plant $\delta^{15}N$ values outside the seagull colony in Surtsey were in the same range (Table 2).

It is striking to see that the $\delta^{15}N$ isotopic signatures of the gull feces and pellets were clearly reflected in the soil signatures in the gull colony (Table 2). On average the soil $\delta^{15}N$ was 12.9 in the soil and 13.2 in the feces and pellets (Table 2). Unfortunately, these signatures could not be determined for all the soils outside the colony due to the extremely low N and C concentrations. They were below the detection limit for the continuous-flow isotope ratio mass spectrometer.

The vegetation in the gull colonly had a substantially higher $\delta^{15}N$ value than the vegetation in the shallow soils outside the colony. The plant $\delta^{15}N$ was on average 17.9 within the gull colony (Table 2), i.e. much closer to the high values found in gull feces and pellets ($\delta^{15}N$ of 13.0) and to the soil in the colony ($\delta^{15}N$ of 12.9; Table 2) or from normal soil and plant $\delta^{15}N$ values in Icelandic grasslands (Edlinger 2016). This strongly supports that the N accumulation seen within the seagull colony is largely derived from the feces and pellets, and does not result from more effective N retention of N-deposition by the more vegetated soils or by N-fixation.

The $\delta^{15}N$ value was significantly higher in plants on deep than shallow soils, both within and outside the seagull colony (Tables 2, 3). In the deep soils within the gull colony the the $\delta^{15}N$ value was even substantially higher than in feces and pellets (21.5 vs. 13.2, respectively; Table 2). The natural abundance of ^{15}N in leaves provides a measure of mineral nutrition that reflects differences in a number of properties and processes, such as the forms of N source (Michelsen *et al.* 1996, Robinson 2001), the type of mycorrhizal infection (Michelsen *et al.* 1998) and differences in signatures among soil layers (Robinson 2001). This

Table 2. Nutritional data of gull feces and pellets, soils and plants at Surtsey inside (+birds) and outside (-birds) the gull colony and for deep and shallow soils. Shallow: up to 10 cm deep; Deep: at least 30 cm deep. bdl: below detection limits.

	%N	%P	%C	C/N ratio	N/P ratio	δ15N(‰)	δ13C(‰)
Gull feces (n=2)							
Mean	8.93	6.22	26.03	2.89	1.47	13.15	-18.79
SD	0.33	1.16	11.25	1.15	0.33	2.52	2.75
Gull pellets (n=2)							
Mean	7.93	6.51	26.47	3.37	1.23	13.31	-18.18
SD	1.77	0.29	3.63	0.30	0.33	0.70	1.71
Soil, +birds, deep (n=3)							
Mean	0.15	0.13	1.91	13.36	1.10	13.99	-28.41
SD	0.07	0.03	0.80	1.57	0.46	0.93	0.67
Soil, +birds, shallow (n=4)							
Mean	0.57	0.11	8.66	14.76	5.54	11.69	-27.54
SD	0.39	0.02	6.58	1.35	4.54	4.86	1.18
Soil, -birds, deep (n=5)							
Mean	0.01	0.10	0.10	13.36	0.08	bdl	bdl
SD	0.00	0.01	0.02	0.69	0.02		
Soil, -birds, shallow (n=4)							
Mean	0.01	0.10	0.13	11.94	0.13	bdl	bdl
SD	0.01	0.01	0.06	2.25	0.09		
Vegetation, +birds, deep (n=3)							
Mean	2.44	0.49	45.42	18.67	5.00	21.51	-27.65
SD	0.23	0.02	0.93	2.04	0.65	0.77	0.29
Vegetation, +birds, shallow (n=4)							
Mean	2.47	0.49	44.88	19.98	5.48	14.81	-29.60
SD	0.17	0.16	1.73	2.75	2.69	3.69	1.12
Vegetation, -birds, deep (n=5)							
Mean	2.06	0.18	42.52	21.09	12.55	1.81	-27.82
SD	0.16	0.04	4.34	0.22	1.57	2.56	0.48
Vegetation, -birds, shallow (n=4)							
Mean	2.18	0.15	40.91	19.30	16.23	0.70	-27.76
SD	0.05	0.02	0.46	0.91	4.71	2.23	0.81

makes it hard to interpret the change in the leaf $\delta^{15}N$ values between deep and shallow soils as so many processes are involved. The data presented here do suggest that, given the differences among deep and shallow soils, that the plants in the deep soils are able to tap nitrogen from deeper layers, although the amount of N there is very low.

The $\delta^{13}C$ signatures in soils and vegetation were relatively constant with values around -28‰. This is in line with the values normally found in soil organic matter and plant material of C3 plants (Farquhar *et al.* 1989) and also in Icelandic grassland soils (Edlinger 2016). The $\delta^{13}C$ signatures in the gull feces and pellets are clearly less negative, but in contrast with ^{15}N, there is no physiological connection between the ^{13}C in these compounds and that in soil organic matter and in plants. These signatures are largely determined by carbon fixation and CO_2 diffusion through the stomata (Buchmann *et al.* 1997, Alstad *et al.* 1999). Some direct effect on soil $\delta^{13}C$ signatures could occur from feces and pellet inputs if those would accumulate as 'guano' in the organic layer of the soil. Leblans (2016), however, addressed this and estimated that the direct C-input from the seabirds could only account for a few percentage of the observed SOC accumulation within the seabird colony and such direct effects should therefore be minimal.

Plant N concentrations (determined on the mix of species present) were higher inside than outside the colony, but the effect was relatively small (Tables 2, 3). This contrasts sharply with the plant P concentrations, as they were about 3 times higher within than outside the colony. As a result, the N/P ratios of plants inside the colony were around 5, which points to strong N limitation (Aerts & Chapin 2000). Outside the colony the N/P ratio was, on the other hand, between 12.5 (deep soils) and 16.2 (shallow soils) which is close to P limitation, as a N/P ratio > 16 indicates P limited plant

Table 3. Results of 2-way analyses of variance on various nutritional parameters in soil and vegetation with soil depth and bird presence as independent parameters. * $P < 0.05$, ** $P < 0.01$, *** $P < 0.001$, N.S.: non-significant; bdl: below detection limits.

	Bird presence	Soil depth	Interaction
Soil			
%N	***	*	*
%P	*	N.S.	N.S.
%C	***	**	N.S.
C/N ratio	N.S.	N.S.	*
N/P ratio	***	*	N.S.
δ15N	bdl		
δ13C	bdl		
Vegetation			
%N	*	*	N.S.
%P	***	N.S.	N.S.
%C	N.S.	N.S.	N.S.
C/N ratio	N.S.	N.S.	N.S.
N/P ratio	***	N.S.	N.S.
δ15N	***	**	N.S.
δ13C	N.S.	*	*

growth (Aerts & Chapin 2000). Soil depth had hardly any effect on these nutritional parameters. One other study has addressed the P availability inside and outside the seagull colony in Surtsey, by looking at the N/P ratios of the same plant species (*Cerastium fontanum* (Hartm.) Greuter & Burdet) growing both inside and outside the colony (Leblans *et al.* 2017). Surprisingly, they found the reverse; the plant N/P ratio was lower outside the seagull colony (ca. 6) compared to inside the colony (ca. 10). The P cycle reserves therefore a further study on Surtsey.

The relative low effect of gulls on the leaf N concentration inside the seagull colony is probably caused by the about 70 times higher carbon stock inside the colony than outside it, whereas the N stock is “only” 30 times higher (data from Leblans *et al.* 2014). This strongly suggests that the higher N accumulation rate in the colony than outside (47 vs 0.7 kg N ha^{-1} yr^{-1}) is translated into a much higher biomass production, and hence N uptake from soil, which results in only a minor increase in leaf N concentration despite the about 70 times higher N input.

In conclusion, in line with other studies, the present study shows the overriding effect of the seagull colony at Surtsey on nutritional characteristics of the soils and vegetation on the island. Due to the very high P richness of the volcanic soils in combination with the high P input by the birds, vegetation productivity is N limited, despite the extremely high N input of 47 kg N ha^{-1} yr^{-1} they produce. However, further studies are needed on P availability for plants outside the seagull colony, and on whether low P availability (relative to N) can possibly be a co-limiting factor for plant productivity there.

ACKNOWLEDGEMENTS

The authors would like to thank Dr Borgþór Magnússon, Icelandic Institute of Natural History, for coordinating the Surtsey excursion in 2013 and the Surtsey Research Society for permitting this study and for logistic support. We further thank the Icelandic Coast Guard for the adventurous helicopter transport to and from the island.

REFERENCES

Aerts, R. & F.S. Chapin, 2000. The mineral nutrition of plants revisited: A re-evaluation of patterns and processes. Advances in Ecological Research 30, 1-67.

Aerts, R., T.V. Callaghan, E. Dorrepaal, R.S.P. van Logtestijn & J.H.C. Cornelissen, 2009. Seasonal climate manipulations result in species-specific changes in leaf nutrient levels and isotopic composition in a sub-arctic bog. Funct. Ecol. 23, 680-688.

Alstad, K.P., J.M. Welker, S.A. Williams & M.J. Trilica, 1999. Carbon and water relations of *Salix monticola* in response to winter browsing and changes in surface water hydrology: an isotopic study using delta C-13 and delta O-18. Oecologia 120, 375-385.

Arnalds, O., 2015. The soils of Iceland. Springer, Netherlands.

Bokhorst, S.F., P. Convey & R. Aerts, 2019. Nitrogen Inputs by Marine Vertebrates Drive Abundance and Richness in Antarctic Terrestrial Ecosystems. Current Biology 29, 1721-1729.

Buchmann, N., W.-Y. Kao & J. Ehleringer, 1997. Influence of stand structure on carbon-13 of vegetation, soils, and canopy air within deciduous and evergreen forests in Utah, United States. Oecologia 110, 109-119.

Edlinger, A.T. 2016. Changes of belowground processes of the carbon and nitrogen cycle in response to soil warming. Will global warming increase the turnover of soil C and N above plant demands and lead to increased leaching losses? (M.Sc. thesis) Dept. of Geosciences and Natural Resource Management 66 p. Copenhagen University, Denmark & University of Natural Resources and Applied Sciences (BOKU), Austria, Copenhagen, Denmark

Farquhar, G.D., J.R. Ehleringer & K. Hubick, 1989. Carbon isotope discrimination and photosynthesis. Ann. Rev. Plant Physiol. Plant Mol. Biol. 40, 503-537.

Leblans N.I.W., 2016. Natural gradients in temperature and nitrogen: Iceland represents a unique environment to clarify longterm global change effects on carbon dynamics. (PhD thesis). 229 p. Joint thesis between Agricultural University of Iceland and University of Antwerp, Reykjavik, Iceland

Leblans, N.I.W., B.D. Sigurdsson, P. Roefs, R. Thuys, B. Magnusson & I.A. Janssens, 2014. Effects of seabird nitrogen input on biomass and carbon accumulation after 50 years of primary succession on a young volcanic island, Surtsey. Biogeosciences 11, 6237-6250.

Leblans, N.I.W., B.D. Sigurdsson, R. Aerts, S. Vicca, B. Magnússon & I.A. Janssens, 2017. Icelandic grasslands as long-term C sinks under elevated organic N inputs. Biogeochemistry 134, 279-299.

Magnússon B., S.H. Magnússon, E. Ólafsson & B.D. Sigurdsson, 2014. Plant colonization, succession and ecosystem development on Surtsey with reference to neighbour islands. Biogeosciences 11, 5521-5537.

Michelsen, A., I.K. Schmidt, S. Jonasson, C. Quarmby & D. Sleep, 1996. Leaf ^{15}N abundance of subarctic plants provides field evidence that ericoid, ectomycorrhizal and non- and arbuscular mycorrhizal species access different sources of soil nitrogen. Oecologia 105, 53-63.

Michelsen A., C. Quarmby, D. Sleep & S. Jonasson, 1998. Vascular plant ^{15}N natural abundance in heath and forest tundra ecosystems is closely correlated with presence and type of mycorrhiza in roots. Oecologia 115, 406-418.

Robinson, D., 2001. δ15N as an integrator of the nitrogen cycle. Trends Ecol. Evol. 16, 153-162.

Sigurdsson, B.D. & G. Stefánsdóttir, 2015. Ecosystem CO_2 flux rates in relaton to vegetation type and age of *Leymus arenarius* dunes on Surtsey. Surtsey Research 13, 9-15.

Sigurdsson, B.D., & B. Magnusson, 2010. Ecosystem respiration, vegetation development and soil nitrogen in relation to breeding density of seagulls on a pristine volcanic island, Surtsey, Iceland. Biogeosciences 7, 883-891.

Stefansdottir, G., A.L. Aradottir & B.D. Sigurdsson, 2014. Accumulation of nitrogen and organic matter during primary succession of *Leymus arenarius* dunes on the volcanic island Surtsey, Iceland. Biogeosciences 11, 5763-5771.

Availability of plant nutrients and pollutants in the young soils of Surtsey compared to the older Heimaey and Elliðaey volcanic islands

BJARNI D. SIGURDSSON[1] AND NIKI I.W. LEBLANS[2]

[1] Agricultural University of Iceland, Hvanneyri 311 Borgarnes, Iceland (bjarni@lbhi.is)

[2] Climate Impact Research Centre, Umeå University, Sweden

ABSTRACT

Surtsey and the older islands in the Vestmannaeyjar archipelago offer a unique possibility to study how sub-Arctic ecosystems develop from unvegetated mineral substrate that lacks soil cover to grasslands with thick Brown Andosol soils. The present study was carried out on Surtsey, Heimaey and Elliðaey in 2013 and involved an incubation of resin membranes in the 0-10 cm topsoil layer in different ecosystems, which were either inside or outside seabird colonies. We compared the effects of seabird presence on soil nutrient availability as well as the importance of time for soil development (at least ca.1600 years vs. 50 years). Further we looked for build-up of Cd and Pb within the seabird colonies. Seabird presence enhanced the availability of most nutrients (N, P, K, Mg, Ca, S, Fe, Mn and Zn) except B and Cu, irrespective of the age of the islands. Soil age was also a significant factor for nutrient availability for all macro- and micro-nutrients except B. Nutrient ratios indicated that N was the most limiting nutrient in all ecosystems, except in the thicker tephra soils on Surtsey where low P availability may lead to co-limitation. The role of P in ecosystem function on Surtesy warrants a futher study. No accumulation of Cd and Pb was found within the seabird colonies.

INTRODUCTION

Primary succession, the chain of processes in which an ecosystem develops on an unvegetated substrate that lacks a developed soil (Walker & Del Moral 2003), is a complex process that depends on the interplay of numerous factors, both biotic and abiotic. Surtsey and the older islands of the Vestmannaeyjar archepelago offer a unique possibility to study some of these factors (cf. Magnusson *et al*. 2014, Leblans *et al*. 2017).

Most studies on Surtsey have focused on community changes in flora, fauna and microbes (e.g. Magnusson *et al*. 2014, Ilieva-Makulec *et al*. 2015, Marteinsson *et al*. 2015) and only few on the underlying carbon and nitrogen processes and C and N accumulation (Sigurdsson & Magnusson 2010, Stefánsdóttir *et al*. 2014, Leblans *et al*. 2014, 2017, Aerts *et al*. 2020). From these studies, it is clear that the establishment of a seabird colony on Surtsey in 1986 has had a large impact on vegetation succession and ecosystem processes. Most studies so far have only focused on the N inputs as the most imporatant driver for ecosystem changes, and assumed that other nutrients would not be limiting. Another article in this issue

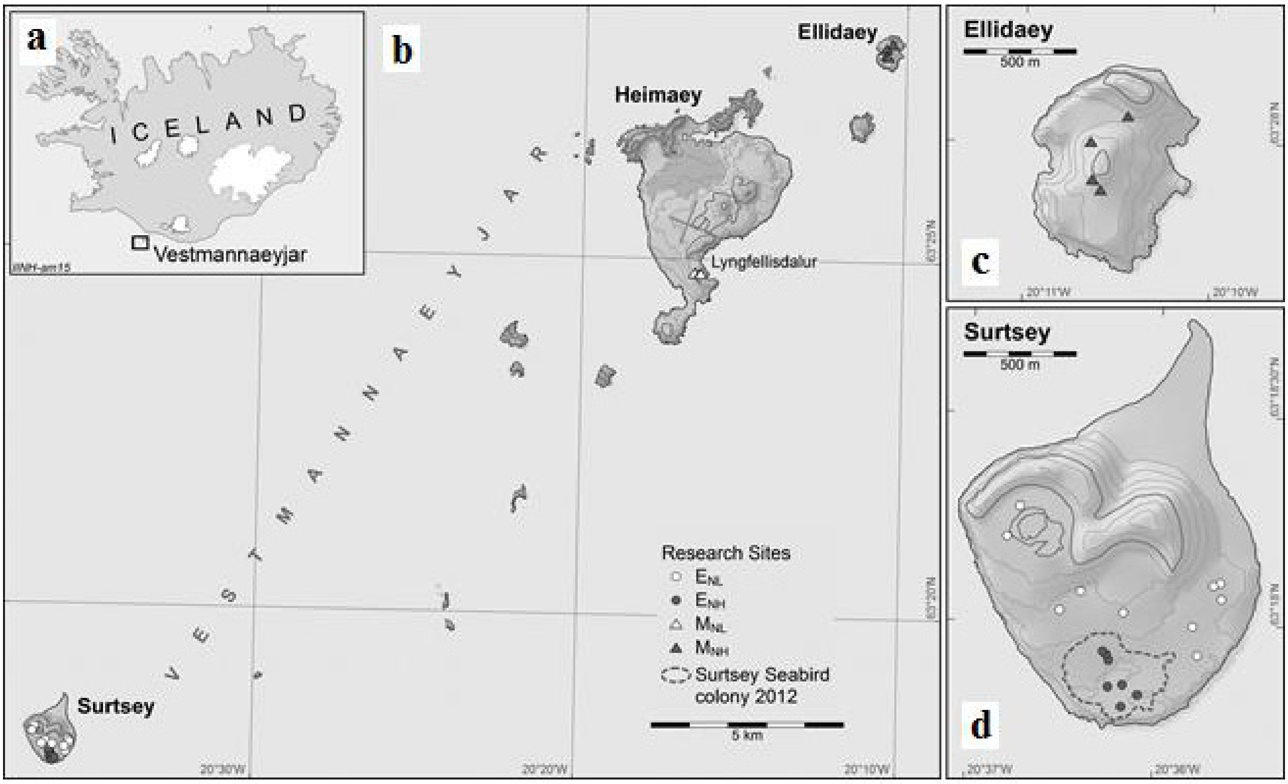

Figure 1. (a) and (b) Location of the Vestmannaeyjar archipelago including the three study islands, Surtsey, Heimaey and Elliðaey, (c) and (d) show the islands Elliðaey and Sterstey in more detail. Circles show the permanent plots at early soil developmental stage under low (○) and high (●) inputs from seabirds within the seagull colony indicated by a dotted line. Triangles show the plots at sites with mature soils under low (Δ) and high (▲) N inputs respectively. Map by Anette Th. Meier.

extends the focus to also involve phosphorus (P), which the seabirds also bring into the ecosystem (Aerts *et al*. 2020). No study has, however, so far looked at the other macro- and micro-nutrients in the Surtsey ecosystems and compared those to the autonomous soil development of the older islands in the Vestmannaeyjar archipelago.

The present study was performed in 2013, when the impact of seabird presence and soil age on soil nutritional availability were studied by incubating resin membranes charged with either anions or cations in the soils of Surtsey (50 years old) and of Heimaey and Elliðaey (ca. 5900 years old). Sampling was performed both inside and outside the seabird colonies on the young and older islands, as well as on both shallow soils formed on lava surfaces and on deeper soils formed in tephra (volcanic ash) deposited during the eruption on Surtsey. The aims were (1) to get a deeper understanding of the nutrient cycle on Surtsey and on potentially limiting nutrients there and (2) to study potential build-up of heavy metals (Cd and Pb) within the seabird colonies.

MATERIAL AND METHODS

Study area

The study was performed on three islands of the volcanic Vestmannaeyjar archipelago (63°250N, 20°170W; south Iceland; Fig. 1) in mid-July 2013. The main vegetation type on the Vestmannaeyjar archipelago is lush grassland, except in areas that are unsuitable for seabird colonization, where heathlands, herb slopes or dry meadows can be found (Magnússon *et al.* 2014). Two pairs of sites with low and high natural seabird inputs were established, one pair with high seabird inputs on Surtsey and Elliðaey and another pair with low seabird inputs at Surtsey and Heimaey (Fig. 1). At Surtsey the soils were at an early developmental stage (50 years old), but both Heimaey (Lyngfellisdalur) and Elliðaey have well-developed soils on bedrocks that both date from eruptions ca. 5900 years ago. The soil profiles at Heimaey and Elliðaey were undisturbed at least since 395 AD, which was determined from the precence of an ash layer from that time >1 m below the surface (Leblans *et al.* 2017). Both the Surtsey and the Heimaey and Elliðaey sites have

Table 1. Distribution of the treatments over the plots used in the study and their dominant plant species.

Islands and experimental category	Plot numbers	Dominant plant species
Elliðaey		
Deep, + seabirds	1, 2, 3, 4	*Festuca richardsonii, Poa* sp., *Stellaria media*
Heimaey		
Deep, no sesbirds	1, 2, 3, 4	*Anthoxantum odoratum, Galium verum, Luzula multiflora*
Surtsey		
Shallow, no seabirds	16, 18, 19, 22	*Leymus arenarius, Honckenya peploides*
Shallow, + seabirds	6, 7, 9, 23	*Festuca richardsonii, Poa* sp., *Pucinellia capillaris.*
Deep, no seabirds	11, 13, 14, 20, 30	*Leymus arenarius, Honckenya peploides*
Deep, + seabirds	1*, 3, 4	*Leymus arenarius, Poa* sp., *Stellaria media*

* *Excluded for macro-nutrients*

different vegetation communites, which represent the differences in seabird influence (Magnússon *et al.* 2014). The Heimaey site is not likely to ever have hosted a seabird colony because of its topographic position, while Elliðaey has topographical conditions that make it highly likely that the island has served as breeding ground for seabirds from early times. The study took place in four permanent 10x10 m study plots that were established at Heimaey and Elliðaey in 2013. These are the same plots that were included in Magnusson *et al.* (2014) and Leblans *et al.* (2017) studies that confirmed the long-term N-accumulation and the contrasting seabird influences at these sites. The vegetation on Elliðaey, which had deep soils with seabird inputs, was similar as in Surtsey, with *Festuca richardsonii*, *Poa* sp., *Stellaria media* as dominant plant species. On Heimaey, which had deep soils without seabird influcecs, the vascular plant community was dominated by *Anthoxantum odoratum* L., *Galium verum* L., *Luzula multiflora* (Ehrh.) Lej.; a herb rich grassland community of low fertility (Magnusson *et al.* 2014) (Table 1).

At Surtsey, the study was conducted in a series of permanent plots that were already established between 1990 and 1995 (Fig. 1), both inside and outside the seagull breeding colony. The seagull colony was originally established in 1986 on the south-western part of the island and by time it has grown in size as the number of birds has increased (Leblans *et al.* 2014). In Surtsey, the plots inside and outside the colony were further divided into plots with shallow soils (≤10 cm soil) formed by wind-borne tephra sands that had covered the basaltic lava surfaces and plots with deep soils (> 30 cm soil) in areas where the tephra sands had been deposited during the eruption (see Leblans *et al.* 2014 for further details). The vegetation on the sandy areas outside the colony on Surtsey was dominated by *Honckenya peploides* (L.) Ehrh. and *Leymus arenarius* (L.) Hochst. The dominant plant species inside the seagull colony were *Poa pratensis* L., *P. annua* L., *Festuca richardsonii* (Hook.) Hultén., with some *Leymus arenarius* and *Stellaria media* (L.) Vill. in deep soils (Table 1). In the area many other studies have already taken place (c.f. Magnusson *et al.* 2014, Leblans *et al.* 2014, 2017, Aerts *et al.* 2020).

Sampling

Soil depth was measured using a 1.2 m long metallic rod pushed down until hitting a rock at 11 places along the S edge of each permanent plot, but recorded as 1.5 m when deeper.

A relative measure for nutrient and pollutant availability was obtained using cation- and anion-exchange membranes (PRS™ probes, Western Ag Innovations Inc.; Saskatoon, SK, Canada). The membranes continuously absorb charged ionic species over the burial period, and the ion availability is calculated as soil flux of exchangable ions. Four sets of cation and anion PRS™ membranes were inserted into the topsoil (0–10 cm depth) at each main study plot in mid-July 2013; 15 – 21 July on Surtsey and 19 – 24 and 19 - 27 July on Heimaey and Elliðaey, respectively. Afterwards, they were sent to Western Ag Innovations Inc. (Saskatoon, SK, Canada) for further analyses.

Data and statistical analyses

Plots where either all PRS™ anion or cation membranes were lost during the incubation period were not included in the analysis. These were two plots on Surtsey, R21 and R8. The reason for the loss of membranes was that seagulls had dragged them out of the soil. One plot, R1, was excluded from the analysis of macro-nutrients on Surtsey as the values were extremely high (10-100 x higher than anywhere else). There was a major dieback of *Poa annua* in this plot following a prolonged drought during summer of 2012, a year before this study took place, which has since then resulted in rapid species turnover and a large increase *in Stellaria media* cover (unpublished data). The plot was therefore an "outlier" for the Surtsey seagull colony as a whole. Further, few samples for the nutrients NO3-N and NH4-N did not quite meet the method detection limits (MDL) of PRS™ which is 2 mg N/10 cm^2, but were still included in the analysis. Similarly, not all Mn and Cu concentrations reached the MDL of 0.2 mg /10 cm^2, but were still included. Finally, Pb and Cd pollutant concentrations never reached the given MDL of 0.2 mg /10 cm^2.

The effets of the chronically elevated seabird inputs and soil age on nutrient and pollutant availability were tested with a two-way ANOVA, with sebird input (low/high) and soil age (young/old) as fixed factors. In case of significant interaction, the pairwise differences were tested by post hoc LSD tests when the requirements of normality and homoscedasticity of the residuals were met. The latter was visually inspected.

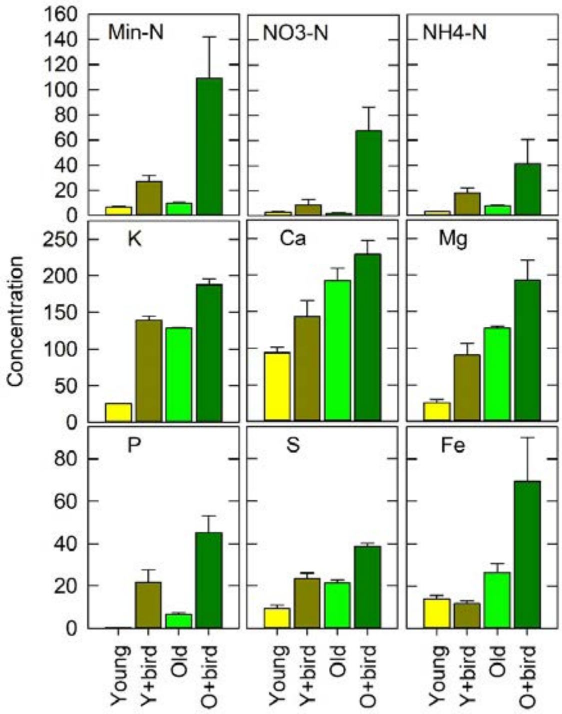

Figure 2. Availability of various macro elements and iron (Fe) after 5-8 day incubation of PRS™ resin probes in 0-10 cm soil depth, or laterally where the soil was thinner, in permanent plots on islands of varying age (Young: Surtsey = 50 years; Old: Heimaey/Elliðaey = ca. 5900 years) in areas with seabird presence (+bird) or not. The unit is mg ion /10 cm^2 resin membrane. Bars show plot means ±SE of n=2-5. Note the different scales on the y-axes. See Table 1 for plot numbers in each category and Table 2 for statistical analysis.

RESULTS AND DISCUSSION

Macro-nutrients

Total mineral N, NO3-N and NO4-N in the topsoil and all the other macro-elements were significantly increased by the seabird precence, both at Surtsey and on the older islands (Fig. 2; Table 2). The significant interaction for both total mineral N and NO3-N seen in Table 2 was caused by the relatively stronger increase on the older islands compared to Surtsey (Fig. 2). The seabird-driven increase in total mineral N was 11-fold on the old isands, while it was only 4-fold on Surtsey. For NO3-N this increase was 36-fold and 3-fold, repectively. Leblans *et al.* (2017) have shown that the seabird N-inputs are somewhat higher within the seabird colony on Elliðaey than on Surtsey, ca. 67 versus 47 kg N /ha /year, compared to ca. 1-2 kg kg N /ha /year background atmospheric N-deposition. The relatively lower seabird response of the total mineral N availability in the topsoil on the younger Surtsey can possibly be explained by the much smaller total soil N stock that has accumulated there (Leblans *et al.* 2017). This lower stock could lead to a relatively higher N uptake by plants on Surtsey in the most active growing season in July (cf. Aerts *et al.* 2020).

The older islands had a significantly higher availability of all macro-nutrients (Table 2; Island age effect) except for NH4-N, which was not significant when compared across all plots (Fig. 2). The NO3-N ratio in the total mineral N was higest (62%) within the very fertile seabird colony on Elliðaey, but lower in the more infertile grassland soil on Heimaey (19%) and on Surtsey (37% across all plots; Table 3).

Macro-nutrient cation availability (Ca, K, Mg) was very high compared to N, P and S (Figure 2; note the different scales on y-axes). This is typical for young basaltic substrates in Iceland (Arnalds 2015). Outside the seabird colony on Surtsey the availability of those cations was significantly lower than within the seabird colony, except for Ca that did not vary

Table 2. Statistical results (p-values) of 2-way analyses of variance on the availability of various elements as a function of seabird presence and island age as independent parameters in Surtsey, Heimay and Elliðaey, as shown in Figures 2-4. Bold font indicates significant differences ($p < 0.05$).

	Seabird presence	Island age	Inter-action
Macro-nutients			
NO3-N	**<0.001**	**<0.001**	**<0.001**
NH4-N	**0.003**	0.07	0.21
Mineral-N	**<0.001**	**0.002**	**0.004**
P	**<0.001**	**0.004**	0.07
K	**0.003**	**0.007**	0.30
Mg	**<0.001**	**<0.001**	0.99
Ca	**0.02**	**<0.001**	0.68
S	**<0.001**	**<0.001**	0.44
Micro-nutrients			
Fe	**0.01**	**<0.001**	**0.006**
Mn	**0.001**	**<0.001**	0.15
Cu	0.06	**<0.001**	0.82
Zn	**0.01**	**0.02**	**0.001**
B	0.90	0.66	0.98
Aluminum and pollutants			
Al	0.45	**<0.001**	0.94
Cd	0.25	**0.009**	0.80
Pb	0.90	**0.008**	0.66

across different plots on Surtsey (Tables 3 and 4). This does not necessarily mean that those extra cations are seabird-borne; they can also accumulate due to more root-growth activity, SOM build-up and decompositon (soil respiration) following primary succession within the seabird colony (Sigurdsson 2015, Sigurdsson & Magnusson 2010, Leblans *et al.* 2014, 2017).

Some of the soils on Surtsey are very thin (or 4-6 cm; Table 3), on top of a basaltic lava bedrock. A tendency for higher average cation availability was seen in plots with the thin soils on Surtsey (Table 3 and 4), but it was only signifcant for Mg. This is the same effect as reported by Aerts *et al.* (2020) for N and P and probably indicates more root-mediated dilution in the deeper tephra soils.

The P availability was significantly enhanced by the seabird presence, irrespective of island age, and it was also on average significantly higher in the older soils (Fig.2; Table 2). Aerts *et al.* (2020) found with isotopic analyses that most of the P in the seabird colony of Surtsey was derived from the seagulls. They also found indications from N/P stociometry of plant biomass that P could possibly be co-limiting outside the seagull colony in Surtsey. This is, however, not supported by Leblans *et al.* (2017) stociometery of *Cerastium fontanum* plants growing in or close to all permanent plots on Surtsey. A non-molar corrected P/N ratio of 0.08 is needed to maintain optimum growth in plants (Linder & Ingestad 1977, Sigurdsson 2001). It is noteworthy that outside the seagull colony at Surtsey the ratio between P and mineral-N availability was exactly 0.08 in the 3 - 6 cm thin soils, but only 0.06 in the topsoil layer of the deeper soils (Table 3). However, this analysis does not include organic P and N that vascular plants can get from symbiotic mycorrhyzal fungi (Chapin *et al.* 2002) and deep-rooted plants may have accessed additional P-stores from below the topsoil. The role of P in the funcitoning of the plant communities outside the seagull colony in Surtsey is therefore still an open question and warrants a futher study.

Sulfur (S) availability also increased significantly both with seabird presence and island age (Fig. 2; Table 2). It had a slight, but significant reduction in topsoil of deeper tephra soils in Surtsey (Tables 3 and 4). Its availability was in a similar range as P on all isands with seabird influence (S/P ratio of 0.9-1.1). The S/P ratio was ca. 3 on Heimaey and as high as 21 outside the seabird colony on Surtsey (Fig. 2). It is therefore unlikely that S will become a limiting nutrient in those island ecosystems compared to N or P, since plants require only ca. half as much S as P for maintaining optimum growth rates (Linder & Ingestad 1977).

Micro-nutrients

The availability of Fe was very high on all islands (Fig. 2), but was only signifcantly increased by seabird precense on the old islands; hence the signicant interaction term in Table 2. Availability of Zn was ca. 1/10 of the Fe, and it had an unexpected spatial trend with the highest availability within the seagull colony on Surtsey, but similar and lower values elsewhere. This also explains the significant interaciton term in Table 2. The relatively high availability of Zn compared to e.g. minearal N (Figs. 2 and 3), with Zn/N ratio of ca. 0.1 on Surtsey and Heimaey, makes it unlikely that Zn plays any important role in the biogeochemistry of the island ecosystems. The Zn/N ratio of 0.0005 are enough to maintain optimum growth of plants (Linder & Ingestad 1977). Similarly Mn values were relatively high (Fig. 3), the lowest Mn values were found outside the seagull colony

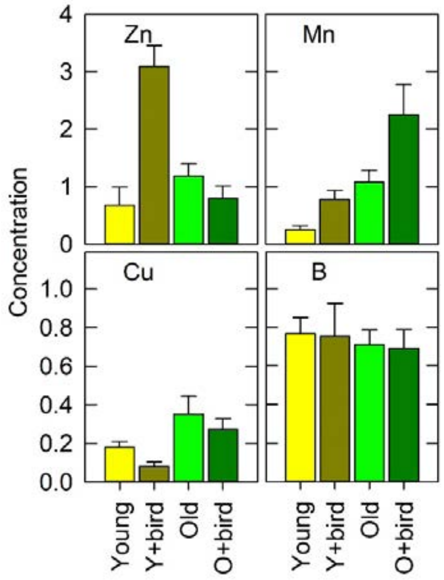

Figure 3. Availability of various micro elements after 5-8 day incubation of PRS™ resin probes in 0-10 cm soil depth, or laterally where the soil was thinner, in permanent plots on islands of varying age (Young: Surtsey = 50 years; Old: Heimaey/Elliðaey = ca. 5900 years) in areas with seabird presence (+bird) or not. The unit is mg ion /10 cm^2 resin membrane. Bars show plot means ±SE of n=3-5. Note the different scales on the y-axes. See Table 1 for plot numbers in each category and Table 2 for statistical analysis.

on Surtsey, but still the Mn/N ratio there was ca. 0.04, which is two orders of magnitude higher than needed to maintain optimum plant growth (Linder & Ingestad 1977). Further, the Mn availability increased significantly both with seabird persence and island age (Table 2), but not with soil depth on Surtsey (Tables 3 and 4).

The Mn/N ratio was highest outside the seagull colony on Surtsey (0.12), but lowest on Elliðaey (0.006) (Figs 2 and 3). According to Linder & Ingestad (1977) a Mn:N ratio of 0.0005 is more than enough for optimum growth of vascular plants; hence the B availability compared to mineral N was still an order of magnitude higher than needed.

The two micro-nutrients with by far the lowest availability in the present study were B and Cu (Fig. 3). The B availability did not change significantly with seabird presence or age of soil (Table 2) nor by soil depth on Surtsey (Table 3). On average it was 0.74 ±0.06 mg B / 10 cm^2.

Copper was the micro-nutrient with the lowest availability in the present study. Something that has also been found in foilage analysis of plants growing on Brown Andosols on mainland Iceland (Sigurdsson 2001). Its availability increased significantly with seabird presence (and plant succession) on Surtsey (Tables 3 and 4), but not overall on the islands (Fig. 3; Table 2). However, it did increase significantly with soil age across both the older islands (Fig. 3; Table 2). Cu is the micro-nutreint included in the present study that plants need least amounts of, or less than 0.0003 Cu/N ratio (Linder & Ingestad 1977). The Cu/N ratio in the seabirds colonies of Surtsey and Elliðaey was ca. 0.003, while it was order of magnitude larger without the seabird presence (ca. 0.03). Hence, Cu seems not to be a limiting element compared to N and possibly P, according to its soil availability found in the present study.

Aluminium and pollutants

The soils in the present study were Al rich (Fig. 4), which is normal for volcanic soils (Arnalds, 2015). The Al availability did not decrease with soil age, but increased significantly which indicates a higher bedrock weathering activity than Al leaching (Fig. 4; Table 2). Further, Al did not vary with soil depth on Surtsey (Tables 3 and 4). An expected increase in the solubility of Al in the more acid soils within the seabird colonies (Sigurdsson & Magnússon 2010, Leblans *et al.* 2017) was not observed. The 5-7 times higher availability of the other cations in the island soils could effectively have buffered that response, as they would be pushed out of the exchange sites before Al.

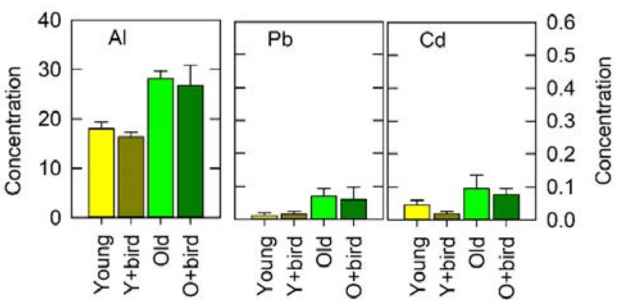

Figure 4. Availability of aluminium and pollutants after 5-8 day incubation of PRS™ resin probes in 0-10 cm soil depth, or laterally where the soil was thinner, in permanent plots on islands of varying age (Young: Surtsey = 50 years; Old: Heimaey/Elliðaey = ca. 5900 years) in areas with seabird presence (+bird) or not, as independent parameters. The unit is mg ion /10 cm^2 resin membrane / 5 days. Bars show plot means ±SE of n=3-5. Note the different scales on the y-axes. See Table 1 for plot numbers in each category and Table 2 for statistical analysis.

Table 3. Soil depth and the availability of various elements after six days incubation of PRS™ resin probes in 0-10 cm soil depth on Surtsey. The unit is mg ion /10 cm2 resin membrane. Numbers are plot means ±SE of n = 2 - 5. See Table 1 for plot numbers in each category and Table 4 for statistical analysis.

	Outside		**Seabirds**	
	Shallow	**Deep**	**Shallow**	**Deep**
Soil depth	3.7 ±2.1	100.0 ±21.9	6.2 ±2.8	39.4 ±9.8
Macro-nutrients				
NO3-N	2.3 ±0.8	3.7 ±1.4	10.5 ±4.3	5.8 ±1.0
NH4-N	3.7 ±0.7	3.0 ±0.7	16.8 ±5.1	21.0 ±9.1
Mineral-N	6.0 ±1.2	6.7 ±1.5	27.2 ±6.0	26.8 ±10.1
P	0.5 ±0.1	0.4 ±0.1	25.8 ±9.0	13.8 ±1.0
K	32.9 ±20.4	19.5 ±2.3	152.5 ±36.0	113.1 ±9.0
Mg	30.4 ±10.6	21.1 ±4.1	107.8 ±20.3	56.1 ±5.7
Ca	92.9 ±15.0	94.0 ±10.6	154.1 ±35.0	122.2 ±0.4
S	9.9 ±4.7	8.5 ±1.6	24.0 ±4.5	22.3 ±3.4
Micro-nutrients				
Fe	13.9 ±4.2	13.9 ±1.1	12.0 ±2.3	11.5 ±0.9
Mn	0.3 ±0.2	0.2 ±0.0	0.9 ±0.3	0.6 ±0.1
Zn	1.0 ±0.8	0.4 ±0.1	3.5 ±0.6	2.6 ±0.3
Cu	0.2 ±0.1	0.2 ±0.0	0.1 ±0.0	0.1 ±0.0
B	0.7 ±0.2	0.8 ±0.1	0.9 ±0.3	0.5 ±0.1
Aluminium and pollutants				
Al	16.4 ±2.8	19.3 ±1.5	16.8 ±1.3	15.9 ±1.4
Cd	0.05 ±0.03	0.05 ±0.02	0.02 ±0.01	0.01 ±0.01
Pb	0.02 ±0.02	0.00 ±0.00	0.01 ±0.01	0.02 ±0.02

Table 4. Statistical results (*p-values*) of 2-way analyses of variance on the availability of various elements on Surtsey, as shown in Table 3. Bold font indicates significant differences ($p < 0.05$).

	Seabird presence	**Soil depth**	**Inter-action**
Soil depth	0.08	**0.001**	0.06
Macro-nutients			
NO3-N	0.09	0.57	0.29
NH4-N	**0.002**	0.66	0.54
Mineral-N	**<0.001**	0.97	0.91
P	**0.003**	0.27	0.28
K	**<0.001**	0.28	0.59
Mg	**0.001**	**0.04**	0.14
Ca	0.08	0.51	0.48
S	**<0.001**	**<0.001**	0.44
Micro-nutrients			
Fe	0.38	0.90	0.92
Mn	**0.01**	0.42	0.53
Cu	**0.02**	0.37	0.41
Zn	**<0.001**	0.14	0.73
B	0.83	0.40	0.14
Aluminum and pollutants			
Al	0.41	0.57	0.30
Cd	0.14	0.82	0.77
Pb	0.70	0.70	0.35

The pollutants Cd and Pd were found with an extremely low availability in the present study and were in fact below the given MDL of 0.2 mg /10 cm^2. Still the membranes yielded some ions, but only on average 0.05 and 0.02 mg /10 cm^2, across all plots, respectively. Since the measurements are so much lower than the MDL of the method, these results are an indication rather than a confirmation of the extremely low values. Both metals can accumulate in oceanic food webs (Kay 1985, Michaels & Flegal 1990). It was therefore of interest if we would find increased accumulation in areas with large seabird presence, which was not the case (Fig. 3; Tables 2-4). However, both metals showed a significant increase in availability with soil age (Table 2). Even then, they only reached ca. half of the MDL for Cd and Pb, so we can conclude that both are very low.

Conclusion

The present study was the first on the availability of most soil macro- and micro-nutrients on Surtsey and the older islands in the Vestmannaeyjar archepelago. The findings support that N is generally the most limiting plant nutrient in these ecosystems. However, in the young, undeveloped soils outside the seagull colonies on Surtsey, P availability could possibly reach co-limitation as N has accumulated by 1-2 kg N / ha / year from atmospheric deposition during the last 50 years (Stefánsdóttir *et al*. 2014). The role of P in ecosystem function hence warrants a futher study on Surtsey.

ACKNOWLEDGEMENTS

The authors would like to thank Dr Borgþór Magnússon, Icelandic Institute of Natural History, for coordinating the Surtsey excursion in 2013, the Surtsey Research Society for permitting this study and Þórdís Bragadóttir and Hekla Hrund Bjarnadóttir for help during fieldwork.

REFERENCES

Aerts, R., R.S.P. van Logtestijn, N.I.W. Leblans & B.D. Sigurdsson, 2020. Effects of sea birds and soil development on plant- and soil-nutritional parameters after 50 years of succession on Surtsey. Surtsey Research 14, 85-90.

Arnalds, O., 2015. The soils of Iceland. Springer, Netherlands.

Chapin III, F.S., P.A. Matson & H.A. Mooney, 2002. Principles of terrestrial ecosystem ecology. Springer: New York, Berlin, London.

Ilieva-Makulec, K., B. Bjarnadottir & B.D. Sigurdsson, 2015. Soil nematode communities on Surtsey, 50 years after the formation of the volcanic island. Icelandic Agricultural Sciences 28, 43-58.

Kay S.H., 1985. Cadmium in aquatic food webs. *In* Gunther F.A. (eds) Residue Reviews. Residue Reviews, vol 96. Springer, New York, NY.

Leblans, N.I.W., B.D. Sigurdsson, P. Roefs, R. Thuys, B. Magnusson, & I.A. Janssens, 2014. Effects of seabird nitrogen input on biomass and carbon accumulation after 50 years of primary succession on a young volcanic island, Surtsey. Biogeosciences 11, 6237-6250.

Leblans, N.I.W., B.D. Sigurdsson, R. Aerts, S. Vicca, B. Magnússon & I.A. Janssens, 2017. Icelandic grasslands as long-term C sinks under elevated organic N inputs. Biogeochemistry 134, 279-299.

Linder, S. & T. Ingestad, 1977. Ecophysiological experiments under limiting and non-limiting conditions of mineral nutrition in field and laboratory. *In* Bicentenary celebration of C.P. Thunberg's visit to Japan, The Botanical Society of Japan, Tokyo, pp. 69-76.

Magnússon B., S.H. Magnússon, E. Ólafsson & B.D. Sigurdsson, 2014. Plant colonization, succession and ecosystem development on Surtsey with reference to neighbour islands. Biogeosciences 11, 5521-5537.

Marteinsson, V., A. Klonowski, E. Reynisson, P. Vannier, B.D. Sigurdsson & M. Ólafsson, 2015. Microbial colonization in diverse surface soil types in Surtsey and diversity analysis of its subsurface microbiota. Biogeosciences 12, 1-13.

Michaels A.F. & A.R. Flegal, 1990. Lead in marine planktonic organisms and pelagic food webs. Limnol. Oceanogr 35 (2), 282-295.

Sigurdsson, B.D., 2001. Environmental control of carbon uptake and growth in a *Populus trichocarpa* plantation in Iceland. PhD thesis. Swedish University of Agricultural Sciences: Uppsala, Sweden, 64 p.

Sigurdsson, B.D. & G. Stefánsdóttir, 2015. Ecosystem CO_2 flux rates in relaton to vegetation type and age of *Leymus arenarius* dunes on Surtsey. Surtsey Research 13, 9-15.

Sigurdsson, B.D. & B. Magnusson, 2010. Ecosystem respiration, vegetation development and soil nitrogen in relation to breeding density of seagulls on a pristine volcanic island, Surtsey, Iceland. Biogeosciences 7, 883-891.

Stefansdottir, G., A.L. Aradottir & B.D. Sigurdsson, 2014. Accumulation of nitrogen and organic matter during primary succession of *Leymus arenarius* dunes on the volcanic island Surtsey, Iceland. Biogeosciences 11, 5763-5771.

Walker, L. R. & R. Del Moral, 2003. Primary succession and ecosystem rehabilitation, Cambridge University Press, Cambridge.

Sea sandwort from Surtsey: chromosomal evidence of active evolution via wide-hybridization

KESARA ANAMTHAWAT-JÓNSSON [1], AUDREY PACE [1] AND SIGURÐUR H. ÁRNASON [1,2]

[1] Institute of Life and Environmental Sciences, School of Engineering and Natural Sciences, University of Iceland, Sturlugata 7, Reykjavík 102, Iceland. [2] Westfjord Iceland Nature Research Centre, Adalstræti 12, 415 Bolungarvík, Iceland.
Corresponding author: Kesara Anamthawat-Jónsson, kesara@hi.is

ABSTRACT

Sea sandwort (*Honckenya peploides*) was among the first species of vascular plants colonizing Surtsey. It is a member of the carnation family, Caryophyllaceae, a coastal plant with circumpolar distribution. The species is dioecious comprising separate female and hermaphrodite (male) plants. Our previous study of this plant revealed high molecular polymorphism, indicating rapid expansion and multiple origins, but low genetic differentiation, suggesting gene flow on Surtsey. The maintenance and/or expansion of populations with high gene diversity on the island are most likely fostered by several factors, one of them being the polyploid nature of the study species providing fixed heterozygosity. We therefore investigated chromosome number diversity of *H. peploides* from Surtsey, in comparison with accessions from Heimaey and other locations within and outside Iceland. Seeds were germinated with and without cold stratification. Chromosomes were isolated from root tips using the cellulase-pectinase enzymatic squash method. DAPI-stained chromosomes were counted from microscopic images that were taken at 1000x magnification. The results show that the most common $2n$ somatic chromosome number of this species is 68 ($2n=4x=68$), but a tetraploid cytotype with 66 chromosomes also exists. The karyotype analysis shows that the species is an autotetraploid, most likely originating via chromosome doubling (whole genome duplication) in a diploid ancestor. Numerous other $2n$ numbers were discovered, from the diploid number $2n=2x=34$ in Heimaey to several different numbers between 40 and 64. The triploid hybrid numbers $2n=3x=51$ (50-52) were discovered from both Surtsey and Heimaey, as well as from other regions. Triploid hybrids serve as a bridge promoting gene flow within populations, promoting heterozygosity in the tetraploid species. All other numbers are aneuploids, most likely deriving from back-crossing of triploid hybrids and the euploid parents. The presence of aneuploids across the species distribution range is due to its ability to propagate asexually by clonal expansion. The presence of the lower ploidy levels within species, together with the extensive aneuploidy, may be an evolutionary characteristic of a pioneering plant, with great dispersal ability and genetic diversity, such as sea sandwort.

INTRODUCTION

Sea sandwort [*Honckenya peploides* (L.) Ehrh.] was among the first four species of vascular plants to colonize Surtsey in 1965-1967, while the island was still in the last phase of cooling down (Friðriksson 1964; Magnússon *et al.* 2009). The other three species are sea rocket (*Cakile arctica* Pobed.), sea lymegrass [*Leymus arenarius* (L.) Hochst.] and sea bluebells [*Mertensia maritima* (L.) Gray]. As the

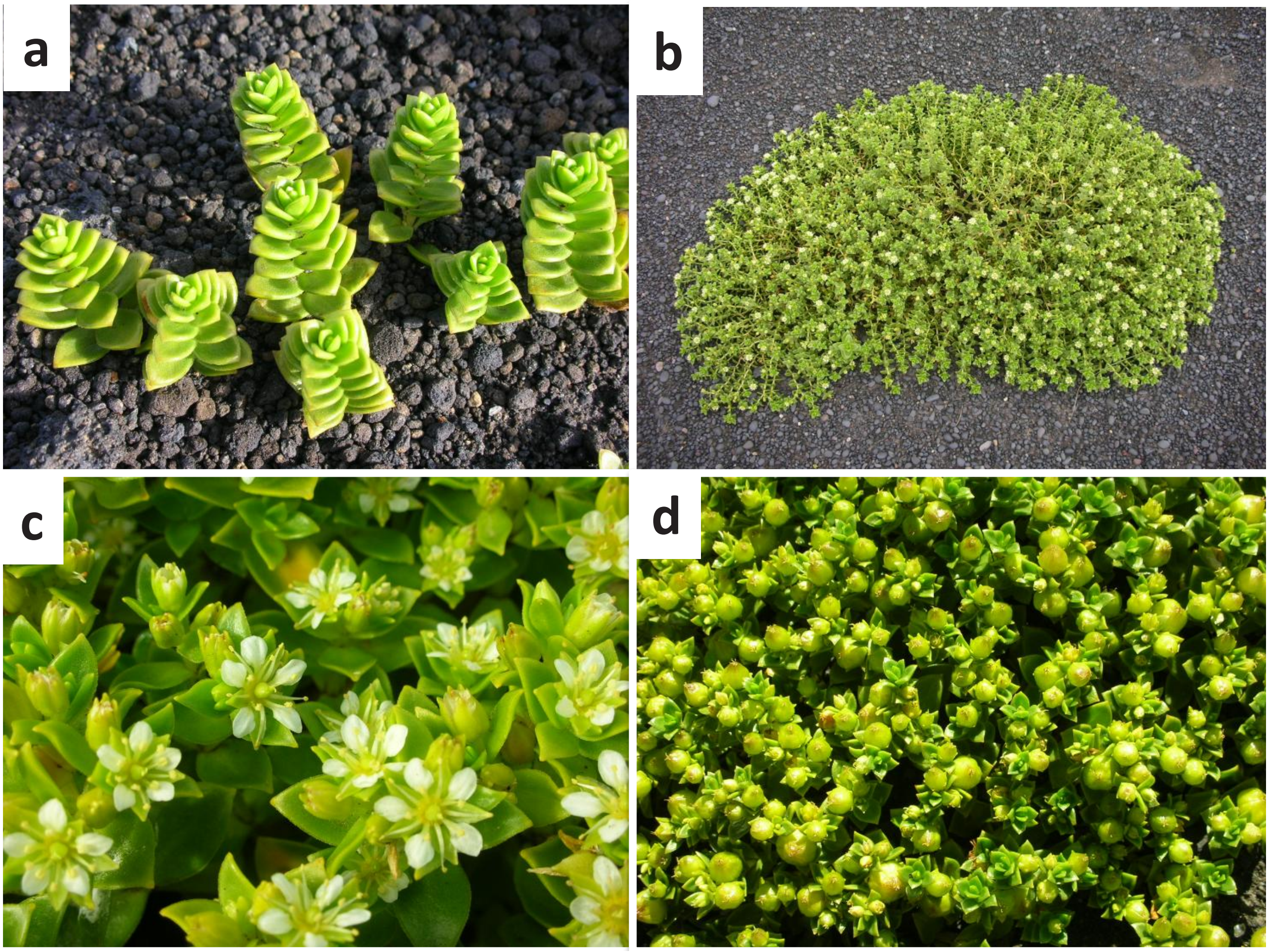

Figure 1. Sea sandwort (*Honckenya peploides)* from Surtsey: (a) young individual plants; (b) fully grown plant in a clonally expanded mat; (c) hermaphrodite flowers showing large petals; and (d) female flowers showing fruit capsules. Photographs by K. Anamthawat-Jónsson, July 2010.

common names imply, they all are coastal plants that colonized the island by means of seed dispersal by sea (Magnússon *et al.* 2014). Since the colonization, *H. peploides* has become the most abundant plant on the island and is a key facilitator of plant and animal colonization, providing substrate binding for plants as well as nesting material for birds (Sigurdsson & Magnússon 2010).

Honckenya peploides (Fig. 1) is the only species within the genus *Honckenya* (L.) Ehrh., belonging to the subfamily Alinoideae in the carnation family Caryophyllaceae. The species has a subdioecious reproductive system, consisting of pistillate (female) plants producing capsules and staminate (male) plants delivering pollen (Malling 1957). The pistillate flowers have a normally developed gynoecium, small petals and non-functional, staminodie-like (aborted) anthers. They produce capsules 6 – 10 mm in size with large seeds. Staminate flowers, on the other hand, have short styles, larger petals and well-developed anthers, producing pollen grains. Some of these staminate flowers have the ability to produce capsules with low seed numbers and are therefore categorized as hermaphrodites. Hermaphrodite seeds develop into female and hermaphrodite plants, in an approximate 1:3 ratio, whereas seeds of female flowers produce about as many hermaphrodites as females (Malling, 1957). The sex determination system is heterogamous for the hermaphrodite.

Both female and male (hermaphrodite) plants co-exist, but the proportion between the two sexes varies among locations. Philipp & Adsersen (2014) found that populations on the southern coast of Iceland had around equal numbers of pistillate and staminate plants, whereas on Surtsey they found pistillate plants predominating, presumably due to their higher water stress tolerance. Sanchez-Vilas & Retuerto (2017) found that the females of *H. peploides* on the Galician coast of Spain had greater water use efficiency than the males. This ability is likely to help maintain high rate of photosynthesis in water-limited conditions, as a female needs to allocate more of its biomass to reproduction. Sexes of dimorphic species often differ in ecophysiological traits and display spatial segregation, and in an evolutionary context, gender specialization appears to be favored in resource-poor environments (Delph & Wolf 2005). Surtsey is a good example – its gender specialization is towards the female sex. Resources especially during the early colonization stages were probably limited due to poor substrate conditions of the sand and the lava/tephra soil. In addition, Philipp & Adsersen (2014) found a tendency towards a higher frequency of hermaphrodite plants on Surtsey with a higher number of seeds per capsule compared to populations on the south coast and the nearby island of Heimaey. They suggested that this arises from the time right after the colonization of Surtsey, when population size was small and the small generalist pollinators were not able to deposit sufficient pollen on pistillate plants, causing the hermaphrodites to have an advantage by being able to set seed after selfing. The result of this initial advantage of the hermaphrodites in combination with the inheritance of the sexes can still be seen due to the longevity of individual plants.

Honckenya peploides reproduces both sexually and asexually (clonal via rhizomes) and displays a large amount of genetic variation within populations in north-western Spain (Sánchez-Vilas *et al*. 2010), Greenland and Svalbard (Eithun 2003), and on Surtsey itself (Árnason *et al*. 2014). An experimental study of Australian seagrass (*Posidonia australis* Hook.f.), a predominantly clonal plant, has demonstrated that a higher level of genetic diversity can benefit the species due to the increased likelihood of those populations having genotypes that can persist under environmental change (Evans *et al*. 2017). As with *H. peploides* we have found a significantly higher level of genetic diversity among island and coastal populations in Iceland (including Surtsey) compared to that of mainland Europe (Árnason *et al.* 2014), which is opposite to the general pattern of oceanic island biogeography (Whittaker *et al.* 2008, Frank 2010). The large genetic variation found in *H. peploides* on Surtsey (and nearby locations) is therefore likely to be an advantage in the ecological context.

Our molecular analysis of *H. peploides* (Árnason *et al*. 2014) has indicated several factors that likely foster the maintenance and/or expansion of populations with high gene diversity on Surtsey. One of these factors is the plant itself. The subdioecious breeding system of the plant causes poor seed set after self-fertilization in the hermaphrodite plants (Tsukui & Sugawara 1992, Eithun 2003), thus reducing inbreeding due to selfing. Although the frequency of seed set by hermaphrodite plants on Surtsey was not as low as predicted, it was still far more inferior to the fertility of the female plants (Philipp & Adsersen 2014). Another important factor promoting high gene diversity within a population is the polyploid nature of a species providing fixed heterozygosity (Soltis & Soltis 2000). The aim of the study reported here was therefore to explore the polyploidy nature of *H. peploides*.

Genetic variation is often maintained through fixed heterozygosity in polyploid species. Fixed heterozygosity has been reported in a number of polyploid arctic plants and seems to be the norm rather than the exception. Brochmann *et al.* (2004) found that all Svalbard polyploids were genetic autopolyploids with fixed heterozygosity at isozyme loci. Furthermore, they found that heterozygosity increases dramatically from diploid to high-level polyploids in 65 arctic taxa. This high level of heterozygosity has been proposed by other authors to be the motive force behind polyploidy expansion into new habitats (Levin 2002, Soltis *et al*. 2015). Brochmann *et al*. (2004) speculated that fixed-heterozygosity as a result of polyploid formation, buffering against inbreeding and drift (environmental filtering), is the cause of the great evolutionary success of polyploids in the arctic region. Out-crossing diploid populations tend to become genetically homogeneous when confronted with bottlenecks and inbreeding, as is often the case when colonization of isolated areas takes place (Aguilar *et al*. 2008, Yuan *et al*. 2012). In fact, ecological modeling generally supports patterns of adaptive niche differentiation in polyploids, with young polyploids often invading new niches and leaving their diploid progenitors behind (Baduel *et al*. 2018). Typical arctic plant populations (usually autopolyploids) have the possibility of retaining genetic variation due to fixed allelic diversity within each individual (Otto & Whitton 2000). The deposit of ancestral genetic material into duplicated genomes guarantees that genetic diversity is maintained

Table 1: Published chromosome numbers for *Honckenya peploides*.

Location	Source	2n =
Spitsbergen, Svalbard	Flovik (1940)	66
Dragor, Denmark	Malling (1957)	68
Sakhalin Island, Russia	Sokolovskaya & Strelkova (1960)	66, 68, 70
Wrangle Island, Russia	Agapova (1993)	66, 68, 70
North Eastern Russia	Zhukova (1966)	68
Eastern Russia	Zhukova (1966)	66
Moneron Island, Russia	Probatova (2004)	34*
North Eastern Asia	Zhukova (1966)	68
Ogotoruk Creek, N.W. Alaska	Johnson & Packer (1968)	68
Meade River, N. Alaska	Packer & McPherson (1974)	68
Western Alaska	Murray & Kelso (1997)	68
Arctic Canada	Löve & Löve (1982)	68
Arctic circumpolar	Löve & Löve (1975)	66, 68, 70
Iceland	Löve & Löve (1950, 1956)	ca. 40, 66
Sweden	Lövkvist and Hultgård (1999)	68

* *indicates diploid.*

despite intense inbreeding, bottlenecks and drift, associated with long distance seed dispersal events or re-colonization of recently barren areas (Soltis *et al*. 2015).

Honckenya peploides is a tetraploid species with a relatively high chromosome number (2n=4x=66, 68, 70) (Table 1) and a large genome (mean 4.33 pg/1C) when compared to other members of Caryophyllaceae (Kapralov *et al*. 2009; Leitch *et al*. 2019). Four subspecies of *H. peploides* have been identified (Jonsell 2001): subsp. *peploides*, distributed from northern Norway to northern Portugal; subsp. *diffusa* (Hornemann) Hultén ex V.V. Petrovsk, which has circumpolar distribution, mainly in Arctic and northern Boreal zones; subsp. *major* (Hooker) Hultén, found in the Northwest Pacific area and on the coasts of north eastern Russia down to Japan; and subsp. *robusta* (Fernald) Hultén, found in northeastern North America. According to Hultén (1971), subsp. *diffusa* is a variety of subsp. *peploides* and therefore we have combined their distribution in the location map of the present research (Fig. 2). Subsp. *peploides* sensu Hultén occurs mainly in the northern parts of Norway, Svalbard, Greenland, Iceland and subarctic Canada (Houle 1997; Jonsell 2001). In Iceland (Kristinsson *et al*. 2018), *H. peploides* can be found on most shorelines from sea level up to 50 m above sea level, with Surtsey being the only place where the plant can be found growing up to 100 m above sea level. Studies from several locations across the whole of the species range report varying tetraploid chromosome numbers, 68±2 (Table 1; Rice *et al*. 2015), but one report includes the diploid number $2n=2x=34$ from an eastern Russian island location that harbors the subsp. *major* (Probatova *et al*. 2004).

Two types of chromosome number variation have been documented for *H. peploides* (Table 1): ploidy variation (diploid $2n=34$ versus tetraploid $2n=68$) and aneuploidy, the number variation within ploidy level,

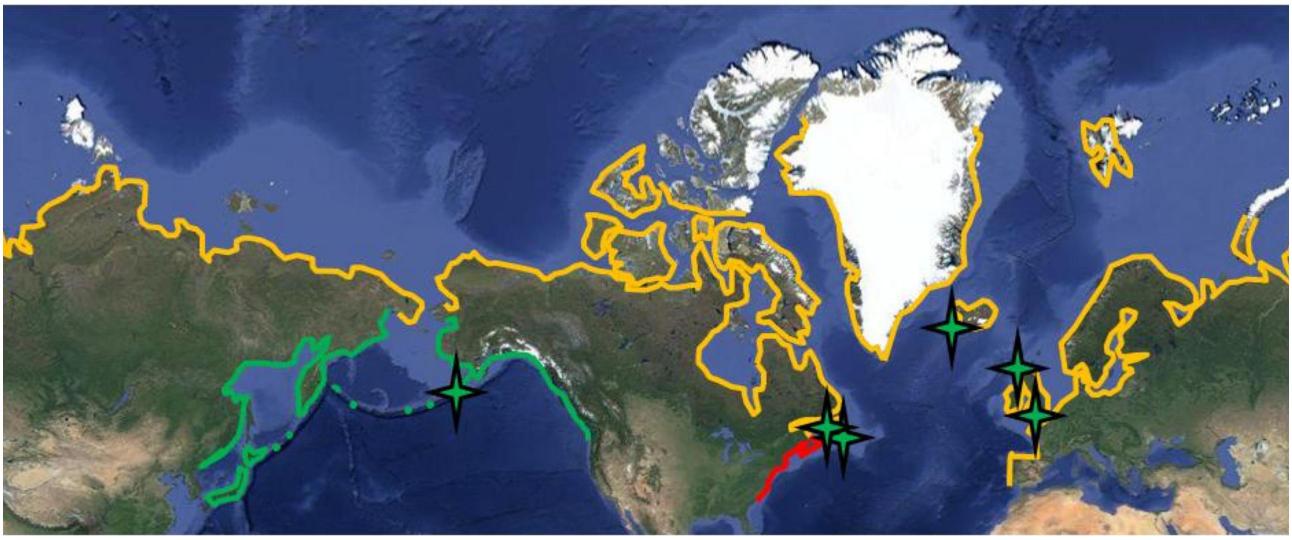

Figure 2. Map of distribution of *Honckenya peploides* and its subspecies: subsp. *peploides* (yellow); subsp. *major* (green); and subsp. *robusta* (red). Stars represent collection locations. From east to west: (1) Keibu, Estonia and Kolobrzeg, Poland; (2) Cornwall, England and Maryport, Scotland; (3) Iceland (Surtsey, Heimaey, Stokkseyri and Seltjarnarnes); (4) Madeleine Island, Canada; (5) Miquelon Island, Canada; and (6) Cold Bay, Alaska. Map modified from Google Earth.

in this case a variation of the tetraploid number (66 and 70). Intraspecific chromosome number variation is wide-spread especially among arctic-alpine plants (Löve & Löve 1975, Al-Shehbaz & O'Kane 2002, Brochmann *et al*. 2004, Grundt *et al*. 2005, Peruzzi *et al*. 2012). These include *Arabidopsis arenosa* (L.) Lawalree (Brassicaceae), which has 2n= 16, 18, 28, 32, 34, 39, 40 (Al-Shehbaz & O'Kane 2002), and *Barnardia japonica* (Thunb.) Schult. & Schult.f. (Hyacinthaceae) with 2n = 16, 18, 26, 27, 34, 35, 36, 43 (Haga & Noda 1976), to name a few. These intraspecific karyotype variants have been termed cytotypes or cytoraces (Stuessy 2009). Some even suggest that various reproductively isolated cytotypes within species may indeed represent cryptic species (Soltis *et al*. 2007). Intraspecific cytotypes can be found allopatrically, parapatrically or in mixed populations. Major courses generating cytotypic variation include hybridization, intraspecific polyploidy, chromosomal rearrangements and dysploidy (Stebbins 1971, Levin 2002, Baduel *et al*. 2018, Mandakova & Lysak 2018).

The relationship between intraspecific variation in chromosome number and variation in physiological, morphological or life history characteristics remains largely unexplored. In some cases, karyotypic variations result in no apparent phenotypic difference between cytotypes as significant gene flow is maintained (Ramsey *et al*. 2008). In other cases, modest karyotypic variations have yielded morphological distinctions, for example in floral and fruit characteristics, as is the case of buttercup (*Ranunculus* L.) (Cires *et al*. 2009), which in turn can affect pollination and pollinator species (Thompson & Merg 2008) and flower sex (as in crowberry (*Empetrum* L.), Suda *et al.* 2004). In *Honckenya*, seed germination of *H. peploides* subsp. *major* (subspecies containing diploid plants) occurred within three weeks at temperatures at least 28°C without prior cold stratification (Voronkova *et al*. 2011a). However, seeds of the tetraploid *H. peploides* began to germinate only after cold stratification (Baskin & Baskin 2001). Variation in morphology can also be seen between *H. peploides* in Greenland, Svalbard and Norway, with the Svalbard ecotypes being generally smaller in all traits measured (M. Philipp, pers. comm.). Such information are useful when attempting to explain these cytotypic differences in the context of ecological preferences and evolutionary adaptation of the sea sandwort in Iceland.

The aim of this study was to find some evolutionary trends in karyotype diversity of *H. peploides* and to distinguish possible variations on a subspecies level. This was achieved by determining chromosome numbers of plants from the young island of Surtsey (57 years old), the older island of Heimaey (over 10 000 years old), and from several other locations across the northern hemisphere. This study may shed light onto the origin and evolution of the species - a major aspect of plant conservation - whilst contributing to the thorough studies that have been performed on the island of Surtsey.

MATERIALS AND METHODS

Plant material

All but one *H. peploides* accessions in this study (Table 2) were raised from seeds. Hp-02 from Seltjarnarnes peninsula is the only accession that was grown from plants collected in the field in September 2012. Live plants of this accession were placed into plastic containers with the native substrate and kept initially at 15°C under a grow lamp with a 12/12 light/dark regime. Seeds from all other locations in Iceland were collected in July 2010 together with plant samples for the molecular study of Árnason *et al*. (2014).

Seed samples were collected from diverse locations on Surtsey, from the low elevation areas located on the northern sand spit, around the eastern slopes and in the vegetation-rich gull colony on the southern side of the island, to the high elevation areas around the western crater Surtungur and on the steep east-facing slope of the crater Surtur. Samples from Heimaey were from Stórhöfdi on the south side of the island and by the harbor in the northern part. Samples from the mainland location Stokkseyri on the southern coast were collected from plants growing by the sea on glacial deposits and fine sand, at the end of a freshwater marsh in between two large glacial rivers.

In order to obtain plant material spanning the world-wide distribution of the species, a correspondence with multiple research institutions around the globe was initiated by the author SHÁ. Through this connection, seeds of *H. peploides* were obtained from both Europe and North America (Fig. 2, Table 2). Locations in Europe include Kolobrzeg, Poland (Hp-16); Keibu, Estonia; Cornwall, England; and Maryport, Scotland. North American locations are Miquelon Island, Canada (Hp-06); Madeleine Island, Canada; and Cold Bay,

Table 2. List of accessions of *Honckenya peploides*, sample locations and obtained 2n somatic chromosome numbers. Chromosome groups: A (66-68); B (60-64); C (54-58); D (50-52); E (44-48); F (~40); G (34). Numbers in bold are of cells shown in Figs 3 and 4.

Location (see also Fig. 1)	Accession	2n number	2n group	Figure
Surtsey, Iceland	Hp 08	68, **68+2B**	A	Fig. 4a
63°18'10.80" N, 20°36'16.92" W	Hp 09	68, 60/62, ~51	A, B, D	
	Hp 21	44/46, **48**	E	Fig. 4b
	Hp 29	68+1B, 62+2B, 60	A, B	
	Hp 30	60/62, 58	B, C	
Heimaey, Iceland	Hp 01	**68**, 66, 55	A	Fig. 4c
63°26'15.64" N, 20°16'02.36" W	Hp 04	>44	E	
	Hp 05	68, 60/62, **51**	A, B, D	Fig. 4d
	Hp 07	58, 51+2B, 50, **34**	C, D, G	Fig. 4e
	Hp 19	66/68, ~60, ~40	A, B, F	
	Hp 25	~68, 62, 58	A, B	
	Hp 27	56+	C	
Stokkseyri, Iceland	Hp 11	**68+1B**, 66	A	Fig. 4f
63°50'16.01" N, 21°03'34.05" W	Hp 17	~60, 56	B, C	
Seltjarnarnes, Iceland 64°09'19.48" N, 22°00'10.58" W	Hp 02	**68**	A	Fig. 3
Kolobrzeg, Poland 54°17'00.57" N, 16°09'45.79" E	Hp 16	**68**, 66	A	Fig. 4g
Miquelon Island, Canada 47°04'32" N, 56°22'46.61" W	Hp 06	~68, 52	A, D	
Cold Bay, Alaska 55°12'00.27" N, 162°42'47.25" W	Hp 10	60/62, **44**	B, E	Fig. 4h
Unknown (Madeleine Island, Canada/ Cornwall, England/ Maryport, Scotland/ Keibu, Estonia)	Hp 13	54+, 44/46	C, E	
	Hp 28	50	D	

Alaska (Hp-10). This Alaskan accession presumably belongs to subspecies *major* (Fig. 2), whereas all other accessions in the present study are from the main subspecies *peploides*/*diffusa*.

Seed stratification, sterilization and germination

Seeds of *H. peploides* obtained from the various locations (Fig. 2, Table 2) were split into two groups, those to undergo stratification and those to be germinated right away. For each accession, one half was stratified by placement into plastic bags with a moist, sandy medium and refrigerated at 2 - 4°C for 12 weeks. The other half was sterilized right away using the procedure described below and placed into the germination chamber directly after. Seeds that had been stratified for up to 12 weeks as well as those that were germinated right away were sterilized in 1% CL solution for 2 min, then rinsed with distilled water and placed in a Petri dish between two sterile filter papers. Petri dishes were then placed under a 12/12 light regime at 15°C during light hours and then moved into a dark refrigerator and kept at 5°C during dark hours until germination. Germination success was estimated visually and noted as % germination per plate. Once germinated, five seedlings from each accession were placed in pots with a mixture of sand and soil. All plants were maintained and grown under 16/8 light/dark regime at 20°C in the Plant Genetics research laboratory growth room located on the second floor of Askja the Natural Sciences building at the University of Iceland, Reykjavík.

Enzymatic root tip squash method of chromosome preparation

Enzymatic root tip squash was performed according to Anamthawat-Jónsson (2001, 2010). Young root tips were harvested from the live plants at mid-day. Root tips were cut to approx. 1 - 2 cm and placed in 15 mL tubes with ice water which were kept on ice at 4°C for 27 h. This was done in order to synchronize mitosis and arrest as many cells as possible in metaphase. Root tips were then placed in another 15 mL tube containing fixative solution of a 1:3 v/v ratio of glacial acetic acid and 96% ethanol. They were allowed to be in this fixative at room temperature for about two hours before keeping them in a freezer at -30°C until use.

To prepare chromosome slides the fixed root tips were submerged in a citrate buffer (0.1 M citric acid monohydrate, 0.1 M trisodium citrate dehydrate, distilled water) for 20 min to dilute off the fixative. The buffer was replaced once during this period of time. Root tips were then placed one at a time onto acid-cleaned slides, which had been washed in chromium trioxide in 80% sulphuric acid for at least 3 hours, rinsed thoroughly and then stored in 96% EtOH in a refrigerator. The root tips were then trimmed down, leaving only the tip (1 - 2 mm) containing the meristematic tissue on the slide. The buffer droplets around the root tip were carefully removed with tissue paper and a 19 µL drop of enzyme mixture containing pectinase (Sigma P7416, 30 units/mL) and cellulase (Merck 1.0232, Onozuka R10, 80 units/mL) was added to each slide. The root tips were placed in the incubator at 37°C for 9 - 10 min for digestion. After incubation the enzyme was reduced with tissue paper. A drop of acetic acid (45%) was added, reduced with tissue paper, and then another drop was added. After resting for 5 min the drop was reduced and re-applied once more. The size of the drop was reduced before extracting the cells under the stereo-microscope. This was achieved by teasing the cloudy meristem tissue above the root cap with a needle and tweezers, releasing the meristem cells into the acetic acid suspension. Surplus root tissue was removed, and the suspension slightly mixed with a needle. The needle and tweezers were cleaned in 70% ethanol in between applications. A clean coverslip was placed on the slide and gently tapped vertically with a needle to scatter the cells. By manually pressing the cover slip firmly between sheets of filter paper the cells were squashed. The coverslip was removed after freezing the slide on dry ice or in liquid nitrogen. The slides were stored in dark and cool place until use.

Prepared slides were stained with 20 µL of the DAPI (1 µL/mL) (4 ’,6-diamidino-2-phenylindole), a fluorochrome that binds to AT-rich regions of DNA, and viewed under a Nikon Eclipse E800 epifluorescence microscope using a UV filter block with 340-380 excitation and 430-450 emission wavelengths (blue). The images obtained with the 100x objective (total magnification x1000) were captured with a Nikon Digital Camera DXM1200F and used for chromosome number determination. Karyotype construction was made from the best images, following Levan *et al.* (1964).

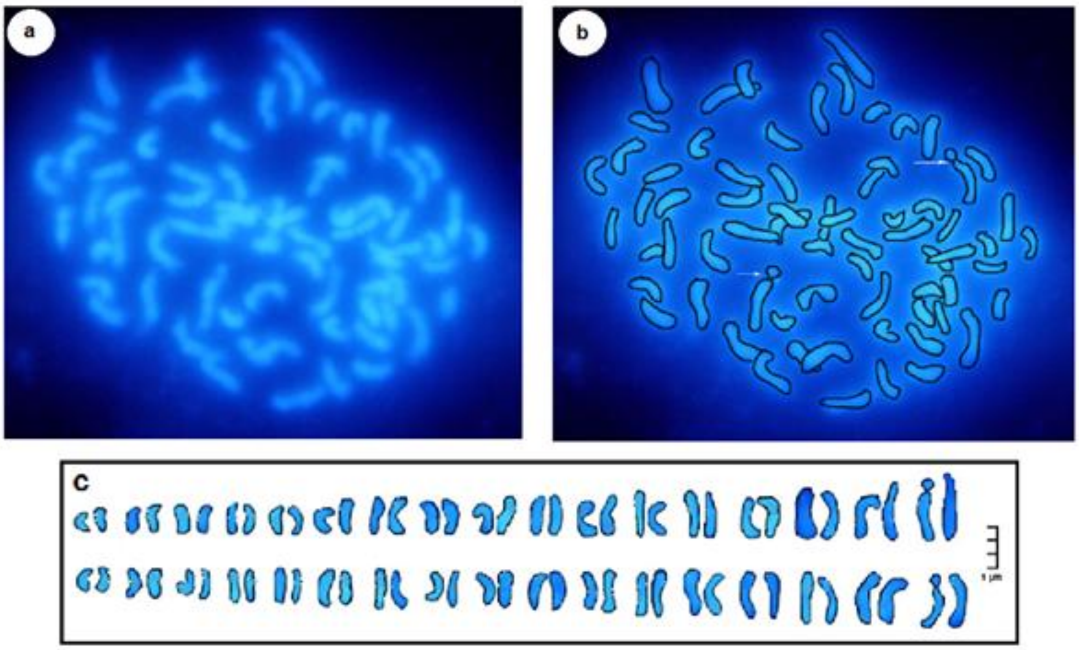

Figure 3. *Honckenya peploides* chromosomes from Seltjarnarnes (accession Hp-02), stained with DAPI taken at 1000x magnification, showing a full tetraploid complement of 68 chromosomes (a), the same chromosomes outlined for pixel size measurement (b), and karyotypically arranged according to relative sizes and morphology (c). Arrow indicates location of satellite, the secondary constriction of NOR bearing chromosome.

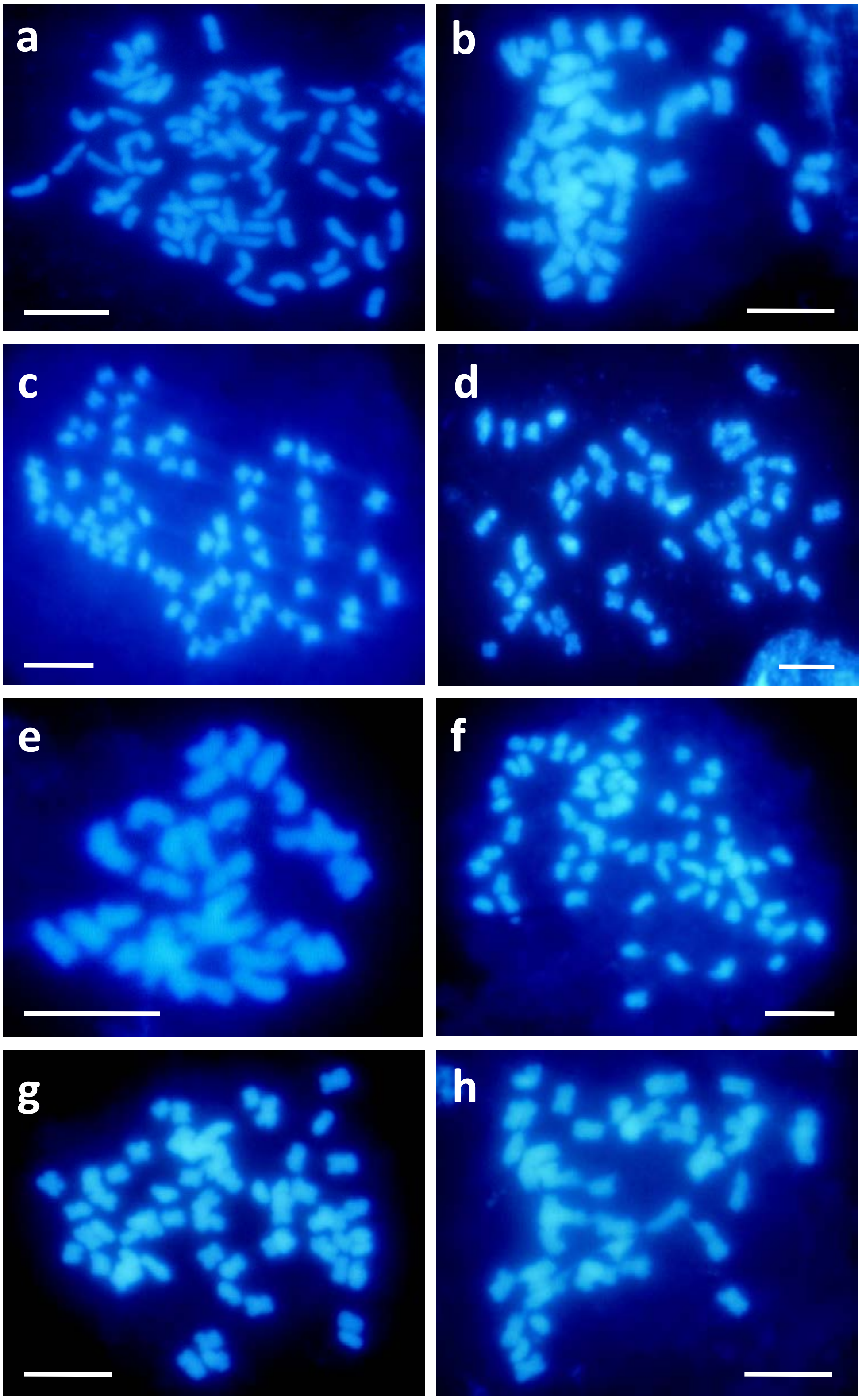

Figure 4. Metaphase cells of *Honckenya peploides* from different accessions showing 2n somatic chromosome numbers (see also Table 2): (a) Hp-08 from Surtsey with 2n=68+2Bs; (b) Hp-21 from Surtsey with 2n=48; (c) Hp-01 from Heimaey with 2n=68; (d) Hp-05 from Heimaey with 2n=51; (e) Hp-07 from Heimaey with 2n=34; (f) Hp-11 from Stokkseyri with 2n=68+1B; (g) Hp-16 from Poland with 2n=68; and (h) Hp-10 from Alaska with 2n=44. Scale bars represent 5 µm.

RESULTS AND DISCUSSION

Ecophysiological differences at subspecies level

The present study shows an example of physiological differences in *Honckenya peploides* at subspecies level. It was tested whether seeds obtained from the various locations outside of Iceland required cold stratification to germinate. Seeds from each accession were split into two groups, those to undergo cold stratification and those to be germinated right away. Prior to germination, with or without stratification, the seed samples were surface sterilized with bleach. The sterilization procedure proved effective at removing most bacterial, mould or fungal contaminants from the seed coat as only 7.1% (22 of 311) of the Petri dishes containing germinating seeds were contaminated. Of the unstratified seeds, only the samples obtained from Cold Bay, Alaska (*H. peploides* subsp. *major*), germinated under the 12/12, 5°C/15°C conditions, with most germination occurring within five to seven days. None of the seeds obtained from other locations, which belonged to the subspecies *peploides/diffusa*, germinated without prior cold stratification. Germination rates following cold stratification for 12 weeks were quite high, with roughly an 80% germination rate in all the non-contaminated plates at 12/12, 5°C/15°C. These results appear to be in good agreement with previous reports on plants from Kamchatka Peninsula in the Russian Far East (Voronkova *et al.* 2011a, 2011b), whereby *H. peploides* subsp. *major* could germinate without prior cold stratification, in the same way as many secondary plant species that succeed the pioneer plants on volcanic substrates. Furthermore, closely related plant species that have the same life history and ecological preferences have different requirements for stratification. For example, the white *Rhododendron aureum* Giorgi requires cold stratification, while seeds of the co-existing red species (*Rh. camtschaticum* Pall.) can germinate spontaneously (Voronkova *et al*. 2011b). Seed dormancy has a genetic basis.

Cold stratification is commonly used for breaking seed dormancy in plants. However, the effects of cold stratification on dormancy release and its physiological characteristics have only been investigated in model species or crop plants. The model plant *Arabidopsis thaliana* (L.) Heynh. which grows in extreme environments, such as on geothermal soil in Iceland (Mandakova *et al*. 2017), will not flower without cold stratification. The plant hormone gibberellin (GA) is best known to stimulate developmental transitions including seed germination, flowering, and the transition from juvenile to adult growth stage. In *Arabidopsis*, GA has been shown to break seed dormancy and is required for normal development of seedlings (Hauvermale *et al*. 2020). Seed dormancy is a critical mechanism that delays germination until environmental conditions are favorable for growth. Plant hormones gibberellin (GA) and abscisic acid (ABA) have long been recognized as key players in regulating dormancy and germination. A gene expression study of seed germination in rice has shown that cold stratification results in a rapid increase of GA and IAA (auxin) promoting germination, and, at the same time, in a rapid decrease of ABA that has a role in dormancy maintenance (Yang *et al.* 2019). Recent data have shown that brassinosteroid (BR) hormones also promote germination by activating GA downstream genes and inactivating ABA signaling (Kim *et al*. 2019). A proteomic study of seed dormancy release has shown a significant increase in expression of numerous genes that are involved in the respiration-related metabolism processes, biosynthesis of amino acids, and translation during the dormancy release of a citrus species after cold stratification (4°C) or gibberellin (GA) treatment (Lu *et al*. 2018). Pioneer species, such as *H. peploides* colonizing Surtsey or any barren and open localities, have a better chance of survival and establishment as their seeds can only germinate after cold stratification (and vernalization) during the preceding winter months, not germinating readily after seed maturation before winter.

Most accessions of Honckenya peploides are tetraploid with 2n=4x=68

The tetraploid somatic chromosome number $2n=4x=68$ is the most common number for *H. peploides* from Surtsey, Heimaey, and other coastal regions in the North Atlantic (Table 2, Figs. 3, 4a, 4c, 4f and 4g). This is the most common chromosome number of *H. peploides* samples world-wide (Table 1) and is the number representing all subspecies in the Chromosome Count Database (CCDB, Rice *et al*. 2015). Furthermore, the present study also shows accurate count with a karyotype of metaphase chromosomes (Fig. 3). To the best of our knowledge, no karyotype of *Honckenya* has been published elsewhere. The karyotype was constructed based on pixel size of DAPI-stained chromosomes (Figs. 3a and 3b) and the sizes were sorted and paired with possible homologs after chromosome morphology (Fig. 3c). Chromosome sizes ranged from 1.36 µm – 4.66 µm while most seem to be metacentric and sub-metacentric chromosomes.

The karyotype (Fig. 3c) reveals two pairs of NORs (Nucleolar Organizing Region) on the largest chromosomes of the complement, although sometimes only one of each pair appears to be actively transcribing, seen as secondary constriction (arrows in Fig. 3b). NORs in a polyploidy species are often variable in size – some are easily detectable as in Fig. 3b, while others are not. This is known to be due to variation in copy numbers of ribosomal (rDNA) repeats, resulting from deletion or amplification at preferential sites over an evolutionary time (Pederson 2011). In addition, not all NORs are active. The major 18S-26S ribosomal genes in the NOR are tandem repeats comprising hundreds or thousands of copies, in ample excess of what would be required to sustain cellular ribosomal synthesis (Rogers & Bendich 1987). Therefore, the number and size of nucleoli in nuclei at interphase are often variable, as some are more active than others. The nucleolus is the site of ribosomal RNA synthesis, i.e. rDNA transcription and rRNA maturation, and ribosome production (McKeown & Shaw 2009). The number of nucleoli in plants has been positively correlated with the ploidy level (Leven 2002; Kim *et al*. 2015). In the present study we found interphase nuclei with two to four nucleoli in the tetraploid accessions.

The karyotype constructed in the present study (Fig. 3) indicates that the species is an autotetraploid, comprising two sets of the homologous diploid chromosome complement. Although several cytological mechanisms are known to induce polyploidy in plants, including somatic chromosome doubling, the most probable route of autopolyploidy is via hybridization of unreduced (2*n*) gametes of diploid parents from different populations within a species (Leitch & Bennett 1997, Ramsey & Schemske 1998), reinforced by reproductive isolation between the diploids and the newly formed tetraploids. Major crop plants of the world are polyploid, for example, wheat, maize, potatoes, banana, cotton, oilseed rape, and coffee beans. Increasing the ploidy level is known to be positively correlated with plant production, both biomass and yield (Leitch & Leitch 2008). But in the ecological and evolutionary context, genome doubling is likely to confer distinct advantages to a polyploid. These advantages allow polyploids to thrive in environments that pose challenges to their diploid progenitors (Madlung 2013). For example, Chao *et al*. (2013) demonstrated that *Arabidopsis thaliana* first-generation autotetraploids had instantaneously enhanced salt tolerance compared to isogenic diploids. Future studies combining genetics, physiology and ecology should shed light onto the underlying physiological mechanism and its genetic basis of such gains in polyploidy.

Another tetraploid chromosome number was discovered in the present study, 2*n*=66 (Table 2, chromosome group A), in accessions from Heimaey and Stokkseyri, Iceland, and from Kolobrezeg, Poland. This number was also reported for Iceland (Löve & Löve 1950). Previous reports have shown three tetraploid numbers, 66, 68 and 70 (68±2) (Table 1; Rice *et al*. 2015, eFlora 2020), and they are hereby referred to as cytotypes. The survey of a wide range of species by Wood *et al*. (2009) has reported that 12 – 13% of all angiosperms display some cytotypic variability. The co-existence of variable cytotypes could be facilitated by ecological barriers to gene flow or by numerous biological reproductive barriers which prevent hybridization between proximal cytotypes (Husband & Sabara 2004). Changes in morphological or physiological characteristics are frequently accompanied by changes in cytotype, often resulting in ecological differentiation between cytotypes (Levin 2002). This might have something to do with the sexual dimorphism and sex chromosome evolution in dioecious species (Charlesworth 2018, 2019). This needs to be investigated, but at least in *H. peploides* sex-specific differences in growth and biomass allocation have been documented (Sanchez-Villas *et al*. 2012, 2017).

The present study shows for the first time the presence of B chromosomes in *Honckenya*, in the accessions from Iceland, i.e. Surtsey, Heimaey and Stokkseyri (Table 2, Figs. 4a and 4f). Supernumerary B chromosomes, as opposed to the standard A chromosomes, are dispensable genetic elements found in hundreds of plant species world-wide (Jones & Rees 1982). Despite the widespread existence, B chromosomes can occur in some members of the population and are absent in others, most probably due to their irregular and non-mendelian inheritance (Jones & Houben 2003). The biological significance of B chromosomes is still inconclusive, but when occurring in low numbers (such as one or two), as in the present study, they tend to be neutral in their phenotypic effects, whereas in high numbers they mostly have a negative effect on the fitness and fertility of the organism (Jones 2018). Nevertheless, recent studies using new and more powerful genomic approaches have begun to show positive effects of plant B chromosomes, for example, in seed germination under drought stress, plant resistance to fungal diseases and plant survival under certain stress conditions (reviewed in Dhar *et al*. 2019). The presence of B chromosomes in the Icelandic accessions of *H. peploides* may be an advantage in the species colonization in extreme environments.

Diploid (2n=2x=34) and triploid (2n=3x=51) chromosome numbers exist across the species distribution range

Diploid chromosome number 2*n*=2*x*=34 and triploid number 2*n*=3*x*=51 (including group D, 2*n*=50-52) are discovered in the present study (Table 2). The diploid number has been documented by Probatova (2004), but the triploid number is reported here for the first time. The diploid number was discovered in one accession from Heimaey (Hp-07, Fig. 4e). On the other hand, the triploid number was detected in two accessions from Heimaey, Hp-05 (Fig. 4d) and Hp-07, accession Hp-09 from Surtsey, accession Hp-06 from Miquelon Island, Canada, and accession Hp-28, which may be from the nearby Madeleine Islands or from a locality in Europe (the plant label showing origin was lost). Furthermore, the presence of only one satellite (NOR bearing) chromosome in triploid cells (e.g. Fig. 4d) confirms that the cells are triploid, as a tetraploid cell has two satellite chromosomes, or one pair (Fig. 3b).

Our study, therefore, presents two important findings about the diploid *H. peploides*. Firstly, the diploid number is no longer unique to the subspecies *major*, but also exists in the subspecies *diffusa*/*peploides*. Secondly, these two localities are geographically different and distant from one another (oceanic islands: Russia-Moneron in the North Pacific versus Iceland-Heimaey in the North Atlantic). This diploid form is probably an ancient relict of the once wide spread species. The whole genome duplication (WGD) event, giving rise to the present-day autotetraploid species, might have happened somewhere before the tetraploid species became widespread, by colonizing new habitats, new islands, and coastal regions, thus replacing the diploid progenitors. The genetic divergence, resulting in geographical and taxonomical variation at the subspecies level, might have taken place during the species radiation, colonization and establishment in a new environment. The alternative scenario is that the WGD event in *H. peploides* had occurred independently multiple times and in different diploid populations. This can only be answered with more research on phylogeographical aspects of this species on a global scale. However, ecological modeling of the temporal evolution of a diploid-autopolyploid system associated with WDG commonly supports patterns of adaptive niche differentiation in polyploids, with young polyploids often invading new niches and leaving their diploid progenitors behind (Baduel *et al*. 2018). In this respect, the former scenario for *H. peploides*, i.e. WGD before tetraploid radiation, seems more likely.

The present study shows that the occurrence of the triploid number 2*n*=3*x*=51 (including group D, 2*n*=50-52) is more frequent than that of the diploid number. In Iceland, the triploid number was found in accessions from Surtsey and Heimaey, but outside Iceland it was detected at least from Miquelon Islands in the Atlantic on the eastern coast of Canada. In all these locations and the surrounding islands and nearby coastal regions, tetraploids are common (Table 2). In Heimaey, both diploid and tetraploid plants co-exist. Populations on the southern shores of the island of Moneron (at the north-eastern end of the Sea of Japan) were found to be diploid (2n=34) (Probatova 2004), however populations from the nearby island of Sakhalin (only about 30 nautical miles north-east of Moneron Island) were found to be tetraploid with three cytotypes (2n=66, 68, 70) (Sokolovskaya & Strelkova 1960). Moreover, populations from the more northerly Wrangle Island were found to be tetraploid and also contained three cytotypes (2n=66, 68, 70) (Goldblatt 1985; Agapova 1993). The triploids must have been formed as offspring of the wide-hybridization between the diploid and the tetraploid plants. Such wide-hybridization may have occurred locally (sympatrically) or within a short dispersal distance during long colonization history of the species. Note that triploid progenies can have different chromosome numbers, depending on cytotypes of the tetraploid parent – they can be 2n=51 (34+68/2), 2n=50 (34+66/2), or 2n=52 (34+70/2). All these three triploid numbers were discovered in the present study (Table 2).

Triploid hybrids play an important role in plant species evolution, especially in the maintenance of the evolutionary dynamics of mixed-ploidy populations (Husband 2004, Anamthawat-Jónsson 2019). Triploid hybrids themselves are normally not able to expand into a sizable population outcompeting the parental accessions or species, due mainly to the loss of fertility following aberrant meiosis of the gamete production. Triploid plants are known to be less fertile than individuals with even numbers of chromosome sets (Stebbins 1971). Difficulties regarding chromosomal pairing and segregation in meiosis make triploids gametophytically unstable, producing a variety of euploid (1n, 2n or 3n) and aneuploid gametes (Husband 2004). Triploids can, however, be partially fertile since they are able to generate some euploid gametes. There is a large difference in triploid fertility among species, with some reported almost completely sterile and others comparatively fertile. The comprehensive survey made by Ramsey & Schemske (1998) showed that triploid pollen fertility, compiled from 41 studies, ranged from 0% to 96.5%, with a mean pollen fertility of 31.9% in triploid angiosperms. Seed set was observed in ten studies, whereas lack of seed setting was observed in seven studies. To sum up, a triploid hybrid normally has a low level of fertility, or in other words, a high level of sterility. This balance functions as a reproduction barrier preventing a hybrid from increasing its population size thus displacing the parental species or population, but keeping its fertility down to the level that maintains a stable hybrid zone, where the two hybridizing taxa (in our case in the diploid-autotetraploid system) are able to coexist across all levels of ecological selection (see review in Wolf *et al*. 2001, Ramsey & Schemske 2002). As with *H. peploides*, triploid hybrids are likely to function as a bridge to gene flow, facilitating the fixation of tetraploids in a new environment.

Aneuploids are common in Honckenya peploides

Aneuploid cells are characterized by incomplete chromosome sets. The present study reveals for the first time numerous chromosome numbers that are categorized as aneuploids, arranged here in groups (Table 2) for the discussion purposes: groups B (60-64); C (54-58); E (44-48) and F (~40). Groups B and C lie between tetraploid and triploid levels, whereas groups E and F are between triploid and diploid levels. Two examples of group E are shown in Fig. 4: 2*n*=48 from Surtsey (Fig. 4b) and 2*n*=44 from Alaska (Fig. 4e).

In the present study, aneuploidy is rather common. It also appears to be more prevalent on oceanic islands than on mainland coastal regions, but this needs further study covering a larger sample size and more location diversity. In contrast, previous reports show that similar aneuploid numbers in *Honckenya* are relatively rare. Most interestingly, the number 2*n*~40 that was discovered by Áskell and Doris Löve was obtained from an Icelandic material, of unknown origin, however (Löve & Löve 1956). Malling (1957) reported a somatic chromosome number of 2*n*=68 for *H. peploides*, after re-examining material from the Baltic Sea. He had received this material from Rohweder, who reported chromosome numbers as low as 2*n*=48 in the same material. Observations from the present study coincide with those reports, suggesting that there might be a cytotype of *H. peploides* with approximately 48 to 50 chromosomes.

Where did aneuploid numbers in *H. peploides* come from, and how? At this point it is necessary to define aneuploidy further. According to Ramsey & Schemske (1998) the term aneuploid refers to a variety of cytotypes, ranging from those which are very similar to euploids (the “hypo-” and “hyper-euploids”, such as 2*x*+1, a hyper-diploid, and 4*x*-1, a hypo-tetraploid), to those with several to many chromosome additions or deletions (e.g. 2*x*+4, 4*x*-3). Other papers define the near-euploid aneuploidy more specifically, and the most common terms are trisomic-monosomic for 2*x*±1 and tetrasomic-nullisomic for 2*x*±2 aneuploids (e.g. Birchler 2013). The best known case in human cytogenetics is the trisomy 21 (with 3 copies of chromosome no. 21) that causes Down syndrome (Hassold & Hunt 2001). But plants tolerate aneuploidy much better (Birchler 2013). In some cases, aneuploid cultivars are even more popular among growers than euploid plants, for example aneuploid tulip cultivars with new colours and flower forms (Marasek-Ciolakowska *et al*. 2014). In wheat breeding, numerous chromosome addition and substitution lines have been produced via wide-crossing between wheat and its wild relatives, in an effort to transfer agronomically important traits to the crop species (e.g. Schwarzacher *et al*. 1992, Andersson *et al*. 2015). In the case of *H. peploides*, the tetraploid cytotypes with 2*n*=4*x*=68±2 discussed in the previous section are a good example of the hypo- and hyper-tetraploid cytotypes.

Aneuploidy with such small deviation (e.g. ±2) from its euploid number may have been the consequence of a mistake in cell division, such as non-disjunction chromosome behavior at the anaphase stage of meiosis-I, or due to chromosome elimination during the metaphase alignment, especially in the embryonic stage of growth (Birchler 2013). Aneuploidy can result from chromosomal rearrangements during an evolutionary time (Mandakova & Lysak 2018). But the most probable route of aneuploid formation is via inter-ploidy hybridization and back-crossing (Ramsey & Schemske 1998, Ramana & Jacobsen 2003, Henry *et al*. 2010). Interestingly, aneuploids which are produced this way are those with several to many chromosome additions or deletions. In the case of *H. peploides*, these are the aneuploids in groups B, C, E and F. They are the intermediate steps towards euploid/tetraploid fixation – they are the cost of polyploidization. Aneuploid plants themselves are considered inferior to their euploid counterparts in numerous ways. Many aneuploids have low viability and fertility (Ramsey & Schemske 1998) and are low in plant productivity and biomass (Birchler 2013). Aneuploid individuals of *Arabidopsis thaliana* exhibited diverse phenotypes affecting a wide variety of traits associated with growth rate, plant morphology, flowering and flower traits (Henry *et al*. 2010). Aneuploids may not be evolutionarily successful due to meiotic problems and genomic imbalance, but they may be different morphologically, which could affect reproduction and pollination preferences, hence becoming a barrier to gene flow (Birchler 2013). The *H. peploides* aneuploids discovered in the present study may play an important role in an ecological and evolutionary context, by maintaining high genetic differentiation and low gene flow within the mixed-ploidy populations. Their inferior fertility is compensated by the species' ability to reproduce asexually, by rhizome spreading and clonal propagation. On Surtsey, the plant can grow and expand into large mat or big clump (Fig. 1). Often daughter clones remain attached to parent clones via rhizomes whose connections sometimes run up to 2 m from the parent plant (Sánchez-Vilas *et al*. 2010). The plants are also perennial and long-lived. In this way, *H. peploides* aneuploids are evolutionary successful.

ACKNOWLEDGEMENTS

This work was partly supported by University of Iceland's Research Fund and ERASMUS Student Exchange Programme. We would like to thank Professor Marianne Philipp and Professor Henning Adsersen, University of Copenhagen, for the samples from Surtsey and Heimaey, and for their supervision and collaboration on the genetic research of this species. We also thank Dr. Borgþór Magnússon and Dr. Sigurður Magnússon, the Icelandic Institute of Natural History, for their knowledge about plant colonization on Surtsey, Dr. Ægir Þór Þórsson and Dr. Lilja Karlsdóttir for their advice on the laboratory work of this project, and we thank all the collaborators who provided seed samples from outside of Iceland.

REFERENCES

Agapova, N.D.,1993. Chromosome numbers in flowering plants of the flora of the U.S.S.R Moraceae-Zygophyllaceae. Nauka.

Aguilar, R., M. Quesada, L. Ashworth, Y. Herrerias-Diego & J. Lobo, 2008. Genetic consequences of habitat fragmentation in plant populations: susceptible signals in plant traits and methodological approaches. Mol. Ecol. 17, 5177–5188. DOI: 10.1111/j.1365-294X.2008.03971.x

Al-Shehbaz, I.A. & S.L. O'Kane, Jr., 2002. Taxonomy and Phylogeny of *Arabidopsis* (Brassicaceae). The Arabidopsis Book 2002(1), 1–22. DOI: 10.1199/tab.0001

Anamthawat-Jónsson, K., 2001. Molecular cytogenetics of introgressive hybridization in plants. Methods Cell Sci. 23, 139–148. DOI: 10.1023/A:1013182724179

Anamthawat-Jónsson, K., 2010. Selected methods in plant cytogenetics. Háskólaprent, Reykjavík, Iceland. ISBN: 978-9979-9967-1-2.

Anamthawat-Jónsson, K., 2019. Hybrid introgression: the outcomes of gene flow. Sci. Asia 45, 203–211. DOI: 10.2306/scienceasia1513-1874.2019.45.203

Andersson, S.C., E. Johansson, M. Baum, F. Rihawi & E. Bouhssini, 2015. New Resistance Sources to Russian Wheat Aphid (*Diuraphis noxia*) in Swedish Wheat Substitution and Translocation Lines with Rye (*Secale cereale*) and *Leymus mollis*. Czech J. Genet. Plant Breed. 51, 162–165. DOI: 10.17221/72/2015-CJGPB

Árnason, S.H., Æ.Th. Thórsson, B. Magnússon, M. Philipp, H. Adsersen & K. Anamthawat-Jónsson, 2014. Spatial genetic structure of the sea sandwort (*Honckenya peploides*) on Surtsey: an immigrant's journey. Biogeosciences 11, 6495–6507. DOI: 10.5194/bg-11-6495-2014

Baduel, P., S. Bray, M. Vallejo-Marin, F. Kolar & L. Yant, 2018. The "Polyploid Hop": Shifting Challenges and Opportunities over the Evolutionary Lifespan of Genome Duplications. Front. Ecol. Evol. 6, article 117. DOI: 10.3389/fevo.2018.00117

Baskin, C.C. & J.M. Baskin, 2001. Seeds: ecology, biogeography, and evolution of dormancy and germination. San Diego, California: Academic Press.

Birchler, J.A., 2013. Aneuploidy in plants and flies: The origin of studies of genomic imbalance. Semin. Cell Dev. Biol. 24, 315–319. DOI: 10.1016/j.semcdb.2013.02.004.

Brochmann, C., A.K. Brysting, I.G. Alsos, L. Borgen, H.H. Grundt, A.-C. Scheen & R. Elven, 2004. Polyploidy in arctic plants. Biol. J. Linn. Soc. 82, 521–536. DOI: 10.1111/j.1095-8312.2004.00337.x

Chao, D.Y., B. Dilkes, H.B. Luo, A. Douglas, E. Yabubova, B. Lahner & D.E. Salt, 2013. Polyploids Exhibit Higher Potassium Uptake and Salinity Tolerance in *Arabidopsis*. Science 341, 658–659.
DOI: 10.1126/science.1240561

Charlesworth, D., 2018. Does sexual dimorphism in plants promote sex chromosome evolution? Environ. Exp. Bot. 146, 5–12.
DOI: 10.1016/j.envexpbot.2017.11.005

Charlesworth, D., 2019. Young sex chromosomes in plants and animals. New Phytol. 224, 1095–1107.
DOI: 10.1111/nph.16002

Cires, E., C. Cuesta, E.L. Peredo, M.A. Revilla & J.A.F. Prieto, 2009. Genome size variation and morphological differentiation within *Ranunculus parnassifolius* group (Ranunculaceae) from calcareous screes in the Northwest of Spain. Plant Syst. Evol. 281, 193–208.
DOI: 10.1007/s00606-009-0201-9

Delph, L.F. & D.E. Wolf, 2005. Evolutionary consequences of gender plasticity in genetically dimorphic breeding systems. New Phytol. 166, 119–128.
DOI: 10.1111/j.1469-8137.2005.01339.x

Dhar, M.K., J. Kour & S. Kaul, 2019. Origin, Behaviour, and Transmission of B Chromosome with Special Reference to *Plantago lagopus*. Genes 10, 152.
DOI: 10.3390/genes10020152

eFloras (2020) 26. *Honckenya* Ehrhart. Flora of North America, vol. 5, Caryophyllaceae, published on the Internet http://www.efloras.org [accessed 13.01.2020]. Missouri Botanical Garden, St. Louis, MO & Harvard University Herbaria, Cambridge, MA.

Eithun, A., 2003. Reproduction, genetic variation and responses to temperature increase in populations of *Honkenya peploides* (L.) Ehrh. in W Greenland, Svalbard and S Norway, M.S. thesis, University of Oslo.

Evans, S.M., A. Verges & A.G.B. Poore, 2017. Genotypic Diversity and Short-term Response to Shading Stress in a Threatened Seagrass: Does Low Diversity Mean Low Resilience? Front. Plant Sci. 8, article 1417.
DOI: 10.3389/fpls.2017.01417

Flovik, K., 1940. Chromosome Numbers and Polyploidy within the Flora of Spitzbergen. Hereditas 26, 430–440.

Franks, S.J., 2010. Genetics, evolution, and conservation of island plants. J. Plant Biol. 53, 1–9.
DOI: 10.1007/s12374-009-9086-y, 2010.

Friðriksson, S., 1964. The colonization of the dryland biota on the island of Surtsey off the coast of Iceland. Natturufræðingurinn 34, 83–89.

Goldblatt, P., 1985. Index to chromosome numbers 1982-1983. Monogr. Syst. Bot. 13, 224.

Grundt, H.H., R. Obermayer & L. Borgen, 2005. Ploidal levels in the arctic-alpine polyploid *Draba lactea* (Brassicaceae) and its low-ploid relatives. Bot. J. Linn. Soc. 147, 333-347.
DOI: 10.1111/j.1095-8339.2005.00377.x

Haga, T. & S. Noda, 1976. Cytogenetics of the *Scilla scilloides* complex. 1. Karyotype, genome, and population. Genetica 46, 161–176.
DOI: 10.1007/BF00121032

Hassold, T. & P. Hunt, 2001. To err (meiotically) is human: the genesis of human aneuploidy. Nat. Rev. Genet. 2, 280–291.
DOI: 10.1038/35066065

Hauvermale, A.L., L. Amber & C.M. Steber, 2020. GA signaling is essential for the embryo-to-seedling transition during Arabidopsis seed germination, a ghost story. Plant Sig. Behav. 15, e1705028.
DOI: 10.1080/15592324.2019.1705028.

Henry, I.M., B.P. Dilkes, E.S. Miller, D. Burkart-Waco & L. Comai, 2010. Phenotypic Consequences of Aneuploidy in *Arabidopsis thaliana*. Genetics 186, 1231-U288.
DOI: 10.1534/genetics.110.121079

Houle, G., 1997. No evidence for interspecific interactions between plants in the first stage of succession on coastal dunes in subarctic Quebec, Canada. Can. J. Bot. 75, 902–915.
DOI: 10.1139/b97-100

Hultén, E., 1971. The circumpolar plants. II. Dicotyledons. K. Sven. Vetenskapsakademiens Handl. 13, 1–463.

Husband, B.C., 2004. The role of triploid hybrids in the evolutionary dynamics of mixed-ploidy populations. Biol. J. Linn. Soc. 82, 537–46.
DOI: 10.1111/j.1095-8312.2004.00339.x

Husband, B.C. & H.A. Sabara, 2004. Reproductive isolation between autotetraploids and their diploid progenitors in fireweed, *Chamerion angustifolium* (Onagraceae). New Phytol. 161, 703–713.
DOI: 10.1046/j.1469-8137.2004.00998.x

Johnson, A.W. & J.G. Packer, 1968. Chromosome numbers in the flora of Ogotoruk Creek, N.W. Alaska. Bot. Not. 121, 403–456.

Jones RN (2018) Transmission and drive involving parasitic B chromosomes. Gene 9, 288.
DOI: 10.3390/genes9080388

Jones, N. & A. Houben, 2003. B chromosomes in plants: escapees from the A chromosome genome? Trends Plant Sci. 9, 417–23.
DOI: 10.1016/S1360-1385(03)00187-0

Jones, R.N. & H.B. Rees, 1982. B chromosomes, Academic Press, London.

Jonsell, B, (2001. Flora Nordica: Chenopodiaceae to Fumariaceae. Bergius Foundation, the Royal Swedish Academy of Sciences.

Kapralov, M.V., M. Stift, & D.A. Filatov, 2009. Evolution of genome size in Hawaiian endemic genus *Schiedea* (Caryophyllaceae). Trop. Plant Biol. 2, 77–83.
DOI: 10.1007/s12042-009-9029-2

Kim, S., D. Lee & A.L. Rayburn, 2015. Analysis of Active Nucleolus Organizing Regions in Polyploid Prairie Cordgrass

(*Spartina pectinata* Link) by Silver Staining. Cytologia 80, 249–258.
DOI: 10.1508/cytologia.80.249

Kim, S.Y., K.M. Warpeha & S.C. Huber, 2019. The brassinosteroid receptor kinase, BRI1, plays a role in seed germination and the release of dormancy by cold stratification. J. Plant Physiol. 241, article 153031.
DOI: 10.1016/j.jplph.2019.153031.

Leitch, I.J. & M.D. Bennett, 1997. Polyploidy in angiosperms. Trends Plant Sci. 2, 470–476.
DOI: 10.1016/S1360-1385(97)01154-0

Leitch, A.R. & I.J. Leitch, 2008. Perspective – Genomic plasticity and the diversity of polyploidy plants. Science 320, 481–83.
DOI: 10.1126/science.1153585

Leitch, I.J., E. Johnston, J. Pellicer, O. Hidalgo & M.D. Bennett, 2019. Angiosperm DNA C-values database (release 9.0, Apr 2019) https://cvalues.science.kew.org/

Levin, D.A., 2002. The role of chromosomal change in plant evolution. Oxford University Press, Oxford, New York. ISBN 0-19-513860-0

Löve, Á. & D. Löve, 1950. Some innovations and nomenclatural suggestions in the Icelandic flora. Bot. Not. 24–60.

Löve, Á. & D. Löve, 1956. Cytotaxonomical conspectus of the Icelandic Flora. Acta Horti Gotob. 20, 65–291.

Löve, Á. & D. Löve D, 1975. Cytotaxonomical Atlas of the Arctic Flora, J. Cramer, Vaduz, Germany.

Löve, Á. & D. Löve, 1982. In IOPB chromosome number reports LXXX. Taxon 31, 324–368.

Lövkvist, B. & U.M. Hultgård, 1999. Chromosome numbers in south Swedish vascular plants. Opera Bot. 137, 1–42.

Lu, Q., Z.S. Zhang, R.T. Zhan & R. He, 2018. Proteomic analysis of Zanthoxylum nitidum seeds dormancy release: Influence of stratification and gibberellins. Ind. Crop. Prod. 122, 7–15.
DOI: 10.1016/j.indcrop.2018.05.044.

Madlung, A., 2013. Polyploidy and its effect on evolutionary success: old questions revisited with new tools. Heredity 110, 99–104.
DOI: 10.1038/hdy.2012.79

Magnússon, B., S.H. Magnússon & S. Friðriksson, 2009. Developments in plant colonization and succession on Surtsey during 1999–2008. Surtsey Res. 12, 57–76.

Magnusson, B., S.H. Magnusson, E. Olafsson & B.D. Sigurdsson, 2014. Plant colonization, succession and ecosystem development on Surtsey with reference to neighbouring islands. Biogeosciences 11, 5521–5537.
DOI: 10.5194/bg-11-5521–2014

Malling, H., 1957. The chromosome number of Honckenya peploides (L.) Ehrh., with a note on its mode of sex determination, Hereditas 43, 517–524,
DOI:10.1111/j.1601-5223.1957.tb03454.x

Mandakova, T. & M.A. Lysak, 2018. Post-polyploid diploidization and diversification through dysploid changes. Curr. Opin. Plant Biol. 42, 55–65.
DOI: 10.1016/j.pbi.2018.03.001

Mandakova, T., H. Thorbjornsson, R. Pisupati, I. Reichardt, M.A. Lysak & K. Anamthawat-Jonsson, 2017. Icelandic accession of *Arabidopsis thaliana* confirmed with cytogenetic markers and its origin inferred from whole-genome sequencing. Iceland Agric Sci. 30, 29–38.
DOI: 10.16886/IAS.2017.03

Marasek-Ciolakowska, A., S.L. Xie, P. Arens & J.M. van Tuyl, 2014. Ploidy manipulation and introgression breeding in Darwin hybrid tulips. Euphytica 198, 389–400.
DOI: 10.1007/s10681-014-1115-3.

McKeown, P.C. & P.J. Shaw, 2009. Chromatin: linking structure and function in the nucleolus. Chromosoma 118, 11–23.
DOI: 10.1007/s00412-008-0184-2

Murray, D.F. & S. Kelso, 1997. Chromosome numbers and notes on the taxonomy of selected Alaskan vascular plants. Rhodora 99, 33–55.

Otto, S.P. & J. Whitton, 2000. Polyploid incidence and evolution. Annu. Rev. Genet. 34, 401–437.
DOI: 10.1146/annurev.genet.34.1.401

Packer, J.G. & G.D. McPherson, 1974. Chromosome numbers in some vascular plants from northern Alaska. Can. J. Bot. 52, 1095–1099.
DOI: 10.1139/b74-138

Pederson, T., 2011. The nucleolus. Cold Spring Harbor Perspectives in Biology 3, a000638.

Philipp, M. & H. Adsersen, 2014. Colonization of an empty island: how does a plant with a plastic gender system respond? Biogeosciences 11, 6657–6665.
DOI: 10.5194/bg-11-6657-2014

Probatova, N., V. Barkalov & E. Rudyka, 2004. Chromosome Numbers of Selected Vascular Plant Species from Sakhalin, Moneron and the Kurile Islands. Bull. Hokkaido Univ. Mus. 2, 15–23.

Ramana, M.S. & E. Jacobsen, 2003. Relevance of sexual polyploidization for crop improvement - A review. Euphytica 133, 3–18.
DOI: 10.1023/A:1025600824483.

Ramsey, J. & D.W. Schemske, 1998. Pathways, mechanisms, and rates of polyploidy formation in flowering plants. Annu. Rev. Ecol. Evol. Syst. 29, 467–501.
DOI: 10.1146/annurev.ecolsys.29.1.467

Ramsey, J. & D.W. Schemske, 2002. Neopolyploidy in flowering plants. Annu. Rev. Ecol. Syst. 33, 589–639.
DOI: 10.1146/annurev.ecolsys.33.010802.150437

Ramsey, J., A. Robertson & B. Husband, 2008. Rapid adaptive divergence in new world Achillea, an autopolyploid complex of ecological races. Evolution 62, 639–653.
DOI: 10.1111/j.1558-5646.2007.00264.x

Rice, A., L. Glick, S. Abadi, M. Einhorn, N.M. Kopelman & et al., 2015 The Chromosome Counts Database (CCDB) – a community resource of plant chromosome numbers. New Phytologist 206, 19–26.
DOI: 10.1111/nph.13191

Rogers, S.O. & A.J. Bendich, 1987. Ribosomal ENA genes in plants: variability in copy number and in the intergenic spacer. Plant Mol Biol. 9, 509–520.
DOI: 10.1007/BF00015882

Sanchez Vilas, J. & R. Retuerto, 2017. Sexual dimorphism in water and nitrogen use strategies in *Honckenya peploides*: timing matters. J. Plant Ecol. 10, 702–712.
DOI: 10.1093/jpe/rtw072

Sanchez-Vilas, J., R. Bermudez & R. Retuerto, 2012. Soil water content and patterns of allocation to below- and above-ground biomass in the sexes of the subdioecious plant Honckenya peploides. Ann. Bot. 110, 839–848.
DOI: 10.1093/aob/mcs157

Sanchez-Vilas, J., M. Philipp & R. Retuerto, 2010. Unexpectedly high genetic variation in large unisexual clumps of the subdioecious plant *Honckenya peploides* (Caryophyllaceae). Plant Biol. 12, 518–525

Schwarzacher, T., K. Anamthawat-Jónsson, G.E. Harrison & *et al*., 1992. Genomic in situ hybridization to identify alien chromosomes and chromosome segments in wheat Theor. Appl. Genet. 84, 778–786.
DOI: 10.1007/BF00227384

Sigurdsson, B.D. & B. Magnusson, 2010. Effects of seagulls on ecosystem respiration, soil nitrogen and vegetation cover on a pristine volcanic island, Surtsey, Iceland. Biogeosciences 7, 883–891.
DOI: 10.5194/bg-7-883-2010

Sokolovskaya, A.P. & O.S. Strelkova, 1960. Geograficheskogo rasprostranenie poliploidnykh idov rasteniy v evraziatskoy arktike. Bot. Zhurn. 45, 370–381.

Soltis, P.S. & D.E. Soltis, 2000. The role of genetic and genomic attributes in the success of polyploids. Proc. Natl. Acad. Sci. 97, 7051–7057.
DOI: 10.1073/pnas.97.13.7051

Soltis, P.S., D.B. Marchant, Y. Van de Peer, & D.E. Soltis, 2015. Polyploidy and genome evolution in plants. Curr. Opin. Genet. Dev. 35, 119–125.
DOI: 10.1016/j.gde.2015.11.003

Soltis, D., P. Soltis, D. Schemske, J. Hancock, J. Thomson, B. Husband & W. Judd, 2007. Autopolyploidy in angiosperms: have we grossly underestimated the number of species? Taxon 56, 13–30.
DOI: 10.2307/25065732

Stebbins GL (1971) Chromosomal Evolution in Higher Plants, J. W. Arrowsmith Ltd, Bristol, UK.

Stuessy, T.F., 2009. Plant taxonomy: the systematic evaluation of comparative data. New York: Columbia University Press.

Suda, J., R. Malcová, D. Abazid, M. Banaš, F. Procházka, O. Šída & M. Štech, 2004. Cytotype distribution in *Empetrum* (Ericaceae) at various spatial scales in the Czech Republic. Folia Geobot. 39, 161–171.
DOI: 10.1007/BF02805244

Thompson, J.N. & H.F. Merg, 2008. Evolution of polyploidy and the diversification of plant-pollinator interactions. Ecology 89, 2197–2206.
DOI: 10.1890/07-1432.1

Tsukui, T. & T. Sugawara, 1992. Dioecy in *Honckenya peploides* var. *major* (Caryophyllaceae). Bot. Mag. 105, 615–624.
DOI: 10.1007/BF02489435

Voronkova, N.M., E.V. Burkovskaya, T.A. Bezdeleva & O.L. Burundukova, 2011a. Morphological and biological features of plants related to their adaptation to coastal habitats. Russ. J. Ecol. 39, 1–7.

Voronkova, N.M., V.P. Verkholat & A.B. Kholina, 2011b. Specific features of plants at early stages of the colonization of loose volcanic matter. Biology Bull. 38, 237–241.
DOI: 10.1134/S1062359011030150

Whittaker, R.J., K.A. Triantis, & R.J. Ladle, 2008. A general dynamic theory of oceanic island biogeography, J. Biogeogr. 35, 977–994.
DOI: 10.1111/j.1365-2699.2008.01892.x

Wolf, D.E., N. Takebayashi & L.H. Rieseberg, 2001. Predicting the risk of extinction through hybridization. Conserv Biol 15:1039–1053.
DOI: 10.1046/j.1523-1739.2001.0150041039.x

Wood, T.E., N. Takebayashi, M.S. Barker, I. Mayrose, P.B. Greenspoon & L.H. Rieseberg, 2009. The frequency of polyploid speciation in vascular plants. Proc. Natl. Acad. Sci. 106, 13875–13879.
DOI: 10.1073/pnas.0811575106

Yang, B., J. Cheng, J. Wang, Y. Cheng, Y. He, H. Zheng & Z. Wang, 2019. Physiological characteristics of cold stratification on seed dormancy release in rice. Plant Growth Regul. 89, 131–141.
DOI: 10.1007/s10725-019-00516-z

Yuan, N., H.P. Comes, Y.R. Mao, X.S. Qi & Y.X. Qiu, 2012. Genetic effects of recent habitat fragmentation in the Thousand-Island Lake region of southeast China on the distylous herb *Hedyotis chrysotricha* (Rubiaceae). Am. J. Bot. 99, 1715–1725.
DOI: 10.3732/ajb.1200054

Zhukova, P.G., 1966. Chromosome numbers in some species of plants of the northeastern part of the U.S.S.R. Bot. Zhurn. 51, 1511–1516.

Seabirds and seals as drivers of plant succession on Surtsey

BORGTHÓR MAGNÚSSON[1], GUDMUNDUR A. GUDMUNDSSON[1], SIGMAR METÚSALEMSSON[1] AND SANDRA M. GRANQUIST[2]

[1] Icelandic Institute of Natural History, Urridaholtsstræti 6–8, 210 Gardabær, Iceland (borgthor@ni.is)

[2]Marine & Freshwater Research Institute, Skúlagata 4, 101 Reykjavík. [2]The Icelandic Seal Center, Brekkugata 4, 530 Hvammstangi, Iceland.

ABSTRACT

Plant colonization and succession on Surtsey have been monitored since 1965. In 2019, the 75th species of vascular plants was detected on the island, 62 species were present and about 40 species had established viable populations. Over the last decade colonization has slowed down and the number of present species not increased. The rising number of seagulls breeding on the island after 1985 had a great impact on plant colonization and vegetation development. While most parts of the island remained barren, a grassland area (13 ha in 2018) developed in the main seagull breeding colony on the southern part of the island. This development is attributed to transfer of nutrients from sea to land by the seagulls. In recent years a dense patch of vegetation, 2 ha in 2018, has also developed on the low, northern spit of the island, where a few pairs of seagulls breed in the spring and grey seals haul out and breed in the fall in considerable numbers. In a survey conducted during the grey seal pupping period in 2019, the seal abundance and spatial distribution was mapped accurately for the first time. The results show that the dense vegetation of the spit and seal distribution are clearly overlapping. The continuous shrinking of the island and its spit has led to an increasing concentration of the seals in their breeding area. Based on a literature survey we estimated the nitrogen (N) input from sea to land by the grey seals as 9-13 kg N/ha in 2019. This compares to an estimated input of 5-30 kg N/ha/yr by the seagulls breeding in the same area during 2015-2019. Within the grey seal and seagull breeding area on the spit of the island, a distinct community of shore plants has developed. Measurements of plant cover and biomass in permanent plots on Surtsey in 2018 and 2019 show that development on part of the spit is reaching a similar state as in the old gull colony on the southern part of the island. This suggests that the grey seals along with the seagulls are important drivers of plant succession on the northern spit. Further research on the effects of the seals on nutrient transfer from sea to land and ecosystem development on Surtsey is recommended.

INTRODUCTION

The island Surtsey was formed in an oceanic eruption starting in November 1963 and coming to an end in 1967. The first vascular plant was found on the island in 1965 and from that time plant colonization and ecosystem development have been closely studied (Fridriksson 1975, Magnússon et al. 2009, 2014, Ólafsson & Ingimarsdóttir 2009, Petersen 2009, Leblans et al. 2014, Sigurdsson & Magnússon 2014, Sigurdsson & Leblans 2020, Aerts et al. 2020). In the early years most of the pioneering plants were shore species adapted to establishment on the sandy and nutrient poor soils of the new island. A few years after the cessation of the eruption the first pairs of seabirds started breeding on the fragile lava cliffs.

However, during the first two decades, the progress was slow and it was evident that some ingredients of the young ecosystem were lacking. This was to change in 1986 with the formation of a seagull colony upon the southern part of the island. The plants and the birds had met and the wheels started turning. Subsequent studies revealed that the nutrient transfer from sea to land and seed dispersal by seagulls had pronounced effects on plant succession, soil development, invertebrate and bird communities, as well as ecosystem functions on the island. Over time, differences developed between the area impacted by the seagulls on the southern lava fields and other areas of the island. This is in line with what several other studies on the impact of seabirds on terrestrial ecosystems have shown (e.g. Sobey & Kenworthy 1979, Lindeboom 1984, Ellis 2005, Havik et al. 2014, Ball et al. 2015).

The low, northern spit of Surtsey is where the first pioneering shore plants (*Cakile*, *Leymus*, *Honckenya*, *Mertensia*) were found on the island during 1965-1969. However, in the beginning vegetation development there turned out to be slower than on slightly higher land apparently because of frequent disturbance by coastal flooding during heavy storms in the wintertime (Friðriksson 2005). Grey seals started breeding on the northern spit as early as 1983 (Jakobsson et al. 2007) but for years it was not evident that they were impacting the development of vegetation in their breeding area. However, after 2010 this was to change. On aerial and satellite images of the island taken in 2012 or later, dense vegetation patches started to become visible on the northern spit in contrast to older images (data not shown). This needed a further investigation. Various studies have shown that seals and sea lions can impact vegetation in and around their colonies through their disturbance and nutrient transfer from the sea to land, as seabirds do (Norton et al. 1997, Farina et al. 2003, Bokhorst et al. 2007, 2019, McLoughlin et al. 2016, Moss 2017).

In this paper we report on our studies of vegetation in permanent plots on Surtsey, including the northern spit, in 2018 and 2019 and long-term trends. In mid-October 2019 we made an aerial survey and a count of grey seals in the breeding colony on the island which allowed a comparison of the seal distribution and the dense vegetation of the northern tip. The results shed a new light on vegetation development on Surtsey and possible impacts of grey seals.

MATERIALS AND METHODS

Study area

Surtsey (63°18´N, 20°36´W) is in the Vestmannaeyjar archipelago off the south coast of Iceland. The islands of Vestmannaeyjar form a young volcanic system with the oldest rock formations dating from 40,000 years BP (Sigurðsson & Jakobsson 2009). Surtsey, the southernmost of the islands, was formed in an eruption in 1963 to 1967. At the end of the eruption the island had reached an area of 2.7 km^2 and a height of 173 m a.s.l. During the eruption, large tephra cones were formed in explosive phases of the two main central craters. The cones were gradually transformed into denser palagonite tuff (Jakobsson et al. 2000). The southern part of the island consists of lava flows from the craters. The northern part is a low spit formed by eroded coastal sediments deposited on the leeward side (Fig. 1). Coastal erosion has taken a heavy toll of the island and by 2018 it was only 1.3 km^2 in area.

The climate of the Vestmannaeyjar area is mild, oceanic and very windy. An automatic weather station has been in operation on Surtsey from 2009. For the period 2009-2019 the mean annual temperature of the island was 6.6 °C and annual precipitation 1009 mm. On the average the length of the frost-free period was 199 days and there were 229 days with precipitation (Petersen & Jónsson 2020). Waters off the southern coast of Iceland are productive and rich in marine life (Astthorsson et al. 2007). Seabirds are particularly

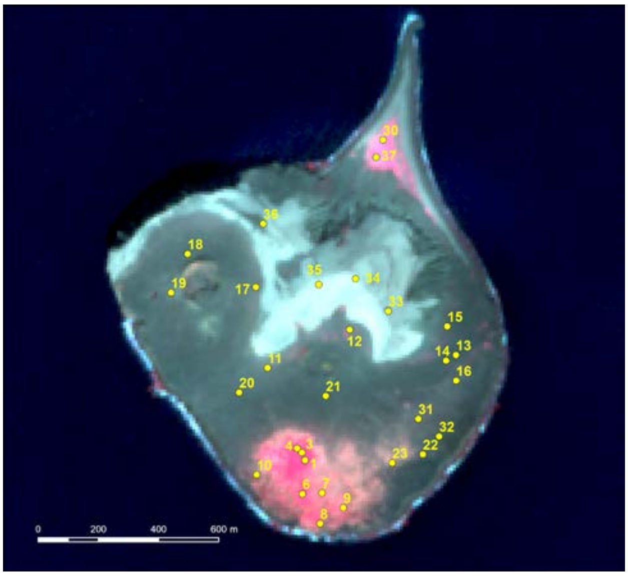

Figure 1. Surtsey and location of permanent plots (dots and numbers), infrared Sentinel image from 6 July 2019. Areas with dense vegetation appear in red color.

abundant on the Vestmannaeyjar islands and large breeding populations of several species are found there, such as the Atlantic puffin (*Fratercula arctica*), northern fulmar (*Fulmarus glacialis*), gannet (*Morus bassanus*), common guillemot (*Uria aalge*), and black guillemot (*Cepphus grylle*) (Hilmarsson 2009); bird nomenclature follows the British Ornitholgists' Union (BOU 2013). The seabirds impact the vegetation with their nutrient transfer, burrowing, nest building and other activities. The vascular flora of the islands consists of some 160 species, and all but a few are present on Heimaey the largest and only inhabited island. The other old islands harbour only 2–28 species, numbers corresponding to their size, but lush seabird grasslands and cliff communities are their main vegetation types. The dominants of the grasslands are the rhizomatous grasses *Festuca richardssonii* and *Poa pratensis*. Among common species of the cliffs are *Cochlearia officinalis, Puccinellia coarctata* and *Armeria maritima* (Friðriksson & Johnsen 1967); plant nomenclature follows Kristinsson et al. (2018). A more detailed description of the study area is given in Magnússon et al. (2014).

Plant sampling and analysis of biomass

Surtsey is visited by a team of field biologists in the middle of July every year. After the initial colonization phase, plant succession has been studied in permanent plots on the island. The first plots were set up in 1990 and the latest in 2014. The location of the plots was chosen subjectively with respect to substrate type and potential influence of seagulls on vegetation development on the island (Magnússon & Magnússon 2000, Magnússon et al. 2009, 2014). Through the years a few plots by the northern shore have been lost due to extreme weather and surf during winter, but replacements have been made. In 2014 plots were established for the first time up on the palagonite ridges on the highest part of the island. In 2018 there were 29 plots in operation on the island (Fig. 1, Table 1). The plots are 10 x 10 m in size and are sampled with line transects. Plant cover is determined by line-intercept method (see Magnússon et al. 2014).

From 1999, plant biomass is harvested every fourth year in 10 x 10 m plots adjacent to the permanent plots, the last sampling occurring in 2019. In each of these plots vegetation is harvested at random coordinates. The vegetation is cut at ground level along a 2 m long line using electric grass clippers. All plant material is collected (green and withered) and dried at 60 °C to constant oven-dry mass in the laboratory (Magnússon et al. 2014).

A biomass estimation for the whole island in 2019 was derived from satellite data. Normalized difference vegetation index (NDVI) was calculated from a Sentinel 2 satellite image corrected for atmospheric affects, acquired 6 July, 2019 with 10 meter pixel size. NDVI is an indicator of the magnitude of photosynthetically active vegetation (Rouse et al. 1974), and it is calculated with the formula:

$$NDVI = (R-IR)/(R+IR),$$

where R is red reflectance and IR is infrared reflectance. NDVI values for each permanent plot were extracted and correlated against the biomass measurements (see Results). After that a biomass map was produced for the whole island from the observed relationship.

Density of seabird nests

Since 2003, density of seabird nests (mainly seagulls) has been determined annually in and around the permanent plots on Surtsey. A 1000 m^2 circular area

Table 1. Permanent plots on Surtsey in 2018, year of establishment, substrate type and relative influence of seabirds and grey seals.

Plot no.	First sampling	Substrate type	Seabird influence	Grey seal influence
1,3,4	1990	Sandy sheet lava	High	
6-10	1994	Sheet lava	High	
22,23	1995	Sheet lava	Moderate	
11-14, 16, 18-21	1994, 1995	Sandy sheet lava	Low	
15,17	1994	Tephra hill slopes	Low	
30, 37	2005, 2014	Coastal sand	Moderate	Moderate
31-32	2008	Block lava	Moderate	
33-36	2014	Palagonite, gravel	Low	

with a center point in the middle of each permanent plot (10 x 10 m) is inspected and nest bowls, occupied in the current season counted. The great black-backed gull (*Larus marinus*), lesser black-backed gull (*L. fuscus*) and herring gull (*L. argentatus*) breed in substantial numbers (200-300 pairs) upon the island (Petersen 2009) and form a dense colony on the southern part. A few fulmar nests (*Fulmarus glacialis*) have also been encountered within the colony and they are included in the nest counts. Fewer and more scattered pairs of great black-backed gulls also breed on the eastern- and northernmost part of the island.

History of seals on Surtsey

Two species of seals breed in Iceland; the harbour seal (*Phoca vitulina*) and the grey seal (*Halichoerus grypus*). Both species are frequently seen in the waters around the Vestmannaeyjar islands and in the early years of Surtsey they were observed in the shallow waters and on the sandy coast of the island, but records are few (Hauksson 1992). Seal populations of Iceland, including the Vestmannaeyjar area, are monitored regularly by aerial surveys. The harbour seal surveys have been conducted since 1980 and are carried out in their moulting period in July-August (Granquist & Hauksson 2019a), while the grey seal surveys have been conducted since 1982 and are carried out during their pupping period in October-November (Hauksson 1992, 2009, 2010, 2015, Georgsdóttir et al. 2018, Granquist & Hauksson 2019b). In recent years, only a few harbour seals have been observed on Surtsey in the harbour seal summer surveys and hardly any in the grey seal autumn surveys. However, no aerial surveys have been conducted during the harbours seals pupping period in May-June, hence there is no direct evidence of them breeding on the island.

Grey seals, on the other hand, have been reported to breed on the northern spit of the island as far back as 1983 (Jakobsson et al. 2007, Hauksson 2015). In all previously conducted surveys of Surtsey between 1986 and 2017 grey seals with pups were observed on the northern spit. Total pup production (number of pups born during the pupping period) is used as an indicator to monitor grey seal abundance. Grey seal pups are born with white lanugo fur and can be assumed to stay at the breeding site until they have moulted and weaned. Females give birth to their pups at different times over the course of a few weeks, and it can be assumed that not all pups born at the site are present at the same time, since pups born early in the period

Table 2. Observations of grey seal pups on Surtsey, based on the aerial surveys (1-5 overflights per survey) that have been carried out since 1982 (in 1998 pups were counted from land). Estimated pup production at the breeding site. Maximum number of pups and adults seen in a single survey each year and dates for maximum observations. Sources are: [1]Hauksson 2015, [2]Granquist & Hauksson 2019b, [3]present study. Methods applied to estimate pup production from either one or several counts are explained in Hauksson 2015 and Granquist and Hauksson 2019b.

Year	Estimated pup production	Maximum number of pups*	Maximum number of adults	Date for maximum observation	Source
1982		0	0	Oct 8	1
1986	42	34	16	Oct 19	1
1988	20	15	11	Nov 21	1
1989	38	73	0	Dec 13	1
1990	29	23	x	Nov 3	1
1992	31	25	10	Nov 2	1
1995	49	39	x	Oct 19	1
1998	x	30	x	Oct 15	1
2002	44	35	x	Nov 6	1
2003	54	37	x	Oct 29	1
2005	63	66	x	Nov 25	2
2008	88	24	10	Sep 25	2
2012	62	55	x	Oct 17	2
2017	134	67	x	Oct 3	2
2019	x	62	32	Oct 18	3

**The maximum number of observed pups includes moulted pups, some of which might not be born in Surtsey, which explain why maximum number of observed pups is sometimes higher than estimated pup production.*

are likely to have weaned and left the area before the last the pups are born. Therefore, a breeding site needs to be surveyed a minimum of four times during the pupping period to obtain a significant estimate of total pup production (Granquist & Hauksson 2019b). The estimated pup production on Surtsey has varied from 20 to 134 and the maximum number of pups seen in a single flight within a year has ranged from 15 to 73 (Table 2), (Hauksson 2015, Granquist & Hauksson 2019b). In the latest grey seal survey in Iceland, which was carried out in 2017, the breeding colony on Surtsey was the largest of all colonies at the south coast with an estimated pup production of 134 (Table 2) and the peak of the pupping period occurred on October 12 (±1 day) (Granquist & Hauksson 2019b).

Distribution of the grey seals in their breeding colony in 2019

To document the distribution of grey seal pups and adults, the colony was photographed vertically from an aircraft, flown in calm weather at 530 m (1680 feet) altitude, around noon on 18 October, 2019. The twin engined Partinavia P-68 Observer aircraft has a hatch in the floor where cameras can be mounted for vertical photography. We used two Canon EOS 5DS R 50.2 MP digital cameras with 50 mm and 105 mm lenses. The programme DotDotGoose (version 1.1.0; Ersts 2019) was used to count the seals from the digital photos. A map was then made showing the seal locations on top of a layer of vegetation distribution of the northern spit.

On 30 October, 2019 a short visit by helicopter was made to the island which allowed a brief walk through and photographing of the seals in their breeding colony.

Changes in island area and patches of dense vegetation based on images

From the early years of the eruption aerial photographs have been taken regularly of Surtsey, bi-annually during the last decades. The photographs have allowed exact monitoring of the erosion of the island and surface changes (Jakobsson et al. 2000). Also, changes in plant cover are noticeable in areas where dense vegetation patches develop. They become visible when total plant cover reaches approximately 20% or more. This has been most obvious on the southern part of the island where a gull colony started to form in 1986. On an aerial photograph from 1988 the first sign of a dense patch of vegetation could be seen in the center of the gull colony. From that year expansion of the dense vegetation area was followed (Magnússon et al. 2009, 2014). After 2010, a patch of dense vegetation also became visible on the low spit on the northern part of the island, on aerial and satellite images. By 2014 small, dense patches of vegetation were visible at old fulmar nest sites in crater walls in the center part of the island. Here we update the development of dense vegetation areas on the island by analysing the series of aerial photographs from 2014, 2016 and 2018. Approximate outlines of the dense vegetation patches, as seen on the aerial photographs (true color) were drawn and changes followed between years. The outlines of the island and the northern spit were also drawn. The northern spit is the only part of the island with low shores, as the southern part has high vertical cliffs. In the geospatial information system ESRI Arc Gis the 10 m contour line and the shoreline for each available year were used to construct a polygon representing the spit. The shoreline was drawn manually so that the software could calculate the area of the polygons for each year.

Data analysis

Vegetation data (vascular plants only) sampled in the permanent plots on Surtsey in 2018 were analysed with a two-way cluster analysis. The cover data were transformed (log+1) prior to analysis. The PC-Ord 6 package (McCune & Mefford 2011) was used for the analysis with the Euclidean distance measure chosen and clustering by Ward´s method. Plant grouping, cover and biomass were compared to seabird and grey seal distribution.

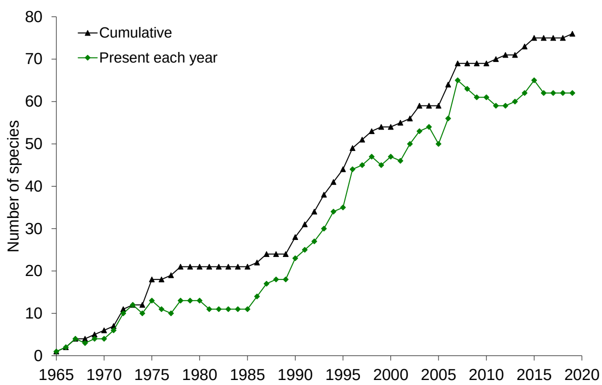

Figure 2. Surtsey colonization curve for vascular plants during the period 1965–2019.

RESULTS

Vegetation: colonization, plant composition and grouping, cover and biomass

By 2019 a total of 76 vascular plants species had been discovered on Surtsey from 1965 and of those 62 had living individuals. One new species, *Tussilago farfara*, was found on the island for the first time in 2019. About 40 species had established viable populations. After two distinct colonization phases during approximately 1965 – 1975 and 1987 – 2007, colonization has slowed down over the last decade (Fig. 2).

In the sampling of the 29 permanent plots (P) on the island in 2018 (Fig. 1), 25 vascular plant species were recorded. The number of species within individual plots varied from 3 to 16. Poorest in species was P32, located on block lava on the eastern part of the island. Richest in species was a nearby P23 at the fringe of the gull colony, on sheet lava (Fig. 1).

The cluster analysis revealed four main groups in the plot assemblage (Fig. 3). The first group, G1, consisted of three plots (P1, 3 & 4) within the gull colony that are characterized by a very dense and

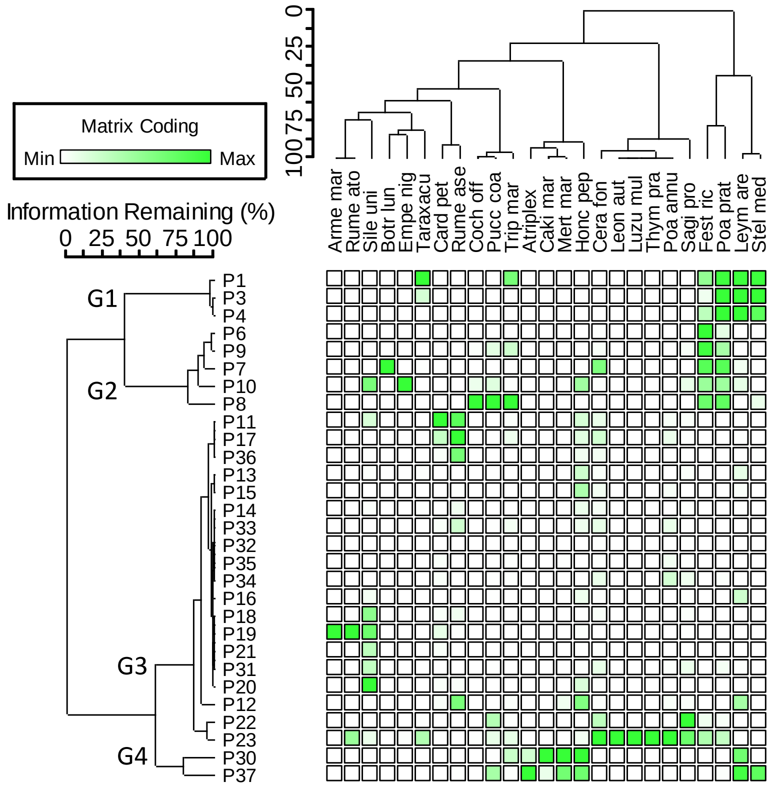

Figure 3. Two-way cluster analysis graph showing grouping of plots (left) and plant species within them (above) on Surtsey in 2018. The species are from left to right: *Armeria maritima, Rumex acetosa, Silene uniflora, Botrychium lunaria, Empetrum nigrum, Taraxacum sp., Cardaminopsis petrea, Rumex acetosella, Cochlearia officinalis, Puccinellia coarctata, Tripleurospermum maritimum, Atriplex sp., Cakile maritima, Mertensia maritima, Honckenya peploides, Cerastium fontanum, Leontodon autumnalis, Luzula multiflora, Thymus praecox, Poa annua, Sagina procumbens, Festuca richardsonii, Poa pratnesis, Leymus arenarius* and *Stellaria media*. Relative abundance of each species within a plot is shown by green color intensity, irrespective of other species.

Table 3. Species richness and total plant cover (%) in permanent plots in 2018 and plant biomass (g dwt./m^2) harvested in 2019. Averages ± s.e. for the four vegetation groups (G1-G4) of the cluster analysis and for all the plots.

	n	Species richness	Plant cover	Biomass
G1	3	5.0 ±0.5	160.6 ±5.3	576.0 ±20.1
G2	5	8.0 ±1.0	78.1 ±12.2	231.7 ±85.1
G3	19	7.1 ±0.6	2.9 ±1.0	7.4 ±1.9
G4	2	9.0 ±1.4	88.3 ±4.8	222.7 ±17.5
All plots	29	7.2 ±0.5	38.4 ±10.0	119.7 ±36.7

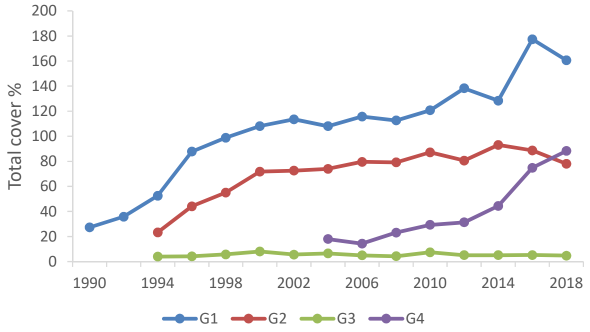

Figure 4. Total plant cover in permanent plots from their establishment. Averages for the four groups (G1-G4) formed in cluster analysis of the 2018 vegetation data, shown in Fig. 3. G1 and G2 plots are within the main gull colony, G3 are outside the colony and G4 are on the northern spit where the grey seal colony hauls out.

layered cover of *Leymus arenarius*, *Poa pratensis* and *Stellaria media*, along with less abundant *Festuca richardsonii*, *Taraxacum sp.* and *Tripleurospermum maritimum.* Total plant cover and biomass was two-fold higher than in any of the other groups and species richness is relatively low (Table 3). The plots are in the old center of the gull colony and on relatively thick tephra soil that overlays the lava underneath.

The second group, G2, consisted of five plots (P6-10) that are also within the gull colony but on lava substrate with little or no tephra on top. The vegetation was lower and not as dense as in G1 as shown by the plant cover and biomass but species richness was higher (Table 3). The most common species of this group (G2) were the grasses *Festuca richardssonii* and *Poa pratensis* but other common species were *Puccinellia coarctata*, *Tripleurospermum maritimum* and *Cochlearia officinalis* (Fig 3).

The third group, G3, consisted of 19 plots (P11-29, 31-36, Fig. 3). These plots are outside the gull colony and on variable substrate (Table 1). They had a very low plant cover and biomass but species richness is intermediate (Table 3). The main species in tephra plots of the group were *Honckenya peploides, Cerastium fontanum, Silene uniflora,*

G1–plot 3. Plant cover: 170%, biomass: 603 g/m^2, dominants: *Poa pratensis, Leymus arenarius, Stellaria media*.

G2–plot 8. Plant cover: 89%, biomass: 169 g/m^2, dominants: *Poa pratensis, Festuca richardsonii, Puccinellia coarctata.*

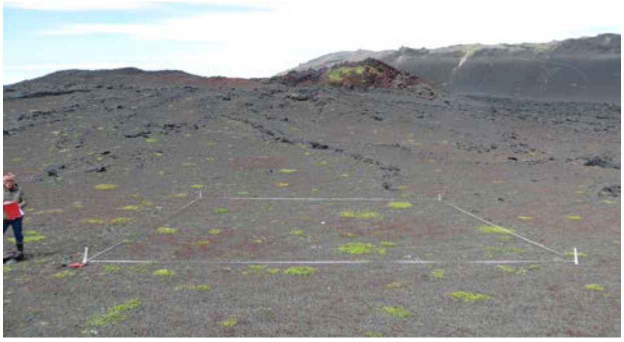

G3–plot 17. Plant cover: 4%, biomass: 10 g/m^2, dominants: *Rumex acetosella, Honckenya peploides, Cerastium fontanum.*

G4–plot 30. Plant cover: 95%, biomass: 248 g/m^2, dominants: *Mertensia maritima, Honckenya peploides, Leymus arenarius.*

Figure 5. Examples of plots within the four main vegetation groups, in 2018 (see Fig. 3). Cover data is from the 2018 season and biomass from 2019. G1 and G2 are within the old gull colony, G3 is outside the colony and G4 is from the grey seal and gull breeding area on the northern spit. Plant cover is a total cover of species within plot, adds to > 100% in dense, layered vegetation. Photos: Borgthór Magnússon 16-18 July 2018.

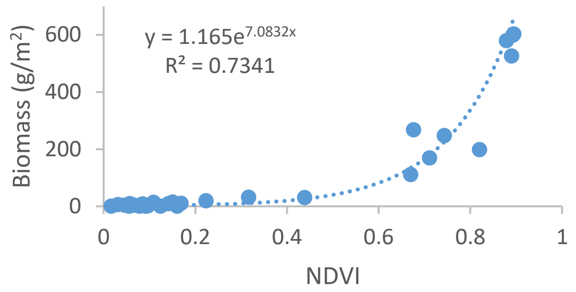

Figure 6. Relationship between plant biomass of permanent plots on Surtsey in mid July 2019 and NDVI of their pixels acquired from a Sentinel 2 image dated 6 July 2019 (see Fig. 1).

Rumex acetosella and *Cardaminopsis petrea*, but in plots on lava or the palagonite ridges *Puccinellia coarctata*, *Cerastium fontanum*, *Sagina procumbens* and *Poa annua*.

The fourth group, G4, consisted of only two plots (P30, 37) that are both on the low, northern spit (Figs. 1 and 3). Within these plots, plant cover, biomass and species richness were relatively high (Table 3). The characteristic species of the plots were the shore plants *Mertensia maritima*, *Cakile maritima*, *Atriplex sp.*, *Honckenya peploides* and *Leymus arenarius*, but other rather abundant species were *Stellaria media* and *Puccinellia coarctata* in one of the plots. The annuals *Cakile maritima* and *Atriplex* sp. were not found in other plots on the island.

The long-term data from the vegetation plots revealed trends in development within them (Fig. 4). A comparison of the four vegetation groups (G1-G4) shows that from as early as 1994, the cover of plots within the gull colony (G1 and G2) increased more or less steadily over time, while that of plots outside the colony (G3) has remained extremely low. In the plots on the northern spit (G4), cover was relatively low in 2004 and 2006 but started to increase from 2008 and took a sharp rise in 2014.

Sampling of biomass adjacent to permanent plots in 2019 reflected the same differences between plots and groups as the species composition and cover measurements in 2018 (Table 3). The biomass in individual plots varied from < 1 to 603 g dwt/m^2, the poorest plots (P33 & 35) being upon the palagonite ridge, and the richest (P3) in the lush grassland of the gull colony. Examples of plots within the four vegetation groups are shown in Fig. 5, underlining the differences in their plant composition, cover and biomass.

The biomass measurements from the middle of July 2019 allow a calibration with NDVI-values of a Sentinel-image covering the island a week earlier. The correlation showed a good exponential relationship between biomass and NDVI (Fig. 6). A new dataset derived by using the best-fit exponential function from the correlation ($y = 1.165e^{7.0832x}$, EXCEL) gave an estimation of biomass for each pixel in the dataset. The outcome is shown on Fig. 7. Over most of the island, biomass was extremely low, but on the other hand, very high within the gull colony on the southern part of the island, as well as in part of the northern spit. A few other areas showed small patches of elevated biomass (Fig. 7). A summing up of these calibrated values gave a biomass of 19,600 kg dry weight for the whole island in 2019.

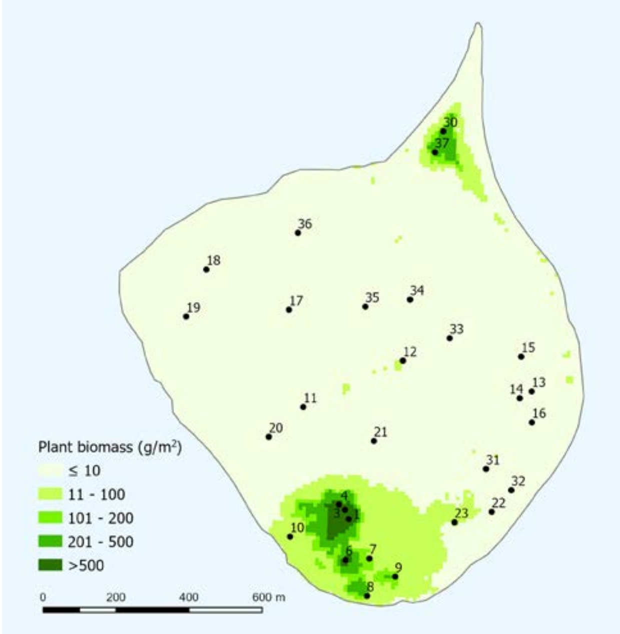

Figure 7. Distribution of plant biomass (dry weight) on Surtsey in 2019, derived from projected NDVI-values and ground-truth biomass measurements by the permanent plots in the same season (see Fig. 6). Hot spots are the seagull colony on the southern part of the island and the grey seal/seagull breeding area on the northern part. Most of the light-green spots on the center part of the island are small breeding colonies of fulmars. Furthest to the right are two old seagull nest sites within *Leymus*-dunes.

Vegetation: expansion of dense growth

With inspection of the series of aerial photographs of Surtsey it is possible to trace and follow the formation and development of dense vegetation patches on the island (Figs. 8 & 9). In 1988 the first patch within the gull colony on the southern part of the island measured 0.03 ha (Fig. 8). Ten years later, in 1998, it had expanded to 6.6 ha, and by 2014 it had reached 13.0 ha. The 2016 and 2018 outlines revealed a small reduction due to an erosion of the island (Fig. 8 & 9).

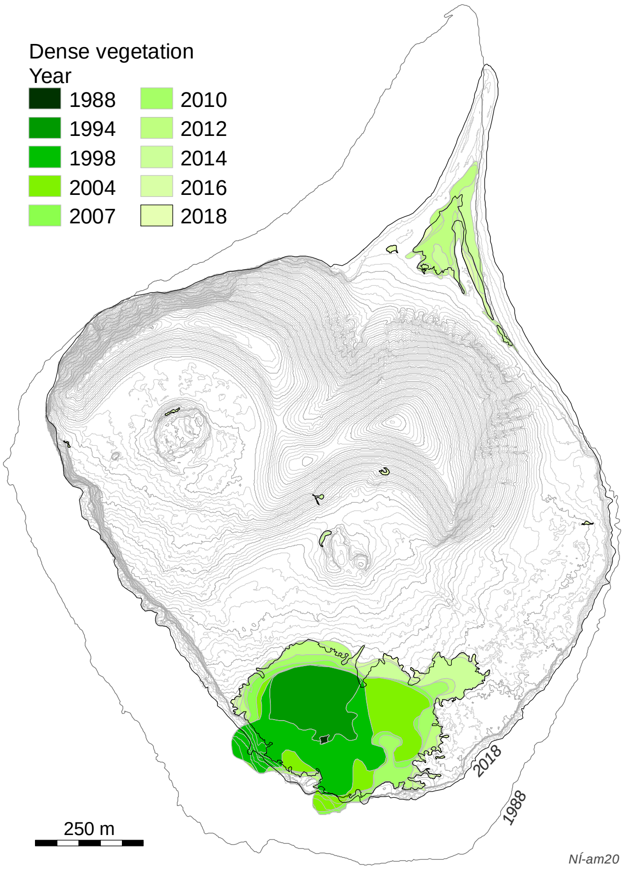

Figure 8. Expansion of dense vegetation on Surtsey during the period 1988-2018. Approximation from aerial images, by Anette Th. Meier. First signs of dense vegetation became visible in 1988 on the southern part of the island, in 2012 on the northern part and in 2014 on the central part. Vegetation patches become visible on aerial photos when plant cover has reached about 20% or more. Contour lines are 2 m.

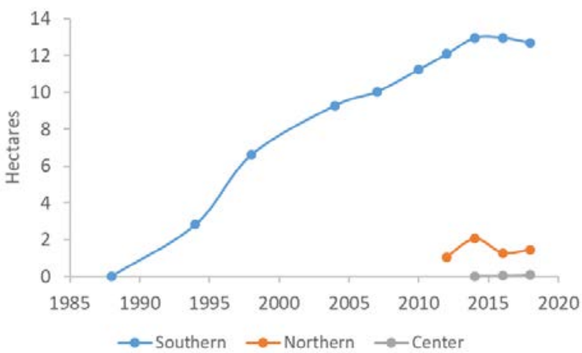

Figure 9. Development of areas of dense vegetation patches on southern, northern and center Surtsey during 1988-2018, as seen and outlined on aerial photographs, see Fig. 8.

On the northern spit a dense vegetation patch of 1.1 ha had become visible in 2012, expanding to 2.1 ha in 2014. After that a reduction in area occurred and it measured 1.5 ha in 2018 (Fig. 8 & 9). The small patches on the center part of the island measured only 0.1 ha in 2018. The total area of dense vegetation patches on the island in 2018, as outlined from aerial photographs, was 14.3 ha in 2018 or approximately 11% of the island´s area.

Seagull nesting density by vegetation plots

From 2003 we have an unbroken 17-year record of nesting density in and around the permanent plots on Surtsey. The total number of nests found each year varies greatly (19-52), being lowest in 2009 and highest in 2017 (Fig. 10). The variation probably reflects feeding conditions in the sea around Surtsey in the spring and during the breeding season. Through the years most of the nests have been within the gull colony area on the southern part of the island. From 2015 nests have also been encountered near plots on the northern spit (Fig. 10).

Average nesting density in plots within the four vegetation classes shows a distinct difference between the plots as well as a change in trends between 2003 and the present (Fig. 11). However, one must bear in mind that nests were not counted during the first 17 years of the gull colony. From 2003 nesting density was high within the two groups, G1 and G2, consisting of plots within the gull colony. The density was markedly higher in G2 but plots within the group are located more towards the edge of the colony than plots in G1 (Fig. 1). Nesting density in the other two groups,

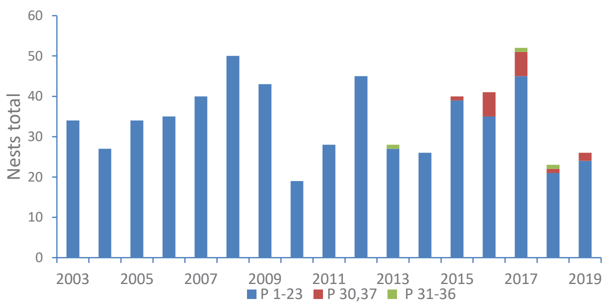

Figure 10. Total number of nests found in a 1000 m^2 circular area by all permanent plots (P1-36) on Surtsey from 2003 to 2019. P1-23 are 21 plots in operation from 2003. P30-37 are 8 plots established in 2013 or later, but prior nesting is improbable. P30 and P37 are on northern spit, (see plot locations on Fig. 1). The nests are all seagull nests except for the years 2012, 2013, 2014, 2018 and 2019, when 1-2 fulmar nests were also found each year and included.

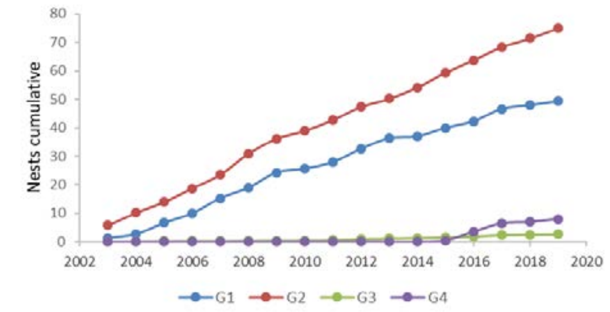

Figure. 11. Cumulative number of gull nests in and around permanent plots from 2003 to 2019 (within a circular area of 1000 m^2), averages for the four groups formed in cluster analysis of the 2018 vegetation data (see Fig. 3).

G3 and G4, remained extremely low over most of the period but from 2016 there was a slight rise, especially in the plots of G4, on the northern spit (Fig. 11).

Grey seal numbers and distribution in 2019

In the aerial survey of Surtsey on 18 October 2019, a total of 94 grey seals was observed on the island, all on the northern tip. Of those 62 were pups and 32 adults. Several females were seen feeding their pups. The seals were on the inner part of the spit and most of them inside the coarse boulder ridge by the shore. The ridge extends to form the northernmost part of the spit where seals were

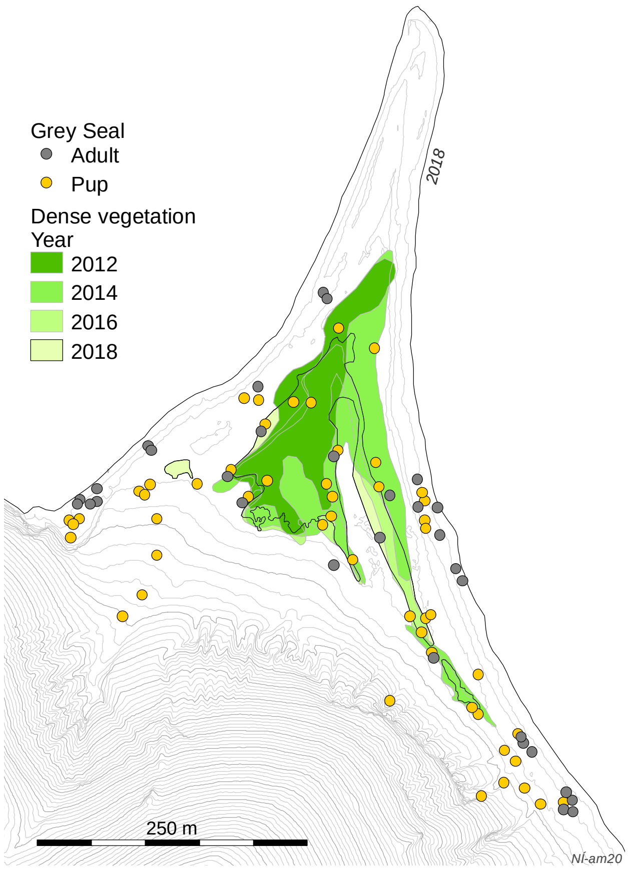

Figure 12. Distribution of grey seals photographed in an aerial survey of Surtsey on 18 October 2019. The expansion of dense vegetation on the northern spit of the island from 2012 is also shown. Approximation from aerial images, by Anette Th. Meier. Contour lines are 2 m.

Figure 13. Grey seals by the northern shore of Surtsey on 18 October 2019. A female with a suckling pup is in the center of the photograph. Four adults and six pups are visible. The withered vegetation is mainly *Leymus* and *Honckenya*. Photo: Gudmundur A. Gudmundsson.

A. A newborn pup in a bed of *Honckenya* on the northern spit.

B. Pups, about 1-week-old on a tephra slope on the eastern side of the spit.

C. Roughly 2-week-old pups within the dense vegetation area of the northern spit.

D. Pup about 4-week-old in a bed of *Leymus* on the eastern side of the spit. The dense white birthcoat is gone and adult fur has developed.

Figure 14. Grey seal pups at different stages of development by the northern shore of Surtsey on 30 October, 2019. Photos: Borgthór Magnússon.

not seen (Fig. 12). Many of the pups and adult seals were within or near the dense vegetation in the central part of the spit (Fig. 12–14). A few of the pups were up in tephra channels on the slopes above the spit. None of these pups were with their mothers which can indicate that they were weaned. At the later stages of the moulting period, the pups start crawling around and exercising their muscles before going to sea.

In the brief visit to the island on 30 October, 2019 it was not possible to thoroughly inspect the whole seal colony. However, pups at different development stages were encountered, from newborns to 4-5 week old pups (Fig. 14). Also, several adult seals were observed, including a female with fresh feces beside her who appeared ready to give birth.

DISCUSSON

Vegetation development

The finding of *Tussilago farfara* on Surtsey in 2019 is the first addition to the vascular flora since 2015. The species has probably been dispersed by wind to the island. From our last account of the flora reaching to 2013 (Magnússon et al. 2014) four other newcomers have been discovered. They are *Ranunculus repens, Epilobium hornemannii, Alchemilla alpina* and *Carex bigelowii*. However, only the last one was present in 2019. There is now a strong indication that the colonization wave driven by the seagulls during 1987-2007 has slowed. The number of present vascular plant species on the island peaked at 65 in 2007, then began to decline. From 2016 to the present the number has stayed at 62 species.

The analysis of the vegetation data sampled in 2018 showed mostly the same trends and differences between areas outside and inside the old seagull colony as revealed in our previous studies (Magnússon & Magnússon 2000, Magnússon et al. 2009, 2014). In 2018/2019, there was ~50-80 times as much cover and biomass in areas with breeding gulls as those where no gulls were present. This change is driven by nutrient transfer from sea to land by the birds. Most important are N and P, but availability of several other nutrients is enhanced in the affected soils (Sigurdsson & Leblans 2020, Aerts et al. 2020).

New in our results of the vegetation analysis of 2018 is that the plots (P30 & P37) on the northern spit are departing from other plots outside the old gull colony, indicating a recent change in the vegetation of the spit. The plots are in the center and lowest part of the spit, where there is more shelter and moisture compared to outer parts of the area. What is most noteworthy among their species is a great increase in the abundance of *Mertensia maritima* in both plots since 2016, also in the abundance of *Cakile maritima, Atriplex, Stellaria media* and *Leymus arenarius* in one or both plots. All the species are known to prefer fertile to richly fertile soils (Nitrogen (Ellenberg) 6-8) according to BRC (2020). *Cakile, Atriplex* and *Stellaria* are annuals that only thrive in relatively nutrient rich environments.

Cakile was the first species found on Surtsey, on the northern shore in 1965 (Friðriksson 1975). In the following years it came and went until 1995, as it was present in 13 years out of 30 (Magnússon et al. 2009). From 1995 there is an unbroken record of the species on the island (unpublished data). In 2014 it started to appear in the plots on the northern spit and increase in abundance. *Mertensia* has an unbroken record of presence on the island from 1971 but does not start to flourish until 2014, in the plots of the spit. Although found earlier *Stellaria* did not gain a foothold on the island until 1988. Its main stronghold became the oldest and richest plots within the gull colony, until it appeared in high abundance in one of the plots on the northern spit in 2018. *Atriplex* has an unbroken record on the island from 2004. It is mostly confined to the dense vegetation on the northern spit were it has thrived in recent years. *Leymus* was the second colonizer of Surtsey, in 1966, and has an unbroken presence since 1973. It has spread widely in sandy areas and in 2012 it was among the most common species on the island (Magnússon et al. 2014). However, its abundance, measured as cover within permanent plots, remained relatively low except in areas impacted by breeding seagulls. Since 2016, its abundance has increased substantially within the plots on the northern spit. The observed changes in distribution and abundance of these species on the northern spit in recent years indicate considerable increase in soil fertility of the area. The low, northern shores of Surtsey receive very little drift of marine algae, as large fucoid beds have not developed on the unstable, littoral substrate off the spit (Jakobsson et al. 2007). Nutrient input upon the beaches and further inland is therefore considered limited via transport of dead algae from the sea.

Distribution of seagulls and seals

The first record of seagulls breeding on the northern spit is from 2005 when one great black-backed gull nest was found (unpublished data). From that time a few pairs have nested in the area amongst driftwood and patches of *Honckenya*. The first nest in or near a permanent plot on the spit was found in 2015. In 2016 and 2017, there were 6 nests recorded in or near the two plots, during a peak in number of breeding gulls on the island. In 2018 and 2019 the number of nests in or near the two plots was down to 2 and 1 (Fig. 10). It can therefore be stated that the seagulls have impacted the vegetation of the northern spit in recent years.

In this study, we have created the first map of the exact distribution of the grey seal breeding colony on the northern spit of Surtsey, which is the only part the island accessible to them. While the map is based on a single overflight, previous data obtained from the regular grey seal censuses carried out since 1982, has shown the grey seals with pups haul out on the northern spit (Granquist and Hauksson 2019b; Erlingur Hauksson pers. comm.). As an example, images taken during the census of 5 October 2017, show dozens of grey seal females and pups, most of them at the eastern and western edges of the spit, under the hill slopes, similar to what we observed in the current study (Granquist and Hauksson, unpublished data). Fewer seals were visible near the center of the spit in early October 2017 compared to late October 2019. In both years many seagulls (75 glaucous, 46 great black-backed and 12 herring gulls in 2019) could be seen on the photos of the spit, some of them amongst the seals and others roosting on the northern tip of the spit. This suggests that the gulls might be attracted to something edible coming from the seals.

Due to continuing marine abrasion, the land surface of Surtsey was reduced from its maximum area of 2.7 km^2 in 1967 to 1.3 km^2 in 2018. The northern spit, where the grey seals haul out to breed, has shrunk accordingly. In 1967 it was 0.3 km^2 or about 30 ha in area (Jakobsson et al. 2000). In 1988 it was reduced to 20.1 ha and by 2018 down to 10.2 ha (Fig. 8, Fig. 15). The grey seals in the breeding colony have therefore concentrated in a smaller area with the passing of time.

It should be noted that estimated total pup production (see Table 2) is a better indicator for grey seal abundance in Surtsey, than a separate single count, which was only possible in 2019. In 2017, when four overflights were

A. 27 July, 2001.

B. 17 July, 2018.

Figure 15. An overview of the northern spit of Surtsey, taken from the same spot in 2001 and 2018. Note the shrinking of the spit over the period and change in vegetation cover in the center part. Photos: Sigmar Metúsalemsson and Borgthór Magnússon.

made the highest number of pups seen in a single flight was 67 on 3 October, and the estimated pup production in the colony that year was 134. The peak of the pupping period in 2017 was 12 October (Granquist & Hauksson 2019b). The number of pups seen in the colony on 18 October 2019 is close to the maximum number recorded in earlier surveys and it should be expected that a higher number of pups were born over the course of the full pupping period (Table 2).

In the brief visit to the island on 30 October 2019, it was not possible to thoroughly inspect the whole seal colony. However, pups at different development stages were encountered, from newborns to 4-5 week-old pups (Fig. 14), as well as an adult female ready to give birth. This further indicates that at the time of inspection of the colony in mid-October some pups were probably unborn and others might have left for the sea. Very little information on grey seal abundance on Surtsey outside of the breeding period exists, but it can be assumed that the island is used by adult grey seals during their moulting period in the spring. Further, information on harbour seal abundance in Surtsey in other times of the year is very scarce. Harbour seals haul-out on land to a large extent during their pupping period in May-June, and it cannot be ruled out that they use Surtsey more at that time of the year than when the surveys have been carried out. This needs to be taken into consideration when effects of seal abundance on plant succession in Surtsey is discussed.

Nutrient transfer by seagulls and seals

In an earlier paper (Magnússon et al. 2009) we attempted to estimate the nutrient transfer of the gulls in their colony based on the excretion and food models for gulls developed in the Netherlands by Hahn et al. (2007). A seasonal estimate of a family unit (parents and offspring) for a lesser black-backed gull and a herring gull was around 0.6 kg N and 0.12 kg P. Taking into account the larger size of the great black-backed gull we here approximate the nutrient input of its family unit to 1 kg N and 0.2 kg P during the breeding season. Therefore, from their nesting density by the plots on the spit in 2015-2019 (0.5-3 nests/1000 m^2 = 5-30 nests/ha) we estimate their nutrient input as 5-30 kg N/ha and 1-6 kg P/ha in a season. This can be compared to an estimated input of 6-60 kg N/ha and 1.2 – 12 kg P/ha in a season in the old gull colony during 2003-2008 (Magnússon et al. 2009). Also to measured average seabird N-accumulation of 47 kg N/ha/yr in the old gull colony soils on Surtsey since 1985 and 1-2 kg of background N-deposition outside the colony (Leblans et al. 2014). The nutrient input of the nesting great black-backed gulls on the northern spit in the last few years is therefore substantial and contributes to the increase in vegetation in the area.

Grey seals are capital breeders as they forage and build up stored blubber that is utilized during the period of breeding and weaning of pups. During this time, they do not forage for food. In mid-September, grey seals start hauling out to breed on the northern spit of Surtsey and the first pups are born. The last females give birth in November-December (Hauksson 2015, Granquist & Hauksson 2019b). The lactation period is short and the pups are abruptly weaned after 2-3 weeks after which a post-weaning land based fasting period starts. During this period the pup moults before going to sea (Fedak & Anderson 1982). After weaning the females mate with the dominant male. Knowledge on grey seal pup development and exact time spent at the breeding site at these different stages is scarce for the Icelandic population. However, in a study of breeding grey seals (17 mothers and pups) on Sable Island, Canada, the average lactation period was 17 days. The average weight of a female at the time of parturition was 196 kg and pup birth mass 17 kg. At the time of weaning a pup had increased its weight 200-300% and the females had lost 35% of their initial body mass (Mellish et al. 1999). Further, Reilly (1991) studied the post weaning fast period of 12 grey seal pups. Their fast period lasted from 10 to more than 28 days. However, among 8 pups that were studied more thoroughly, the average post weaning fast lasted for 16 days on the average.

Can it be assumed that a 200 kg grey seal female and its pup transfer more nutrients from sea to land than a pair of black-backed gulls (2 x 2.5 kg) breeding in the same area? Water and energy metabolism of free-living grey seal pups during their post-weaning fast was studied by Reilly (1991). The average water output of the pups was 521 ml/day. The daily urine output fell with fasting time, from 4.8 to 2.1 ml/kg/day. Nitrogen in pup urine was 3.4 g/day (24 h) at initial capture but fell to 1.8 g/day at final capture (Reilly 1991). These values can be used to speculate about the possible nutrient output from the seals on Surtsey. Assuming a female/pup weight ratio of 6 over the period of lactation (17 days), (Mellish et al. 1999), the same urine output per kg and the higher urine N-value (3.4), a post weaning period of 16 days (Reilly 1991) and the N-output value for the pups as 2.6 g N/day over the period (average of the higher and lower value found by Mellish et al. 1999). The outcome will therefore be: female lactation period 6 x 3.4 g N/day x 17 days = 347 g N; pup lactation period 3.4 g N/day x 17 days = 58 g N, pup post weaning period 2.6 N/day x 16 days = 42 g N. This exercise gives a total nitrogen output from a female and its pup of 447 g N, assuming that the females urinate on land only during the period of lactation. Feces from the females and the pups are not included, but defecation appears to be limited during the period of fasting (Reilly 1991). The N-output from a grey seal female and its pup estimated here is therefore only about half of the estimated output from a pair of black-backed gulls and their chicks.

As stated above, there were 62 grey seal pups and 32 adults seen on the northern spit of Surtsey in October 2019. Considering that the estimated pup production in 2017 was estimated to 134, it is likely that over the whole 2019 breeding season there were more than 100 pups born in the colonly, in an area of approximately 5 ha. The N-output from the seals could therefore be of the order 20-30 females with pups per ha x 0.45 kg N = 9-13 kg N/ha, compared to to the 1-2 kg of background N-deposition on most of Surtsey (Leblans et al. 2014).

The grey seals breed in the fall after the period of vegetation growth. A portion of nutrients coming from the seals to the top soil may be washed or leached away from the plant root zone and not be as readily available as nutrients released from breeding seagulls in the spring and summer. However, as mentioned above, data on grey seal abundance during other periods of the year, such as the moulting period in the spring, is lacking. There are other possible sources of nutrients associated with the seals. When giving birth the females release the placenta and its fluids which are a sources of energy and nutrients and appear to attract seagulls (see earlier). Also, they may release feces at the site before giving birth. At moulting the pups change coats and the birth hairs are left in place, some of them will blow away but others be buried in the sand, eventually decomposing and adding nutrients to the soil. Here we have not considered the males present in the breeding colony and their possible inputs. Another source of nutrients are animals that die on land. In the summer of 2019 three carcasses of long-dead seals were encountered on the western spit of Surtsey. To our knowledge dead seals have not been found previously on the spit, although it can be expected that some of the pups do not survive.

Earlier studies (e.g. Farina et al. 2003, Doughty et al. 2016, Moss 2017, Bokhorst et al. 2019) have suggested that marine mammals and seabirds can be important vectors of marine nutrients to terrestrial systems. Our results support these findings. The animals obtain their food from productive oceans and breed on islands or in other remote areas. At the breeding sites soil nutrient concentrations are affected and plant growth enhanced. These effects have become very clear in the continuing studies of plant colonization and ecosystem development on Surtsey. The seagulls are more mobile than the seals, so they exert their influence over a much larger area on the island.

With continued erosion of Surtsey the northern spit will probably disappear before the turn of this century, while the island core will remain for thousands of years (Jakobsson et al. 2000). As the older neighboring islands, Surtsey will be girthed by high cliffs and not accessible to seals. Their impact on the island ecosystem will therefore be far more short-lived than that of the seabirds.

ACKNOWLEDGEMENTS

The Surtsey Research Society has provided logistic support for the study. Transport to the island has been provided by the Icelandic Coast Guard and the Vestmannaeyjar Rescue Team. Anette Th. Meier made maps of vegetation and seal distribution. Bjarni D. Sigurdsson, Erling Ólafsson, Matthías V. Alfredsson, Niki Leblans, Pawel Wasowicz, Sigurdur H. Magnússon and Starri Heidmarsson have taken part in biological expeditions to the island in recent years and contributed in various ways. Erlingur Hauksson provided valuable information on the grey seals. Aerial survey of the island in October 2019 was made with Úlfar Henningsson at Gardaflug. Eric dos Santos made valuable comments and corrections on the manuscript.

REFERENCES

Aerts, R., R.S.P. Van Logtetijn, N.I.W. Leblans & B.D. Sigurdsson, 2020. Effects of seabirds and soil development on plant and soil nutritional parameters after 50 years of succession on Surtsey. Surtsey Research 14, 85-90.

Astthorsson, O.S., A. Gislason & S. Jonsson, 2007. Climate variability and the Icelandic marine ecosystem. Deep-Sea Research 54, 2456-2477.

Ball, B.A., C.R. Telliz & R.A. Virginia, 2015. Penguin activity influences soil biogeochemistry and soil respiration in rookeries on Ross Island, Antarctica. Polar Biology 38, 1357-1368.

Biological Records Centre (BRC), 2020. Online Atlas of the British and Irish Flora. https://www.brc.ac.uk/plantatlas/ (accessed January 26, 2020).

Bokhorst, S., A. Huiskes, P. Convey & R. Aerts, 2007. External nutrient inputs into terrestrial ecosystems of the Falkland Islands and Maritime Antarctic region. Polar Biology 30, 1315-1321.

Bokhorst, S., P. Convey & R. Aerts, 2019. Nitrogen inputs by marine invertebrates drive abundance and richness in Antarctic ecosystems. Current Biology 29, 1721-1727.

British Ornithologists' Union (BOU), 2013. The British List: a checklist of birds of Britain, 8th Edn., Ibis, 155, 635-676.

Doughty, C.E., J. Roman, S. Faurby, A. Wolf, A. Haque, E.S. Bakker, Y. Malhi, J.B. Dunning Jr. & J.-C. Svenning, 2016. Global nutrient transport in a world of giants. PNAS 113, 868-873.

Ellis, J.C. 2005. Marine birds on land: a review of plant biomass, species richness and community composition in seabird colonies. Plant Ecology 181, 227-241.

Ersts, P.J. DotDotGoose (version 1.1.0). American Museum of Natural History, Center for Biodiversity and Conservation. Available from http://biodiversityinformatics.amnh.org/open_source/dotdotgoose. Accessed on 1st July 2019.

Farina, J.M., S. Salazar, K.P. Wallem, J.D. Witman & J.C. Ellis, 2003. Nutrient exchanges between marine and terrestrial ecosystems: the case of the Galapagos sea lion *Zalophus wollebaecki*. Journal of Animal Ecology 72, 873-887.

Fedak, M. A. & S.S. Anderson, 1982. The energetics of lactation: accurate measurements from a large wild mammal, the grey seal (*Halichoerus grypus*). Journal of Zoology 198, 473 -479.

Fridriksson, S., 1975. Surtsey. Evolution of life on a volcanic island. Butterworths, London, 198 pp.

Friðriksson, S., 2005. Surtsey. Ecosystem formed. Varði, Reykjavík, 112 pp.

Friðriksson. S.F. & B. Johnsen, 1967. The vascular flora of the outer Westman Islands. Societas Scientarium Islandica, Section IV, 37-67.

Georgsdóttir, G.I., E. Hauksson, G. Gudmundsson & E.R. Unnsteinsdóttir, 2018. Selalátur við strendur Íslands. Fjölrit Náttúrufræðistofnunar 56, 23 pp.

Granquist, S.M. and E. Hauksson, 2019a. Population estimate, trends and current status of the Icelandic harbour seal (*Phoca vitulina*) population in 2018. Marine and Freshwater Research Institution, HV 2019-36. 22 pp.

Granquist, S.M. & E. Hauksson, 2019b. Aerial sensus of Icelandic grey seal (*Halichoerus grypus*) population in 2017. Pup production, population estimate, trends and current status. Marine and Freshwater Research in Iceland, HV 2019-02, 19 pp.

Hahn, S., S. Bauer & M. Klassen, 2007. Estimating the contribution of carnivorous water birds to nutrient loading in freshwater habitats. Freshwater Biology 52, 2421-2433.

Hauksson, E., 1992. Observations on seals on the island of Surtsey in the period 1980-1989. Surtsey Research Progress Report 10, 41-42.

Hauksson, E., 2009. Seals in Surtsey, the period 1980-2005. Surtsey Research 12, 167-170.

Hauksson, E., 2010. Niðurstöður af talningum útselskópa úr lofti haustin 2005, 2008 og 2009. Áætlaðar stofnstærðarbreytingar útsels við Ísland 2005 til 2008/9. Handrit Rannsjá fjölrit. Nr. 1. 12 pp.

Hauksson, E., 2015. Observations on seals on the island of Surtsey in the period 1980-2012. Surtsey Research 13, 41-43.

Havik, G., A. Catenazzi & M. Holmgren, 2014. Seabird nutrient subsidies benefit non-nitrogen fixing tress and alter species composition in South American coastal cry forests. Plos One 9, 1, e86381, 8 pp.

Hilmarsson, J.Ó., 2009. Fuglalíf Vestmannaeyja (Birdlife of Vestmannaeyjar), in: Vestmannaeyjar, Árbók Ferðafélags Íslands 2009, 28-73, edited by J.V. Sigurðsson, Ferðafélag Íslands, Reykjavík.

Jakobsson, S.P., G. Gudmundsson & J.G. Moore, 2000. Geological monitoring of Surtsey, Iceland 1967-1998. Surtsey Research 11, 99-108.

Jakobsson, S.P., B. Magnússon, E. Ólafsson, G. Þorvarðardóttir, K. Gunnarsson, S. Baldursson & Æ. Petersen, 2007. Nomination of Surtsey for the UNESCO World Heritage List, edited by: Baldursson,S. & Á. Ingadóttir, Icelandic Institute of Natural History, Reykjavik, 124 pp.

Kristinsson, H., J.B. Hlíðberg & Þ.E. Þórhallsdóttir, 2018. Flóra Íslands. Blómplöntur og byrkningar (The Flora of Iceland). Vaka-Helgafell, Reykjavík, 741 pp.

Leblans, N.I., B.D. Sigurdsson, P. Roefs, R. Thuys, B. Magnússon & I.A. Jansen, 2014. Effects of seabird nitrogen input on biomass and carbon accumulation after 50 years of primary succession on a young volcanic island, Surtsey. Biogeosciences 11, 4415-4427.

Lindeboom, H.J., 1984. The nitrogen pathway in a penguin rookery. Ecology 65, 269-277.

Magnússon, B. & S.H. Magnússon, 2000. Vegetation succession on Surtsey during 1990-1998 under the influence of breeding seabirds. Surtsey Research 11, 9-20.

Magnússon, B., Magnússon, S.H. & S. Fridriksson, 2009. Developments in plant colonization and succession on Surtsey during 1999 – 2008. Surtsey Research 12, 57-76.

Magnússon B., S.H. Magnússon, E. Ólafsson & B.D. Sigurdsson, 2014. Plant colonization, succession and ecosystem development on Surtsey with reference to neighbour islands. Biogeosciences 11, 5521-5537.

McCune, B. & M.J. Mefford, 2011. PC-ORD. Multivariate Analysis of Ecological Data, Version 6. MjM Software, Gleneden Beach, Oregon, USA.

McLoughlin, P.D., K. Lysak, L. Debeffe, T. Perry & K.A. Hobson, 2016. Density-dependent resource selection by a terrestrial herbivore in a response to sea-to-land nutrient transfer by seals. Ecology 97, 1929-1937.

Mellish, J.E., S.J. Iverson & W.D. Bowen, 1999. Variation in milk production and lactation performance in Grey seals and consequences for pup growth and weaning characteristics. Physiological and Biochemical Zoology 72, 677-690.

Moss, B., 2017. Marine reptiles, birds and mammals and nutrient transfer among the seas and the land: An appraisal of current knowledge. Journal of Experimental Biology and Ecology 492, 63-80.

Norton, D.A., P.J. Delaange, P.J. Garnock-Jones & D.R. Given, 1997. The role of seabirds and seals in the survival of coastal plants: lessons from New Zealand *Lepidium* (Brassicaceae). Biodiversity and Conservation 6, 765-785.

Ólafsson, E. & M. Ingimarsdóttir, 2009. The land-invertebrate fauna on Surtsey during 2002-2006, Surtsey Research 12, 113-128.

Petersen, G.N. & T. Jónsson, 2020. The climate of Surtsey. Surtsey Research 14, 9-16.

Petersen, Æ., 2009. Formation of a bird community on a new island Surtsey, Iceland. Surtsey Research 12, 133-148.

Reilly, J.J., 1991. Adaptations to prolonged fasting in free-living weaned gray seal pups. American Journal of Physiology 260, 677-690.

Rouse, J.W., R.H. Haas, J.A. Schell & D.W. Deering, 1974. Monitoring Vegetation Systems in the Great Plains with ERTS. In: *Third Earth Resources Technology Satellite-1 Symposium. Volume 1: Technical Presentations, section A.* https://ntrs.nasa.gov/archive/nasa/casi.ntrs.nasa.gov/19740022614.pdf

Sigurdsson, B.D. & N.I.W. Leblans, 2020. Availability of plant nutrients and pollutans in the young soils of Surtsey compared to the older Heimaey and Elliðaey volcanic islands. Surtsey Research 14, 91-98.

Sigurdsson, B.D. & B. Magnusson, 2014. Ecosystem respiration, vegetation development and soil nitrogen in relation to breeding density of seagulls on a pristine volcanic island, Surtsey, Iceland. Biogeosciences 7, 883-891.

Sigurðsson, I.A. & S.P. Jakobsson, 2009. Jarðsaga Vestmannaeyja (Geological history of Vestmannaeyjar), in: Vestmannaeyjar, Árbók Ferðafélags Íslands 2009, 14-27, edited by J.V. Sigurðsson, Ferðafélag Íslands, Reykjavík.

Sobey, D.G. & J.B. Kenworthy, 1979. The relationship between herring gulls and the vegetation of their breeding colonies. Journal of Ecology 67, 469-496.

Hydrozoan colonization and succession in the tidal and subtidal zones in Surtsey during the period 1967 to 1984

STEFFEN LUNDSTEEN†, ERLINGUR HAUKSSON[1] AND KARL GUNNARSSON[2]

[1] Fornistekkur 14, 109 Reykjavík, Iceland
[2] Marine and Freshwater Research Institute, Skúlagata 4, 101 Reykjavík, Iceland
Address for correspondence: email: karl.gunnarsson@hafogvatn.is

ABSTRACT
This article reports on results of investigations of hydrozoans collected in Surtsey, Iceland in the period 1967 – 1984. Samples were collected in the intertidal zone and by divers in the subtidal zone down to 40 m. A list and illustrations of hydrozoan species found in the intertidal and subtidal rocky bottom in Surtsey are presented. Species numbers increased steadily during the study period and in 1984 a total of 37 species were recorded in Surtsey making hydrozoans one of the most diverse marine invertebrate groups in Surtsey. Among hydrozoans found during the study are 8 species not previously recorded in Iceland. Apart from dispersal by planktonic medusa, rafting of polyps on floating objects drifting to Surtsey is thought to be important for colonisation of hydrozoan fauna in Surtsey. At the end of the investigations period, 20 years after formation of rocky shores on the island, number of species seemed to be continually increasing.

INTRODUCTION
The island Surtsey (63° 18’N, 20° 36’W) was born in a series of volcanic eruptions between 1963 and 1967. When the eruptions stopped in 1967 the island had reached 2.7 km^2 in area. Since then the island has diminished considerably due to intensive erosion of the shoreline by heavy waves and now covers less than half its original size. The erosion of the shore has been most severe at the southwestern part of the island but slightest on the eastern side. (Jakobsson *et al.* 2000).

Surtsey is situated about 30 km off south coast of Iceland. The distance from Heimaey, the largest island in Vestmannaeyjar archipelago, is 20 km and about 3 km are from nearest rock rising above sea surface, Geirfuglasker.

† Steffen Lundsteen passed away in September 2018. Steffen was a marine biologist working at the Århus University, Denmark. Steffen was a skilled research diver with long experience in working with benthic biota. He joined Surtsey marine research in 1980 and took part in sampling, identified the hydrozoan species and made the illustrations that are presented in this paper. He passed away, way too soon, and we his co-authors (EH & KG) remember him with gratitude for his friendship and collaboration.

https://doi.org/10.33112/surtsey.14.11

Monitoring colonisation and succession of benthic organisms started already 1964 in the intertidal zone a year after the eruption started and in 1968, divers started sampling in subtidal slopes of the Island. In the beginning studies were done every year but after 1971 intervals between samplings have become increasingly longer (Jónsson 1970, Jónsson *et al.* 1987, Sigurðsson 1999, 2000, Gunnarsson & Hauksson 2009). The studies have focused on hard substrate where macrofauna and -flora have developed. Most of the marine macrofaunal groups found in Surtsey has been reported on, in a series of articles by Sigurðsson (1968, 1970, 1972, 1974, 1999, 2000), Hauksson (1982, 1992, 2000) and Gunnarsson & Hauksson (2009). However, hydrozoans that are prominent element of the fauna on subtidal rocky substrate, have been largely omitted hitherto.

The first systematic studies of hydrozoan fauna of Iceland date from the beginning of 20th century (Sæmundsson 1902, 1911). Sæmundsson (1911) registered 60 species of hydrozoans living at the Icelandic coast. Later, works of Broch (1916, 1918) and Kramp (1938) added to the list of hydrozoa known from Iceland and extending it to 90 species. Extensive sampling of benthic animals in Icelandic waters during the BIOICE program added significantly to knowledge of the hydrozoa fauna of Iceland its species and their distribution. Schuchert (2000, 2001), after analysing of the BIOICE material and revising older records, lists 129 species of hydrozoans found in Icelandic waters.

Here we present results of studies on the colonisation and succession of hydrozoans on rocky substrate in intertidal and shallow subtidal zone in Surtsey during the period from 1967 to 1984. The paper is primarily based on species analysis by Steffen Lundsteen.

MATERIAL AND METHODS

Most of the intertidal coastline of Surtsey is covered by basaltic rocks or cliffs, except the northern part, which is of sand (Calles *et al.* 1982). In the subtidal zone, substrate off the northern part is sand, but along the east, south and the west it consists of boulders and large rocks in the shallow parts, but in the deeper parts sand becomes more common between rocks, and below 25 m sand covers large part of the bottom.

The sea around Surtsey is influenced by the North Atlantic current with salinity of 35.1 and surface temperatures that reach 12 to 13°C during late summer and falls to 6°C in winter (Marine and Freshwater Research Institute 2020). Visibility of the waters in the area is reduces by outflow of several large glacial rivers at the south coast of Iceland.

The material was collected in 1967, 1968, 1969, 1970, 1971, 1974, 1977, 1980 and 1984. The intertidal zone was sampled in the first three sampling years. Sampling of the subtidal zone started in 1968 and followed in all subsequent sampling years. Samples from the intertidal zone were collected during landing excursions on the coast. Samples from the subtidal were taken by divers at different depths at several stations around the island. Emphasis was on taking samples from all types of substrates and habitats. The sea conditions can be very rough at the island and sampling stations had to be chosen according to weather conditions, prevailing during sampling expeditions. The subtidal zone was sampled at depths between 5 to 40 m. However, most of the samples were from 10 m to 30 m. Faunal samples were preserved in 70% isopropanol for later examination. For further information about the sampling procedure see Sigurðsson (1968, 1970, 1972, and 1974) and Hauksson (1982 and 1992).

From the tidal belt 21 samples were examined and 113 samples from the subtidal zone. Samples were first sorted into higher taxonomic groups with hydrozoans grouped separately. Examination of hydrozoan samples and species identification was done under a stereo microscope with camera lucida as a drawing aid. Species occurrence in samples was recorded along with types of substrate on which hydrozoans were growing. Species names have been updated in accordance with the WoRMS database (2020). Authorities of scientific names of hydrozoan species mentioned in text are given in Table 2.

RESULTS

Hydrozoans were a prominent part of hard bottom faunal community that had developed in the subtidal zone in Surtsey (Fig. 1). The species with highest frequency, occurring in more than 40% of samples, during 3 of the latest sampling years were *Bougainvillia muscus, Clytia gracilis, Diphasia rosacea, Ectopleura larynx, Halecium undulatum, Obelia geniculata, O. longissima* and *Phialella quadrata* (Table 1).

Most of the species recorded had relatively wide depth distribution throughout the subtidal zone, although a few of the species that were first found

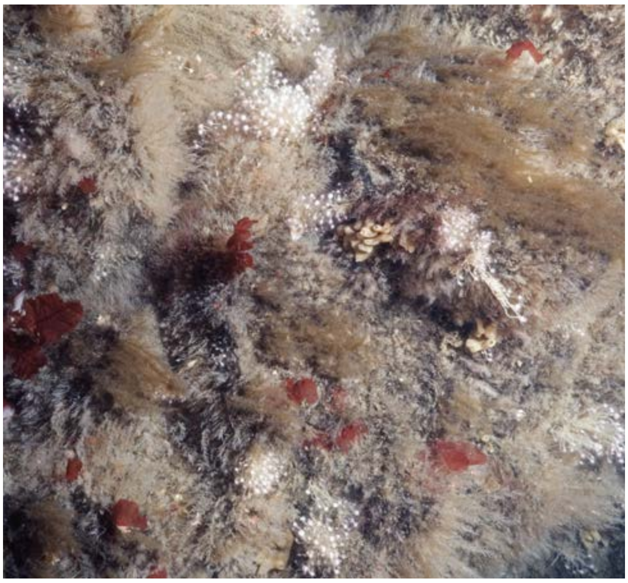

Figure 1. Hydrozoans are a prominent part of the hard bottom benthic fauna in the subtidal zone around Surtsey. Photo taken at 25 m depth in Surtsey in June 1984.

at the end of the study period had only settled at 20 to 30 m depth (Table 1). In 1967 four species were found in the intertidal zone all of them were drift specimens attached to subtidal algae or stones cast ashore with other subtidal animals attached. All those 4 species have since been found every year growing in the subtidal zone (Table 2). In 1968 when direct sampling in the subtidal zone started, 10 species were found. Since then number of species found each sampling year have increased steadily (Fig. 2). In 1984, there were 27 species found in Surtsey. In total 37 hydrozoan species were registered in Surtsey, for the period 1967 – 1984.

Many of the species were missing in one or more sampling years after they were first found. It is quite likely in those cases that some of the smaller or the rarer once have been overlooked. Bigger and more prominent species are more likely to be found if present. The fact that they were absent in some of the sampling years but not others, indicates that they are opportunistic, appearing only when conditions

Table 1. Vertical and horizontal distribution of Hydrozoan species found in Surtsey in the year 1984. Species with the highest frequency of occurrence during the last three sampling years are marked with an asterix.

	North-East		East				South-East					South				West			
	10m	15m	5m	10m	15m	30m	5m	10m	15m	20m	30m	10m	15m	20m	30m	10m	15m	20m	30m
*Bougainvillia muscus**		x				x				x	x			x	x		x	x	x
Calycella syringia	x									x	x	x			x			x	
Campanulina pumila	x	x	x						x	x			x	x	x		x	x	
Clytia gracilis	x	x								x			x	x	x		x	x	x
Clytia hemisphaerica	x										x								
*Diphasia rosacea**	x	x		x		x				x	x		x	x	x		x	x	x
*Ectopleura larynx**	x	x			x	x			x	x	x		x	x	x			x	x
Eudendrium arbuscula										x									
Eudendrium capillare																			x
Eudendrium rameum											x								
Filellum serpens	x			x					x	x			x	x					
Gonothyraea loveni							x				x								
Halecium beanii											x		x						
Halecium curvicaule	x					x				x	x			x			x		
Halecium muricatum											x								
*Halecium undulatum**	x						x			x	x		x	x			x	x	x
Lafoeina tenuis	x									x				x				x	
Mitrocomella polydiademata										x									
Obelia dichotoma		x		x	x		x			x	x								
*Obelia geniculata**	x	x	x	x	x	x	x	x	x	x	x	x	x	x		x	x		x
Obelia hyalina											x								
*Obelia longissima**	x	x	x			x	x		x	x	x		x	x	x		x	x	x
Orthopyxis integra	x			x					x	x				x			x		
*Phialella quadrata**		x								x	x		x	x	x	x			x
Podocoryna carnea										x									
Sarsia lovenii										x									
Sarsia tubulosa											x							x	x
Zanclea implexa											x								x

Table 2. Order of arrival of hydrozoan species in Surtsey from the beginning of colonisation until 1984. Species not recorded in Iceland before are marked with asterix.

Species	1967	1968	1969	1970	1971	1974	1977	1980	1984
Ectopleura larynx (Ellis & Solander, 1786)	x	x	x	x	x	x	x	x	x
Obelia geniculata (Linnaeus, 1758)	x	x	x	x	x	x	x	x	x
Obelia longissima (Pallas, 1766)	x	x	x	x	x	x	x	x	x
Phialella quadrata (Forbes, 1848)*	x	x	x	x	x	x	x	x	x
Bougainvillia muscus (Allman, 1863)		x	x	x	x	x	x	x	x
Diphasia rosacea (Linnaeus, 1758)		x			x	x	x	x	x
Clytia hemisphaerica (Linnaeus, 1767)		x				x	x	x	x
Lafoeina tenuis Sars, 1874*		x		x	x			x	x
Obelia dichotoma (Linnaeus, 1758)		x		x		x	x	x	x
Corymorpha nutans M. Sars, 1835		x							
Calycella syringa (Linnaeus, 1767)			x	x	x	x	x	x	x
Eudendrium rameum (Pallas, 1766)			x	x	x	x	x	x	x
Podocoryna carnea M. Sars, 1846			x	x	x		x	x	
Clytia gracilis (M. Sars, 1850)				x	x	x	x	x	x
Orthopyxis integra (MacGillivray, 1842)				x	x	x	x	x	x
Halecium curvicaule Lorenz, 1886				x	x	x	x	x	x
Aequorea forskalea Péron & Lesueur, 1810				x					
Halecium labrosum Alder, 1859					x	x	x		
Cuspidella humilis Hincks, 1866					x				
Filellum serpens (Hassall, 1848)						x	x	x	x
Rhizorhagium roseum M. Sars, 1874						x	x	x	
Halecium muricatum (Ellis & Solander, 1786)						x	x		x
Eudendrium capillare Alder, 1856*							x		x
Halecium halecinum (Linnaeus, 1758)							x		
Hydrallmania falcata (Linnaeus, 1758)								x	
Opercularella lacerata (Johnston, 1847)								x	
Tiaropsis multicirrata (M. Sars, 1835)*								x	
Campanulina pumila (Clark, 1875)								x	x
Eudendrium arbuscula Wright, 1859*								x	x
Gonothyraea loveni (Allman, 1859)								x	x
Halecium undulatum Billard, 1921								x	x
Zanclea implexa (Alder, 1856)*								x	x
Halecium beanii (Johnston, 1838)									x
Eudendrium ramosum (Linnaeus, 1758)									x
Mitrocomella polydiademata (Romanes, 1876)*									x
Sarsia lovenii (M. Sars, 1846)*									x
Sarsia tubulosa (M. Sars, 1835)									x

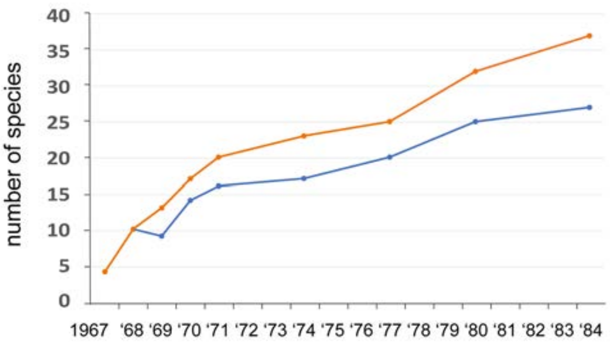

Figure 2. Changes in number of hydrozoan species registered in Surtsey during the period 1967 to 1984. Blue curve: number of species found each sampling year. Orange curve: cumulative number of species recorded in Surtsey.

are favourable or substrate freely available. Most species did not appear to be substrate specific and were alternatively found growing on stones, shells or other hydrozoans. Exceptions are *Ectopleura larynx* that was rarely found on other substrate than rocks, *Filellum serpens* was only found on other hydrozoans, *Obelia geniculata* was mostly found attached to algae and *Corymorpha nutans* was found growing in sand.

Eleven species were detected in all the subsequent sampling years since they were first found, for at least four sampling years. Those are *Bougainvillia muscus, Calycella syringia, Clytia gracilis, Ectopleura larynx, Eudendrium rameum* (Fig. 6), *Filellum serpens, Halecium curvicaule, Obelia geniculata,* *O. longissima*, *Orthopyxis integra* and *Phialella quadrata*. Additionally, *Clytia haemispherica*, *Diphasia rosacea* and *Obelia dichotoma* were found consistently in the last 4 to 5 sampling years (Table 1) although originally found earlier.

Eight of the species found in Surtsey had not been recorded for Iceland before (cf. Schuchert 2001). Those are the following:

1. *Aequorea forskalea* Péron & Lesueur, 1810; Hydroid stage referred to this specie was found in Surtsey in 1970 at 40 m depth growing on a *Mytilus edulis* shell.
2. *Eudendrium arbuscula* Wright, 1859 (Fig. 3); Fertile colonies of this species were found in Surtsey in August 20, 1971 at 20 m depth. It was found again, in 1980, attached to a stipe of the kelp *Laminaria hyperborea*, and in 1984 on calcareous plates of a *Balanus* sp.
3. *Lafoeina tenuis* Sars, 1874; First found in 1968 and subsequently in 1970, 1971, 1980 and 1984, growing on shells of *Mytilus edulis* and on other hydrozoans.
4. *Mitrocomella polydiademata* (Romanes, 1876); Found in 1984 at 20 m depth, growing on stolons of *Obelia longissima* (cf. Cornelius 1995, Schuchert 2001 regarding identification of *M. polydiademata*).
5. *Phialella quadrata* (Forbes, 1848); This species was first found in Surtsey 1967 in the intertidal zone on stone cast ashore and was since found in all sampling years at depths from 5 to 40 m. It was a common species in Surtsey and was found growing mostly on other hydrozoans but also on shells, stones and occasionally on algae.
6. *Sarsia lovenii* (M. Sars, 1846); Found in 1984 at 20 m depth growing on stone.
7. *Tiaropsis multicirrata* (M. Sars, 1835); First found in 1980 at 15 m depth, growing on stone.
8. *Zanclea implexa (Alder, 1856)* (Fig. 4); First found in 1980 growing at 25 and 30 m depth on shells of *Heteranomia squamula* (Linnaeus, 1758).

Figure 3. *Eudendrium arbuscula* Wright, 1859. Surtsey West coast 20.08.1971 at 20 m depth. **a**, habitus of a colony; **b**, hydranth with female gonophores, note terminal button with nematocysts; **c**, feeding hydranth with a basal band of nematocyst; **d**, nematophore with nematocysts covering its apex. Scale bars; 1 mm, for ***a*** on the left side and for ***b***, ***c*** and ***d*** on right side.

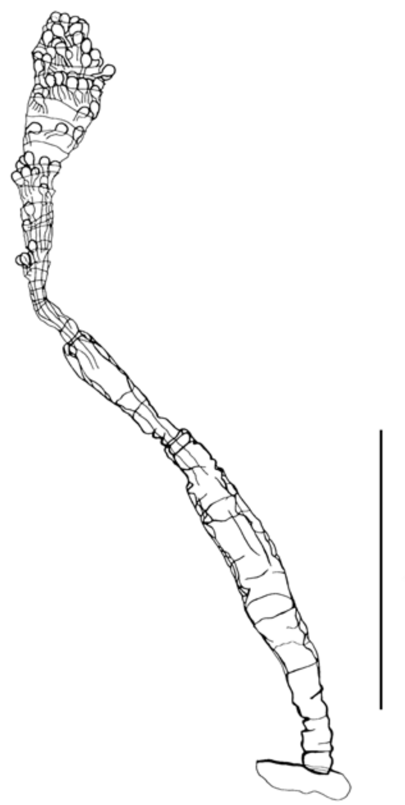

Figure 4. *Zanclea implexa* (Alder, 1856). Surtsey West coast, 29.07.1980, at 30 m depth. A specimen with single hydranth having capitate tentacles. Scale bar; 1 mm.

DISCUSSION

The number of hydrozoa species found in Surtsey increased rapidly from the start of the observations in 1967 until about 1971 when 19 species were found (Fig. 1), some of which are illustrated here for taxonomic clarity (Figs 3–8). Since then the increase in number of species recorded slowed down and at the end of the observation period in 1984, 37 species had been found. Previously 129 hydrozoa species have been recorded from Iceland (Schuchert 2001). Additional 8 species were recorded during the present study. The hydrozoan fauna of Surtsey makes up a relatively high percentage of the hydrozoan fauna of Iceland, or about 27 %. A high percentage considering that a large part of the species previously recorded in Icelandic waters are deep water species that one would not expect to find in shallow waters as studied here (Schuchert 2001).

Hydrozoans are one of the most diverse groups of the faunal community in Surtsey. Their importance in terms of cover of rocky substrate is least at shallower depths where seaweed species dominate. In deeper waters, their coverage increases and below 20 m depth hydrozoans cover more than 50 % of the hard substrate (Gunnarsson & Hauksson 2009).

High abundance of *Bougainvillia muscus* in Surtsey is unexpected. Previously only one colony of this species has been reported from southern Iceland (Kramp 1938). Its early establishment and abundance in Surtsey, might have been facilitated by large open spaces available for colonisation. On the other hand, the conspicuous species *Tubularia indvisa*, was not found in Surtsey, though this was to be expected as it is present at nearby shores and is probably common there (Sæmundsson 1911; Kramp 1938).

The life cycle of the hydrozoans is typically characterized by the alternation of three stages: benthic polyp stage, planktonic medusa and planula (Boero *et al.* 2002, Cornelius 2002). Dispersal can occur by planktonic medusa or planula drifting with currents or by rafting of the polyp stage attached to natural or anthropogenic, floating objects drifting at the surface of the sea. Planula are commonly produced, but usually only last a few hours. It is therefore unlikely that planula stage has any significance in dispersal of hydrozoans to Surtsey. The medusae live stages last from a few hours up to a month (Bouillon *et al*. 2004). Only some of the species found in Surtsey have an independent medusa stage, which lasts for several days, and could therefore contribute to their dispersal to the island.

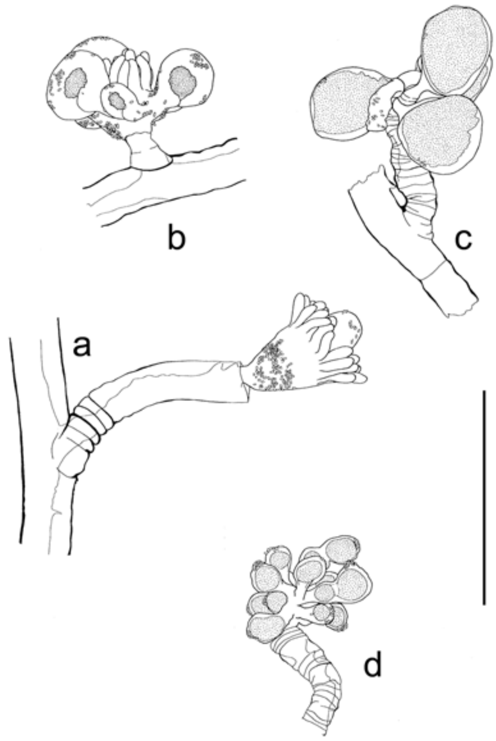

Figure 6. *Eudendrium rameum* (Pallas, 1766). Surtsey North-West coast, 26.07 1969, 28 – 30 m depth. **a**, feeding hydranth with nematocysts spread at its lower part; **b**, **c**, female gonophores with spread nematocysts; **d**, male gonophores with small patches of apical nematocysts. Scale bar: 1 mm

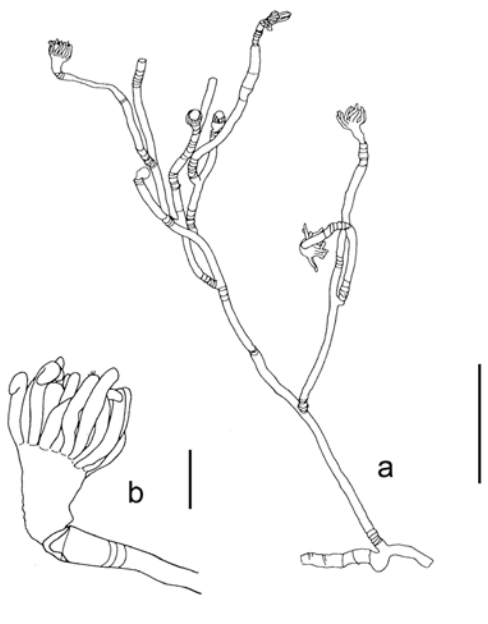

Figure 5. *Eudendrium capillare* Alder, 1856. Surtsey South coast, 11.07.1977, 20 m depth. **a**, habitus of a colony; **b**, details of a feeding hydranth. Scale bars; **a** 1 mm, **b**: 0.1 mm.

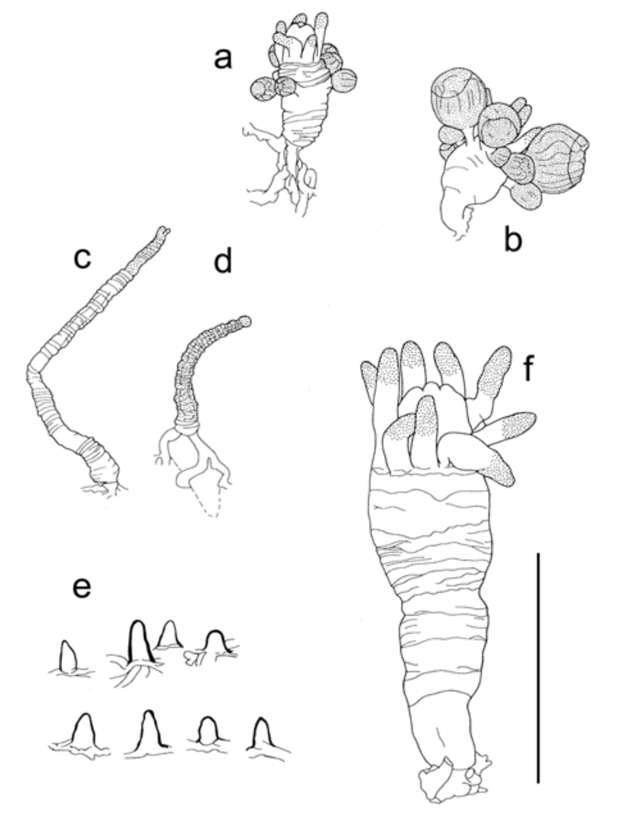

Figure 7. *Podocoryna carnea* M. Sars, 1846. Surtsey East coast, 09.07.1977, 20 m depth. **a, b,** hydranths bearing medusa buds; **c**, **d,** dactylozoids; **e**, spines of hydrorhiza; **f**, solidary feeding hydranth. Scale bar: 1 mm.

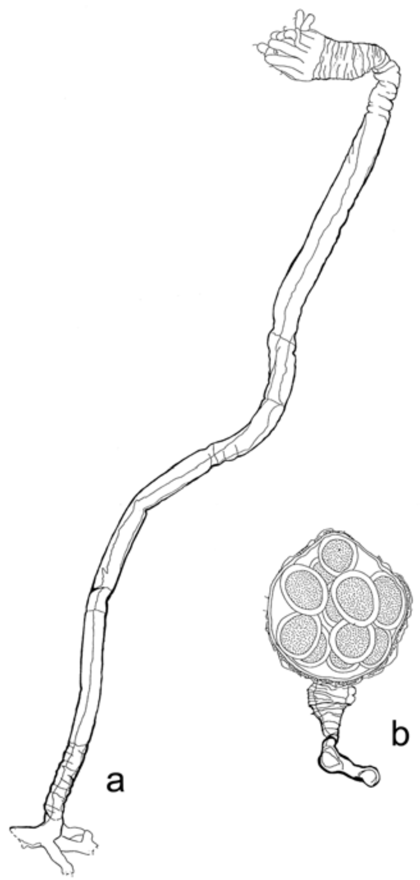

Figure 8. *Rhizorhagium roseum* M. Sars, 1874. Surtsey W, 10.07.1977, 10 m depth. **a**, habitus of a specimen with a single hydranth, **b**, sporosac with eggs. Scale bar: 1 mm.

Rafting probably plays an important role in the dispersal of hydrozoa species to Surtsey. Natural derived rafts such as drifting seaweeds, vegetation turfs, tree branches and driftwood have been found stranded on the shores of Surtsey. In addition, flotsam, plastic floats, bottles and other floating anthropogenic objects are regularly found cast ashore. Ingólfsson (1995) considers rafting on clumps of seaweed an important factor in the dispersal of marine intertidal fauna and has hypothesised that rafting might have been the main factor for benthic fauna repopulating the shores of Iceland and the Canadian Maritime after the last glacial maximum (Ingólfsson 1992).

Hydrozoans are amongst the most common epizoic fauna on rafts drifting in the Oceans (Tiel & Gutow 2005). The tsunami event that occurred 2011 in Japan resulted in large-scale wrecking of maritime structures. This left great amount of debris floating in the ocean, substantial part of which was transported by currents across the Pacific to the west coast of North America. These structures supported diverse fauna that was carried along across the ocean (Carlton *et al.* 2017). Among the most diverse of the attached organisms were hydrozoans (Choon *et al.* 2018).

Significant changes were observed in the development of hydrozoan fauna in Surtsey during the study period. Species numbers were steadily rising, and frequency of the species changed. At the end of the study period in 1984 species were still being added to the hydrozoan fauna of Surtsey, 20 years after formation of rocky shores. Continued studies of hydrozoan sampled in Surtsey along with studies of the fauna attached to floating objects that drift to Surtsey will further help elucidate mode of arrival and the development of the hydrozoan fauna in Surtsey.

ACKNOWLEDGEMENTS
Financial support came from Icelandic Fisheries Fund, Icelandic Research Fund, Icelandic Democracy Fund and Danish National Research Foundation. We are grateful to the crew and divers on mb Sæör, rv

Árni Friðriksson and rv Bjarni Sæmundsson for their assistance during sampling expeditions. Thanks, are due to Kay W. Petersen, Zoologisk Laboratorium in Copenhagen, for assistance with identification of hydrozoans and to Svanhildur Egilsdóttir, Marine and Freshwater Research Institute, Iceland for editing figures. We are also grateful to Guðmundur Guðmundsson Institute of Natural History, Iceland for useful comments on an earlier draft of the manuscript.

REFERENCES

Boero, F., Bouillon, J., Piraino, S. & Schmid, V. 2002. Asexual reproduction in the Hydrozoa (Cnidaria). *In* R.N. Hughes (ed.). Reproductive biology of invertebrates. Vol. XI. Progress in asexual reproduction. Oxford & IBH Publishing Co. Pvt. Ltd., New Delhi. pp. 141–158.

Bouillon, J., Medel, M.D., Pages, F., Gili, J.M., Boero, F. & Gravili, C. 2004. Fauna of the Mediterranean Hydrozoa. Sci. Mar. 68, 5–438.

Broch, H. 1916. Hydroida. Part 1. Danish Ingolf-Expedition 5, part 6, 66 pp.

Broch, H. 1918. Hydroida, Part II. Danish Ingolf-Expedition 5, part 7, 200 pp.

Calles, B., Lindé, K. & Norrman, J.O. 1982. The geomorphology of Surtsey island in 1980. Surtsey Research Progress Report 9, 117–132.

Carlton, J.T., Chapman, J.W., Geller, J.B., Miller, J.A., Carlton, D.A., McCuller, M.I., Treneman, N.C., Steves, B.P. & Ruiz, G.M. 2017. Tsunami-driven rafting: Transoceanic species dispersal and implications for marine biogeography. Science 357, 1402–1406.

Choong, H.H.C., Calder, D.R., Chapman, J.W., Miller, J.A., Geller, J.B. & Carlton, J.T. 2018. Hydroids (Cnidaria: Hydrozoa: Leptothecata and Limnomedusae) on 2011 Japanese tsunami marine debris landing in North America and Hawaiʻi, with revisory notes on *Hydrodendron* Hincks, 1874 and a diagnosis of Plumaleciidae, new family. Aquatic Invasions 13, 43–70

Cornelius, P.F.S. 1992. Medusa loss in leptolid Hydrozoa (Cnidaria), hydroid rafting, and abbreviated life-cycles among their remote-island faunae: an interim review. *In:* J. Bouillon, F. Boero, F. Cicocna, I.M. Gili & R.G. Hughes (eds). Aspects of Hydrozoan Biology. Sci. Mar. 56(2-3), 245–261.

Cornelius, P.F.S. 1995. North-West European Thecate Hydroids and their Medusa. Part 1. *In*: R.S.K. Barnes & H. Crother (eds). Synopsis of the British Fauna (New Series) No 50. Field Studies Council, Shrewsbury i-vii, 1-437.

Gunnarsson, K. & Hauksson, E. 2009. Succession and benthic community development in the sublittoral zone at the recent volcanic island, Surtsey, southern Iceland. Surtsey Research 12, 161–166.

Hauksson, E. 1982. A survey of the subtidal fauna of Surtsey in 1974. Surtsey Research Progress Report 9, 59–61.

Hauksson, E. 1992. Studies of the subtidal fauna of Surtsey in 1980-1987 and changes in subtidal fauna from 1964 to 1987. Surtsey Research Progress Report 10, 33–42.

Hauksson, E. 2000. A survey of the benthic coastal fauna of Surtsey, Iceland, in 1997. Surtsey Research 11, 85–88.

Ingólfsson, A. 1992. The origin of the rocky shore fauna of Iceland and the Canadian Maritimes. Journal of Biogeography 19, 705–712.

Ingólfsson, A. 1995. Floating clumps of seaweed around Iceland: natural microcosms and a means of dispersal for shore fauna. Mar. Biol. 122, 13–21.

Jakobsson, S.P., Guðmundsson, G. & Moore, J.G. 2000. Geological monitoring of Surtsey, Iceland, 1967-1998. Surtsey Research 11, 99–108.

Jónsson, S. 1970. Meeresalgen als erstbesiedler der vulkaninsel Surtsey. Schr. Naturv. Ver. Schlesv. -Holst. Sonderband, 21–28.

Jónsson, S., Gunnarsson, K. & Briane, J.-P. 1987. Évolution de la nouvelle flore marine de l´île volcanique de Surtsey, Islande. Journal of the Marine Research Institute, Reykjavik 10(1), 1–30.

Kramp, P.L. 1938. Marine Hydrozoa. Hydroida. Zoology of Iceland 2(5a), 1–82.

Marine and Freshwater Research Institute 2020. Sea surface temperatures at the Icelandic coast. http://www.hafro.is/Sjora/, searched on 16 March 2020.

Schuchert, P. 2000. Hydrozoa (Cnidaria) of Iceland collected by the BIOICE programme. Sarsia 85, 411–418.

Schuchert, P. 2001. Hydroids of Greenland and Iceland (Cnidaria, Hydrozoa). Meddelelser om Grönland, Bioscience 53. Copenhagen, The Danish Polar Center 2001, 184 pp.

Sigurðsson, A. 1968. The coastal invertebrate fauna of Surtsey and Vestmannaeyjar. Surtsey Research Progress Report 4, 95-107.

Sigurðsson, A. 1970. The benthonic coastal fauna of Surtsey in 1968. Surtsey Research Progress Report 5, 70–77.

Sigurðsson, A. 1972. The benthic coastal fauna of Surtsey in 1969. Surtsey Research Progress Report 6, 91–96.

Sigurðsson, A. 1974. Report on the sampling of the benthic fauna of Surtsey 1970, 1971 and 1974. Surtsey Research Progress Report 7, 20–21.

Sigurðsson, A. 1999. Botndýr við Surtsey. Náttúrufræðingurinn 68(3–4), 201–207.

Sigurðsson, A. 2000. A survey of the benthic coastal fauna of Surtsey in 1992 and comparison with earlier data. Surtsey Research 11, 75–83.

Sæmundsson, B. 1902. Bidrag til Kundskaben om de islandske Hydroider. Videnskabelige Meddelelser fra Dansk Naturhistorisk Forening i København 1902, 47-74, plates 1–2.

Sæmundsson, B. 1911. Bidrag til Kundskaben om de islandske Hydroider. II. – Videnskabelige Meddelelser fra Dansk Naturhistorisk Forening i København 63**,** 67–107.

Tiel, M. & Gutow, L. 2005. The ecology of rafting in the marine environment. II. The rafting organisms and communities. Oceanography and Marine Biology, Annual Review 43, 279–418.

WoRMS (2020). Hydrozoa. Accessed at: http://www.marinespecies.org/aphia.php?p=taxdetails&id=1337 on 2020-03-26.